SEVENTH FRAMEWORK PROGRAMME

THEME 6: Environment (including climate change)

Contract for: **Collaborative Project**

D.4.2
Model Implementation Report

Project acronym:	BRIDGE
Project full title:	SustainaBle uRban planning Decision support accountinG for Urban mEtabolism
Contract no.:	211345
Date:	30/06/2011
Document Reference:	211345_017_TR_UPM
Book Captain:	Roberto San José (UPM)
Authors:	Roberto San José (UPM), Juan Luis Pérez (UPM)
Contributors :	Donatella Spano (CMCC), Serena Marras (CMCC), David Pyles(CMCC), Matthias Falk (CMCC), Carlos Borrego (UAVR), Myriam Lopes (UAVR), Ana Isabel Miranda (UAVR), Jorge Humberto Amorim(UAVR), Pedro Cascão (UAVR), Joana Martins (UAVR), José Manuel Martins (UAVR), Anabela Carvalho (UAVR), Sue Grimmond (KCL), Mario Iamarino (USBa), Leena Järvi (UHEL), Simone Kotthaus (KCL), Fredrik Lindberg (GU and KCL), D. Kolokotsa (NKUA), K. Gobakis (NKUA), A. Synnefa (NKUA), M. Santamouris (NKUA), Veldhuizen Ab (ALTERRA), Grégoire Pigeon (CNRM)
Issue:	1.0
Deliverable no.:	D.4.2
Dissemination Level:	RE

Document Status Sheet

Issue	Date	Author	Comments
1.0	April 8/2011	R. San José, J.L. Pérez (UPM)	
	April 26/2011	Donatella Spano, Serena Marras, David Pyles, Matthias Falk (CMCC)	Added contribution on WRF-ACASA results
	April 26/2011	Carlos Borrego, Myriam Lopes, Ana Isabel Miranda, Jorge Humberto Amorim, Pedro Cascão, Joana Martins, José Manuel Martins, Anabela Carvalho (UAVR)	Added contribution on UAVR model results
	3 june 2011	Sue Grimmond (KCL), Mario Iamarino (Università degli Studi della Basilicata), Leena Järvi (University of Helsinki, and KCL), Simone Kotthaus (KCL), Fredrik Lindberg (Göteborg University and KCL)	Sent round for review by all co-authors
	12 June 2002	Sue Grimmond (KCL), Mario Iamarino (Università degli Studi della Basilicata)	Version submitted

Table of Contents

List of Figures

1 INTRODUCTION

1.1 Definitions and Acronyms

Acronyms

ACASA Advanced Canopy-Atmosphere-Soil Algorithm (CMCC)

CAMO Cellular Automata Traffic Model (UPM)

CAMx Comprehensive Air quality Model with extensions (ENVIRON)

CMAQ Community Multiscale Air Quality Modelling System (US EPA)

EMIMO An emission model (UPM)

MICROSYS Microscale Air Quality Simulation System (UPM)

MM5 NCAR Mesoscale Meteorological Models (US NCAR)

TREM Transport Emission Model for Line Sources (UAVR)

URBAIR Urban air quality model (UAVR)

VADIS Microscale air quality model (UAVR)

WRF Weather Research & Forecasting Model (US NCAR, NCEP, FSL, AFWA, FAA, University of Oklahoma)

1.2 Purpose of the document

Thidocument decribes how the selected models will be implemented, including input data preprocessing and model configurations .An analysis of the models results will be also included.

1.3 Document References

Anandakumar K. (1999). A study on the partition of net radiation into heat fluxes on a dry asphalt surface. Atmos. Env. 33, 3911-3918.

Asaeda T. & Ca V. T. (1993). The subsurface transport of heat and moisture and its effect on the environment: a numerical model. Boundary-Layer Meteorol. 65, 159-178.

Businger J.A., Wungaard J.C., Izumi Y. & Bradley E.F. (1971).Flux-Profile Relationships in the Atmospheric Surface Layer.J. Atmos. Sci., 28, 181–189.

Cambell G.S. & Norman J.M (1998).Introduction to Environmental Biophysics.Springer Science, US.de Bruin H.A.R. &Holtslag A.A.M. (1982). A simple parameterization of surface fluxes of sensible and latent heat during daytime compared with the Penman–Monteith concept. J. Appl. Meteor., 21, 1610–1621.

Cook R, Touma JS, Beidler A, Strum M. Preparing highway emissions inventories for urban scale modeling: a case study in Philadelphia. Transp Res Part D Transp Environ 2006;11:396–407

Chen, F., Y. Liu, H. Kusaka, M. Tewari, J-W Bao, C-F Lo, and K-H Lau, 2004: Challenge of Forecasting Urban Weather with NWP Models. *5th MM5 and WRF Users Workshop*, 21-25 June, Boulder, Colorado.

Chen, F., Kusaka, H., Tewari, M., Bao, J.-W., Kirakuchi, H., 2004. Utilizing the coupled WRF/LSM/Urban modeling system with detailed urban classification to simulate the urban heat island phenomena over the greater Houston area. In: Proceedings of the 5th Conference on Urban Environment, 22–26 August 2004, Vancouver, BC, Canada

Doll D., Ching J. K. S. &Kaneshiro J. (1985).Parameterisation of subsurface heating for soil and concrete using net radiation data.Boundary-Layer Meteorol. 32, 351-372.

Dyer A.J., (1974). A review of flux-profile relationships.Boundary-Layer Meteorol.7, 363-372.Fuchs M. & Hadas A. (1972).The heat flux density in a non-homogeneous bare loessial soil.Boundary-Layer Meteorol. 3, 191-200.

Dudhia, Numerical study of convection observed during the winter monsoon experiment using a mesoscale two-dimensional Model, *J. Atmos. Sci.* **46** (1989), pp. 3077–3107

Falk, M., Pyles, R.D., Marras, S., Spano, D., Snyder, R.L., Paw U, K.T., 2010. A Regional Study of Urban Fluxes from a Coupled WRF-ACASA Model. American Geosciences Union Fall Meeting. San Francisco, California

Grell, G. A., and D. Devenyi, 2002: A generalized approach to parameterizing convection combining ensemble and data assimilation techniques. Geophys. Res. Lett., **29(14),** Article 1693.

Grimmond C.S.B. & Oke T. R. (1991).An Evaporation-Interception Model for Urban Areas. Water Resour. Res. 27, 1739-1755.

Grimmond C.S.B. & Oke T.R. (1999). Aerodynamic properties of urban areas derived from analysis of surface form. J. Appl. Meteorol. 38, 1262-1292.

Grimmond C.S.B. & Oke T.R. (2002). Turbulent Heat Fluxes in Urban Areas: Observations and a Local-Scale Urban Meteorological Parameterization Scheme (LUMPS). J. Appl. Meteorol. 41, 792-810.

Grimmond C.S.B., Cleugh H.A. & Oke T.R. (1991).An objective urban heat storage model and its comparison with other schemes.Atmos. Env.25B, 311-174.

Grimmond, C.S.B. & Oke, T.R. (1999) Heat storage in urban areas: Local-scale observations and evaluation of a simple model. J. Appl. Meteorol. 38, 922-940.

Hamilton IG, Davies M, Steadman P, Stone A, Ridley I, Evans S (2009). The significance of the anthropogenic heat emissions of London’s buildings: A comparison against captured shortwave solar radiation. *Building and Environment* 44: 807-817. DOI: 10.1016/j.buildenv.2008.05.024.

Högström U. (1988).Non-dimensional wind and temperature profiles in the atmospheric surface layer: A re-evaluation.Boundary-Layer Meteorol.42, 55–78.

Hedayat, A., Davilu, H., Barfrosh, A. A., & Sepanloo, K. (2009). Estimation of research reactor core parameters using cascade feed forward artificial neural networks. Progress in Nuclear Energy, 51(6), 709-718

Hong, S.-Y., Dudhia, J., 2003. Testing of a new non-local boundary layer vertical diffusion scheme in numerical weather prediction applications. In: Proceedings of the 16th Conference on Numerical Weather Prediction, Seattle, WA.

Järvi L. & Grimmond C.S.B. (2010)SurfaceUrban Energy and Water Balance Scheme (SUEWS): New developments and evaluation. Manuscript in preparation.

Jiang, D., Zhang, Y., Hu, X., Zeng, Y., Tan, J., & Shao, D. (2004). Progress in developing an ANN model for air pollution index forecast. Atmospheric Environment, 38(40 SPEC.ISS.), 7055-7064

Kanda M., Kanega M., Kawai T., Moriwaki R. & Sugawara H. (2007). Roughness lengths for momentum and heat derived from outdoor urban scale models. J. Appl. Meteorol. Clim. 46, 1067-1079.

Kolokotroni, M., Davies, M., Croxford, B., Bhuiyan, S., & Mavrogianni, A. (2010). A validated methodology for the prediction of heating and cooling energy demand for buildings within the urban heat island: Case-study of london. Solar Energy, 84(12), 2246-2255.

Kusaka, H., H. Kondo, Y. Kikegawa, and F. Kimura, 2001: A simple single-layer urban canopy model for atmospheric models: Comparison with multi-layer and slab models. *Bound.-Layer Meteorol.*, 101, 329-358.

Kusaka, H. and F. Kimura, 2004: Coupling a single-layer urban canopy model with a simple atmospheric model: Impact on urban heat island simulation for an idealized case. *Journal of the Meteorological Society of Japan*, 82, 67-80.

Lin, Y.L., R. D. Farley, and H. D. Orville, 1983: Bulk parameterization of the snow field in a cloud model. J. Appl. Meteor., **22,** 1065-1092

Loridan T,CSB Grimmond, BD Offerle, DT Young, T Smith, L Jarvi, F Lindberg (2010). Local-Scale Urban Meteorological Parameterization Scheme (LUMPS): longwave radiation parameterization & seasonality related developmentsJournal of Applied Meteorology & Climatology. doi: 10.1175/2010JAMC2474.1

MacDonald R.W., Griffiths R.F. & Hall D.J. (1998). An improved method for estimation of surface roughness of obstacle arrays.Atmos. Env. 32, 1857-1864.

McCaughey J. H. (1985). Energy balance storage terms in a mature mized forest at Petawawa Ontario - a case study. Boundary-Layer Meteorol. 31, 89-101.

Maqsood, I., Khan, M.R., Abraham, A., (2004). An ensemble of neural networks for weather forecasting. Neural Computer Applications 13, 112–122

Meyn S. K. (2001). Heat fluxes through roofs and their relevance to estimates of urban heat storage. M. Sc. Thesis. Department of Earth and Ocean Sciences, The University of British Columbia, Vancouver.

Marras, S., Spano, D., Pyles, R.D, Falk, M., Snyder, R.L., Paw U, K.T., 2010. Application of the ACASA model in urban environments: two case studies. AMS Conference on Ninth Symposium on the Urban Environment, Keystone, Colorado, USA, August 2-6 2010

Marras, S., Pyles, R.D, Sirca, C., Paw U, K.T., Snyder, R.L., Duce, P., Spano, D., 2011. Evaluation of the Advanced Canopy-Atmosphere-Soil Algorithm (ACASA) model performance over Mediterranean maquis ecosystem. Agric. Forest Meteorol., 151: 730-745.

Meyers, T.P., and Paw U, K.T., 1986. Testing of a higher-order closure model for modelling airflow within and above plant canopies. Bound. Lay. Meteorol. 31, 297-311

Meyers, T.P., and Paw U, K.T., 1987. Modelling the plant canopy micrometeorology with higher-order closure principles. Agric. For. Meteorol. 41, 143-163

Mihalakakou, P., Flokas, H., Santamouris, M., Helmis, C., 2000. Application of Neural Networks to the simulation of the Heat Island over Athens, Greece using synoptic types as a predictor. J. Applied Meteorology 41, 519-527.

Mlawer, S.J. Taubman, P.D. Brown, M.J. Iacono and S.A. Clough, Radiative transfer for inhomogeneous atmospheres: RRTM, a validated correlated-k model for the longwave, J. Geophys. Res. **102** (D14) (1997), pp. 16663–16682

Narita K., Sekine T. &Tokuoka T. (1984). Thermal properties of urban surface materials – Study on heat balance at asphalt pavement. Geogr. Rev. Japan 57, 639-651.

Novak M. D. (1982). The moisture and thermal regimes of a bare soil in the Lower Fraser Valley during spring. Ph.D. Thesis, The University of British Columbia, Vancouver

Nunez M. (1974).The energy balance of an urban canyon. Ph.D. Thesis, The University of British Columbia, Vancouver

Offerle B., Grimmond C.S.B. & Oke T.R. (2003).Parameterization of Net All-Wave Radiation for Urban Areas.J. Appl. Meteorol. 42, 1157-1173.

Pyles, R.D., Weare, B.C., Paw U, K.T., 2000. The UCD Advanced Canopy-Atmosphere-Soil Algorithm: Comparison with observations from different climate and vegetation regimes. Q.J.R. Meteorol. Soc.,126: 2951-2980

Pyles, R.D., Weare, B.C., Paw U, K.T., Gustafson W., 2003. Coupling between the University of California, Davis, Advanced Canopy-Atmosphere-Soil Algorithm (ACASA) and MM5: Preliminary Results for July 1998 for Western –North America. J Appl. Meteorol. 42: 557-569

Ruano,A.E., Crispim, E.M., Conceicão, E.Z.E., Lúcio,M.M.J.R., (2006). Prediction of building's temperature using neural networks models. Energy Building 38, pp682–694.

Sailor DJ, Lu L (2004). A top-down methodology for developing diurnal and seasonal anthropogenic heating profiles for urban areas. *Atmospheric Environment* 38: 2737-2748. DOI: 10.1016/j.atmosenv.2004.01.034.

Santamouris, G. Mihalakakou, N. Papanikolaou and D. N. Assimakopoulos, 1999. A Neural Network Approach for Modelling the Heat Island Phenomenon in Urban Areas During the Summer Period Geophysics Research Letters, 26, 3, pp337-340.

Skamarock, W.C., Klemp, J.B. Dudhia, J., Gill, D.O., Barker, D.M., Duda, M.G., Huang, X.Y., Wang, W., Powers, J.G., 2008. A Description of the Advanced Research WRF Version 3. NCAR/TN–475 + STR - NCAR TECHNICAL NOTE

Souch C., Grimmond C. S. B. & Wolfe C. (1998). Evaporation rates for wetlands with different disturbance histories: Indiana Dunes National Lakeshore. Wetlands 18, 216-229.

Staudt, K., E.Falge, R.D.Pyles, K.T.PawU, and T.Foken, 2010. Sensitivity and predictive uncertainty of the ACASA model at a spruce forest site. Biogeosciences, 7, 3685-3705. www.biogeosciences.net/7/3685/2010/.

Song, Q. (2010). On the weight convergence of Elman networks. IEEE Transactions on Neural Networks, 21(3), 463-480.

Taesler R. (1980). Studies of the development and thermal structure of the urban boundary layer in Uppsala, Part I: Experimental program; and Part II: Data, analysis and results. Report 61, Met. Instit., Uppsala University, Uppsala.

Tasadduq I., Rehman S., Bubshait K., 2002. Application of neural networks for the prediction of hourly mean surface temperatures in Saudi Arabia. Renewable Energy 36, 545-554.

Van Ulden A.P. & Holtslag A.A.M. (1985).Estimation of atmospheric boundary layer parameters for boundary layer applications.J. Clim. Appl. Meteorol. 24, 1196-1207.

Voogt J.A & Grimmond C.S.B. (2000).Modeling surface sensible heat flux using surface radiative temperatures in a simple urban terrain.J. Appl. Meteorol. 39, 1679-1699.

Yap D. H. (1973). Sensible heat fluxes in and near Vancouver, BC. Ph.D. Thesis, The University of British Columbia, Vancouver.

Yi, J., & Prybutok, V. R. (1996). A neural network model forecasting for prediction of daily maximum ozone concentration in an industrialized urban area. Environmental Pollution, 92(3), 349-357

Yoshida A., Tominaga K. &Watatani S. (1990).Field measurements on energy balance of an urban canyon in the summer season. Energy and Buildings 15, 417-423.

Yoshida A., Tominaga K. &Watatani S. (1991).Field investigation on heat transfer in an urban canyon.Heat transfer – Japanese Research 20, 230-244

1.4 Project Overview

This overview is an introduction to the BRIDGE Project. Who is familiar with the Project can skip this section because its content is already known.

BRIDGE is a joint effort of 14 European Organizations aiming at incorporating sustainability aspects in urban planning, accounting for relations between **urban metabolism** and **urban structure**. BRIDGE also aims at devising of innovative **strategies** for urban planning in Europe.

BRIDGE will provide the means to close the gap between bio-physical sciences and urban planners and to illustrate the advantages of accounting for urban metabolism issues on a routine basis in design decisions. BRIDGE will focus on the following components of urban metabolism: **Energy**, **water**, **carbon and pollutants**. There are many challenges of the sustainable urban planning with regards to the above components (for example to optimize energy efficiency of urban structure, to minimize primary water consumption, to minimize the emissions to atmosphere, etc.)

BRIDGE will exploit the advances in bio-physical sciences to develop a Decision Support System (**DSS**) which will be used to support the decision making needed to achieve the above challenges by proposing quantitative measures and guidelines for sustainable use of energy and materials in urban planning. This DSS will reflect the multidimensionality nature of the urban metabolism, as operationalised in intelligible and transferable **indicators** easily understood by a non-scientific public. Decision making means selecting among **alternatives**. The development of this DSS will be based on an analytical and a design component linking the bio-physical processes with socio-economic parameters in order to estimate the environmental impacts of urban metabolism components and the potential socio-economic implications related to these impacts.

The fluxes of each of the above urban metabolism components will be measured and modeled in BRIDGE case studies, in order to calculate the net-fluxes into or out of the city environment. The measured and simulated datasets will be integrated in the DSS and the environmental impacts of the respective physical flows will be assessed. A cost-benefit analysis will be used to contras the environmental impacts against the cost of “fixing” such impacts.

Five European cities have been selected as BRIDGE **case studies**: **Helsinki**, Finland; **Athens**, Greece; **London**, United Kingdom; **Firenze**, Italy and **Gliwice**, Poland. In order to develop a method that will be welcomed by local governments, it is important to involve them in the project from the beginning. The project uses a **Community of Practice** (CoP) approach, which means that in the **case studies**, local stakeholders and scientists of the BRIDGE project meet on a regular basis in order to learn from each other. The CoP will make clear what aspects are important for the future users of the BRIDGE products. This approach will also be used to create an “umbrella” CoP across the participating cities to exchange ideas and experience of BRIDGE on a European level.

2 IMO-CMAQ. UPM MODELS

2.1 Brief description

Weather Research and Forecasting (WRF) model is designed as the next generation model after the PSU/NCAR-MM5 which has been described in the D4.1 “Model Selection Report”. WRF uses a high-order accurate discretization schemes for the time and space, with new microphysics schemes.

The WRF system is in the public domain and is freely available for community use. WRF was developed at the National Center for Atmospheric Research (NCAR) which is operated by the University Corporation for Atmospheric Research (UCAR). It is designed to be a flexible, state-of-the-art atmospheric simulation system that is portable and efficient on available parallel computing platforms. WRF is suitable for use in a broad range of applications across scales ranging from meters to thousands of kilometres.

UPM has used the WRF ARW solver, which will be described. The equation set for ARW is fully compressible, Eulerian and nonhydrostatic with a run-time hydrostatic option. It is conservative for scalar variables. The model uses terrain-following, hydrostatic-pressure vertical coordinate with the top of the model being a constant pressure surface. The horizontal grid is the Arakawa-C grid. The time integration scheme in the model uses the third-order Runge-Kutta scheme, and the spatial discrimination employs 2nd to 6th order schemes.

The model supports both idealized and real-data applications with various lateral boundary condition options. The model also supports one-way, two-way and moving nest options. It runs on single-processor, shared- and distributed-memory computers. The Figure 1 illustrates the component programs of the WRF Modeling System.

In order to better represent the physical processes involved in the exchange of heat, momentum, and water vapour in urban environment in mesoscale model, an UCM (Urban Canopy Model) is coupled to the WRF model. The main purpose of the coupled model is to improve the description of lower boundary conditions and to provide more accurate forecasts for urban regions. The UCM is a single layer model which has a simplified urban geometry. Some of the features of the UCM include, shadowing from buildings, reflection of short and long wave radiation, wind profile in the canopy layer and multi-layer heat transfer equation for roof, wall and road surfaces. More information about UCM can be found in D4.1 Model Selection Report (2.3). We have used the WRF 3.1 version

The Community Multi-scale Air Quality (CMAQ) modelling system has been designed to approach air quality as a whole by including state-of-the-science capabilities for modelling multiple air quality issues, including tropospheric ozone, fine particles, toxics, acid deposition, and visibility degradation. In this way, the development of CMAQ involves the scientific ... expertise from each of these areas and combines the capabilities to enable a community modelling practice. CMAQ was also designed to have multi-scale capabilities so that separate models were not needed for urban and regional scale air quality modelling. With the model's ability to handle a large range of spatial scales, CMAQ can be used for urban and regional scale model simulations. By making CMAQ a modelling system that addresses multiple pollutants and different spatial scales, CMAQ has a "one atmosphere" perspective that combines the efforts of the scientific community

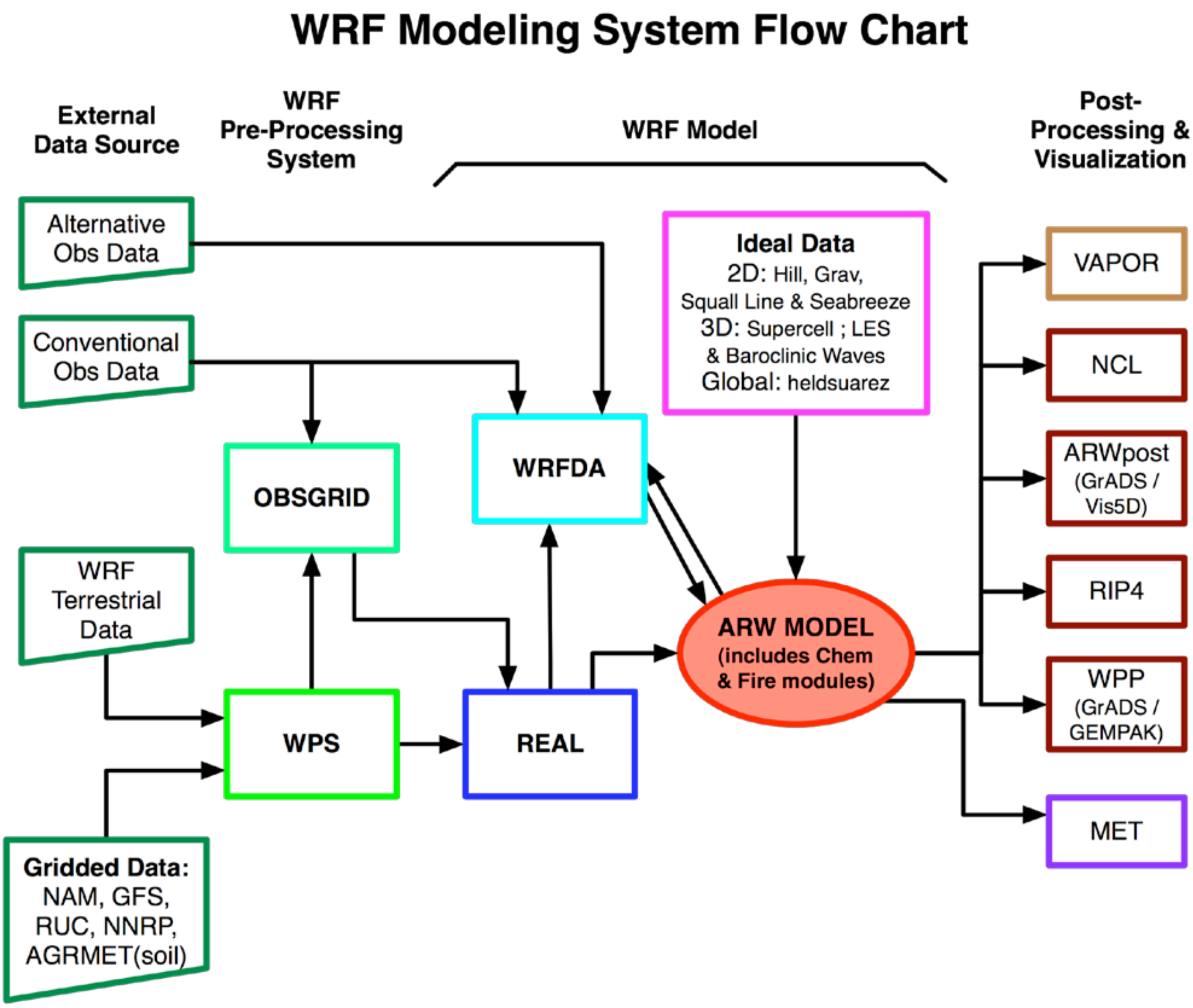

Figure 1: Flow chart and component programs of the WRF Modeling System

To implement multi-scale capabilities in CMAQ, several issues, such as scalable atmospheric dynamics and generalized coordinates, which depend on the desired model resolution, are addressed. Meteorological models may assume hydrostatic conditions for large regional scales, where the atmosphere is assumed to have a balance of vertical pressure and gravitational forces with no net vertical acceleration on larger scales. However, on smaller scales such as urban scales, this assumption cannot be made.

A set of governing equations for compressible non-hydrostatic atmospheres is available to better resolve atmospheric dynamics at smaller scales. These non-hydrostatic equations are more appropriate for finer regional scale and urban scale meteorology. Because CMAQ is designed to handle scale dependent meteorological formulations and a large amount of flexibility, CMAQ's governing equations are expressed in a generalized coordinate system. This approach ensures consistency between CMAQ and the meteorological modeling system.

The generalized coordinate system determines the necessary grid and coordinates transformations, and it can accommodate various vertical coordinates and map projections. The CMAQ modeling system simulates various chemical and physical processes that are thought to be important for understanding atmospheric trace gas transformations and distributions. More information about CMAQ can be found in D4.1 Model Selection Report (4.1.1.2). We have used the CMAQ 4.6 version

An off-line linkage between WRF and CMAQ has been implemented through the MCIP interface processor, the similar way that the MM5-CMAQ coupling described in the D4.1 Model Selection Report (4.1.1.2).

Anthropogenic Green House Emissions (GHG), are calculated using EMIMO (UPM) model, using 5 minutes resolution, hourly CO2 & CH4 emission inventory from Institute of Economics and the Rational of Energy (IER), University of Stuttgart. Figure 2

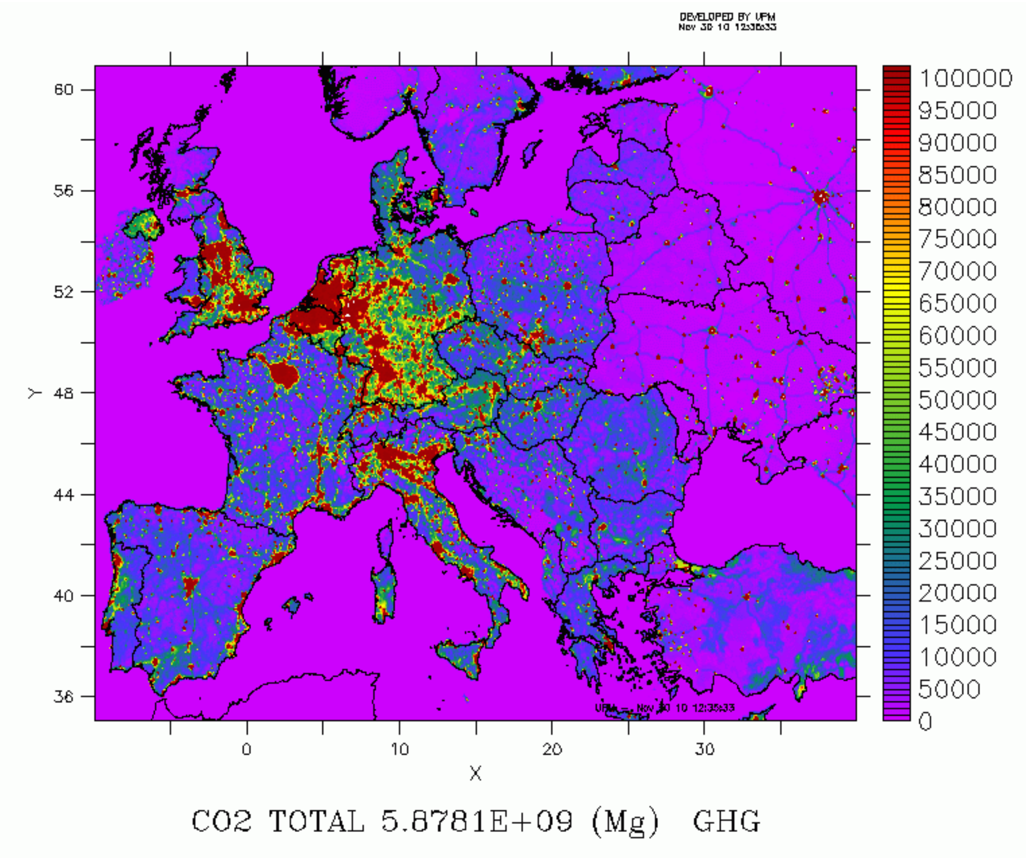

Figure 2: Annual CO2 anthropogenic emission over Europe. IER emission inventory

To produce biosphere CO2 emissions, we have implemented the Vegetation Photosynthesis and Respiration model (VPRM). VPRM takes into an account the CO2 uptabke by photosynthesis and the CO2 emission by respiration.

VPRM is linked with the WRF/UCM model. VPRM uses air temperature at 2 meters and downward short wave radiation at ground surface as input. In addition VPRM uses Land Surface Water Index (LSWI) and Enhanced Vegetation Index (EVI) from MODIS satellite data.

VPRM calculates hourly Net Ecosystem Exchange as a sum of Gross Ecosystem exchange and Respiration. The results can be positive (emission) or negative (deposition), for example Figure 3.

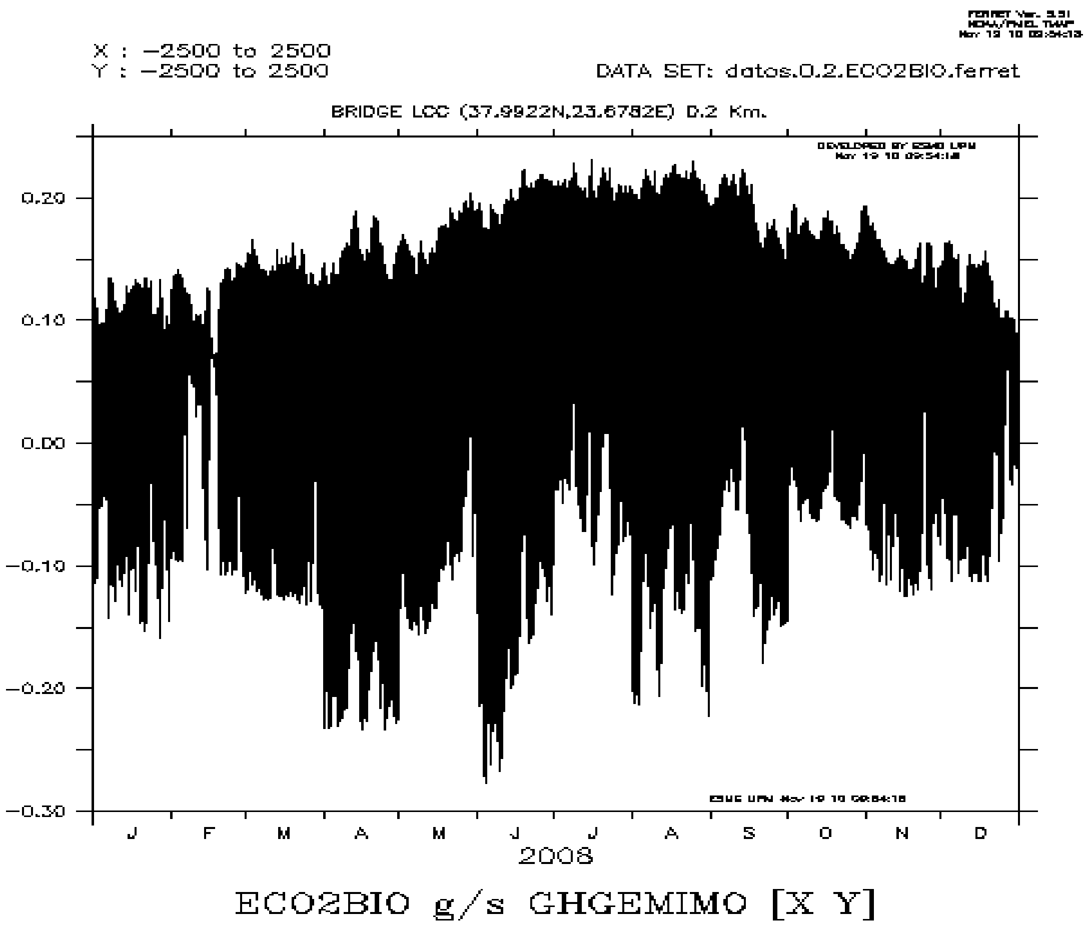

Figure 3: Net Ecosystem Exchange of CO2 for ATHENS spatial average (g/s)

2.2 Architecture and domains

The implemented models have been run over 5 European cities, Athens, Firenze, Helsinki, Gliwice and London, Figure 4 . WRF/UCM has been implemented for all cities and CMAQ to Athens and Firenze. The chemical results over the rest of the cities are provided by the CAMx model run by UAVR.

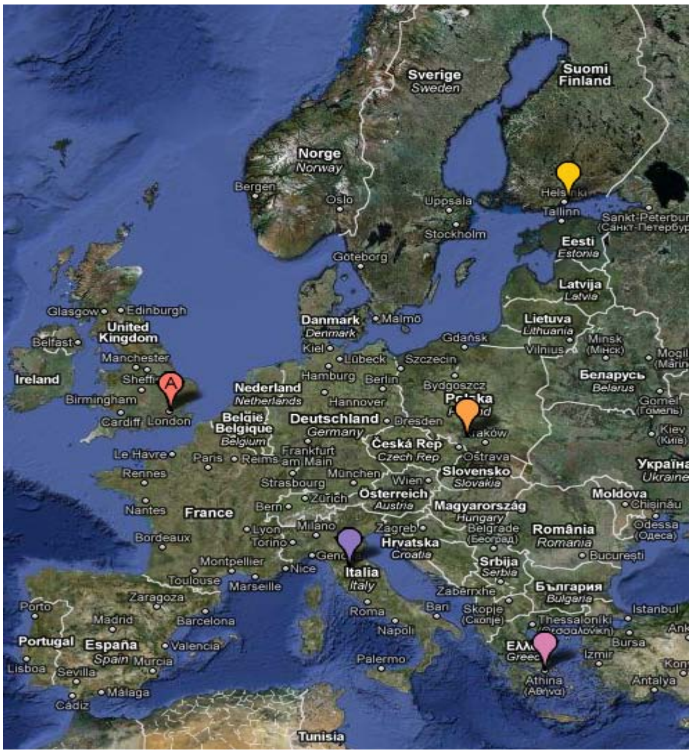

Figure 4: Bridge European Cities

Two domains have been set, Figure 5 First level: 37*37 grid cells, 5.4 km. grid resolution with the lower left corner located at coordinates x =-121500 m. and y = -121500 m. And the second level: 28*28 grid cells, 0.2 km. grid resolution with the lower left corner located at coordinates x =-2700 and y = -2700. WRF/UCM-CMAQ is run using the Lambert Conformal Conic projection. Chemical simulations have to be run with one grid cell less by each side, to make the coupling of the WRF and CMAQ domains. So the chemical domains are 34 by 34 grid cells at level 1 and 25 by 25 grid cells at the second level. The first level is used to supply boundary conditions to the second level chemical simulations.

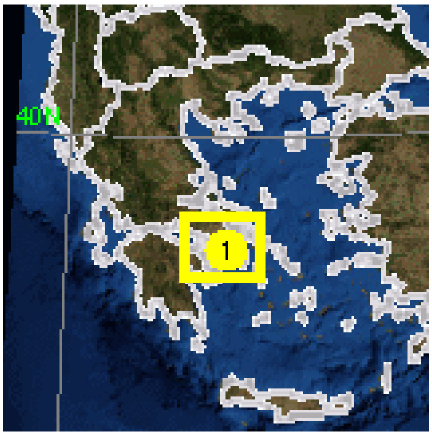

Figure 5: Example of the level 1 and 2. Athens domains

We run the WRF model using the initial and boundary conditions from the global model GFS (Global Forecast System). The data are on 1.0x1.0 degree grids, every 6 hours. They are available on the surface, at 26 mandatory (and other pressure) levels from 1000mb to 10mb, in the surface boundary layer and at some sigma layers, the tropopause and a few others. Parameters include surface pressure, sea level pressure, geopotential height, temperature, sea surface temperature, soil values, ice cover, relative humidity, u- and v- winds, vertical motion, vorticity and ozone.

2.3 Setup and configuration

We have implemented the following configuration in WRF:

Cumulus parameterization: Grell 3D ensamble scheme [Grell et al. 2002]. Scheme for higher resolution domains allowing for subsidence in neighbouring columns.

PBL scheme and diffusion: Yonsei Universtiy (YSU) PBL [Hong et al. 2003]. Non-local-K scheme with explicit entrainment layer and parabolic K profile in unstable mixed layer. The YSU PBL scheme is a first order nonlocal scheme, with a counter gradient term in the eddy-diffusion equation. YSU scheme is dependent upon the bulk Richardson number.

Explicit moisture scheme: Lin et al. Scheme microphysics [Lin et al, 1983]. In this scheme six classes of hydrometeors are included: Water vapour, cloud water, rain, cloud ice, snow, and graupel. suitable for real-data high-resolution simulations.

Radiation schemes: Rapid radiative transfer model (RRTM) longwave radiation [Mlawer et al. 1997]. This RRTM, which is taken from MM5, is a spectral-band scheme using the correlated-k method. It uses pre-set tables to accurately represent longwave processes due to water vapour, ozone, CO2, and trace gases (if present) as well as accounting for cloud optical depth. An accurate scheme using look-up tables for efficiency. Accounts for multiple bands, trace gases, and microphysics species

Simple cloud-interactive shortwave radiation scheme Dudhia radiation [Dudhia , 1989]. Simple downward integration allowing efficiently for clouds and clear-sky absorption and scattering. It uses look-up tables for clouds

Land surface model: Noah/UCM [Chen et al. 2004]. Unified NCEP/NCAR/AFWA scheme with soil temperature and moisture in four layers, fractional snow cover and frozen soil physics. Included UCM option with surface effects for roofs, walls, and streets.

2.4 Input data preprocessing.

To run the models it is necessary to generate several type of input data (D4.1 Input data), each supplied by different sources. Some of them, like emissivity and albedo have been generated uniformly for the 5 BRIDGE cities, while others such as topography, and land uses, had to be treated individually for each city, because the original data source are different by each city.

2.4.1 Emissivity

Emissivity data have been provided by FORTH. Data are images which are in geotiff format and they are got from the MODIS satellite. One image each 16 days (summer 2008), with an area of 65 km2, and 1 km of spatial resolution. The original data have been preprocessed to be ready to run the model. The following operations have been implemented:

- Projection transformation from Geographic coordinates to Lambert Conformal Conic, which is used by de models.
- Resample of the raster data from 1km to 200 meters.
- Selection of the model domain area.
- Average values by each model grid cell to avoid no data values by clouds.

In the Figure 6 we show the emissivity map for Firenze, with different values of emissivity for different land uses.

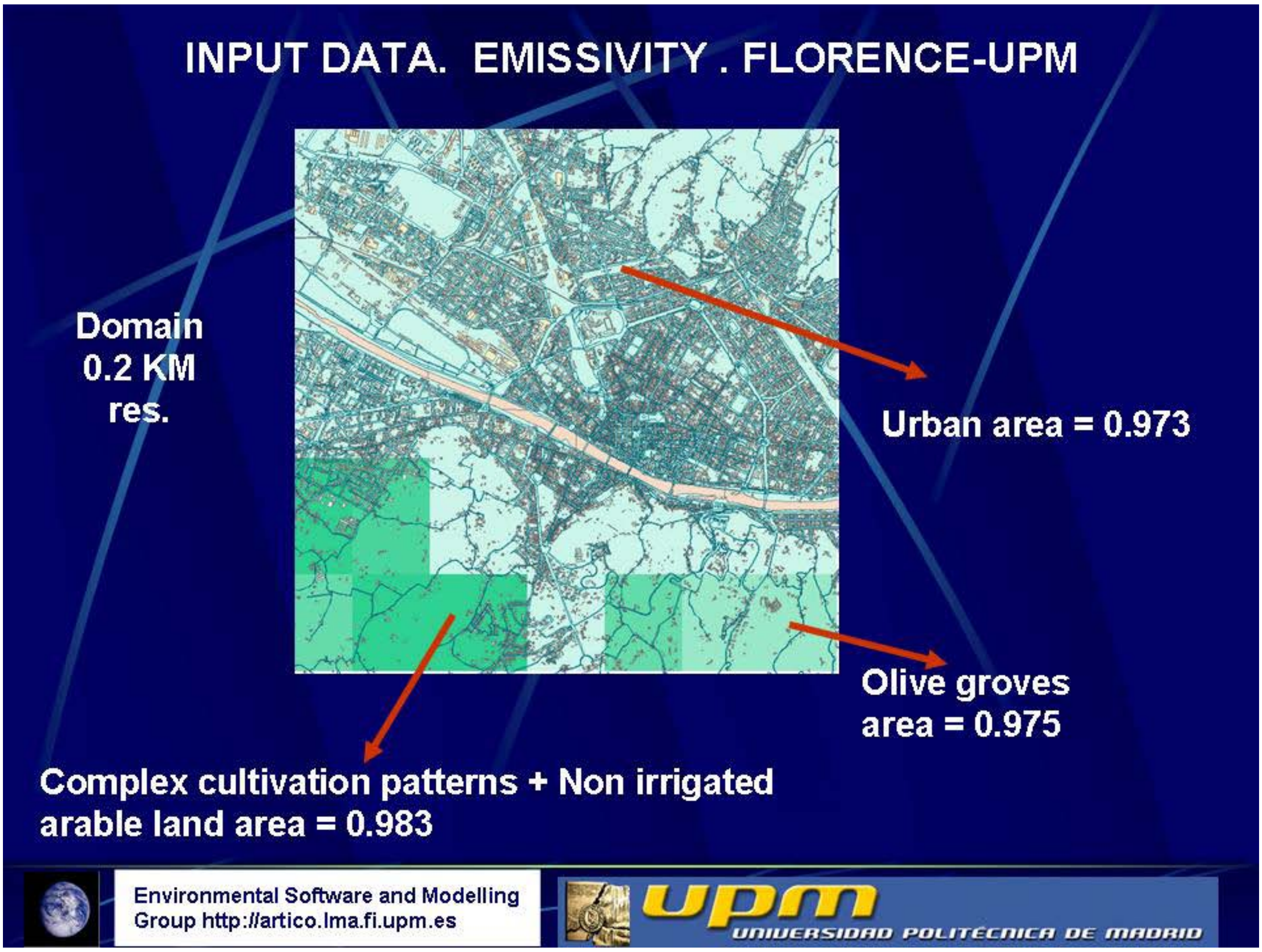

Figure 6: Emissivity map for Firenze

2.4.2 Albedo

Albedo data have been provided by FORTH. Data are images which are in geotiff format and they are got from the MODIS satellite. One image each 16 days (summer 2008), with an area of

extension of 65 km2, and 1 km of spatial resolution. The data are available for 3 fixed AOT (Aerosol Optimal Thickness) values (0.1, 0.5, 0.9) . If no more information is available to fix de best AOT value, we use as default value 0.5 Albedo data change with the solar zenith angle, one data is available by each ten degrees (0º, 10º,…,90º).

The original data have been preprocessed to be ready to run the model the same way to the emissivity data. In the Figure 7 we show the albedo map for Firenze, with different values of albedo for different land uses.

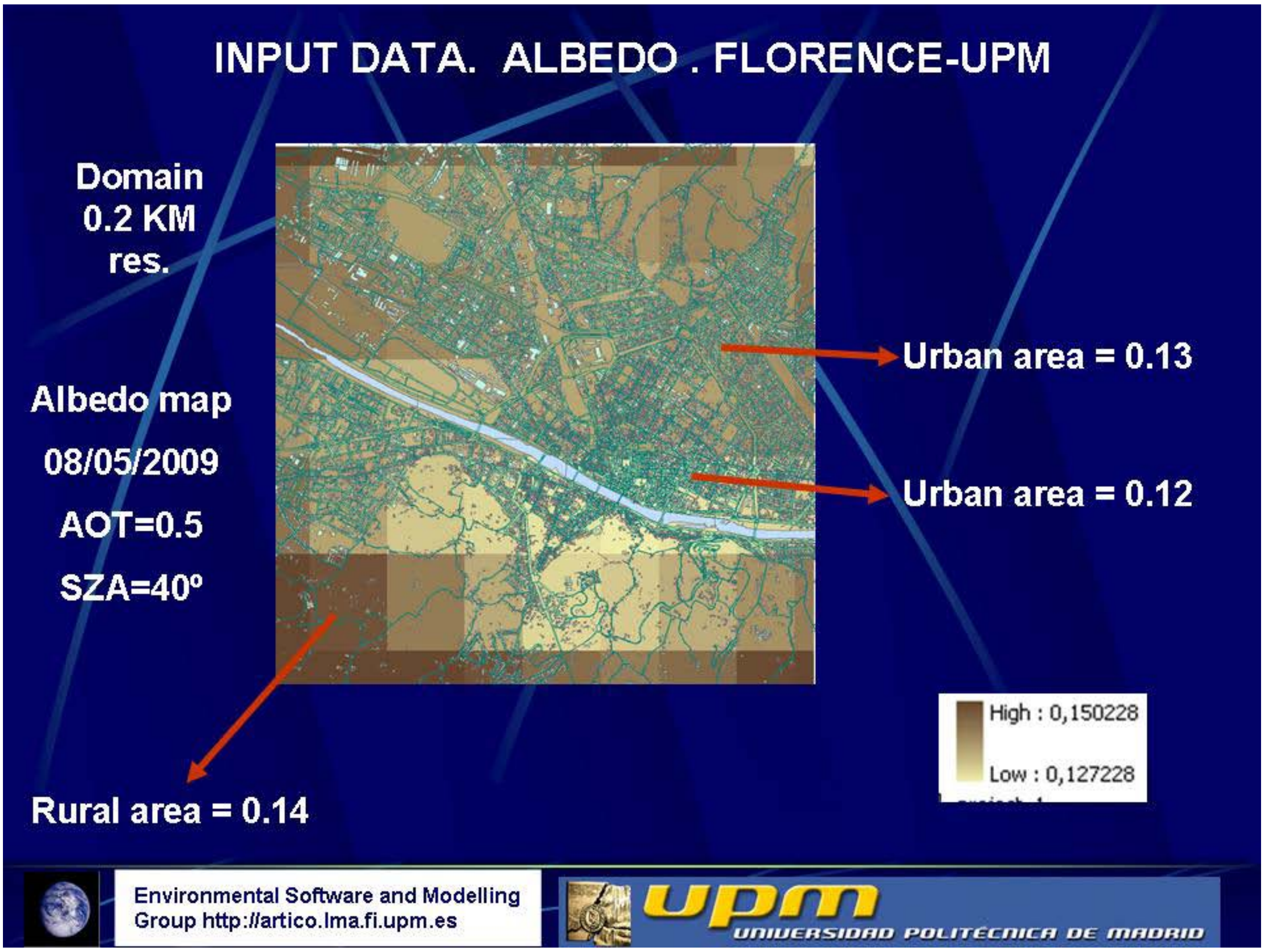

Figure 7: Albedo map for Firenze

In order to get hourly values the following formula can be applied:

$$ALB\_h = (WSA*0.001)*C + (BSA*0.001)*(1-C)$$

C is a factor fixed from a lookup table, there are 2 tables one for continental areas and other for marine areas. The value is defined by a solar zenith angle (SZA) and AOT. The radiation scheme included in the WRF calculates the SZA value each hour.

BSA (Black Sky Albedo value) and WSA (White sky Albedo value) are data supply in the Albedo images from MODIS. The Figure 8 , show hourly values of albedo for 4 different values of AOT, calculated to the Firenze city.

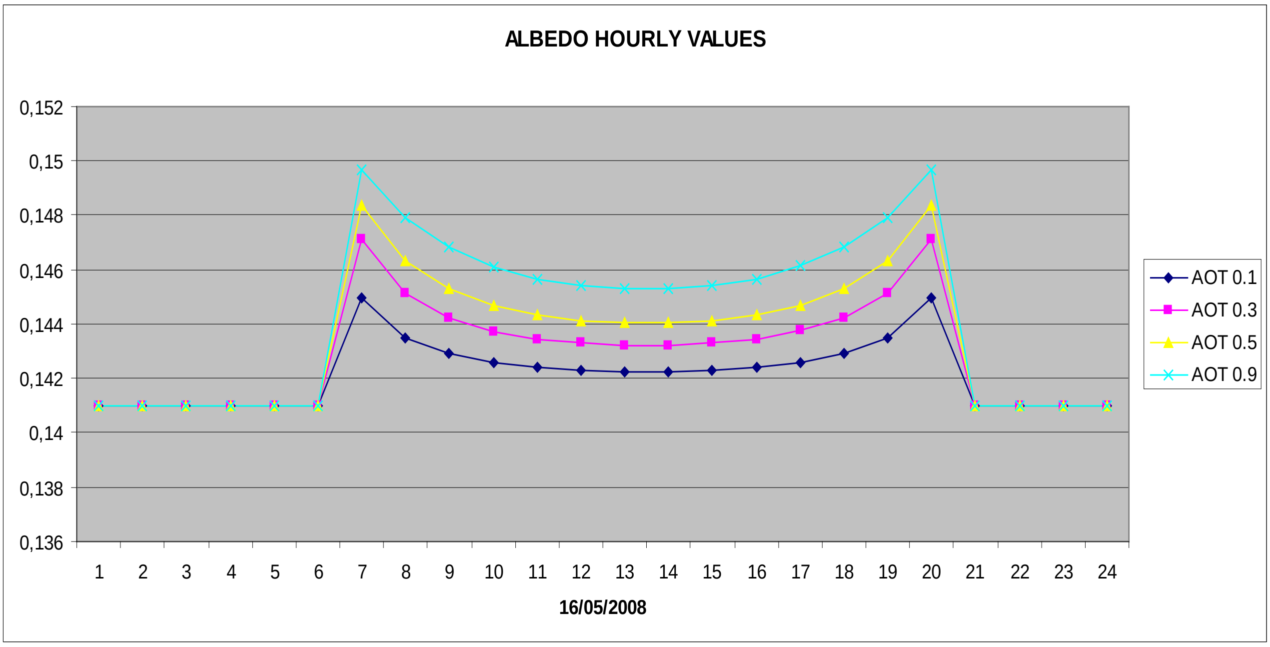

Figure 8: Albedo hourly values for different AOT values

2.4.3 Land uses

Corine Land Cover (CLC 200) raster data with 100 meters of resolution are used by default. These data are improved with the supplied information by the city authorities.

The *Corine Land Cover* is referring to a European programme establishing a computerized inventory on land cover of the 27 EC member states and other European countries, at an original scale of 1: 100 000, using 44 classes of the 3-level Corine nomenclature.

It is produced by the European Environment Agency (EEA) and its member countries and is based on the results of IMAGE2000, a satellite imaging programme undertaken jointly by the Joint Research Centre of the European Commission and the EEA Figure 10

The CLC classification is different that the USGS/UCM used in WRF/UCM-CMAQ models, described in D4.1 “Model Selection Report”. So we need translate CLC land uses to USG-UCM classification. The following correspondences have been implemented:

Indust. or commercial units (clc) → Com/Indust/Transport urban (usgs/ucm)
Discontinuous urban frabic (clc) → Low density urban (usgs/ucm)
Continuous urban frabic (clc) → High density urban (usgs/ucm)

Sport and leisure facilites (clc) → Com/Indust/Transport urban (usgs/ucm)
Road/Rail network (clc) → Com/Indust/Transport urban (usgs/ucm)

Green urban area (clc) → Grassland (usgs/ucm)
Olive groves (clc) → Deciduous broadleaf forest (usgs/ucm)Non-
Irrigated arable land (clc) → Dryland cropland/pasture (usgs/ucm)
Complex cultivation patterns (clc) → Mixed cropland/pasture (usgs/ucm)
Transitional woodland-shrub (clc) → Mixed shrubland/grassland (usgs/ucm)
Forest (clc) → Mixed forest (usgs/ucm)
Water courses (clc) → Water bodies (usgs/ucm)

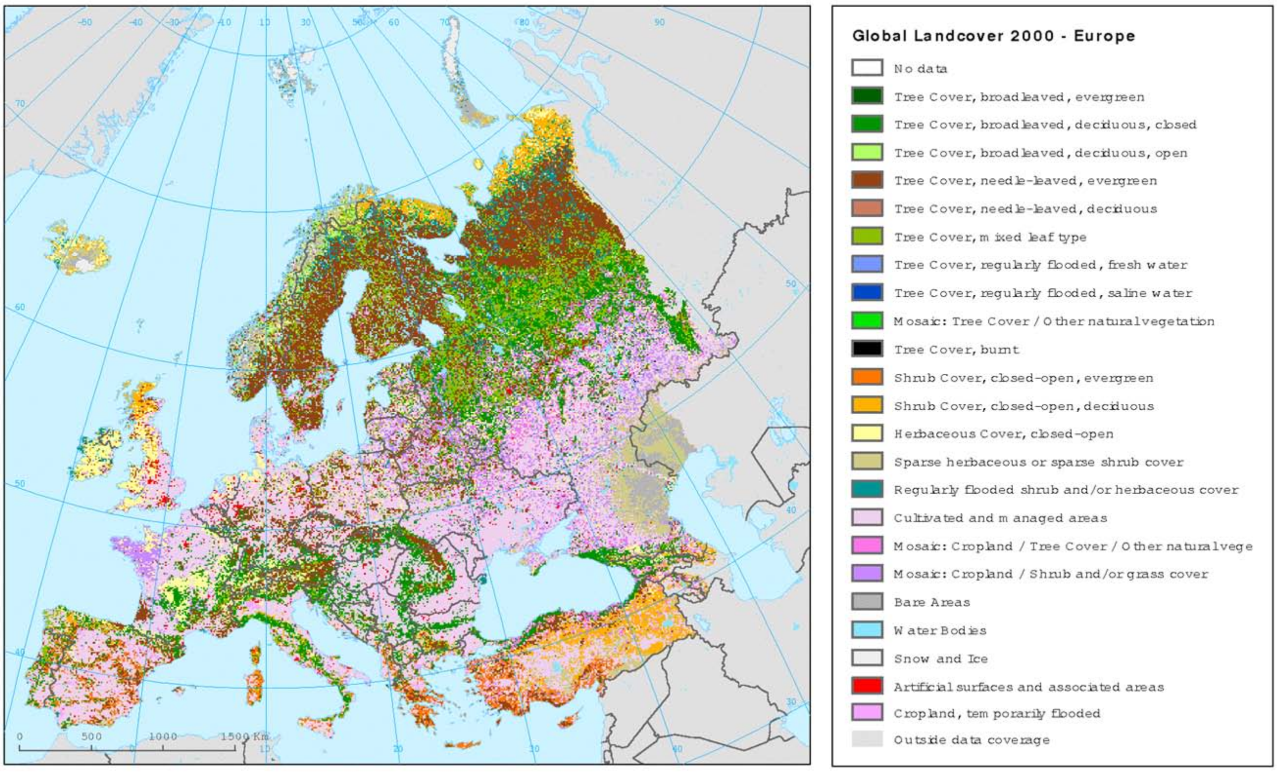

Figure 9: Europe land use data CLC 2000

In Firenze the city authorities have send several layers of information about land uses. The most useful were roads, water and gardens. The Figure 10 shows the land use data for Firenze city.

In Helsinki the information about land use was very completed. So it was not necessary to use the CLC data. The Helsinki classification (user) is different that the USGS/UCM used in WRF/UCM-CMAQ models, described in D4.1 “Model Selection Report”. So we need translate CLC land uses to USG-UCM classification (usgs/ucm). The following correspondences have been implemented

Detached houses (user) → Low density urban (usgs/ucm)
Block house areas (user) → High density urban (usgs/ucm)
Holiday resorts (user) → Low density urban (usgs/ucm)

Sea areas (user) → Water bodies (usgs/ucm)
Road transportation area (user) → Com/Indust/Transport urban (usgs/ucm)
Row and attached small houses (user) → Low density urban (usgs/ucm)
Forest (user) → Mixed forest (usgs/ucm)

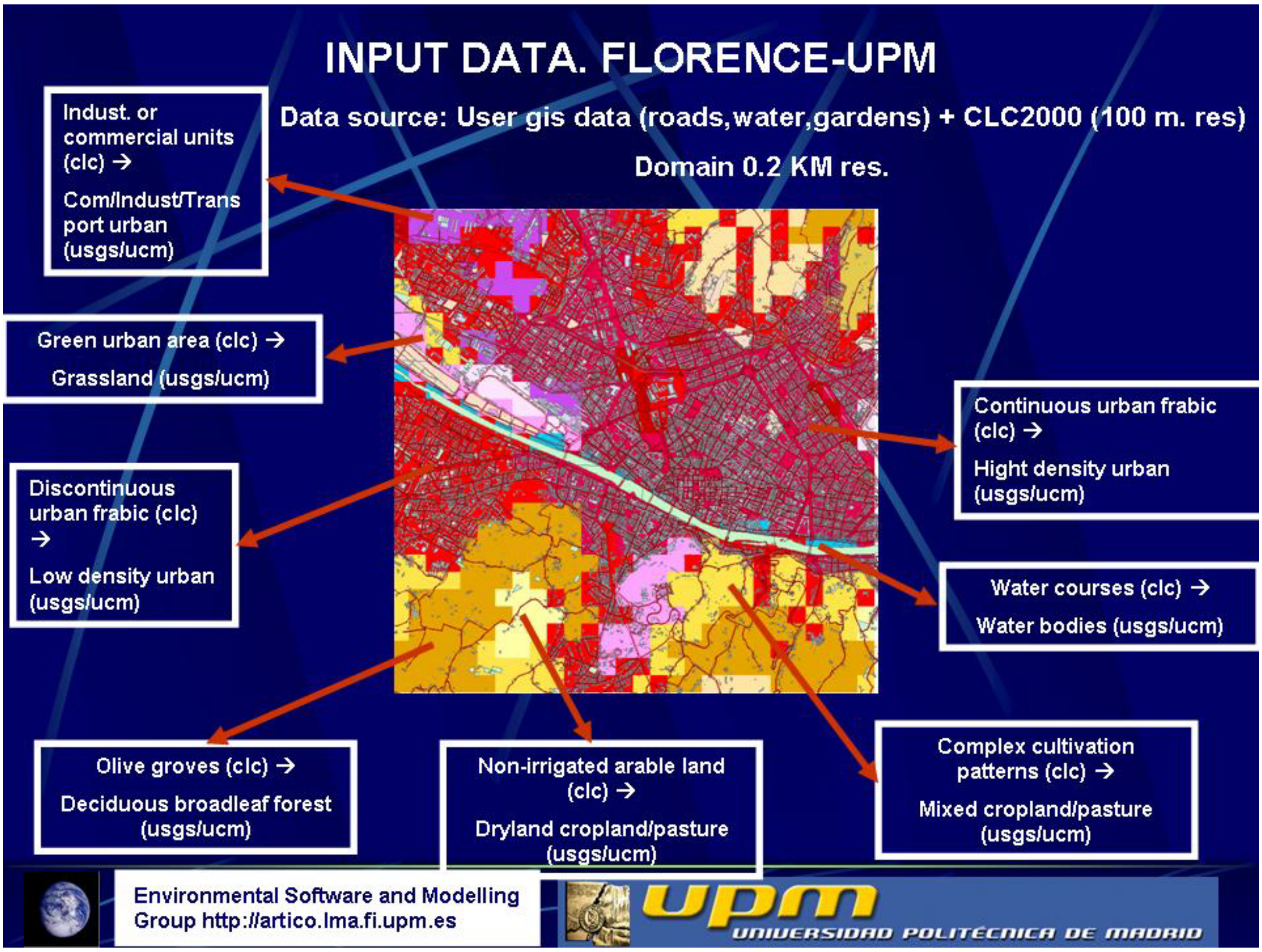

Figure 10: Land use data for Firenze

The Figure 11 shows the land use data for Helsinki city.

In Athens we received land use data for Greece following the CLC classification, so we need only to translate CLC categories to USGS/UCM categories, following the rules described at the beginning of the document. The Figure 12 shows the land use data for Athens city.

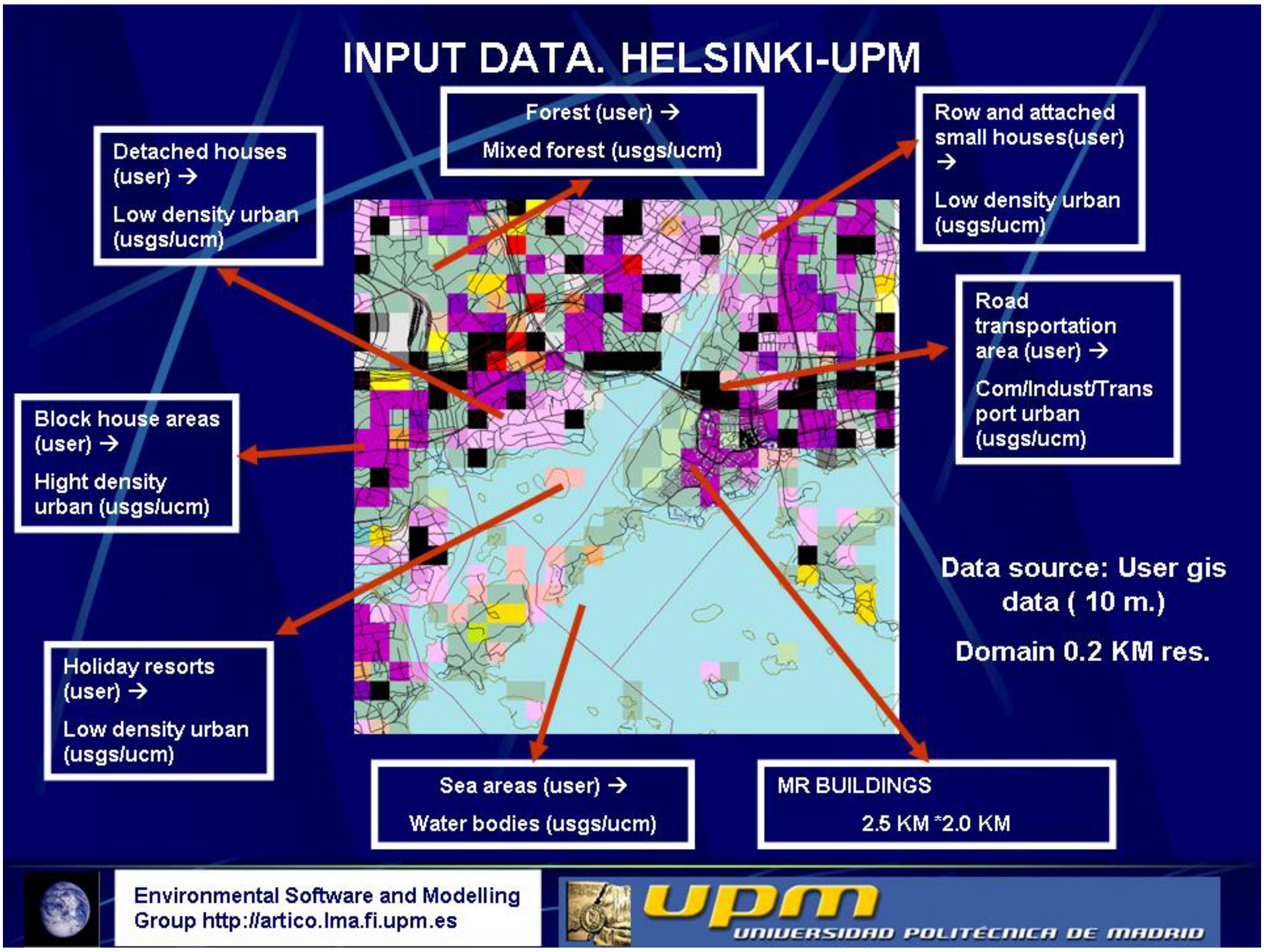

Figure 11: Land use data for Helsinki

In Gliwice we received land use data for Poland following the CLC classification, so we need only to translate CLC categories to USGS/UCM categories, following the rules described at the beginning of the document. The

Figure *13* shows the land use data for Gliwice city.

In London we only have CLC land use data, so we need only to translate CLC categories to USGS/UCM categories, following the rules described at the beginning of the document. The Figure 14 shows the land use data for London city.

2.4.4 Topography

Aster GDEM raster data with 30 meters of resolution are used by default. These data are improved with the supplied information by the city authorities.

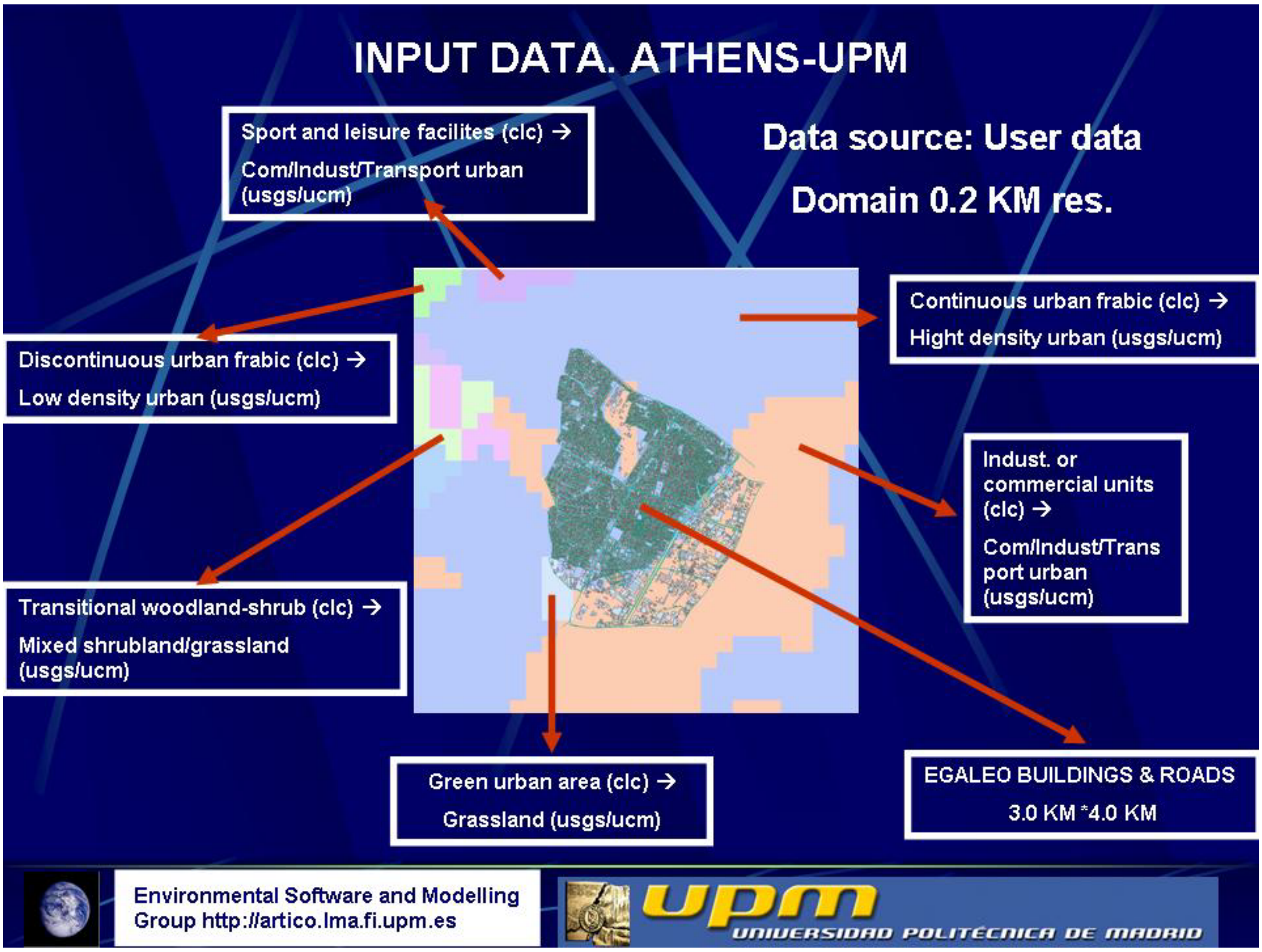

Figure 12: : Land use data for Athens

Aster GDEM is an easy-to-use, highly accurate DEM covering all the land on earth, and available to all users regardless of size or location of their target areas. ASTER GDEM was produced using ASTER data acquired from the start of observation to the end of August, 2008 in cooperation with the Japan-US ASTER Science Team. The coordinate system has reverted to latitude and longitude from the UTM system used for ASTER data previously. Figure 15

In Firenze the city authorities have send topographic information through the point vector file. This information has been combined with ASTER GDEM data and produced the final topography map. The Figure 16 shows the topography data for Firenze city.

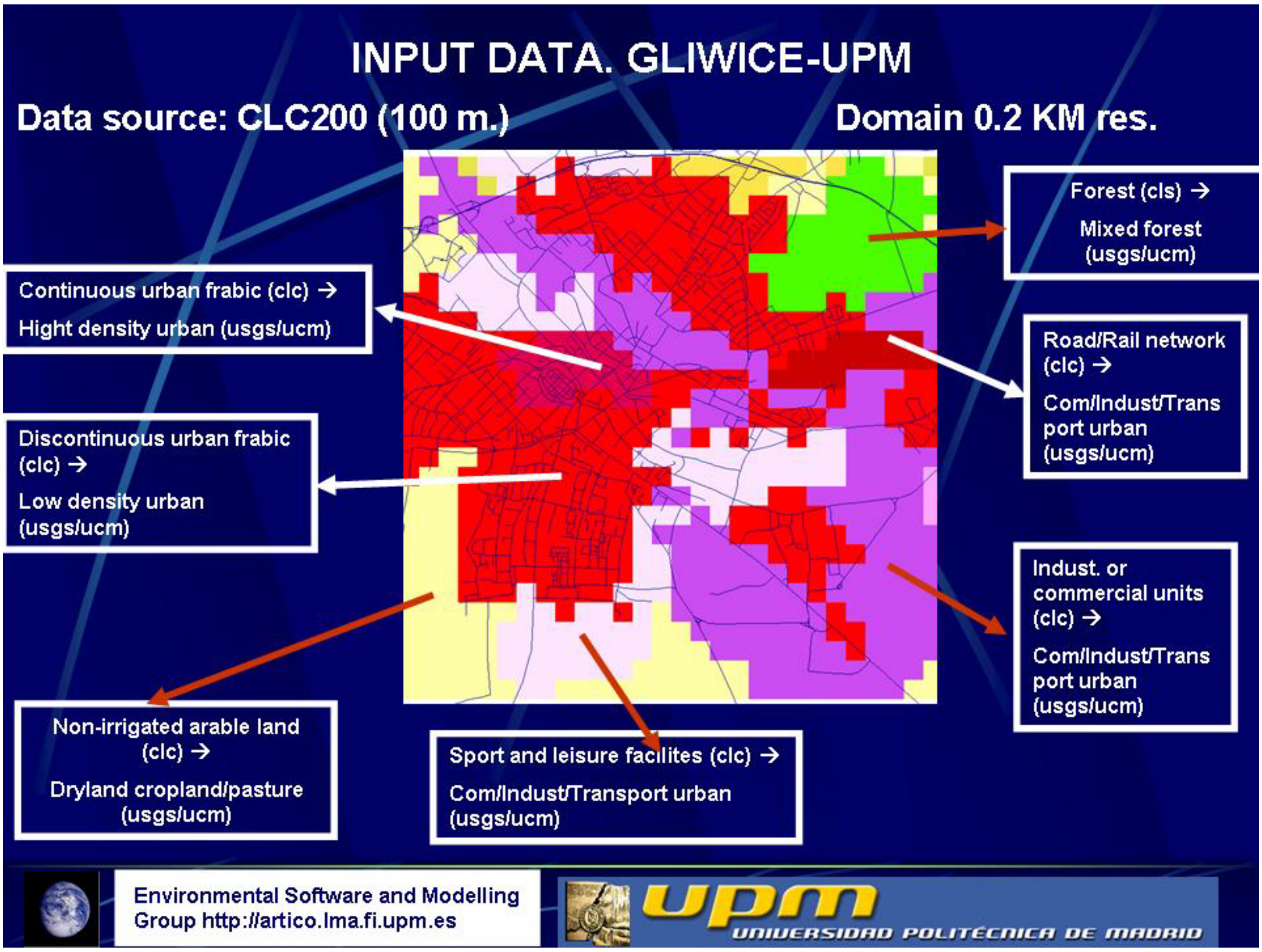

Figure 13: Land use data for Gliwice

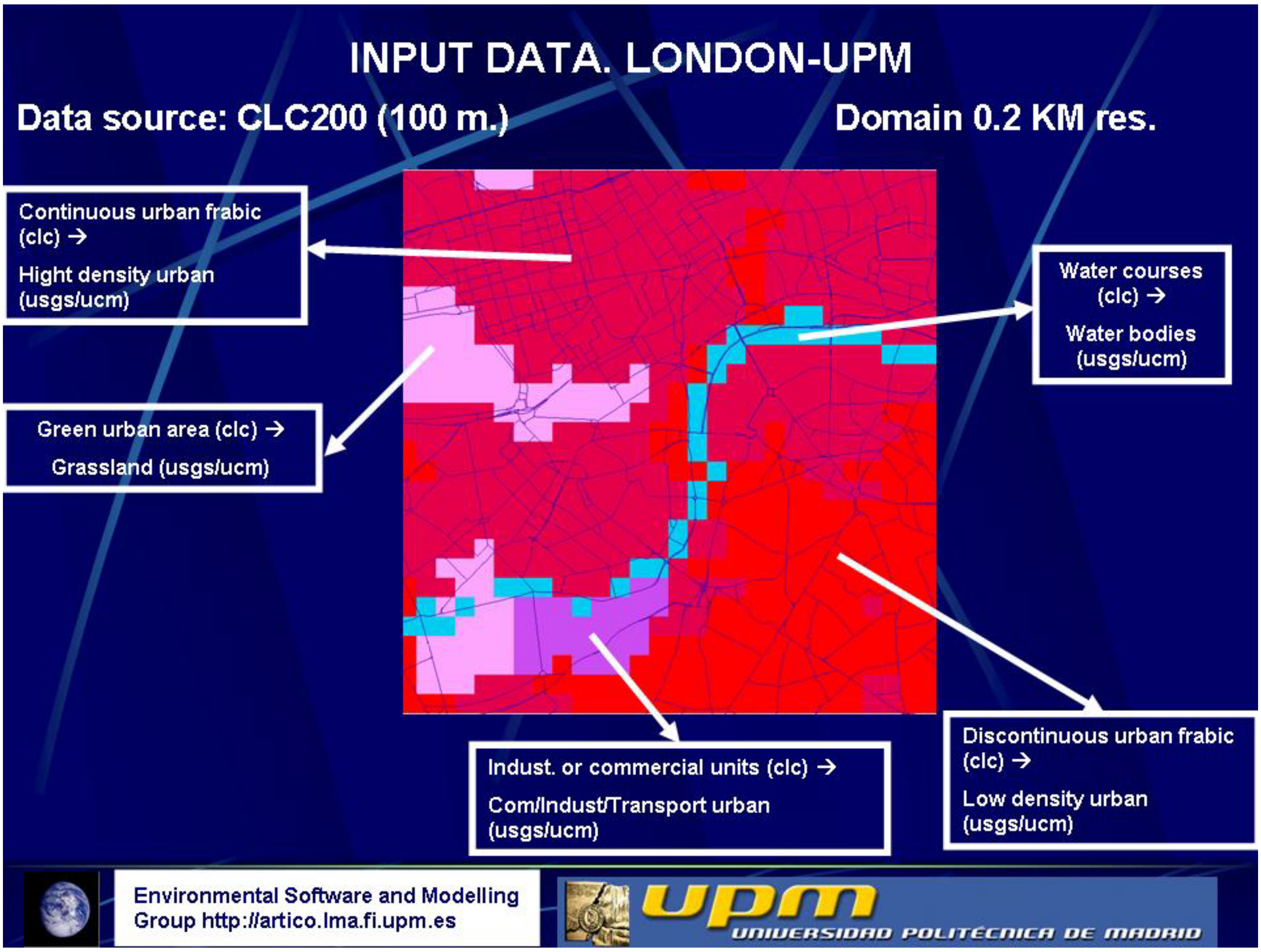

Figure 14: Land use data for London

Figure 15: European topography ASTER GDEM 30s resolution

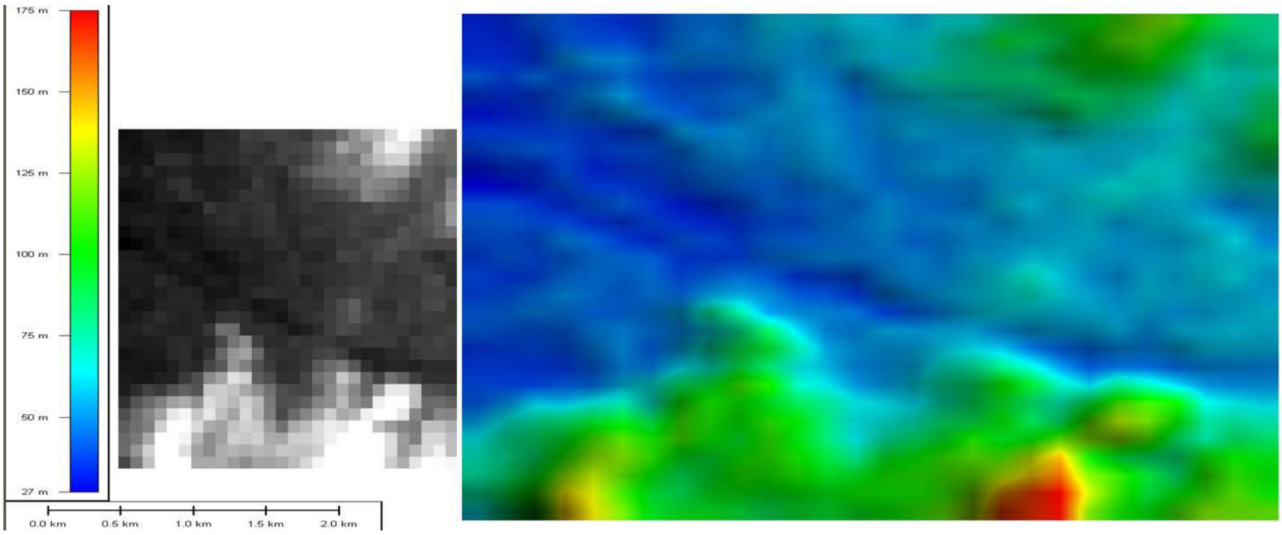

Figure 16: Firenze topography

In Helsinki the information about topography was very rich, Terrain height was received as contours with enough spatial resolution. So it was not necessary to use the ASTER GDEM data. The Figure 17 shows the topography data for Helsinki city.

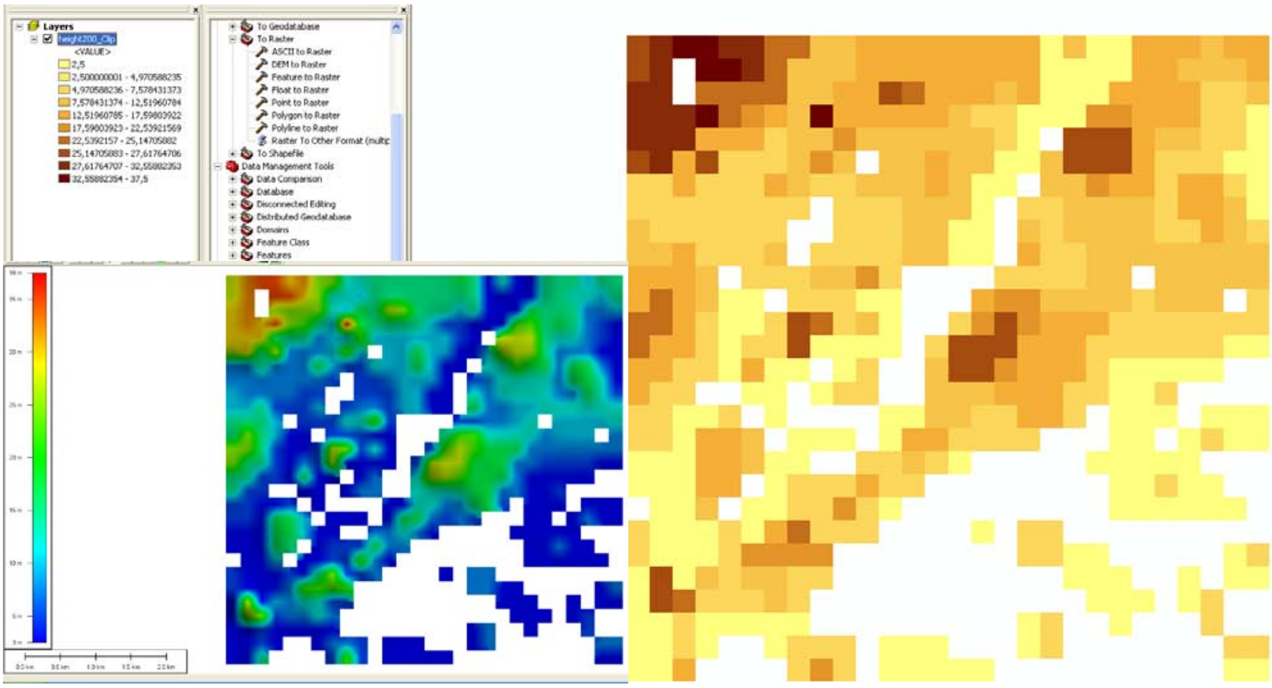

Figure 17: Helsinki topography

In Athens the only information about topography available is from ASTER GDEM. The Figure 18 shows the topography data for Athens city.

In Gliwice the only information about topography available is from ASTER GDEM. The Figure 19 shows the topography data for Gliwice city.

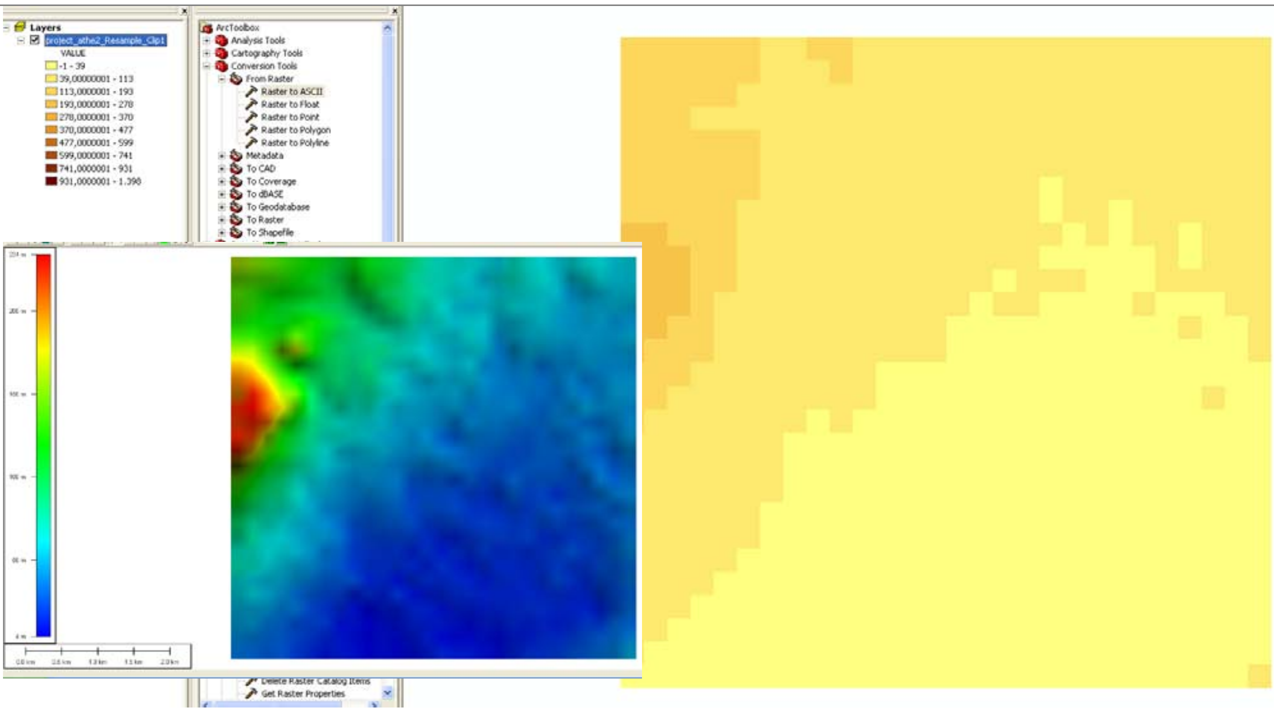

Figure 18: Athens topography

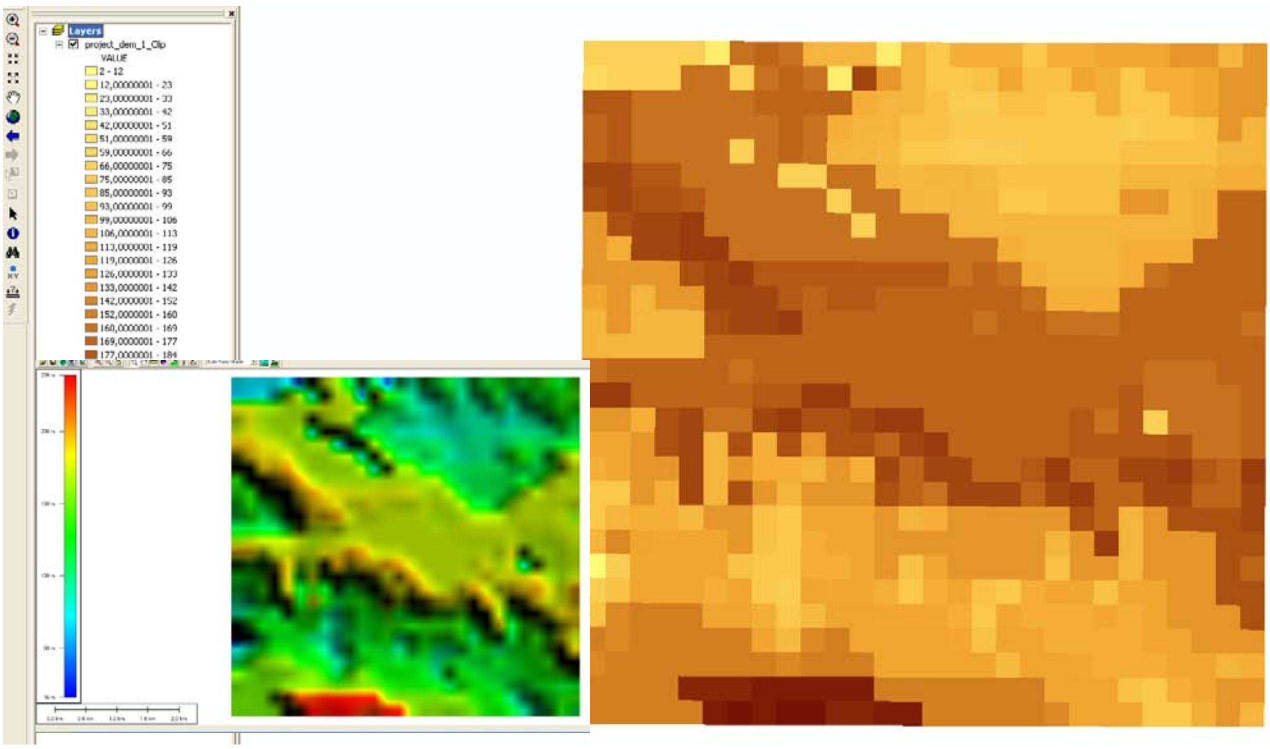

Figure 19: Gliwice topography

2.4.5 Emissions

EMIMO emission model developed by UPM uses a top down approach to estimate emissions, including traffic emissions. Some spatial surrogates, such as population, building density, roads, land use, are used to allocate macro-scale emissions to grid cells as required by the air quality model as CMAQ (Cook et al. 2006)

In BRIDGE, the grid based emission inventory for urban areas have been established using traffic flow to transport snap activities and land uses plus building density to the rest of snap activities.

Cities authorities have sent information about traffic flow at some measurement points of the city. Krigging interpolation procedure is applied to estimate the traffic flow in each grid for Firenze (Figure 20) and Athens (Figure 21), according to the streets distributions.

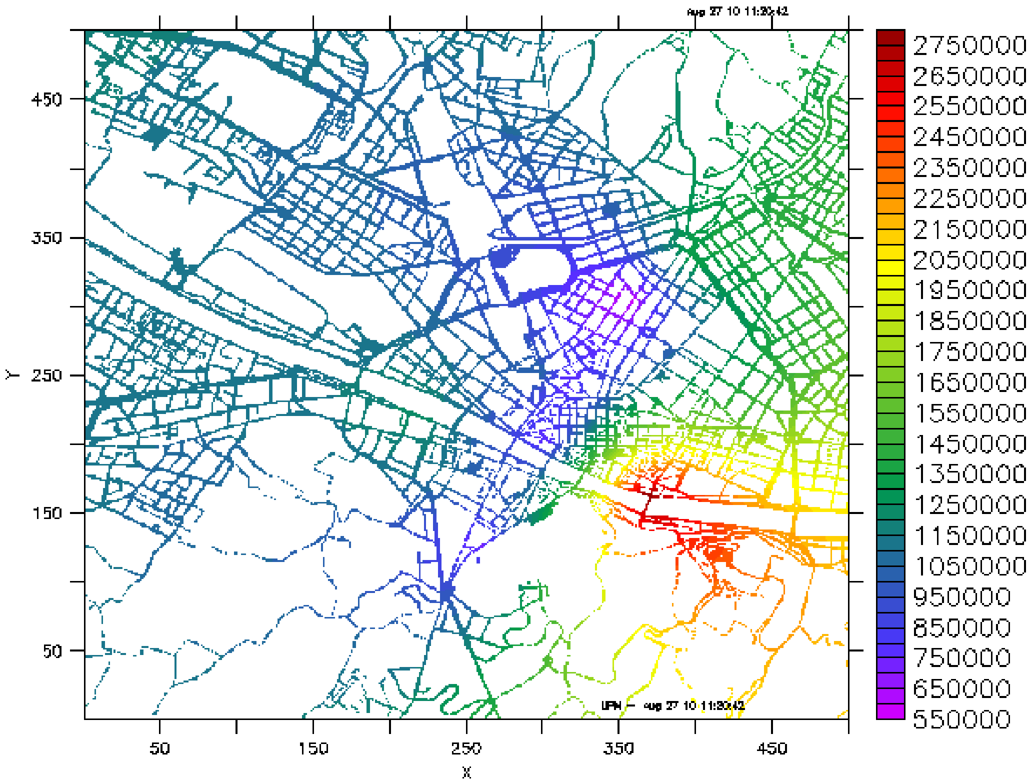

Figure 20: Firenze Vehicles/year. Krigging interpoloation results

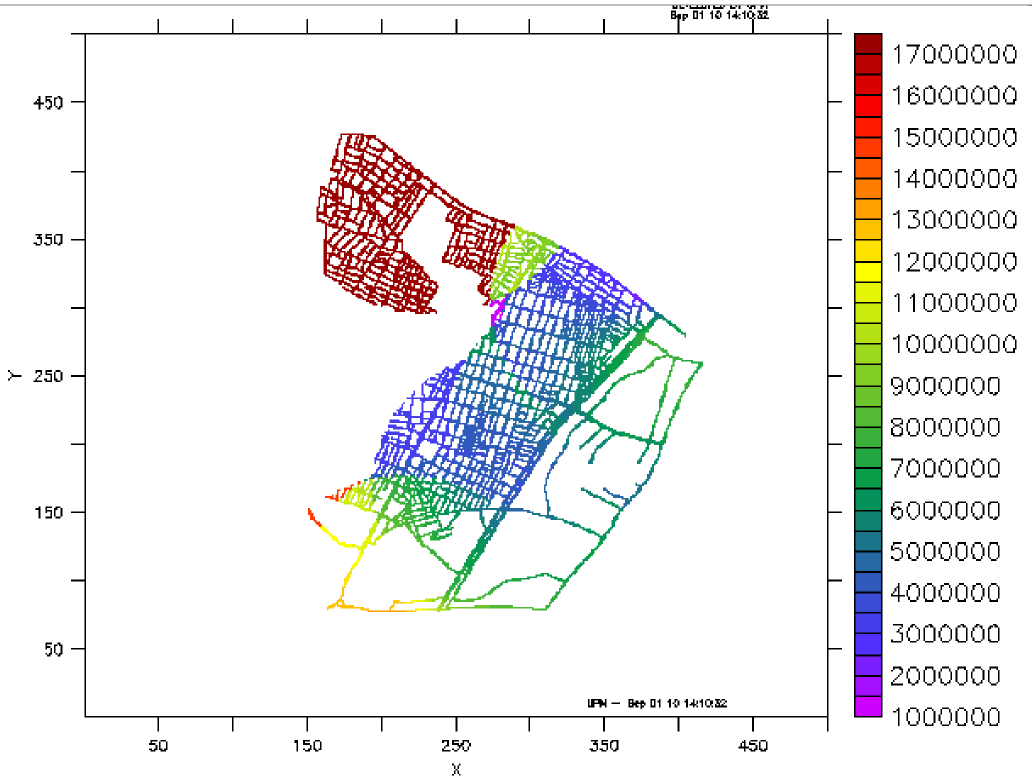

Figure 21: Athens Vehicles/year. Krigging interpolation results

The last figures show that the distribution of traffic flow in the urban areas is not uniform and it is agreement with the measurement values.

2.5 Output data

UPM models have been run in off-line mode. Off-line mode means that the simulations have been run over parallel computer platform and after finished it, the data are sent to the BRIDGE DSS system. It is due to the complexity and computer power required, as described in the D4.1 “Models Selection Report”.

UPM have supplied 2 sets of data:

a) Data to be uploaded into the DSS and will be used to calculate "indicators" and as input data for the "on-line models.

The list of the selected variables is:

2D Variables

Meteorological, Energy and Water:
T2:"Temperature at 2 meters height (Kelvin units)"
PSFC:"Surface Pressure (Pa units)"

U10:"X Wind Component at 10 meters height (m/s units)"
V10:"Y Wind Component at 10 meters height (m/s units)"
GRDFLX:"Downward Ground Heat Flux (w/m2 units)"
PBLH:"Planet Boundary Layer Height (m units)"
HFX:"Upward Sensible Heat Flux at the surface (w/m2 units)"
LH:"Upward Latent Heat Flux at the surface (w/m2 units)"
SFROFF:"Surface Runoff (mm units)"
UDROFF:"Underground Runoff (mm units)"
RAIN:"Rain (mm units)"
ALBEDO:"Surface Albedo (-- units)"
EC:"Canopy Water Evaporation (w/m2 units)"
EDIR:"Direct Soil Evaporation (w/m2 units)"
ETT:"Total Plant Transpiration (w/m2 units)"
GLW: "Downward Long Wave Flux (w/m2 units)"
Q2: "Humidity at 2 meters height (Kg/Kg units)"
SWDOWN: "Downward Short Wave Flux (w/m2 units)"
Z0:"Roughness length (m units)"

Air pollution:
SO2:“SO2 concentration (ug/m3)“
NO2:“NO2 concentration (ug/m3)"
NO: “NO concentration (ug/m3)"
CO:“CO concentration (ug/m3)"
O3:“O3 concentration (ug/m3)"
PM10:“PM10 concentration (ug/m3)"
PM25:“PM25 concentration (ug/m3)"

Green House Emissions (GHG):
EMISCO2:“CO2 emission (g/s)“
EMISCH4:“NO2 emission (g/s)"

3D Variables

Meteorological, Energy and Water:
TEMP3D:"Temperature (Kelvin units)"
PRS3D:"Pressure (Pa units)"
U:"X Wind Component (m/s units)"
V:"Y Wind Component (m/s units)"

The files distribution is implemented through a FTP service. One compressed ASCII file is generated by each variable. The name of the file follows the agreed format which is explained in the Figure 22. The name includes information about data dimension, provider partner, bridge city, base case or alternative, variable, data version and time period.

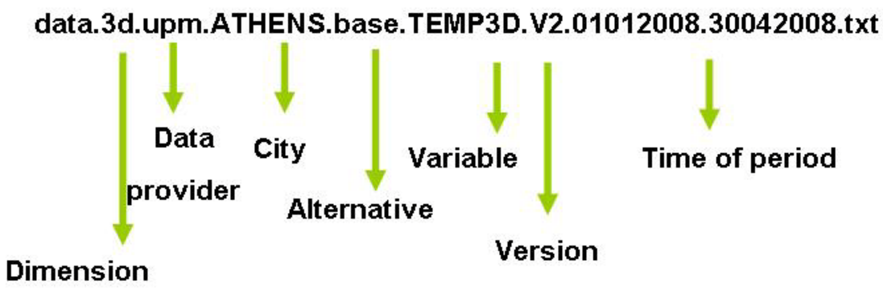

Figure 22: Data file name format

The file contains start with a header with information about projection, simulation domain, variable and temporal information. We use a simple ASCII format based on: **date(dd/mm/yyyy) hour(hh:mm) X_Coordinate Y_Coordinate Height_above_ground Value.**

b) Full 3d output in NETCDF format to be used by the off-line models such as CAMx (UAVR).

2.5.1 2 meter winds

The model outputs do not include winds at 2 meter height. This data is a request from the BRIDGE indicators list, so extra calculations are requested to produce 2 meter winds. Wind speed increases approximately logarithmically with height. The variation from a log-profile depends largely on atmospheric stability. Atmospheric stability refers to the stratification of the air near the surface. A stable stratification will reduce mixing (and surface stress), and an unstable stratification will increase mixing.

The **Log wind profile** is a semi-empirical relationship used to describe the vertical distribution of horizontal wind speeds. The equation to estimate the wind speed (u) at height z (meters) above the ground is described in the Figure 23

$$u_z = \frac{u_*}{\kappa}\left[\ln\left(\frac{z-d}{z_0}\right) + \psi(z, z_0, L)\right]$$

Figure 23: Log wind profile equation

where u_* is the friction velocity (m s^{-1}), κ is von Karman's constant (~0.41), d is the zero plane displacement, z_0 is the surface roughness (in meters), and ψ is a stability term where L is the Monin- Obukhov stability parameter. Under neutral stability conditions, $z / L = 0$ and ψ drops out.

Zero-plane displacement (d) is the height in meters above the ground at which zero wind speed is achieved as a result of flow obstacles, in our case buildings. It is generally approximated as $^2/_3$ of the average height of the obstacles.

Roughness length (z_0) is a corrective measure to account for the effect of the roughness of a surface on wind flow, and is between $^1/_{10}$ and $^1/_{30}$ of the average height of the roughness elements on the ground.

We have information about wind at 10 meters height and 35 meters height (first vertical level of the model), with this information and the log wind profile, we have produced 2 meter winds. In the Figure 24 can be observed the evolution of the wind speeds at 35 and 10 meters height calculated by the WRF/UCM model and the 2 meters calculated using a log wind profile. The results are consistent with the maximum wind speed at 35 meters and minimum at 2 meters height.

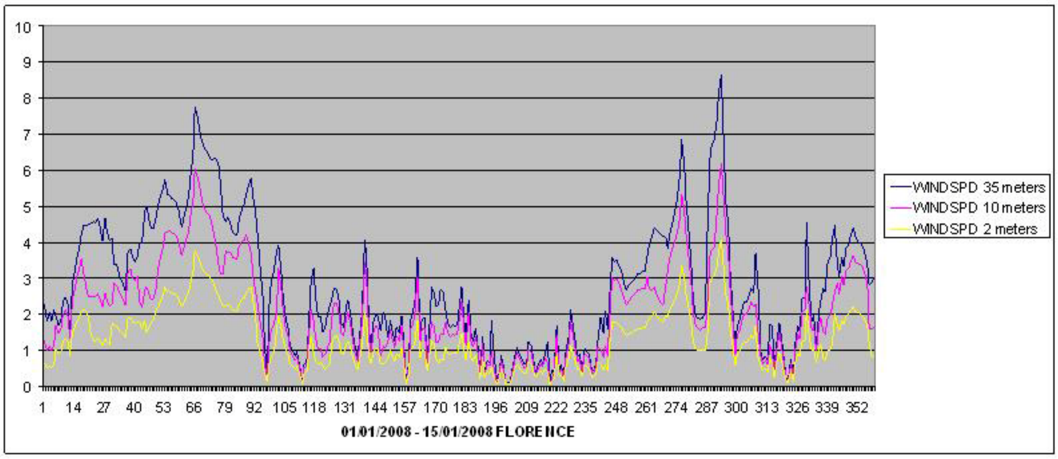

Figure 24: Wind speed, 35,10,2 meters over Firenze 01-15/01/2008

2.6 Base run results.

The results of the base run for full year 2008 , we will be analyzed in the next section. Results have been obtained using the WRF/UCM-EMIMO_CMAQ system described in the last sections. Quality assurance and Quality control process have been described in the D4.3 document “QA/QC”. Base runs for the 5 Bridge cities have been completed for the meteorological and energy parts and Athens and Firenze for the air pollution subject. Annual average results are presented.

2.6.1 Athens

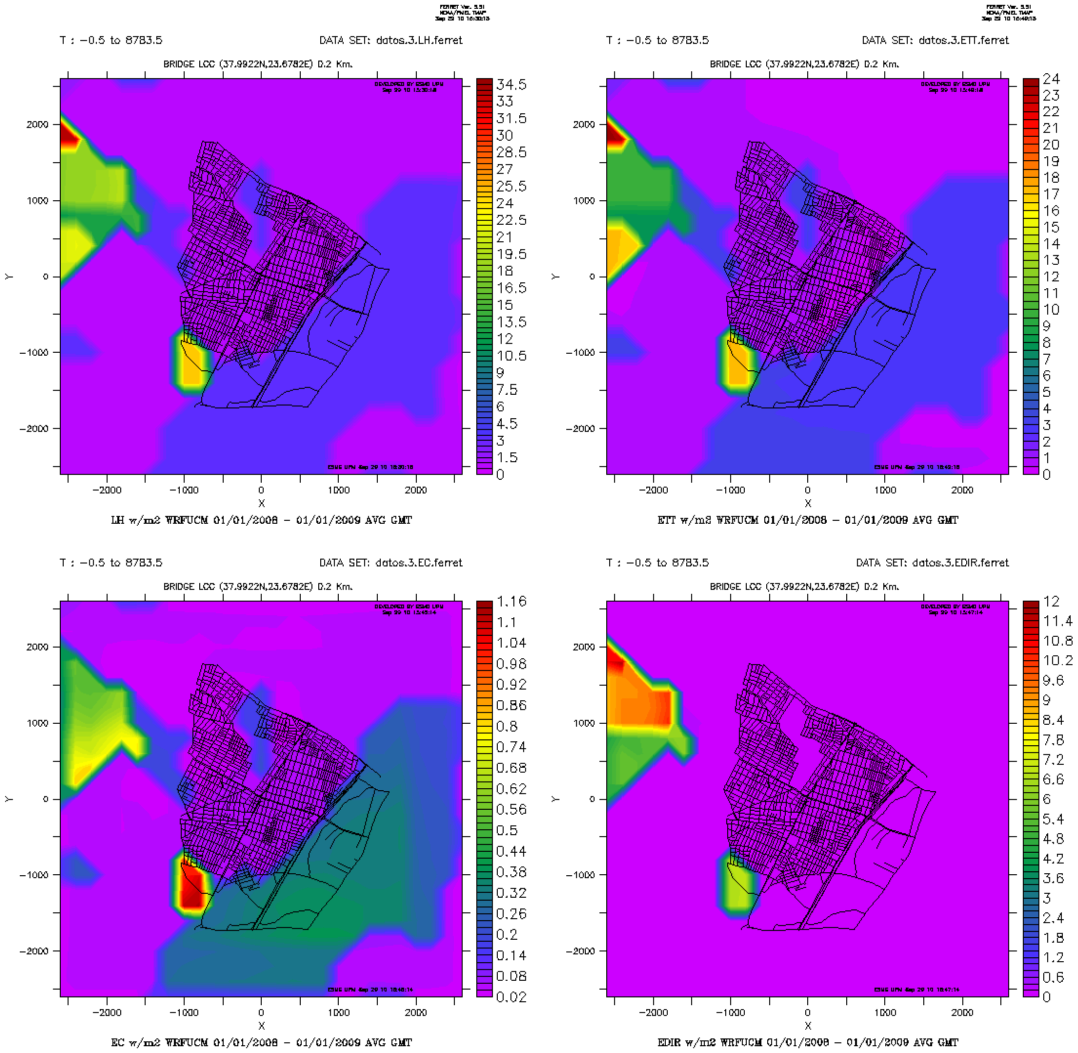

Figure 25: Latent heat flux (upper-left), Total plant transpiration (upper-right), Canopy water evaporation (bottom-left) and direct soil evaporation (bottom-right) fluxes. 2008 annual average, domain 0.2 km resolution over Athens

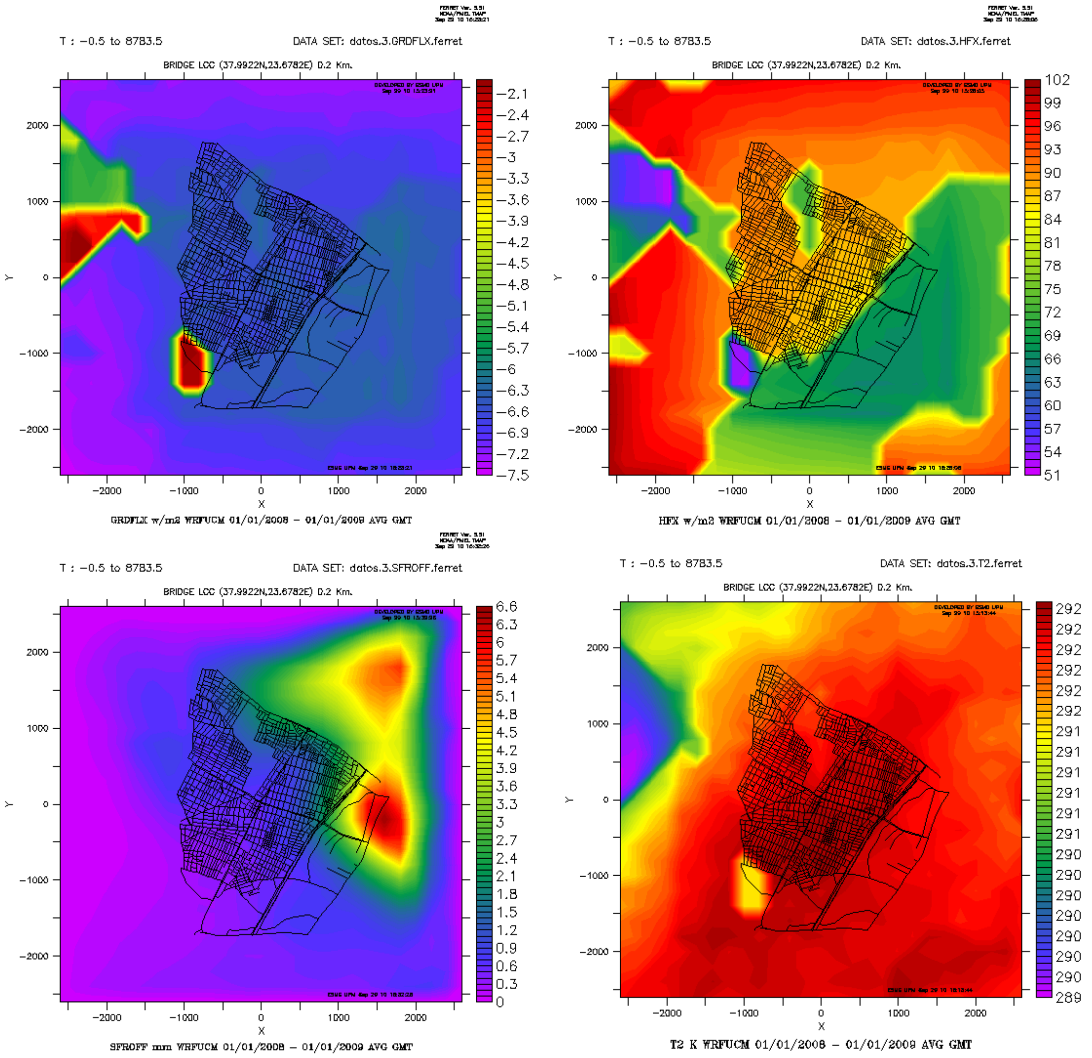

Figure 26: Ground heat flux (upper-left), Sensible heat flux (upper-right), Surface runoff (bottom-left), and Air temperature (bottom-right). 2008 annual average, domain 0.2 km resolution over Athens

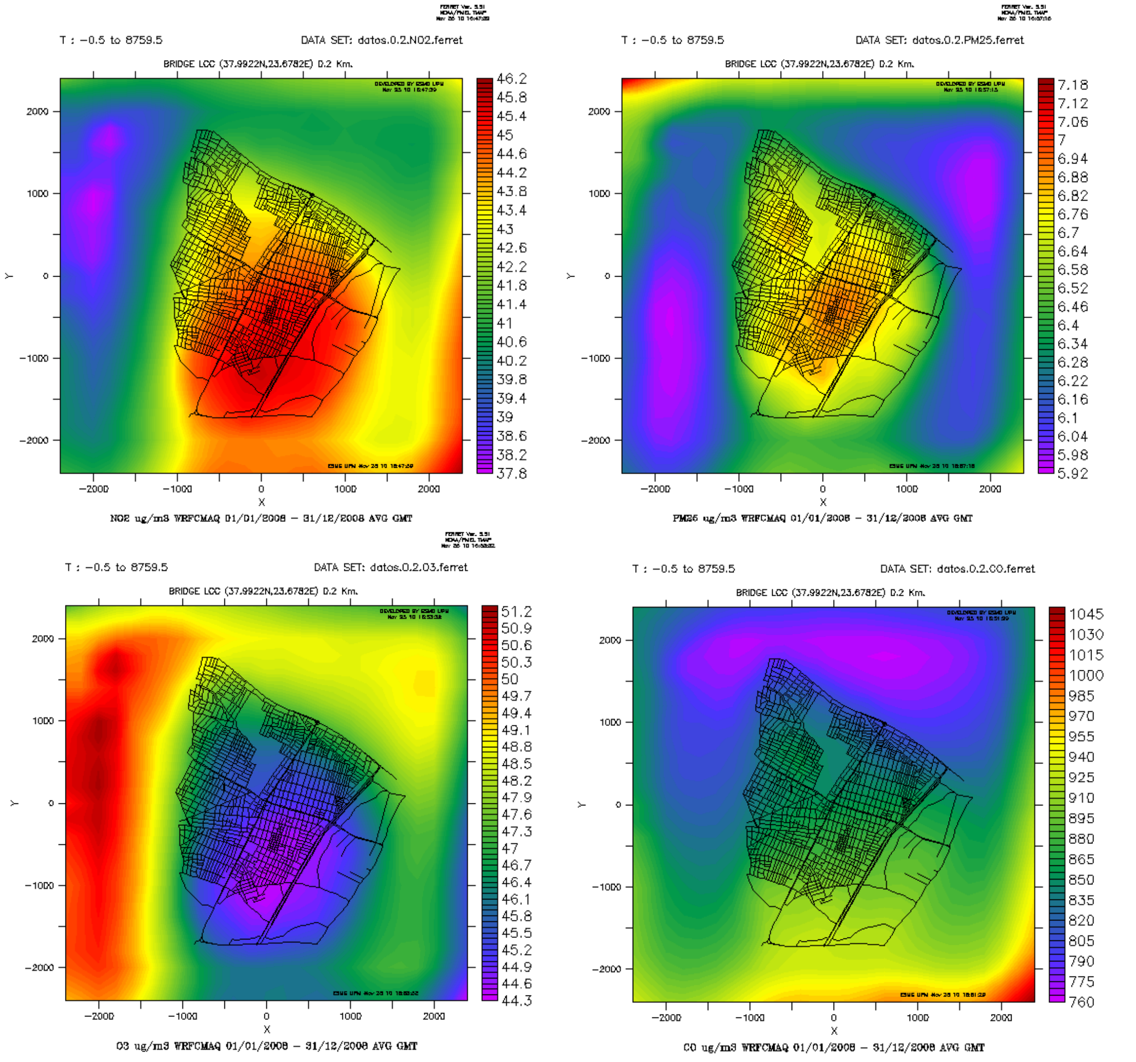

Figure 27:NO2 (upper-left), PM25 (upper-right), O3 (bottom-left), and CO (bottom-right). 2008 annual average, domain 0.2 km resolution over Athens

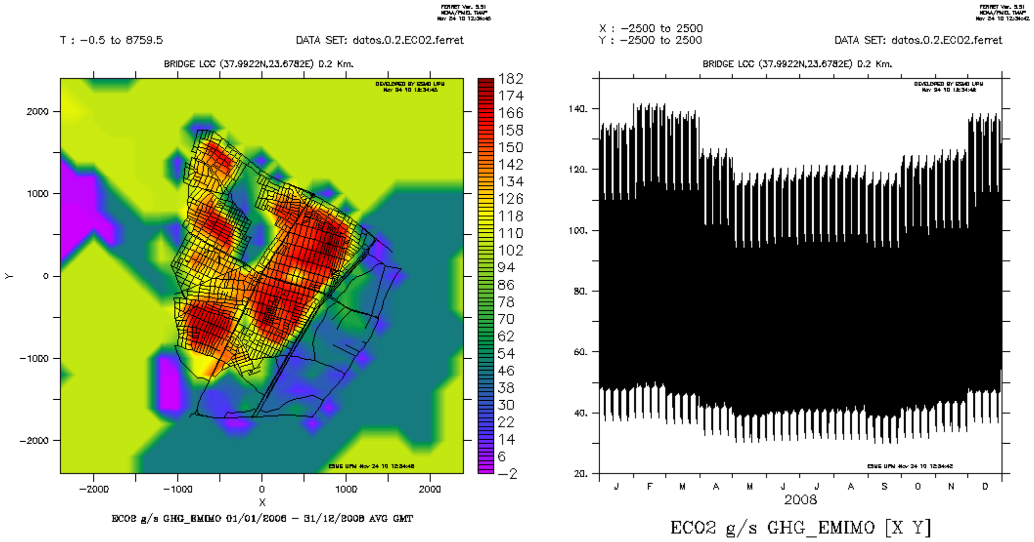

Figure 28: CO2 emission. 2008 annual average (left) and spatial average (right), domain 0.2 km resolution over Athens

2.6.2 Helsinki

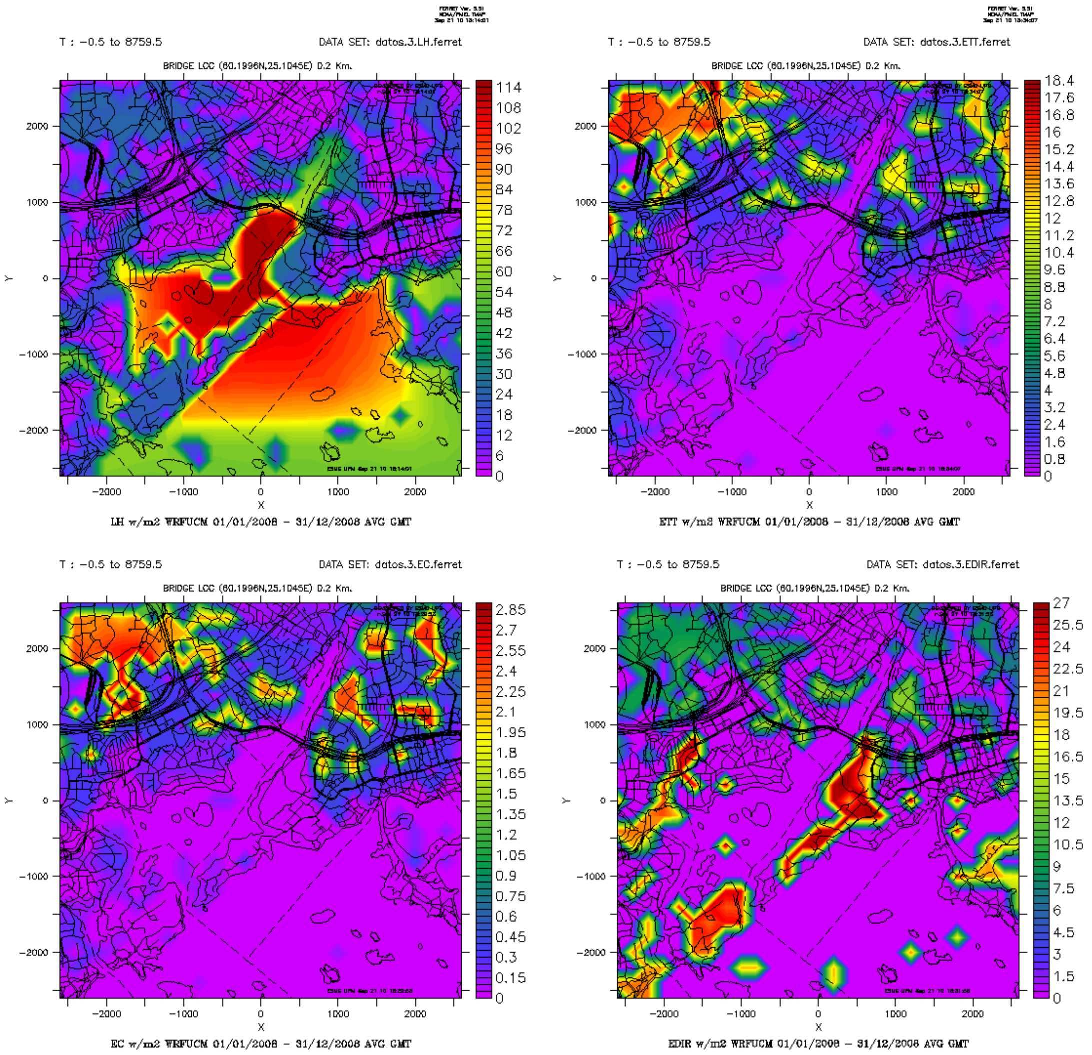

Figure 29: Latent heat flux (upper-left), Total plant transpiration (upper-right), Canopy water evaporation (bottom-left) and direct soil evaporation (bottom-right) fluxes. 2008 annual average, domain 0.2 km resolution over Helsinki

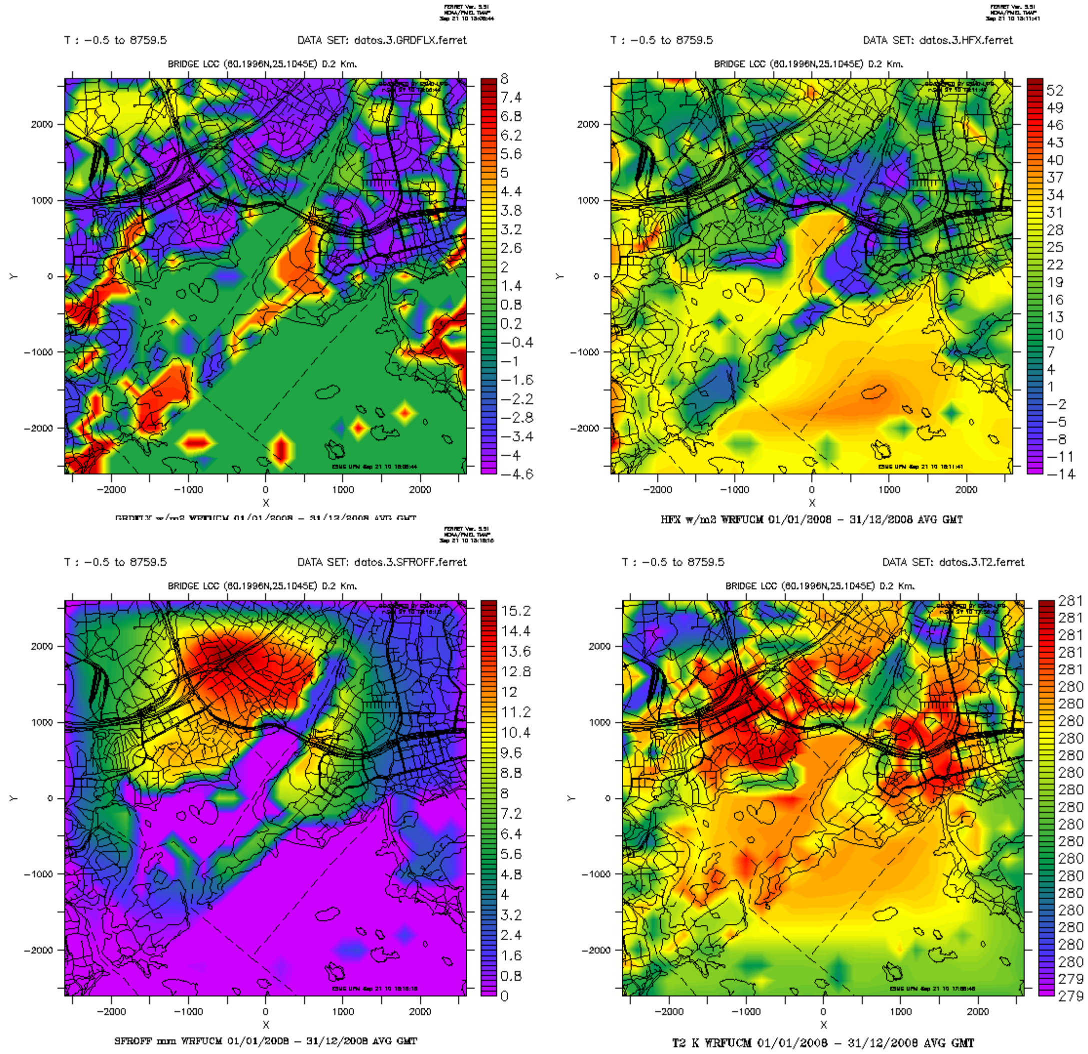

Figure 30: Ground heat flux (upper-left), Sensible heat flux (upper-right), Surface runoff (bottom-left), and Air temperature (bottom-right). 2008 annual average, domain 0.2 km resolution over Helsinki

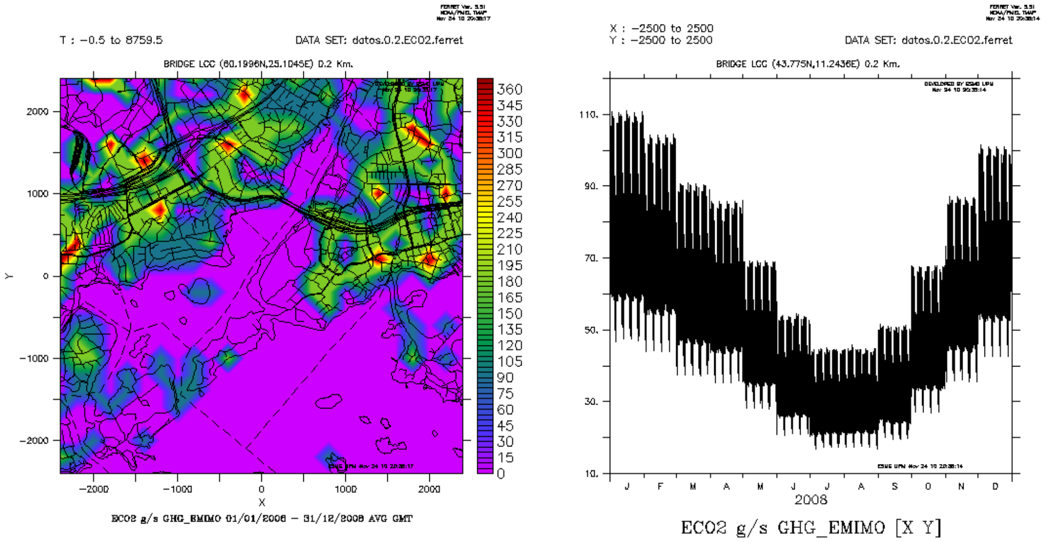

Figure 31: CO2 emission. 2008 annual average (left) and spatial average (right), domain 0.2 km resolution over Helsinki

2.6.3 Gliwice

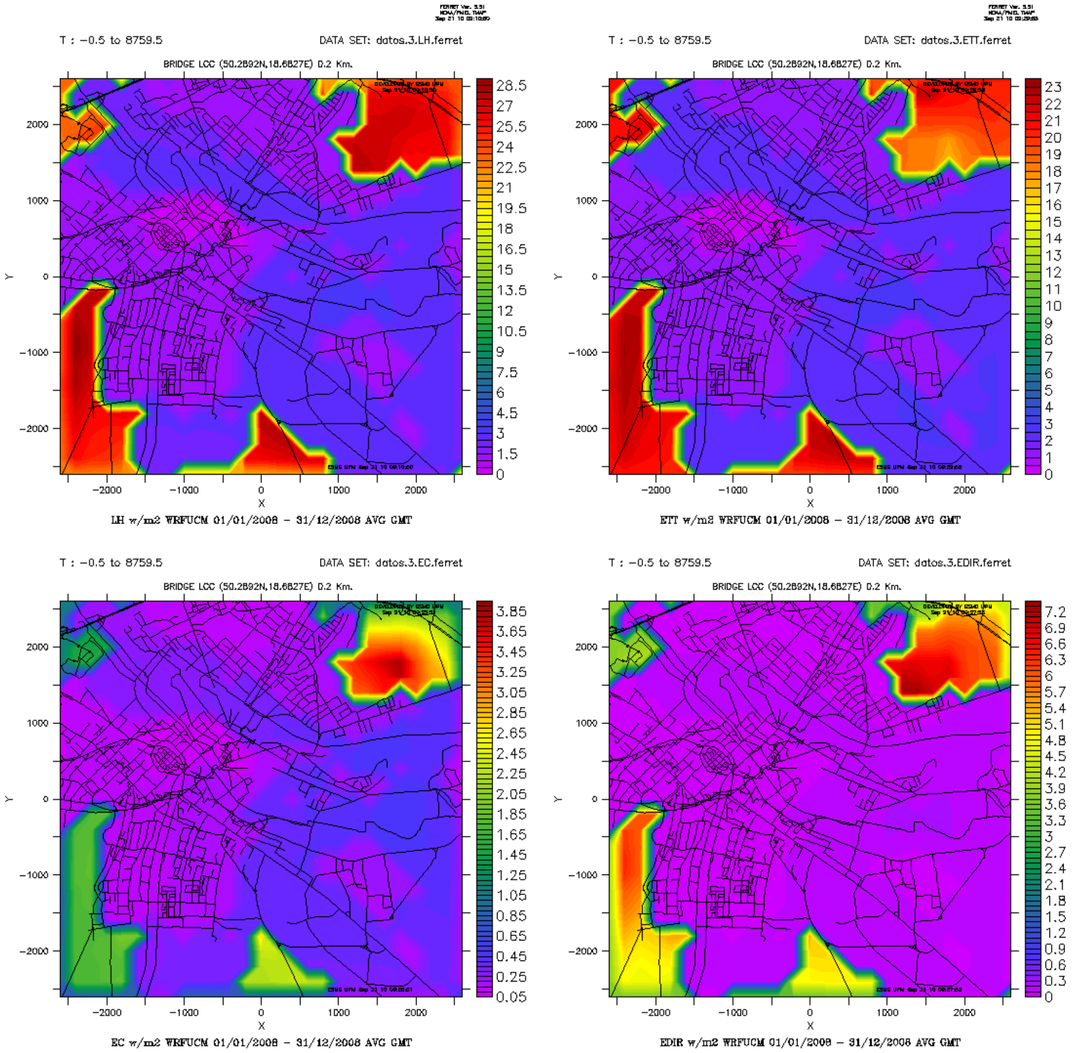

Figure 32: Latent heat flux (upper-left), Total plant transpiration (upper-right), Canopy water evaporation (bottom-left) and direct soil evaporation (bottom-right) fluxes. 2008 annual average, domain 0.2 km resolution over Gliwice

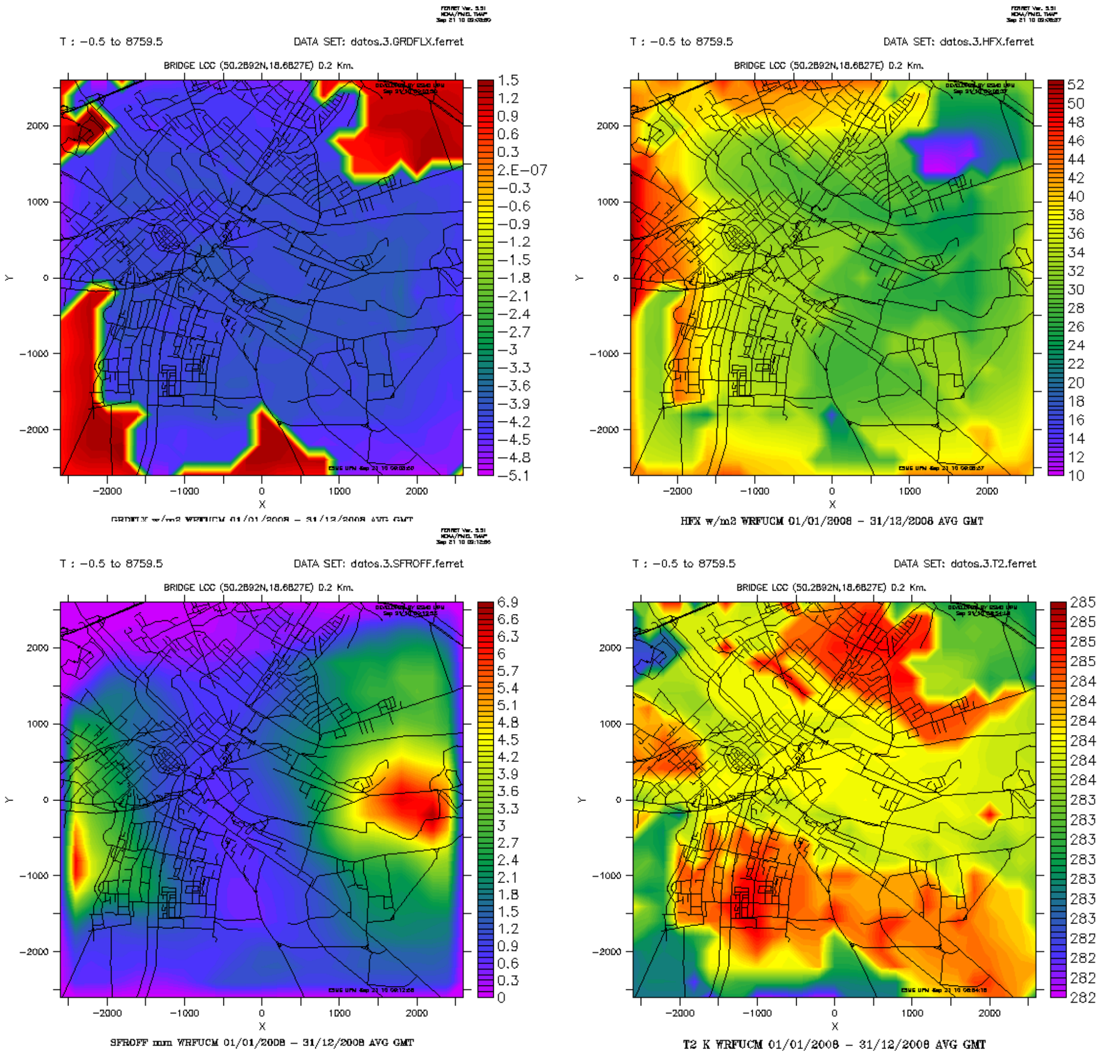

Figure 33: Ground heat flux (upper-left), Sensible heat flux (upper-right), Surface runoff (bottom-left), and Air temperature (bottom-right). 2008 annual average, domain 0.2 km resolution over Gliwice

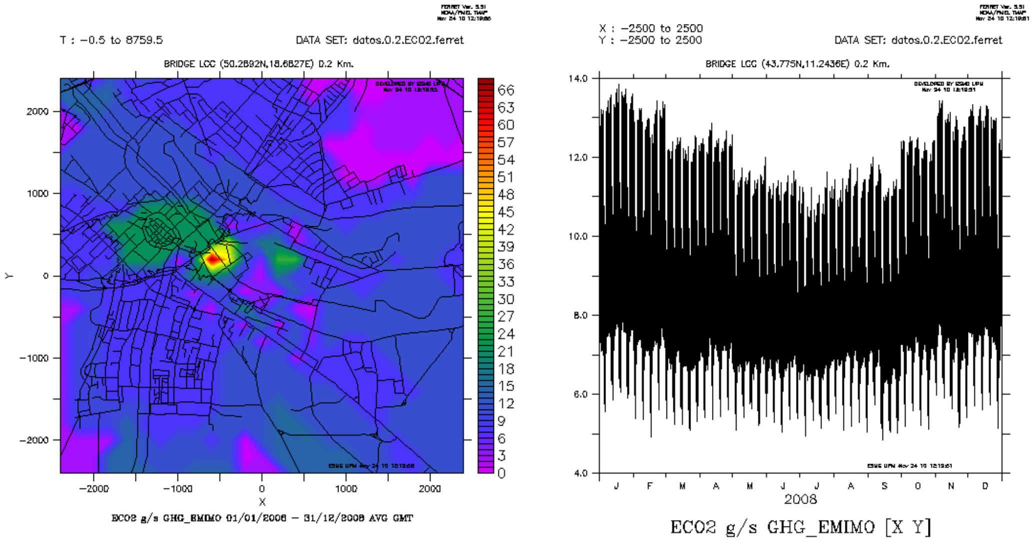

Figure 34: CO2 emission. 2008 annual average (left) and spatial average (right), domain 0.2 km resolution over Gliwice

2.6.4 Firenze

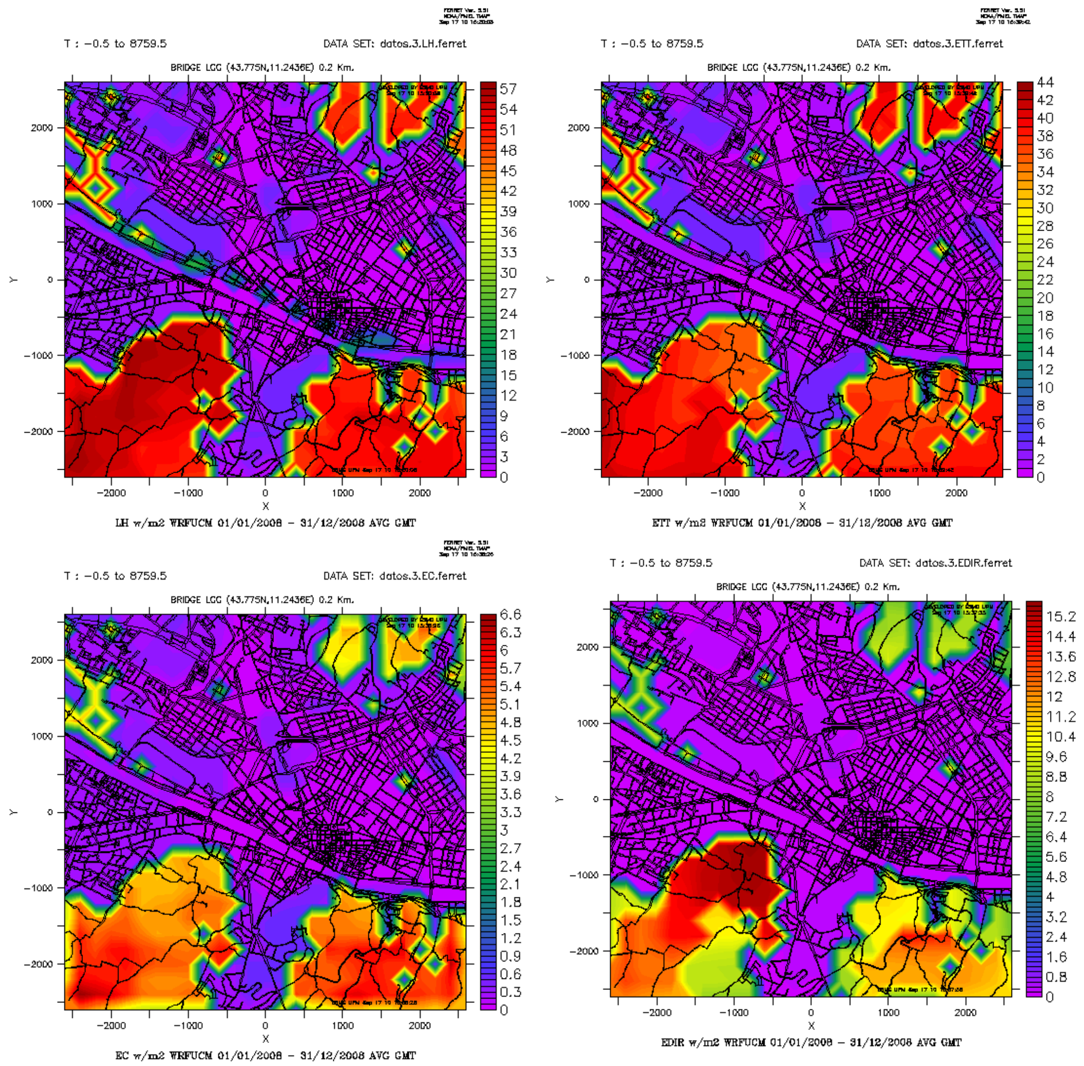

Figure 35: Latent heat flux (upper-left), Total plant transpiration (upper-right), Canopy water evaporation (bottom-left) and direct soil evaporation (bottom-right) fluxes. 2008 annual average, domain 0.2 km resolution over Firenze

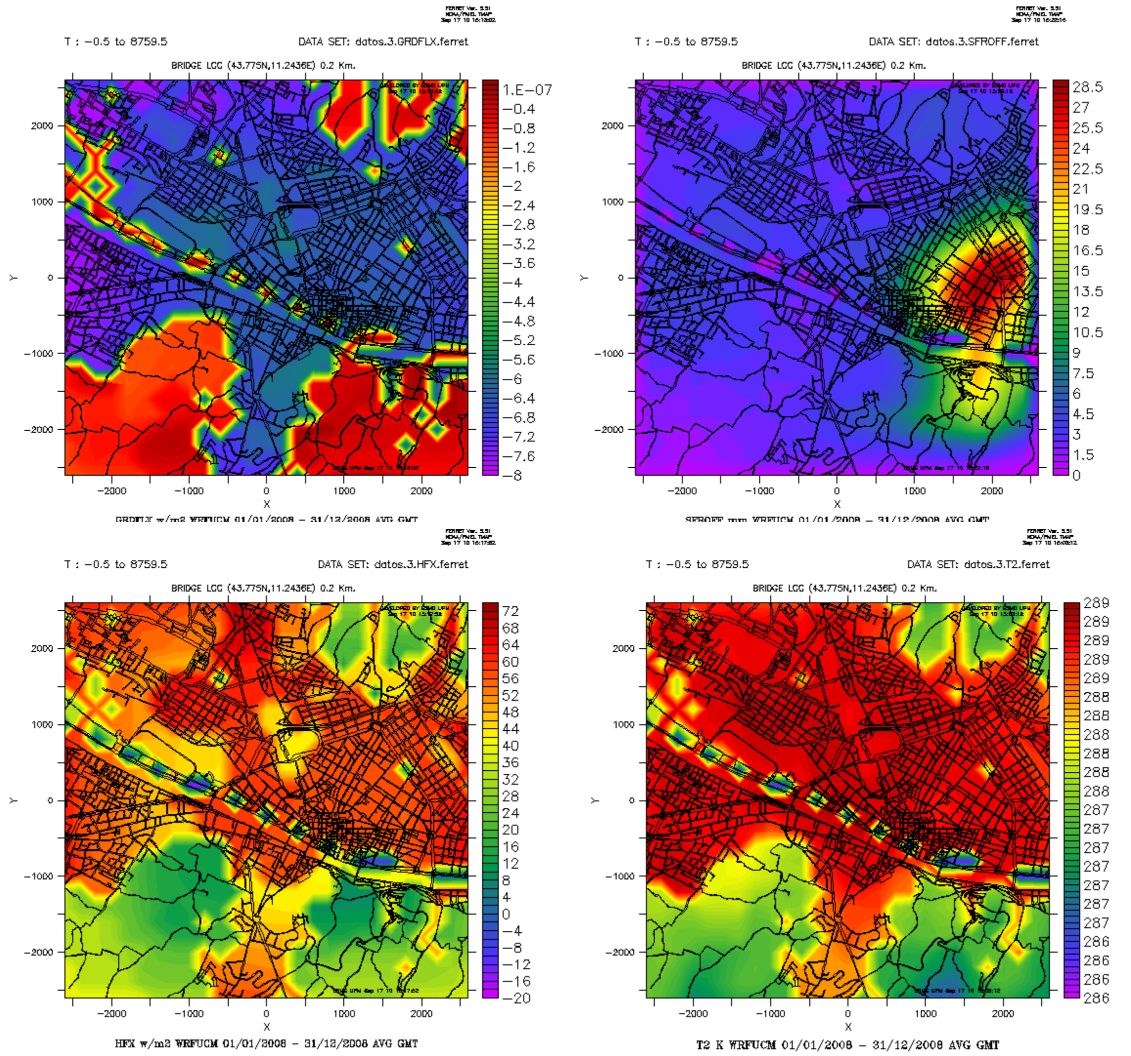

Figure 36: Ground heat flux (upper-left), Surface runoff (upper-right), Sensible heat flux (bottom-left), and Air temperature (bottom-right). 2008 annual average, domain 0.2 km resolution over Firenze

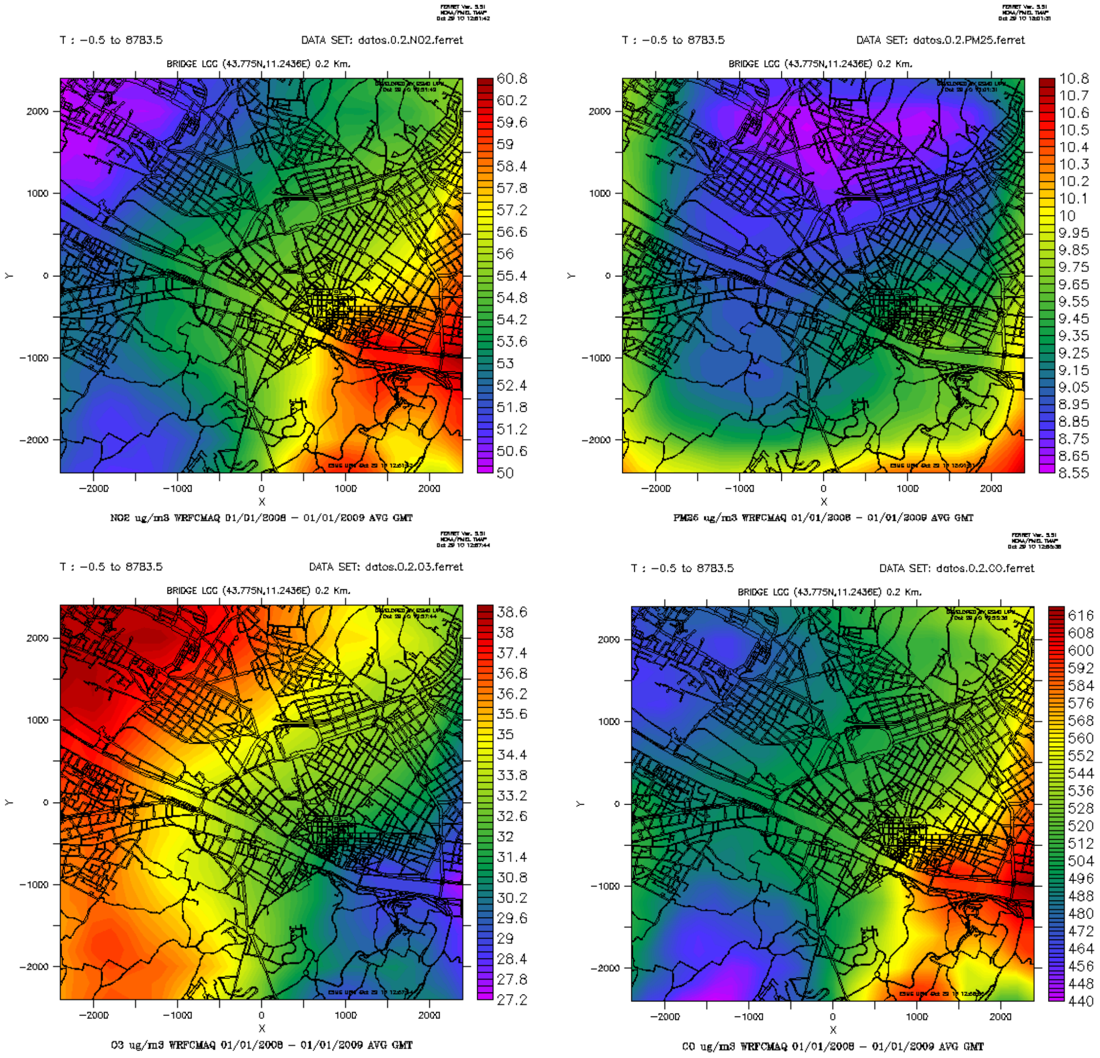

Figure 37:NO2 (upper-left), PM25 (upper-right), O3 (bottom-left), and CO (bottom-right). 2008 annual average, domain 0.2 km resolution over Firenze

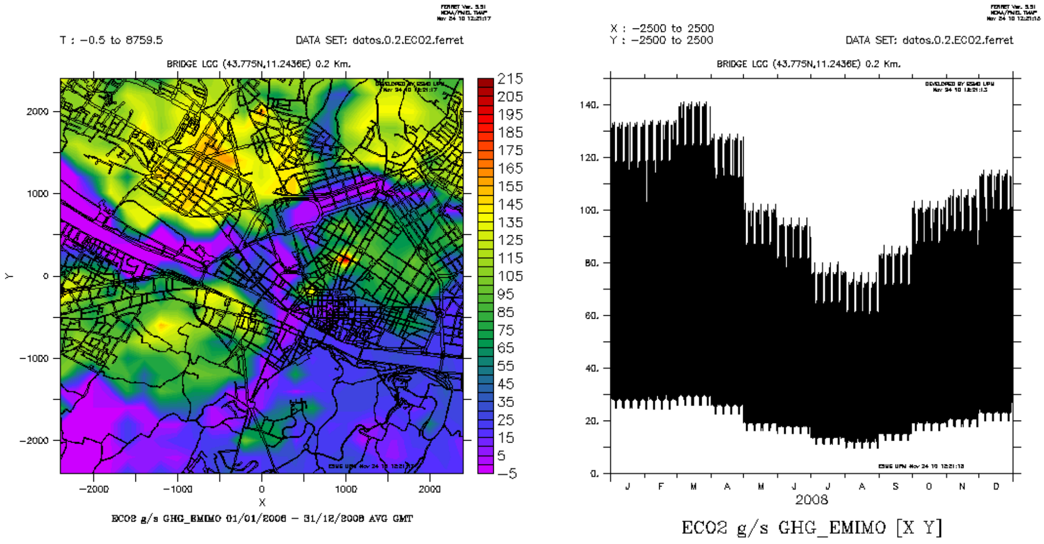

Figure 38: CO2 emission. 2008 annual average (left) and spatial average (right), domain 0.2 km resolution over Firenze

2.6.5 London

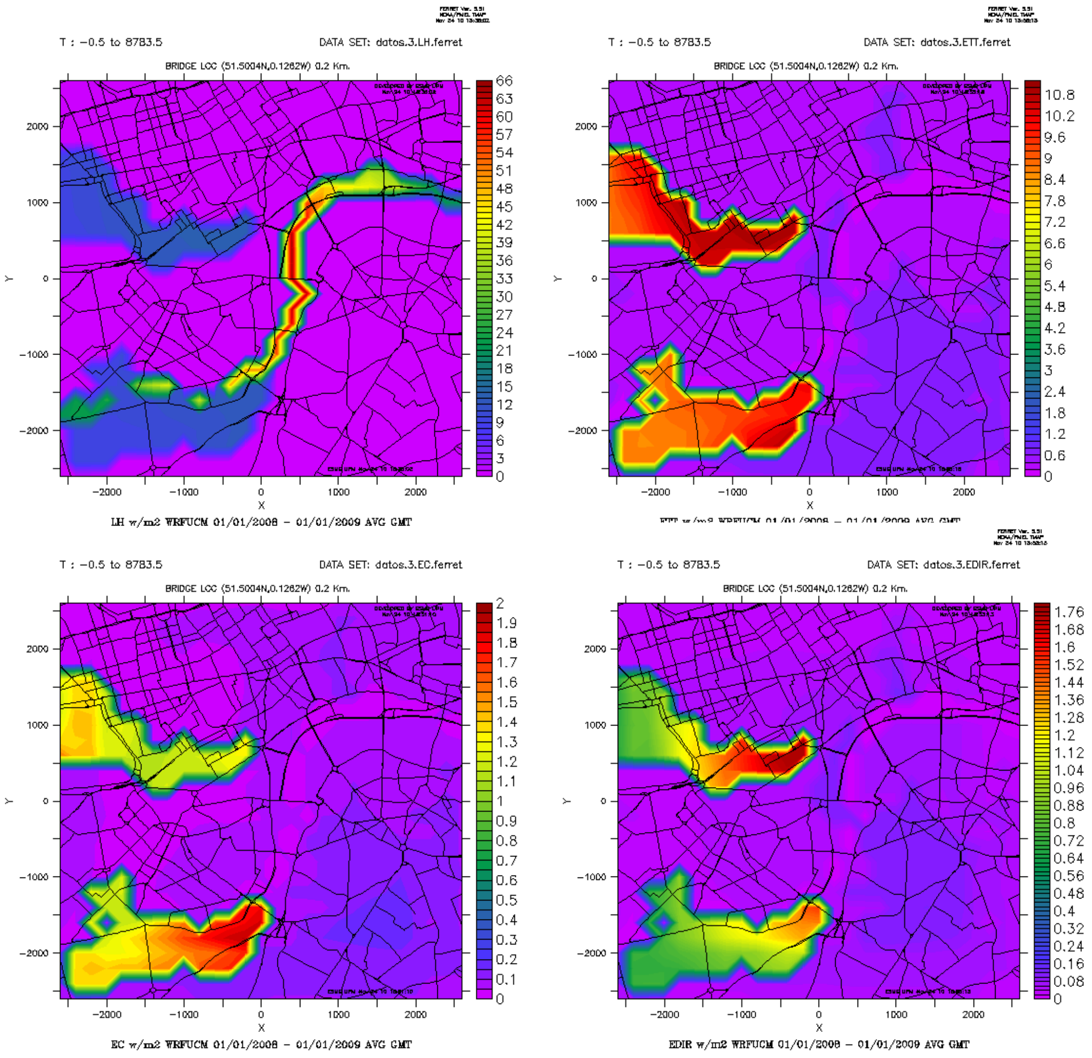

Figure 39: Latent heat flux (upper-left), Total plant transpiration (upper-right), Canopy water evaporation (bottom-left) and direct soil evaporation (bottom-right) fluxes. 2008 annual average, domain 0.2 km resolution over Firenze

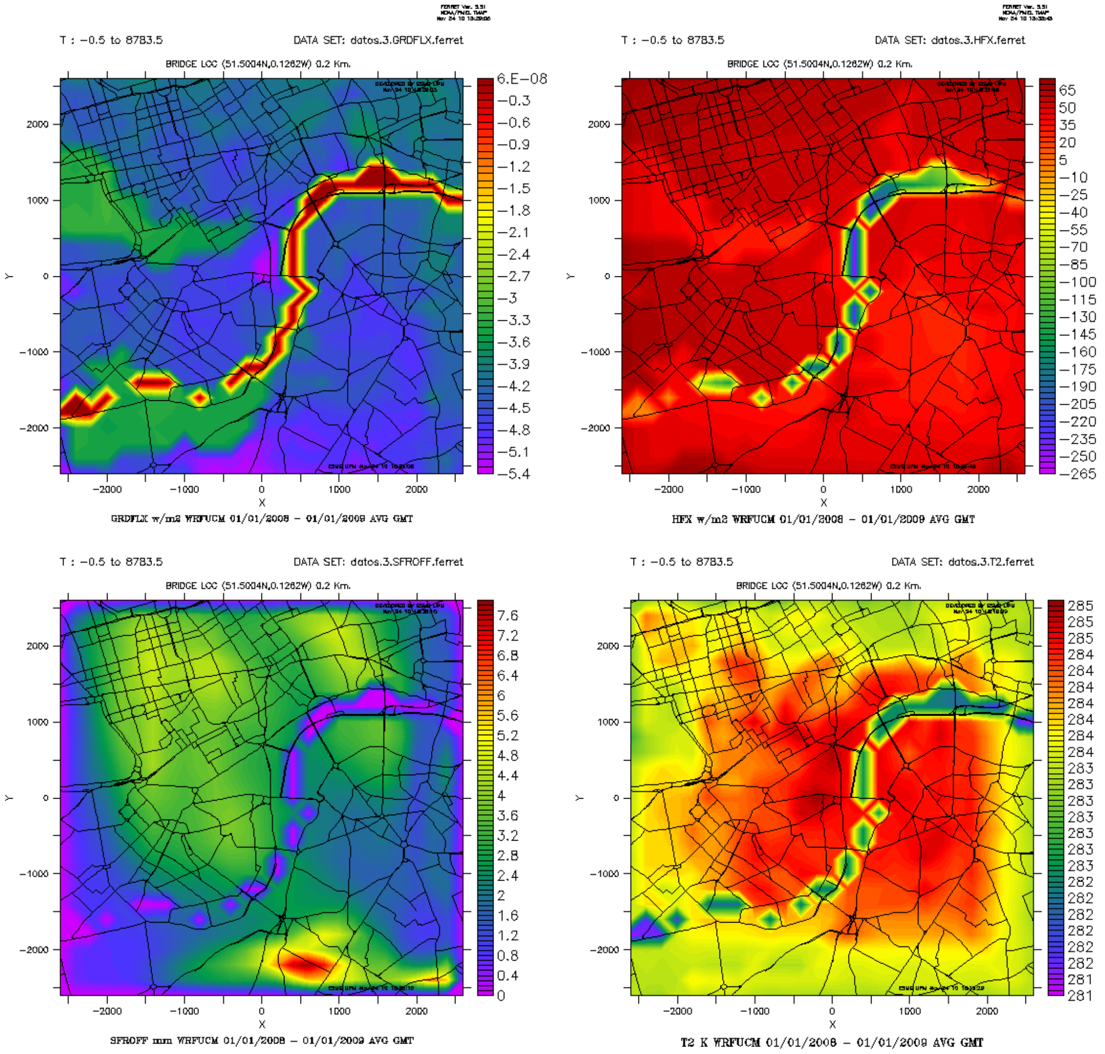

Figure 40: Ground heat flux (upper-left), Surface runoff (upper-right), Sensible heat flux (bottom-left), and Air temperature (bottom-right). 2008 annual average, domain 0.2 km resolution over Firenze

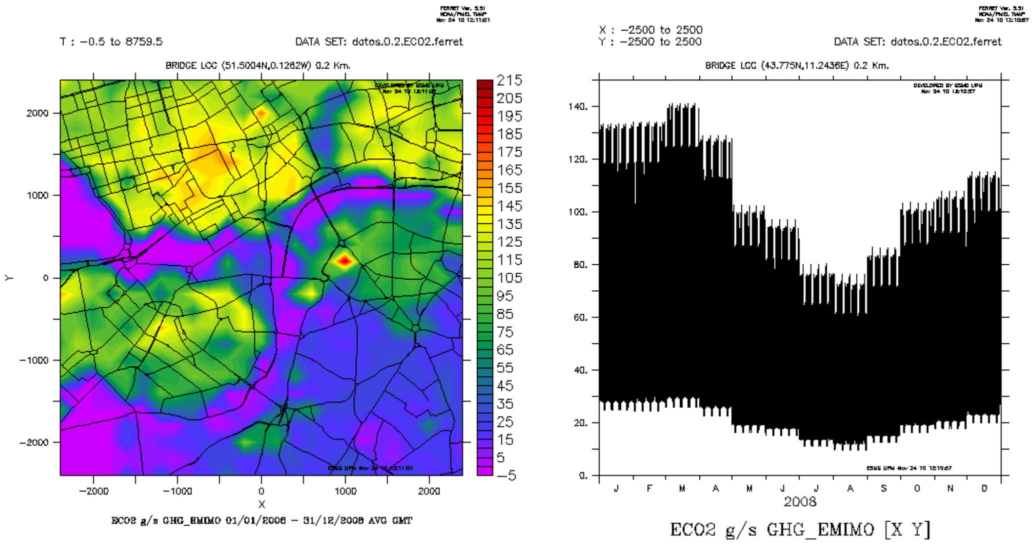

Figure 41: CO2 emission. 2008 annual average (left) and spatial average (right), domain 0.2 km resolution over London

2.7 Alternatives

Three alternatives have been simulated by city. The alternatives have been defined by the city planners. The modelers have translated the alternative to modeling language. Once the alternative has been implemented into the model, a new simulation has to be run. The differences between alternatives and base run show the impact of the planning alternatives for all variables included in the model.

2.7.1 Athens

Alternative 1: Apply cool materials on all buildings at Egaleo municipality and on roads The area of application is the urban fabric of Egaleo municipality: In Figure 42, it is the polygon ABMKJA excluding the polygon 1234 (which is open/green space).

Here we need to apply cool materials, this means that the albedo of buildings should be changed to 85% (from a base case of 20%) and the albedo of roads will be increased to 45% (from a base case of 5%)

This alternative has been implemented into the model, changing albedo of buildings from 0.2 to 0.85 and albedo roads from 0.05 to 0.2.

Alternative 2: In this case, the planning alternative regards the land use change of Eleonas from Brownfield industrial/ area to Urban fabric. Eleonas which is a Brownfield/ industrial area adjacent to the Egaleo municipality. In Figure 42 , it is shown by the polygon CDEFGLMC. New roads have been planned, Figure 43 (red lines) and a new emission map have to be calculated.

This alternative has been implemented into the model, changing Eleonas land uses from Industrial/Commercial urban area to high density urban.

Alternative 3: In this case, the planning alternative regards the land use change of Eleonas from Brownfield industrial/ area to Green spaces, Figure 43, rose color. Eleonas which is a Brownfield/ industrial area adjacent to the Egaleo municipality. In Figure 42 , it is shown by the polygon CDEFGLMC.

This alternative have been implemented into the model, changing Eleonas land uses from Industrial/Commercial urban area to grassland

Figure 42: Map of municipality of Egaleo

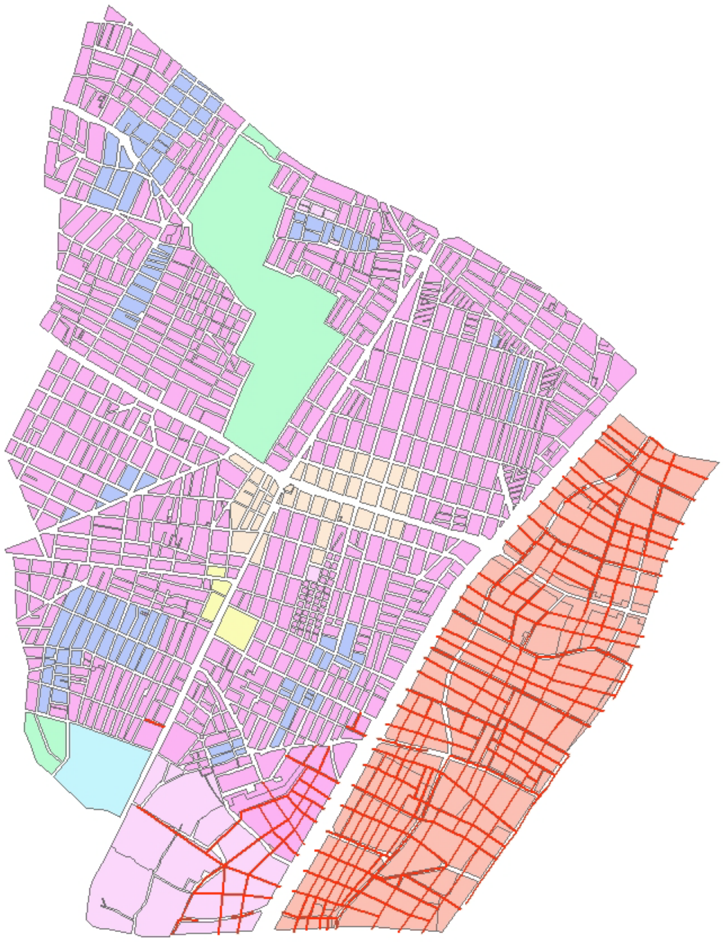

Figure 43: Athens alternatives, new roads (red) and land use shapefiles

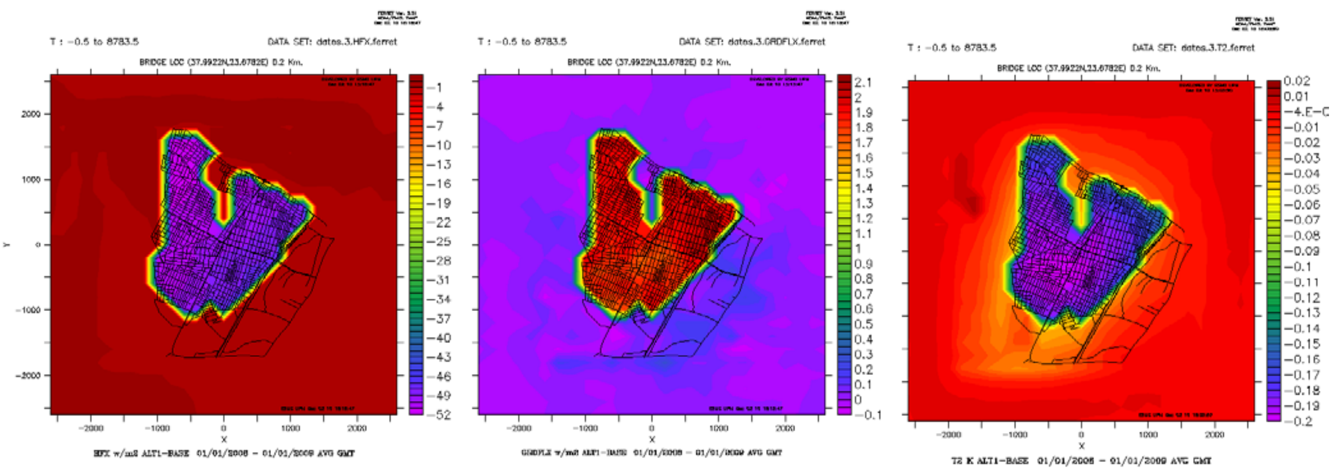

Figure 44: Differences between alternative 1 and base run annual average of Sensible heat flux (left), Ground heat flux (middle),and Air temperature (right), domain 0.2 km resolution over Athens

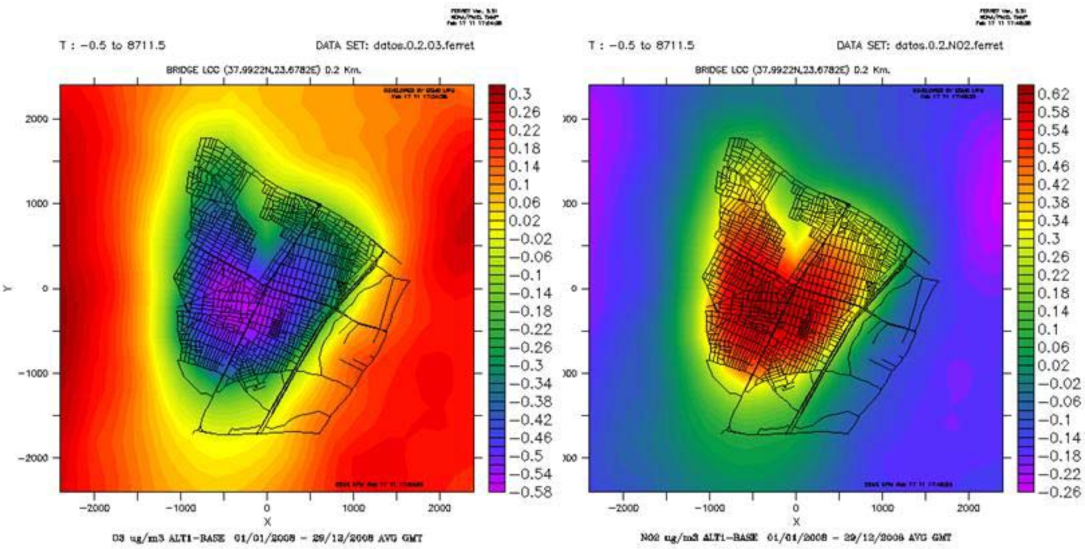

Figure 45: Differences between alternative 1 and base run annual average of Ozone (left) and Nitrogen Dioxide (right). domain 0.2 km resolution over Athens

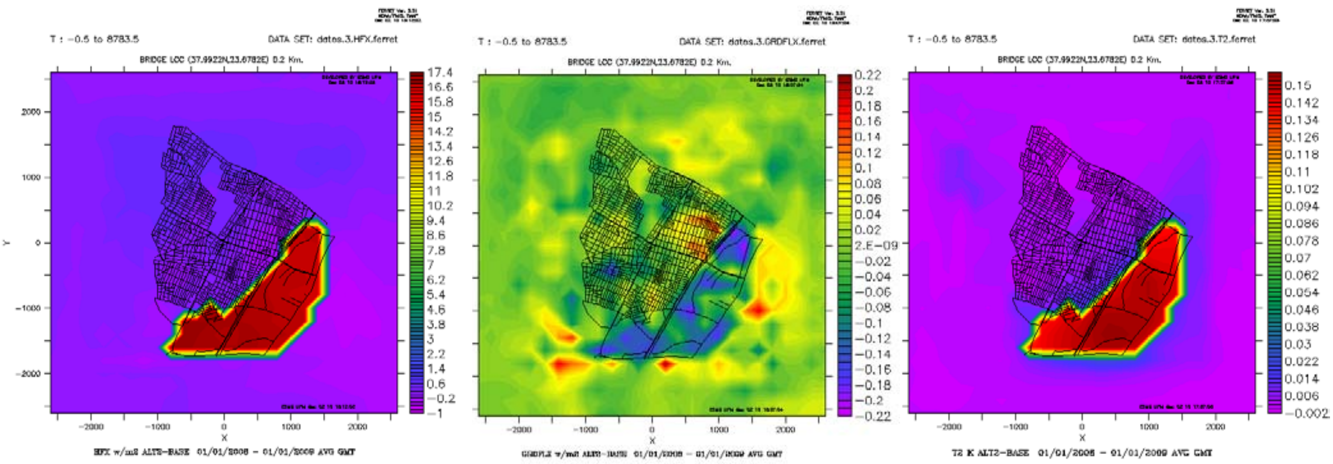

Figure 46: Differences between alternative 2 and base run annual average of Sensible heat flux (left), Ground heat flux (middle),and Air temperature (right), domain 0.2 km resolution over Athens

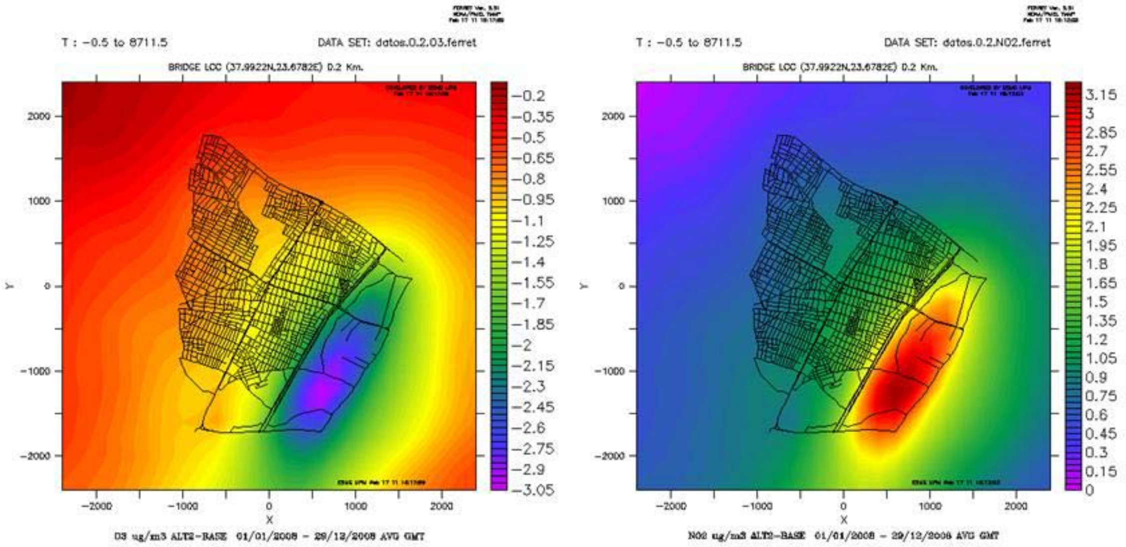

Figure 47: Differences between alternative 2 and base run annual average of Ozone (left) and Nitrogen Dioxide (right), domain 0.2 km resolution over Athens

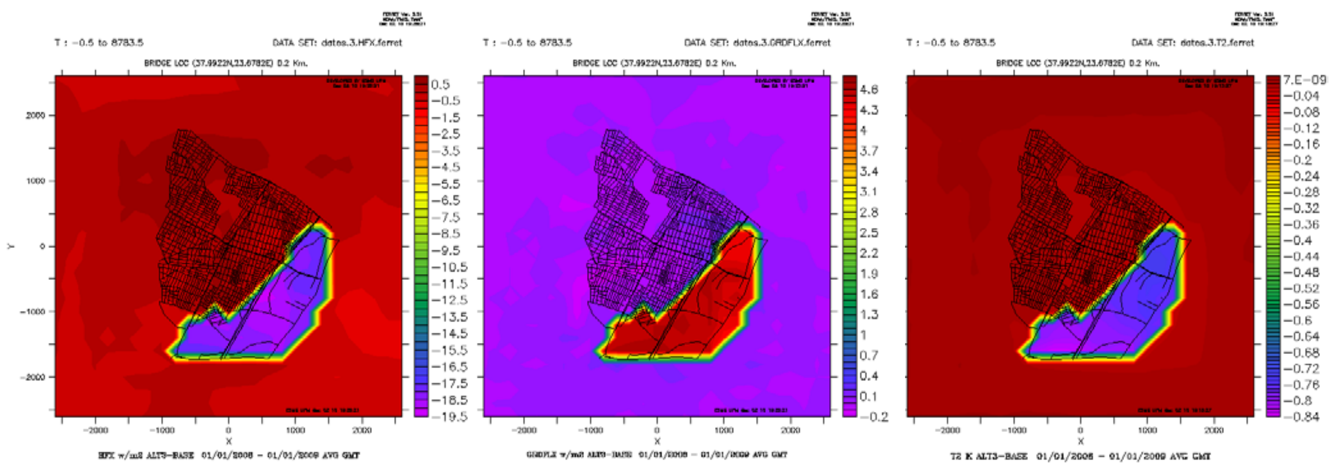

Figure 48: Differences between alternative 3 and base run annual average of Sensible heat flux (left), Ground heat flux (middle),and Air temperature (right), domain 0.2 km resolution over Athens

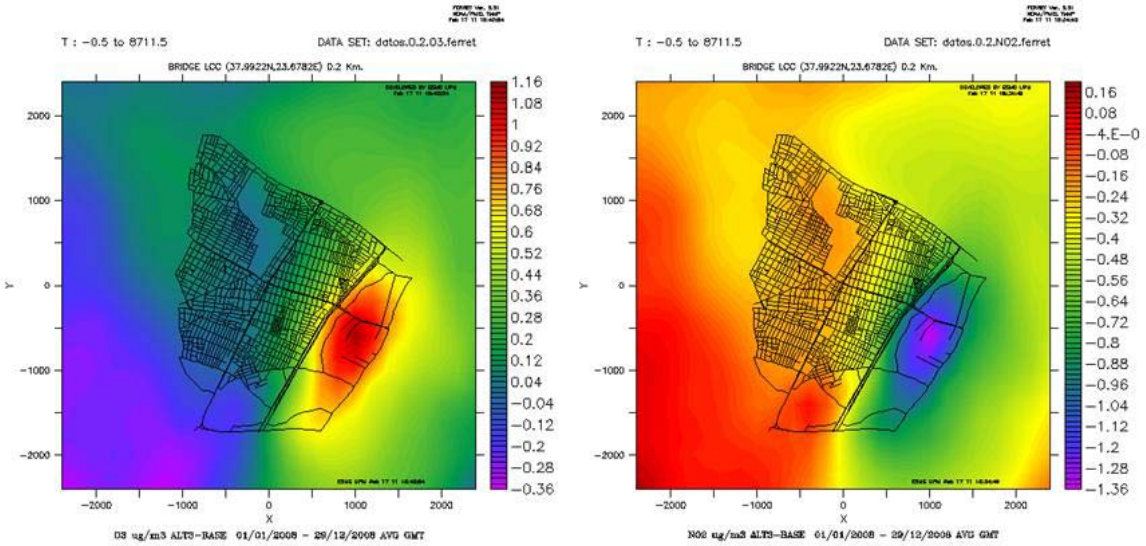

Figure 49: Differences between alternative 1 and base run annual average of Ozone (left) and Nitrogen Dioxide (right), domain 0.2 km resolution over Athens

2.7.2 Helsinki

Helsinki alternatives consist in build 3 different groups of residential buildings over a green area. The information about the new buildings was sent by PDF files, without coordinates, Figure 50. So, it was necessary to develop a geo-location process of the buildings from PDF to a GIS system. This work was developed by UAVR, Figure 51. The alternatives were implemented into the model, changing the land uses from green are to urban areas where the new buildings was located.

Figure 50: Helsinki alternatives PDF file.

Figure 51: Helsinki alternatives in GIS format.

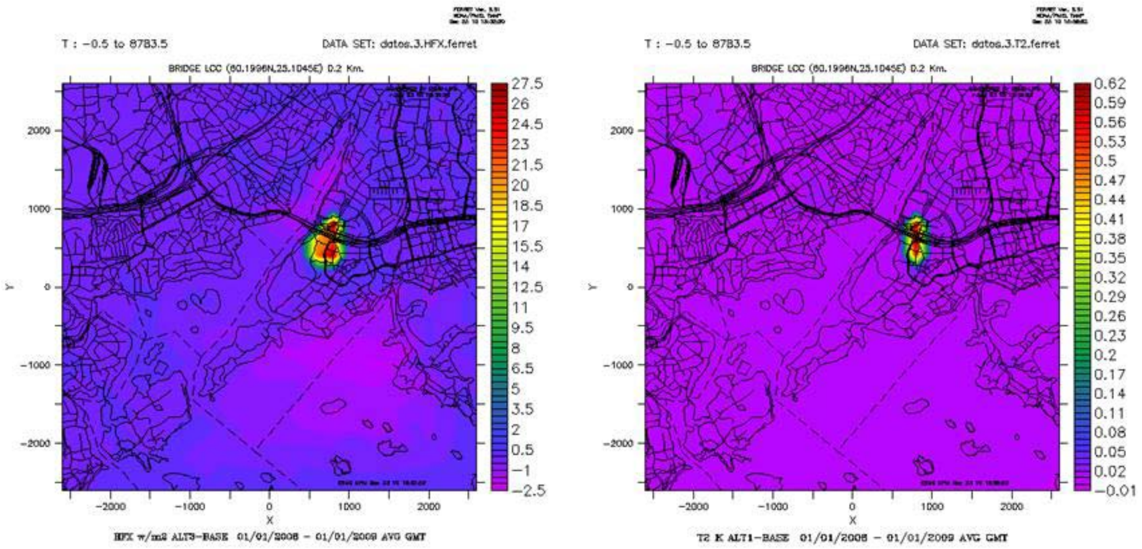

Figure 52: Differences between alternative 1 and base run annual average of Sensible heat flux (left), Air temperature (right), domain 0.2 km resolution over Helsinki

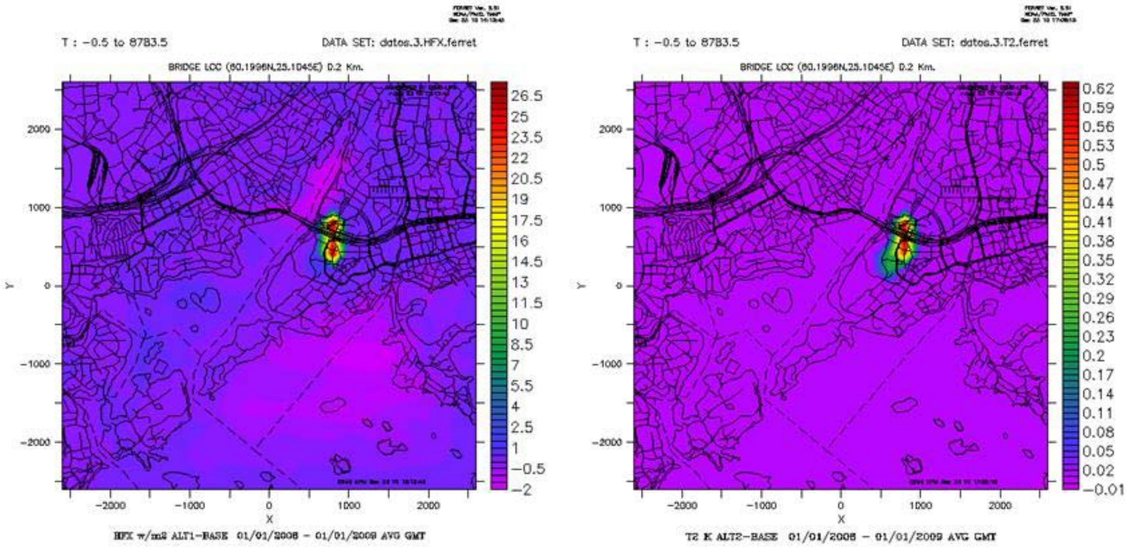

Figure 53: Differences between alternative 2 and base run annual average of Sensible heat flux (left), Air temperature (right), domain 0.2 km resolution over Helsinki

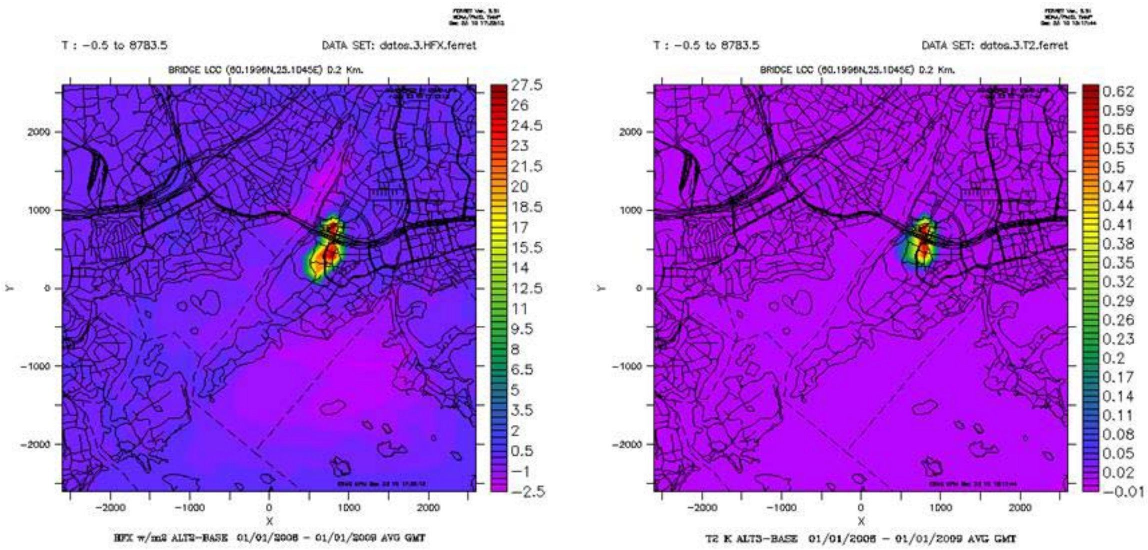

Figure 54: Differences between alternative 3 and base run annual average of Sensible heat flux (left), Air temperature (right), domain 0.2 km resolution over Helsinki

2.7.3 Gliwice

Alternative 1: Construction of Gliwice Central Arena. The alternative were implemented into the model, changing the land uses from Commercial to High density urban area in 2 200 meters resolution grid cells where the new building was located.

Alternative 2: Construction of The Centre of New technologies. The alternative were implemented into the model, changing the land uses from Low density urban to High density urban area in 1 200 meters resolution grid cells where the new building was located.

Alternative 3: Constitutes construction of both new buildings.

ESRI shape format coverages as well as map composition have been sent to know the exact location of the new buildings. In the Figure 55, we can see the Gliwice Central Arena, yellow building and the Centre of New Technologies, green buildings.

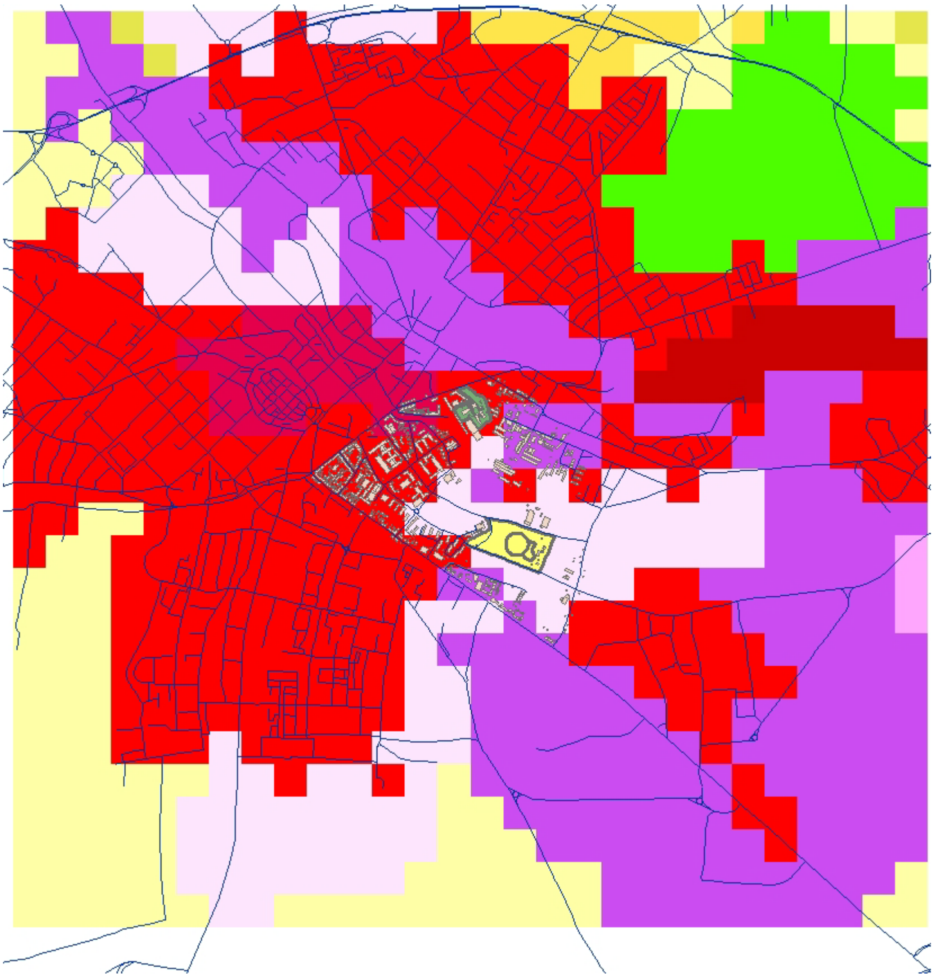

Figure 55: Gliwice alternatives location. Background land use map.

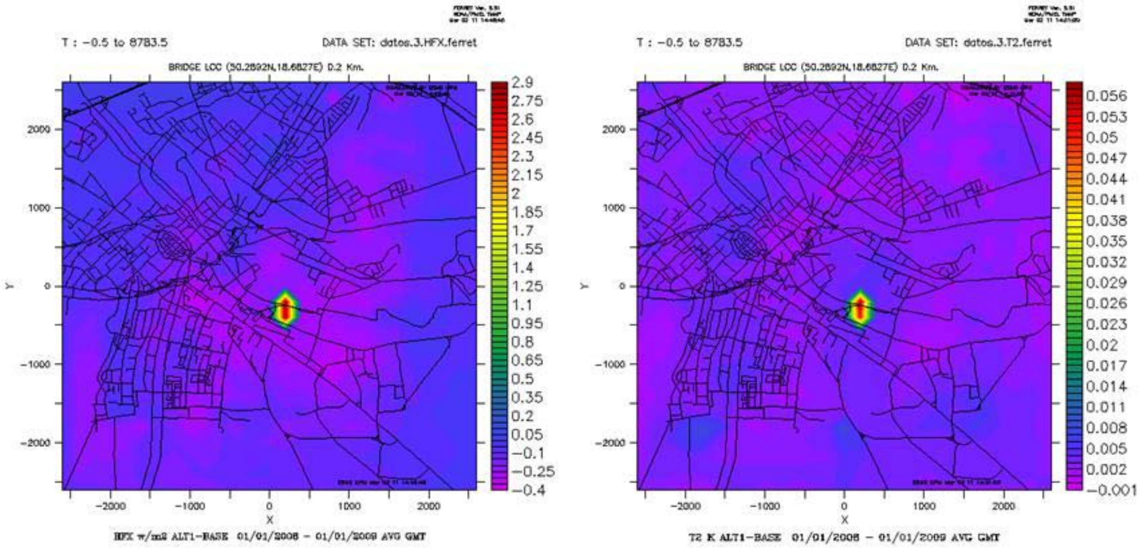

Figure 56: Differences between alternative 1 and base run annual average of Sensible heat flux (left), Air temperature (right), domain 0.2 km resolution over Gliwice.

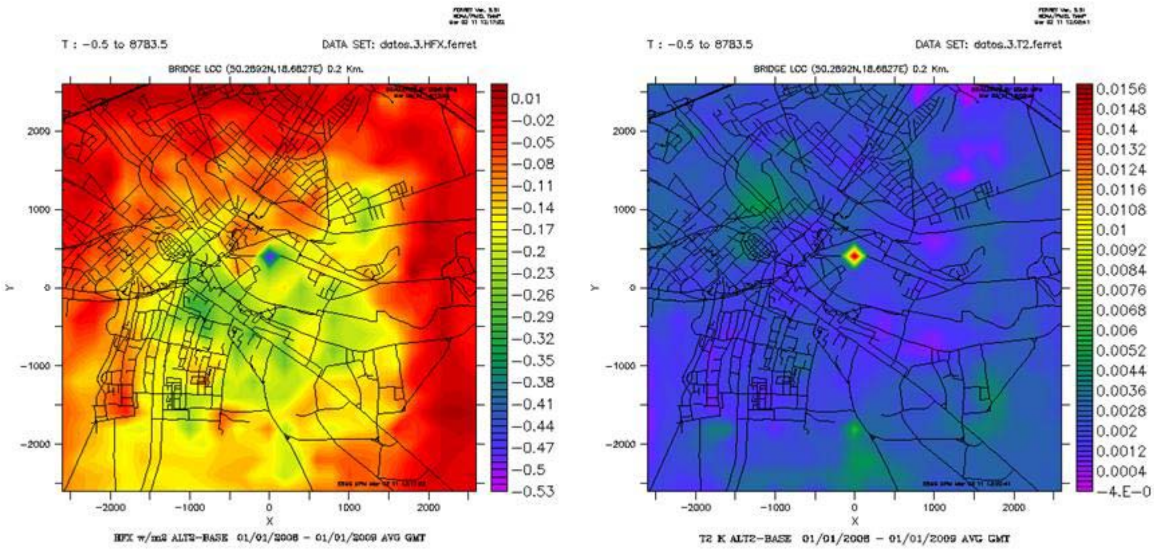

Figure 57: Differences between alternative 2 and base run annual average of Sensible heat flux (left), Air temperature (right), domain 0.2 km resolution over Gliwice.

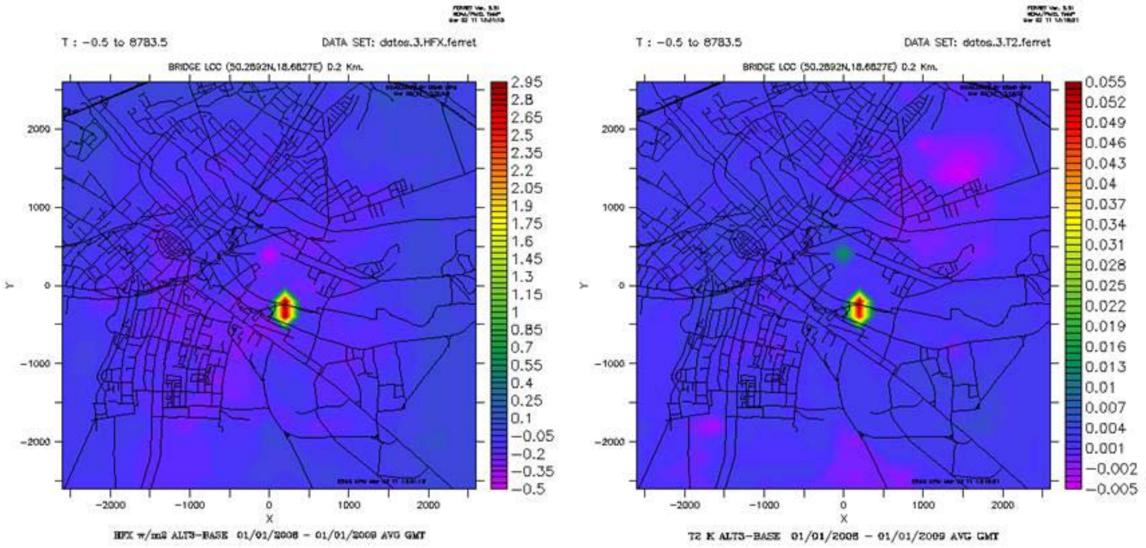

Figure 58: Differences between alternative 2 and base run annual average of Sensible heat flux (left), Air temperature (right), domain 0.2 km resolution over Gliwice.

2.7.4 Firenze

Alternative1: Complete reforestation of a green area and a sport arena in the Cascine Park, Figure 59, yellow eclipse. The alternative is an increase of trees (deciduous) by about 27% of the total. This alternative have been implemented into the model, changing land uses from sport hall and grassland to deciduous trees.

Alternative 2: Redevelopment of a former industrial area (FIAT) in the north of the Cascine Park, San Donato Park, Figure 59, blue eclipse. This alternative has been implemented into the model, changing land use from industrial to grassland.

Alternative 3: Implementation of both planning alternatives (alternatives 1 and 2).

In all alternatives no new emission has been considered, so the air pollution differences are due to the different meteorological information produced by each alternative.

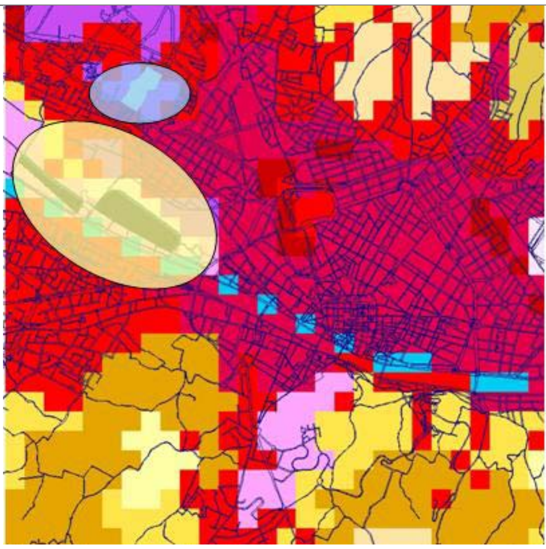

Figure 59: Alternatives for Firenze, land uses

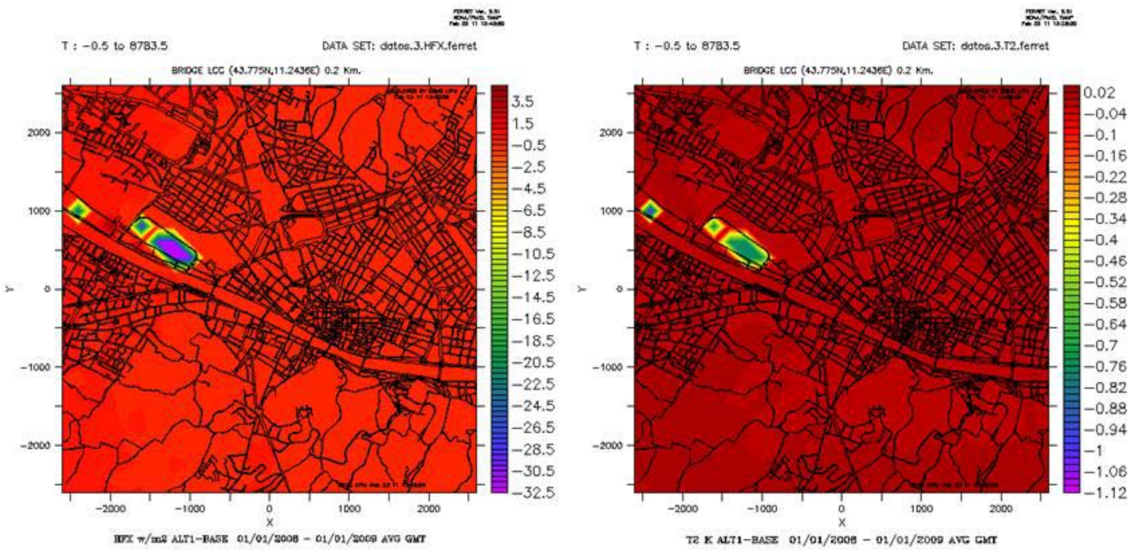

Figure 60: Differences between alternative 1 and base run annual average of Sensible heat flux (left), Air temperature (right), domain 0.2 km resolution over Firenze

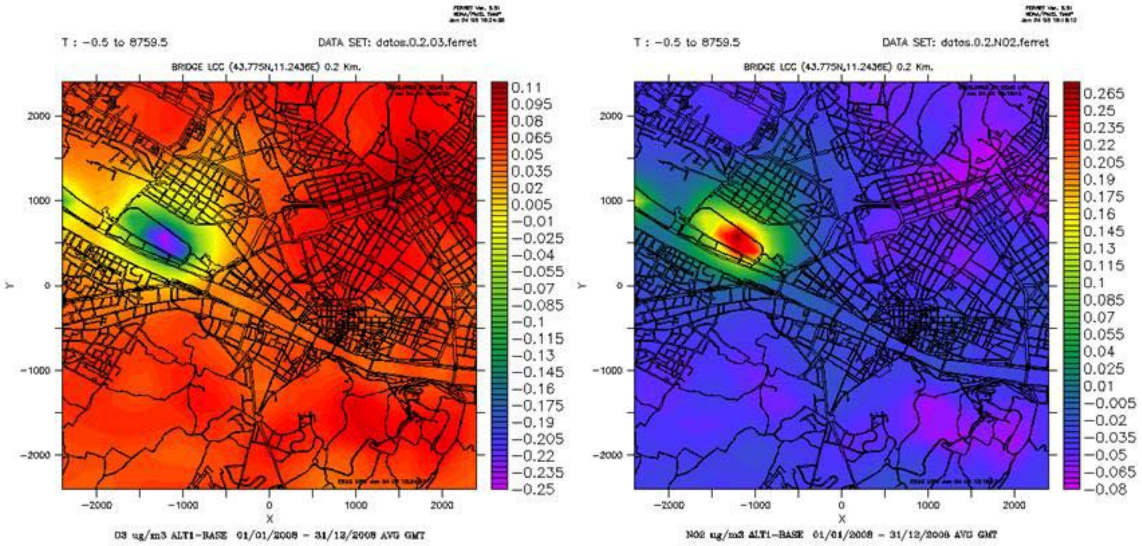

Figure 61: Differences between alternative 1 and base run annual average of Ozone (left) and Nitrogen Dioxide (right). domain 0.2 km resolution over Firenze

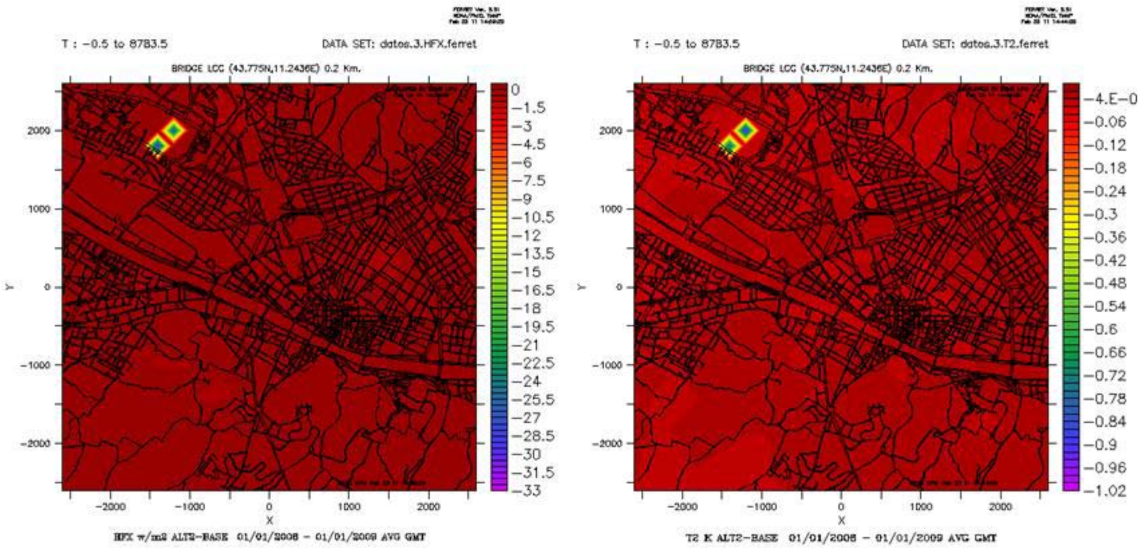

Figure 62: Differences between alternative 2 and base run annual average of Sensible heat flux (left), Air temperature (right), domain 0.2 km resolution over Firenze

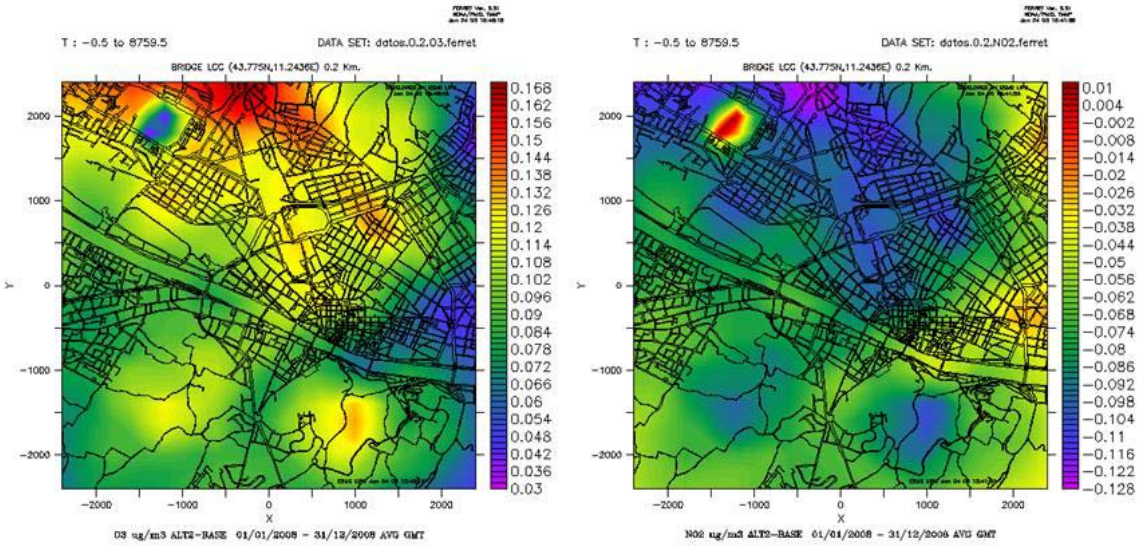

Figure 63: Differences between alternative 2 and base run annual average of Ozone (left) and Nitrogen Dioxide (right). domain 0.2 km resolution over Firenze

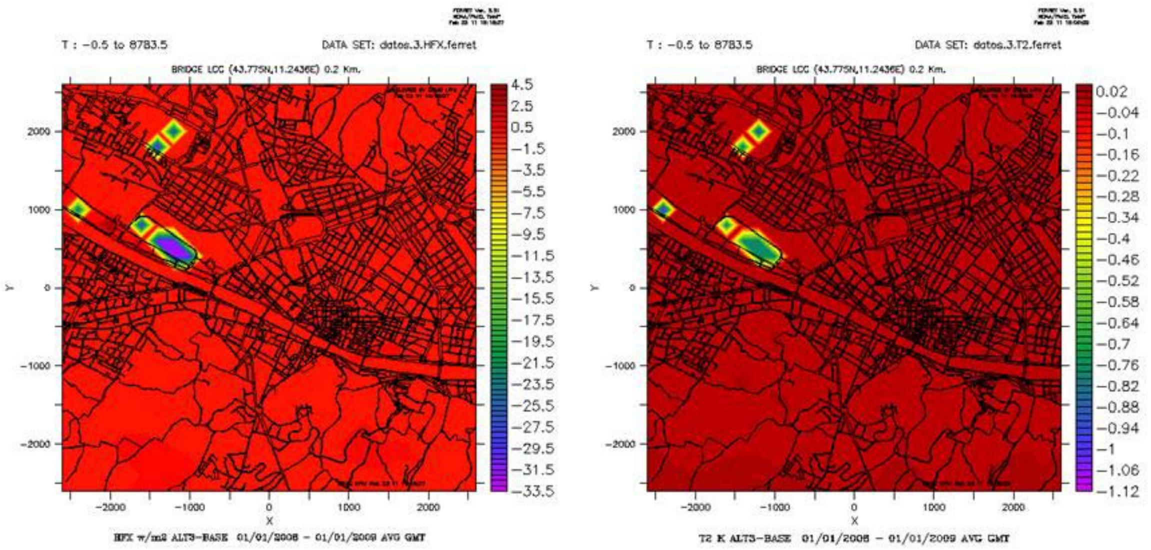

Figure 64: Differences between alternative 3 and base run annual average of Sensible heat flux (left), Air temperature (right), domain 0.2 km resolution over Firenze

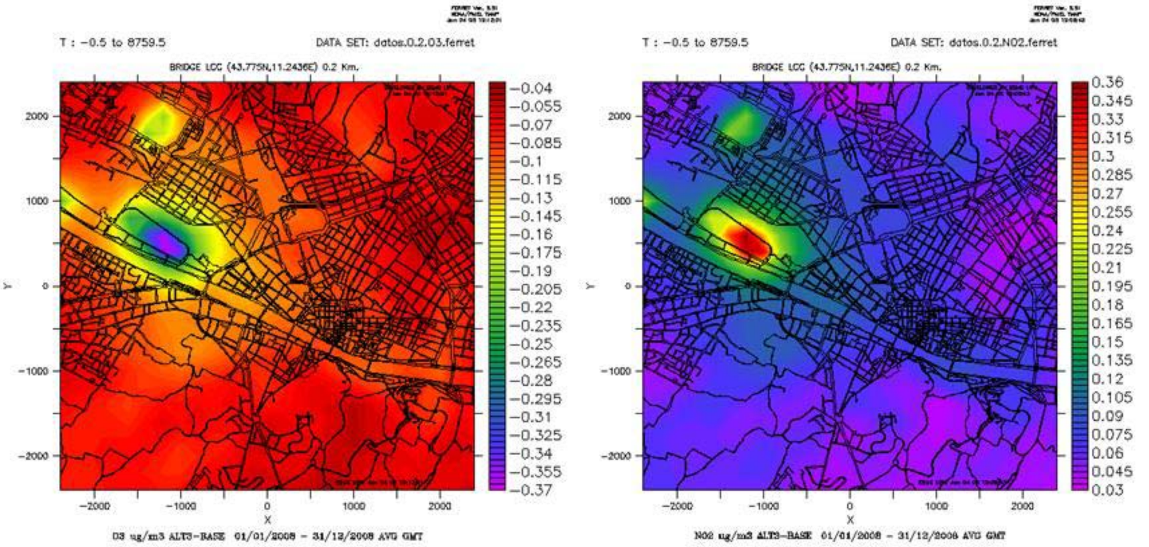

Figure 65: Differences between alternative 3 and base run annual average of Ozone (left) and Nitrogen Dioxide (right). domain 0.2 km resolution over Firenze

2.7.5 London

Alternative 1: Add new street trees.
Alternative 2: Add green roofs on flat roofs.
Alternative 3: Add both street trees plus green roofs.

A land cover analysis for the Central Activity Zone London has been received. It was developed by Fredrik Lindberg and Sue Grimmond. Rules used to add vegetation in the Central Activity Zone, Central London. These are based on discussions between Matthew Thomas (Greater London Authority), Dr Fredrik Lindberg (KCL, University of Göteborg) and Prof Sue Grimmond (KCL). Land cover data for both alternatives and fractions of flat, intermediate and sloping roofs per 200 meters resolution grid cells have been received.

To implement the London alternatives some considerations have to be taking into account. WRF/UCM works with 23 land use types + one urban land use type. When UCM is included the urban land use type is split into three types.

The land cover data are based on 7 characteristics (buildings, roads, water, grass, conifer, deciduous, shrubs). The first step is to establish a correspondence between land cover information and USGS+UCM land use types. We have decided the following, the maximum fraction of land cover will be used to assign the land use, using this transformations:

Buildings and roads --> urban
water --> Water Bodies
grass --> Grassland

conifer	-->	Evergreen Broadleaf
deciduous	-->	Deciduous Broadleaf
shrubs	-->	Shrub land

To implement the changes in the land use, we have taken the following criteria: Check if those grid cells have changed respect the base WRF/UCM land use classification and change them if so. These changes affect to 2.17% of the grid cells in the alternative1, 0.51% in the alternative 2 and 3.32% in the alternative 3. The changes are from urban land use to decidious broadlif in alternative 1 and grassland in alternative 2.

The new street trees and green roofs, make changes in 3 important parameters of the UCM, like as, roof width, road width, and fraction of urban by each type or urban: Commercial/Industrial/Transport, high urban, low urban.

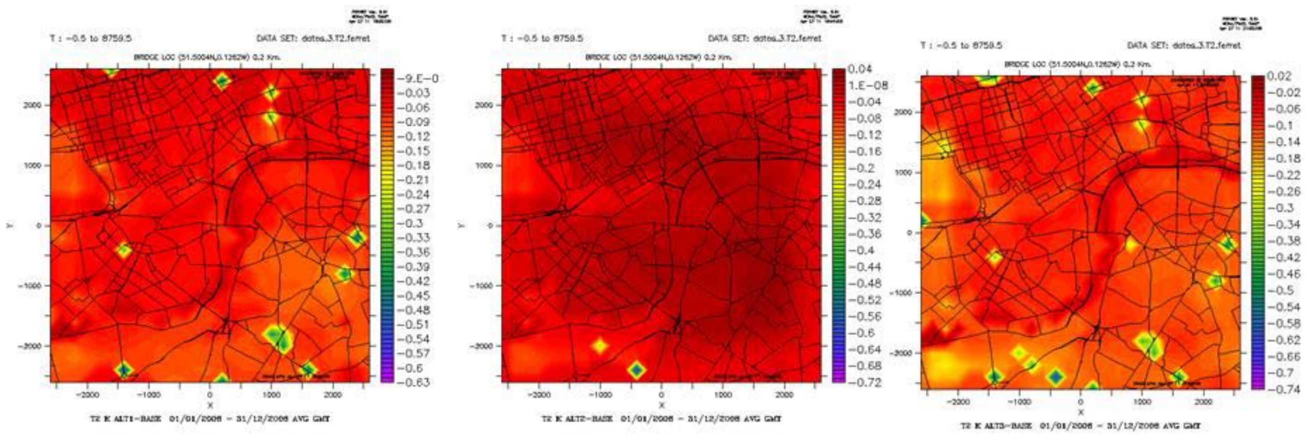

Figure 66: Differences between alternatives and base run annual average of Air temperature, domain 0.2 km resolution over London. Alternative 1 (left), Alternative 2 (middle), Alternative 3 (right)

2.8 Climate scenarios

The selection and analysis of outputs for different climate scenarios helps to understand the uncertainty on future projections derived from climate data. The dynamical downscaling from global outputs to local models allows increasing the spatial and temporal resolution of the projected climate scenarios. The scenario selection is derived from the work developed by the WP7.

For the climate data, results from the global model CCSM have been selected. The Community Climate System Model (CCSM) is a coupled climate model for simulating the earth's climate system. Composed of four separate models simultaneously simulating the earth's atmosphere, ocean, land surface and sea-ice, and one central coupler component, the CCSM allows researchers to conduct fundamental research into the earth's past, present and future climate states.. CCSM3 output data is disseminated via the Earth System Grid (ESG).

The CCSM outputs cover a global Gaussian grid with T85 resolution and 26 vertical levels with a hybrid coordinates system. The data have been transformed to a fixed grid with 1.5º horizontal spatial resolution and 17 pressure vertical levels. The new data are ready to be used by the WRF/UCM modelling system. The transformation process includes a regridding procedure and vertical interpolation. The changed CCSM outputs have been used as boundary and initial conditions to run the WRF/UCM model.

Different IPCC future scenarios have been simulated with the CCSM model to know the future clime, Figure 67. Each scenario has a different emission inventory, Figure 68.

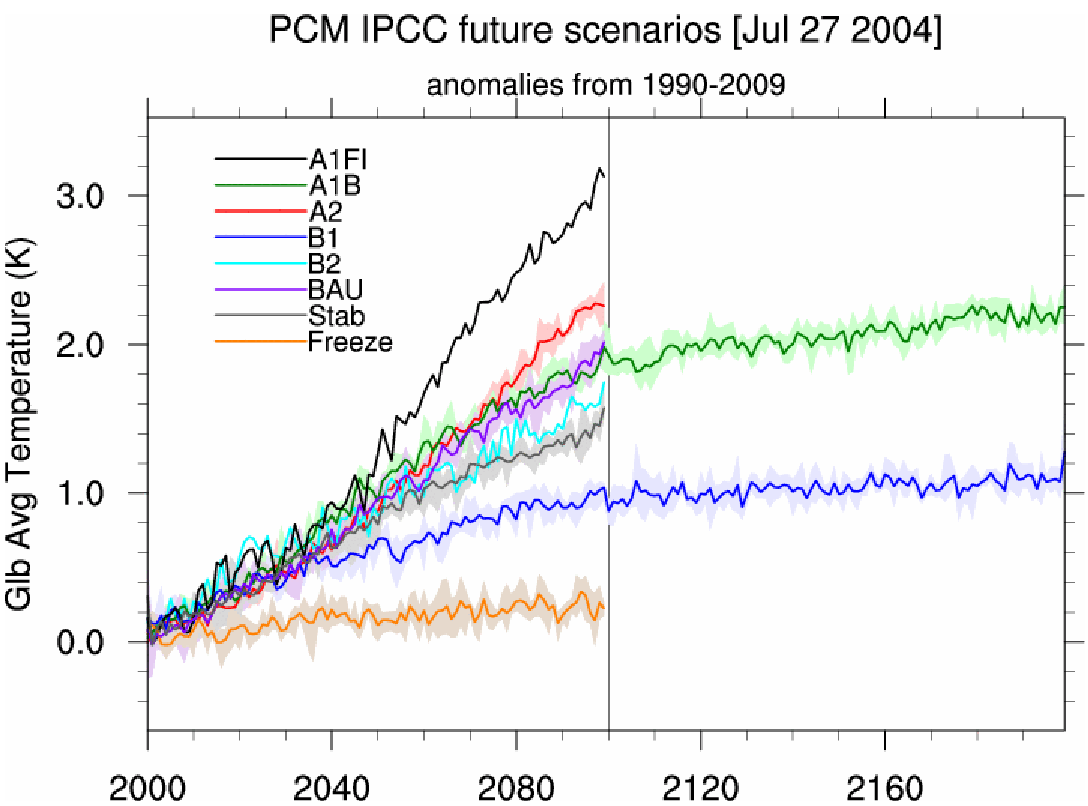

Figure 67: Anomalies of Temperature for IPCC scenarios with CCSM model.

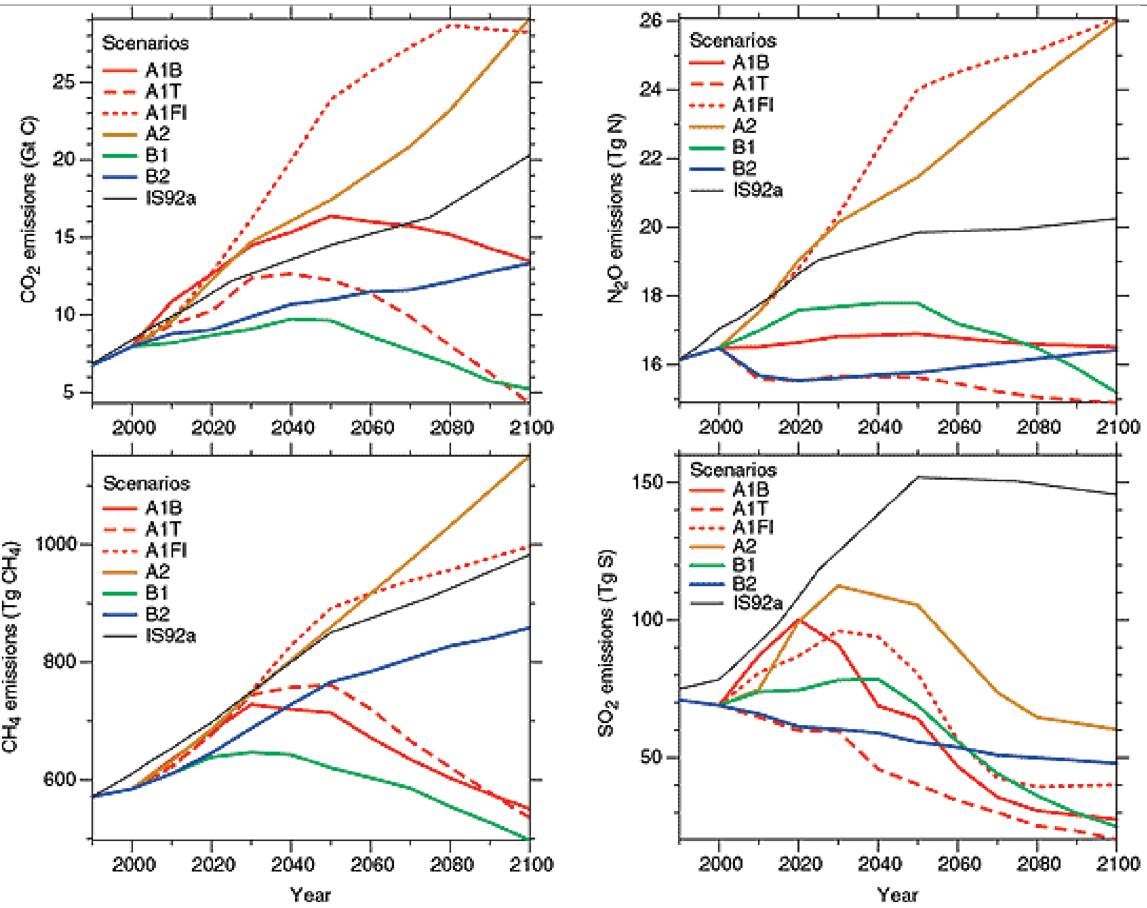

Figure 68: Emission values for the IPCC scenarios

The time period selected was July, August and September 2030 to the future scenarios, and a 2008 base scenario. In order to get the best initial and boundary conditions, only 6 hourly data available can be used. The following table summarizes the 6 hourly data available:

Case name	Time span	Description
b30.030e	**1900 - 1999**	**20th century (20C3M)**
b30.036e	**2000 - 2099**	**climate change commitment (Commit)**
b30.040e	**2000 - 2099**	**IPCC SRES A1B scenario (SRESA1B)**
b30.099a	**2000 - 2099**	**IPCC SRES A1FI scenario (SRESA1FI)**
b30.042e	**2000 - 2099**	**IPCC SRES A2 scenario (SRESA2)**
b30.041e	**2000 - 2099**	**IPCC SRES B1 scenario (SRESB1)**

We have selected commitment scenario as base scenario and SRESA2, SRESA1FI, SRESB1 as future scenarios. A correspondence between BRIDGE scenarios defined in the D 7.1. and IPCC scenario have to be developed and it is the following:

BRIDGE 1 (SCE1) – A2
BRIDGE 2 (SCE2)– A1FI
BRIDGE 3 (SCE3) – B1

BRIDGE SCENARIO 1 (D 7.1): <u>BRIDGE in wonderland</u>

- Gradual transition to renewable energy sources
- Efficient use of energy
- Cleaner uses of fossil energy
- Low level of climate change
- Socially balanced society
- Highly productive economy

CCSM IPCC SCENARIO: A2 (medium emission scenario)

- A very heterogeneous world
- Strengthening regional cultural identities
- Emphasis on family values and local traditions
- High population growth
- Less concern for rapid economic development

BRIDGE SCENARIO 2 (D 7.1): <u>Climate change is a burning issue</u>

- Energy is not that big a problem
- Economy is growing
- Climate change is a serious threat
- It is absolutely necessary cut GHG emissions
- It is absolutely necessary absorb GHG

CCSM IPCC SCENARIO: A1FI (worst emission scenario)

- Very rapid economic growth
- Low population growth
- New and more efficient technology
- Economic and cultural convergence
- Reduction in regional differences in per capita income

BRIDGE SCENARIO 3 (D 7.1): <u>Lack of energy in freezing the economy</u>

- Energy shortage
- Reduced mobility leads to urban concentration
- Resource are diverted for fast increase of renewable sources
- Fossil energy sources are almost depleted

CCSM IPCC SCENARIO: B1 (best emission scenario)

- Convergent world
- Rapid changes in economic structures
- Reduction in materials intensity

- Introduction of clean and resource-efficient technologies

2.8.1 Athens

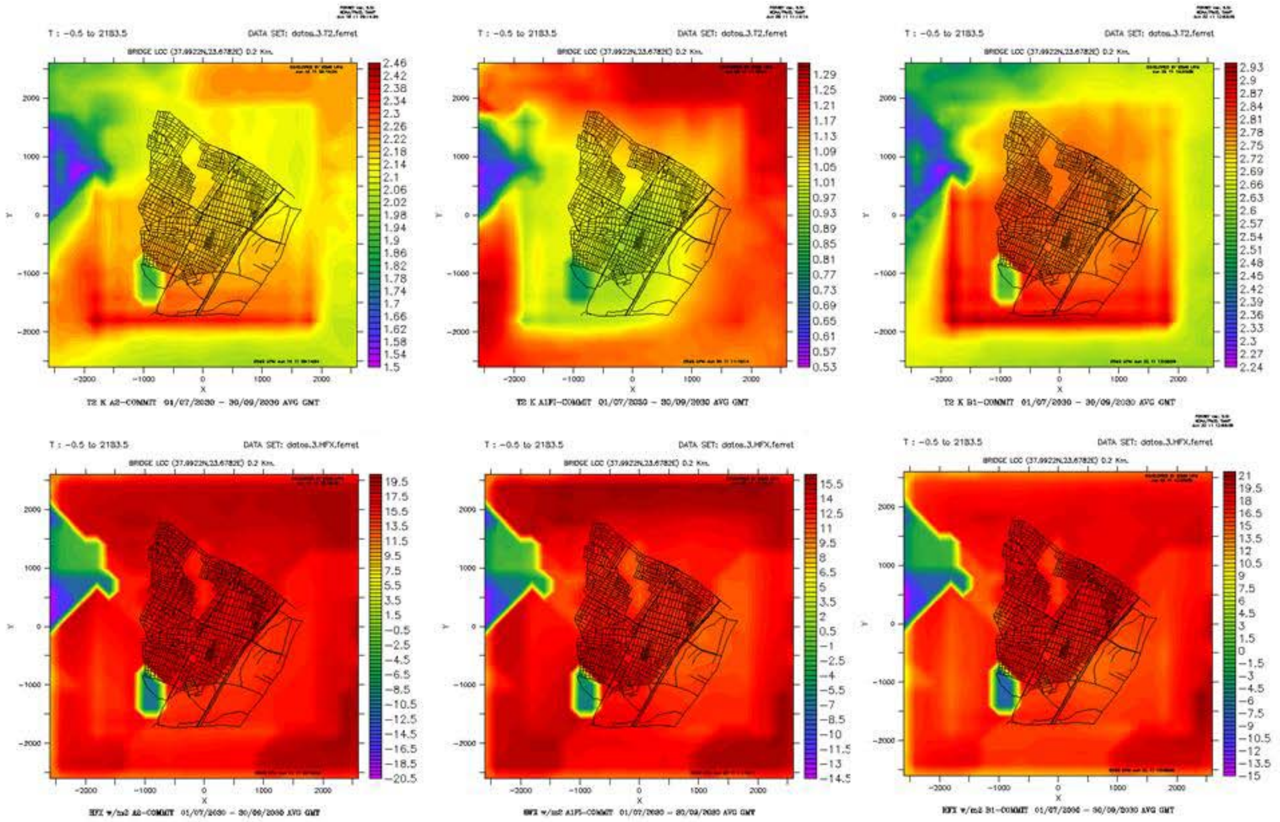

Figure 69: Differences between year 2030 and base run 2008, Scenario 1 (left), Scenario 2 (middle), Scenario 3 (right). Annual average of Sensible heat flux (bottom) and Air temperature (top), domain 0.2 km resolution over Athens

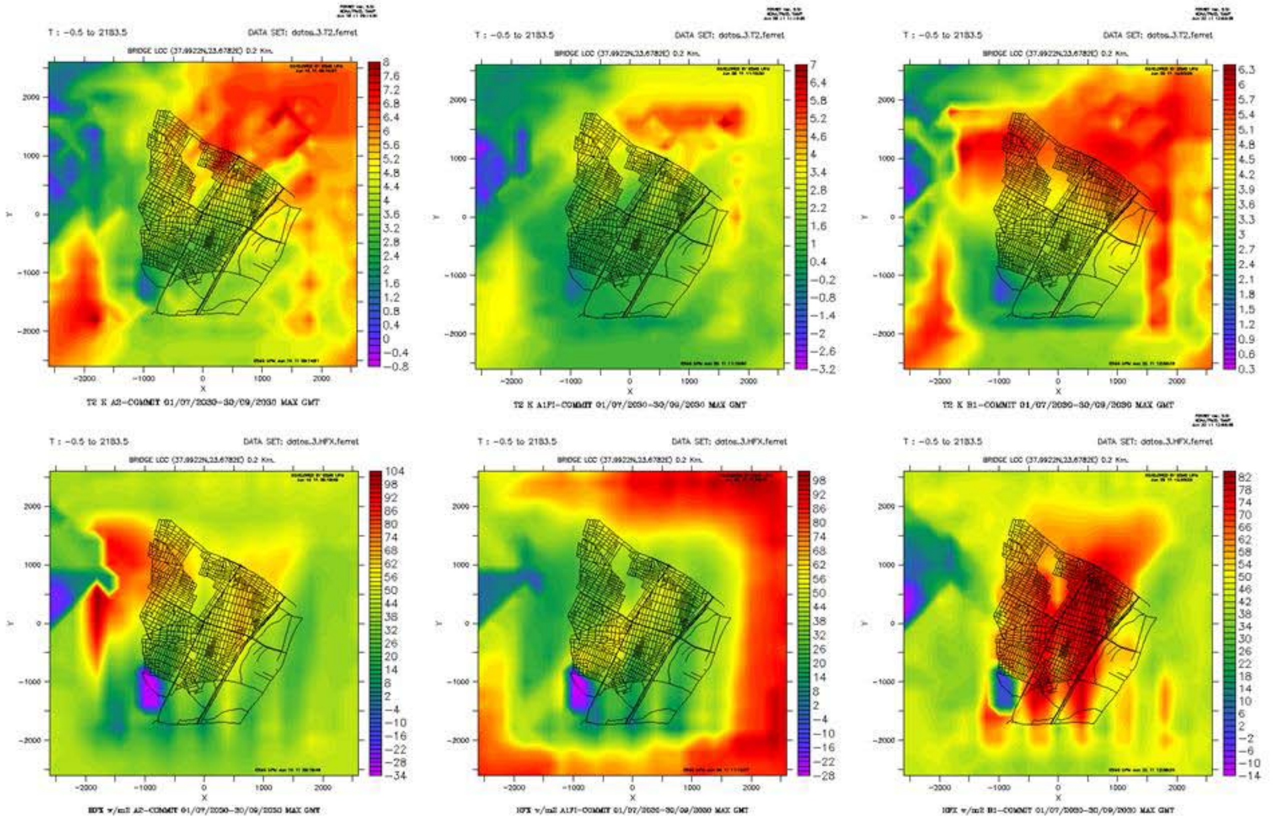

Figure 70 : Differences between year 2030 and base run 2008, Scenario 1 (left), Scenario 2 (middle), Scenario 3 (right). Annual maximum of Sensible heat flux (bottom) and Air temperature (top), domain 0.2 km resolution over Athens.

2.8.2 Helsinki

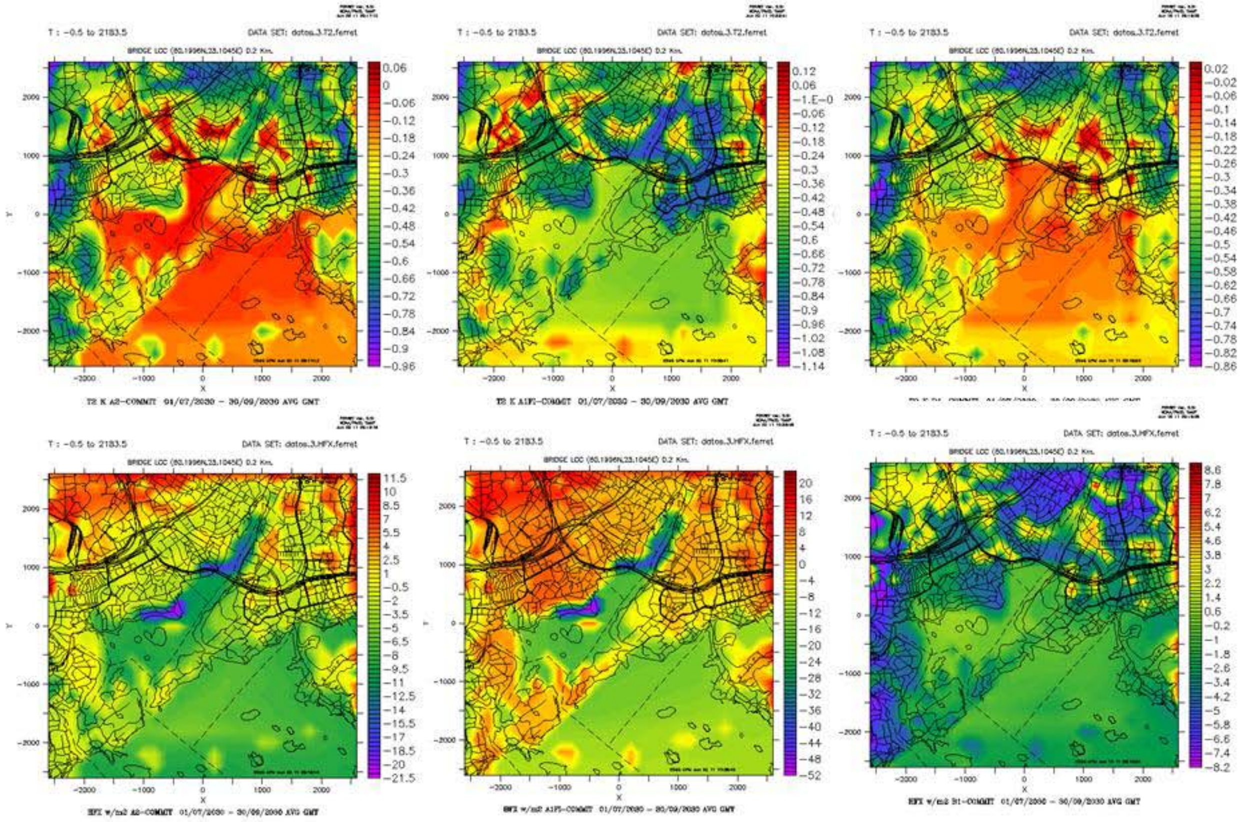

Figure 71 : Differences between year 2030 and base run 2008, Scenario 1 (left), Scenario 2 (middle), Scenario 3 (right). Annual average of Sensible heat flux (bottom) and Air temperature (top), domain 0.2 km resolution over Helsinki.

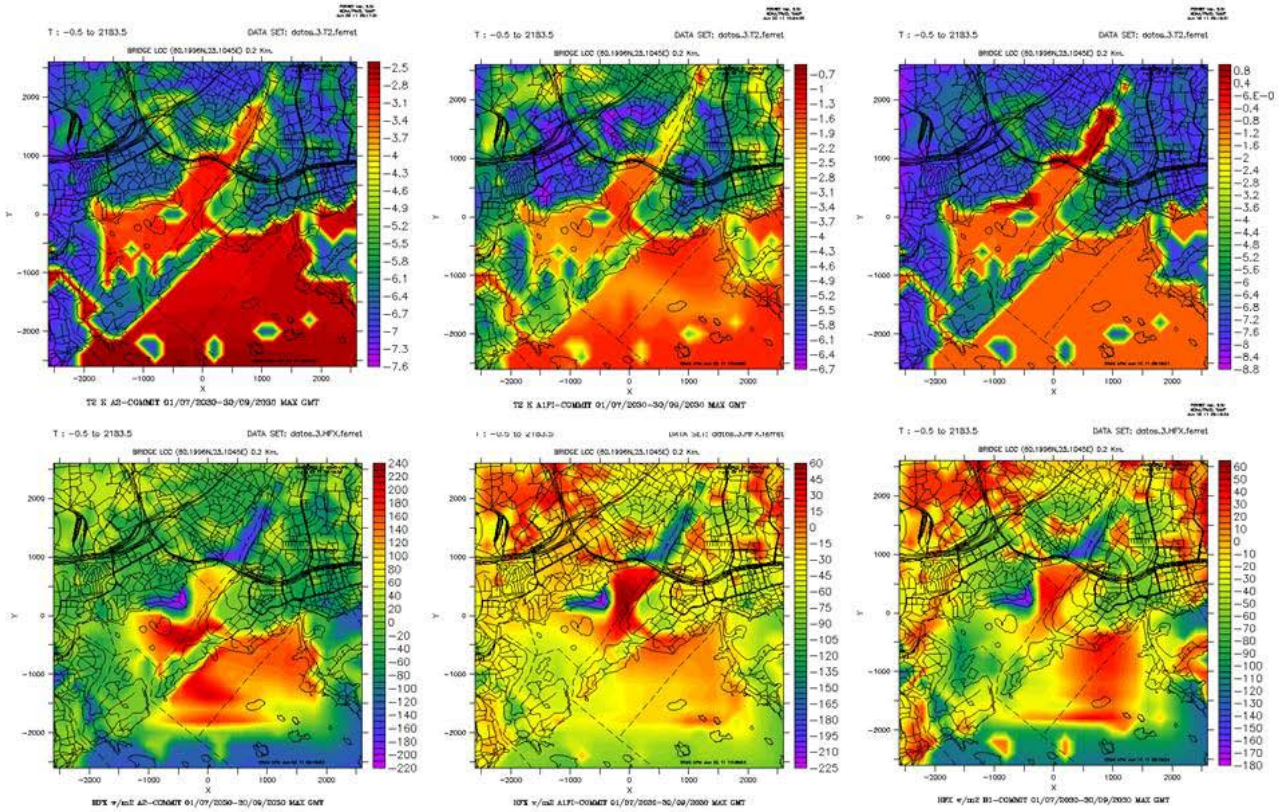

Figure 72: Differences between year 2030 and base run 2008, Scenario 1 (left), Scenario 2 (middle), Scenario 3 (right). Annual maximum of Sensible heat flux (bottom) and Air temperature (top), domain 0.2 km resolution over Helsinki.

2.8.3 Gliwice

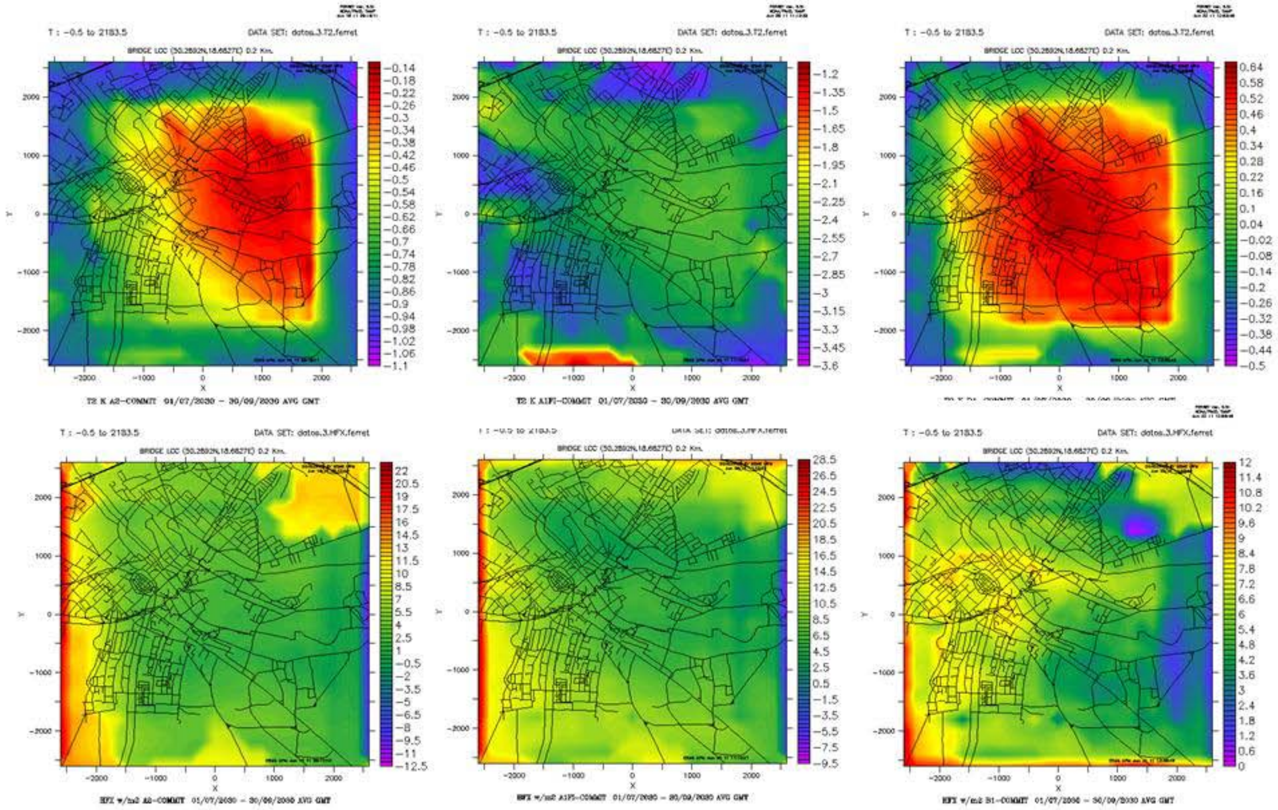

Figure 73: Differences between year 2030 and base run 2008, Scenario 1 (left), Scenario 2 (middle), Scenario 3 (right). Annual average of Sensible heat flux (bottom) and Air temperature (top), domain 0.2 km resolution over Gliwice.

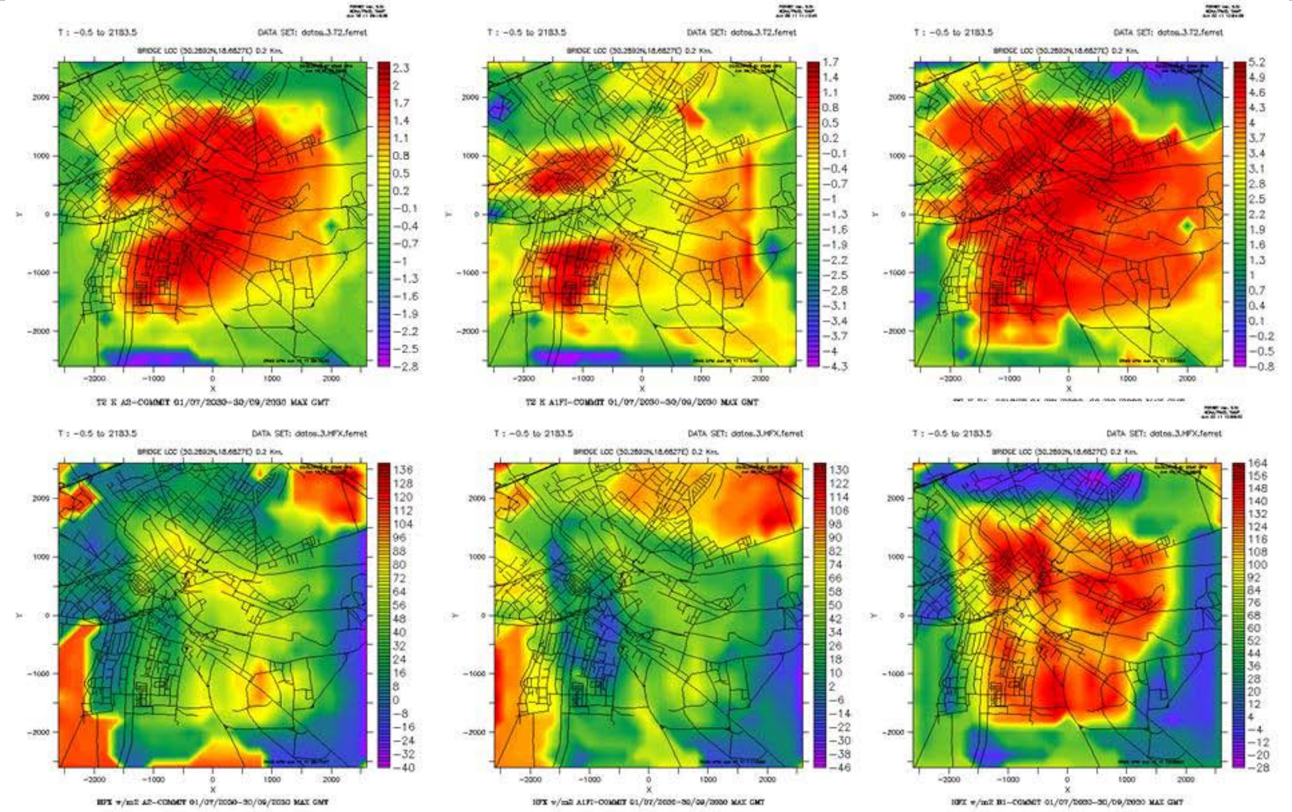

Figure 74: Differences between year 2030 and base run 2008, Scenario 1 (left), Scenario 2 (middle), Scenario 3 (right). Annual maximum of Sensible heat flux (bottom) and Air temperature (top), domain 0.2 km resolution over Gliwice.

2.8.4 Firenze

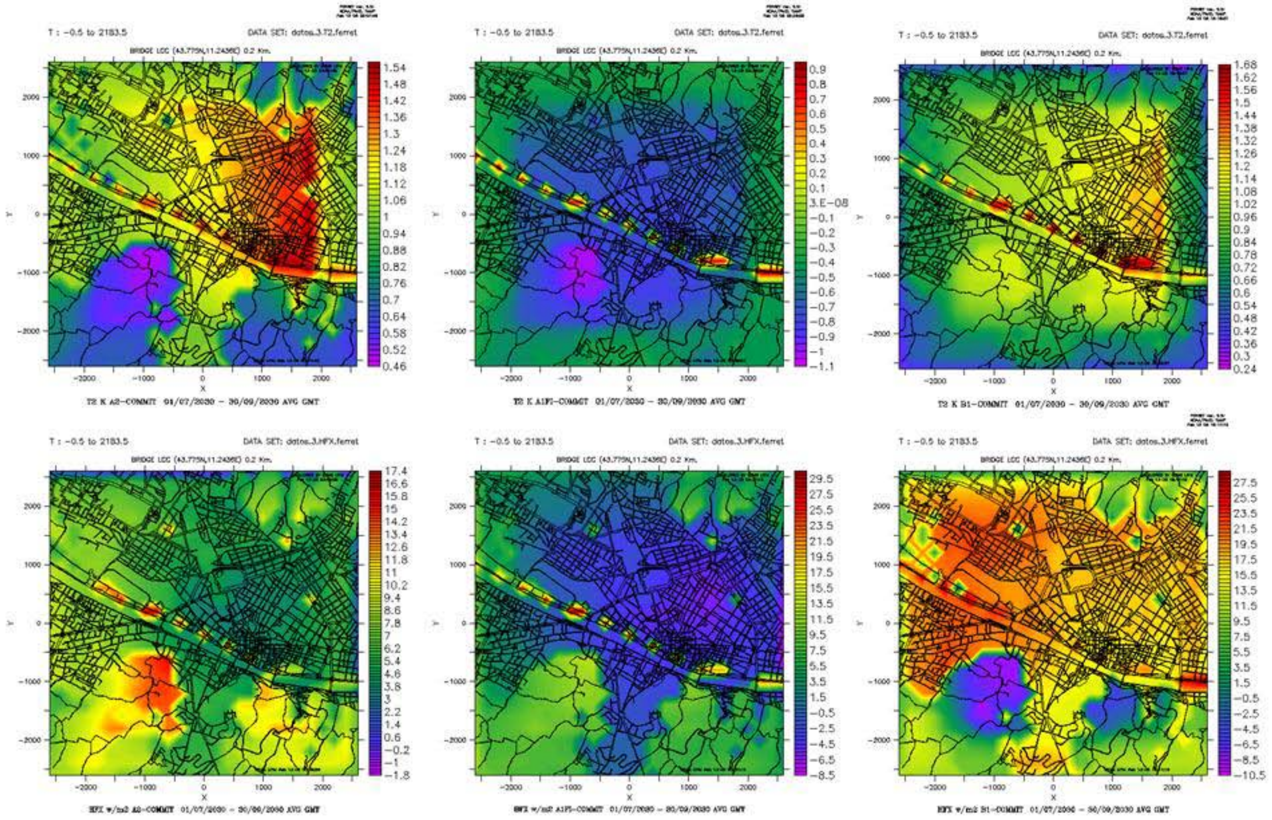

Figure 75 : Differences between year 2030 and base run 2008, Scenario 1 (left), Scenario 2 (middle), Scenario 3 (right). Annual average of Sensible heat flux (bottom) and Air temperature (top), domain 0.2 km resolution over Firenze.

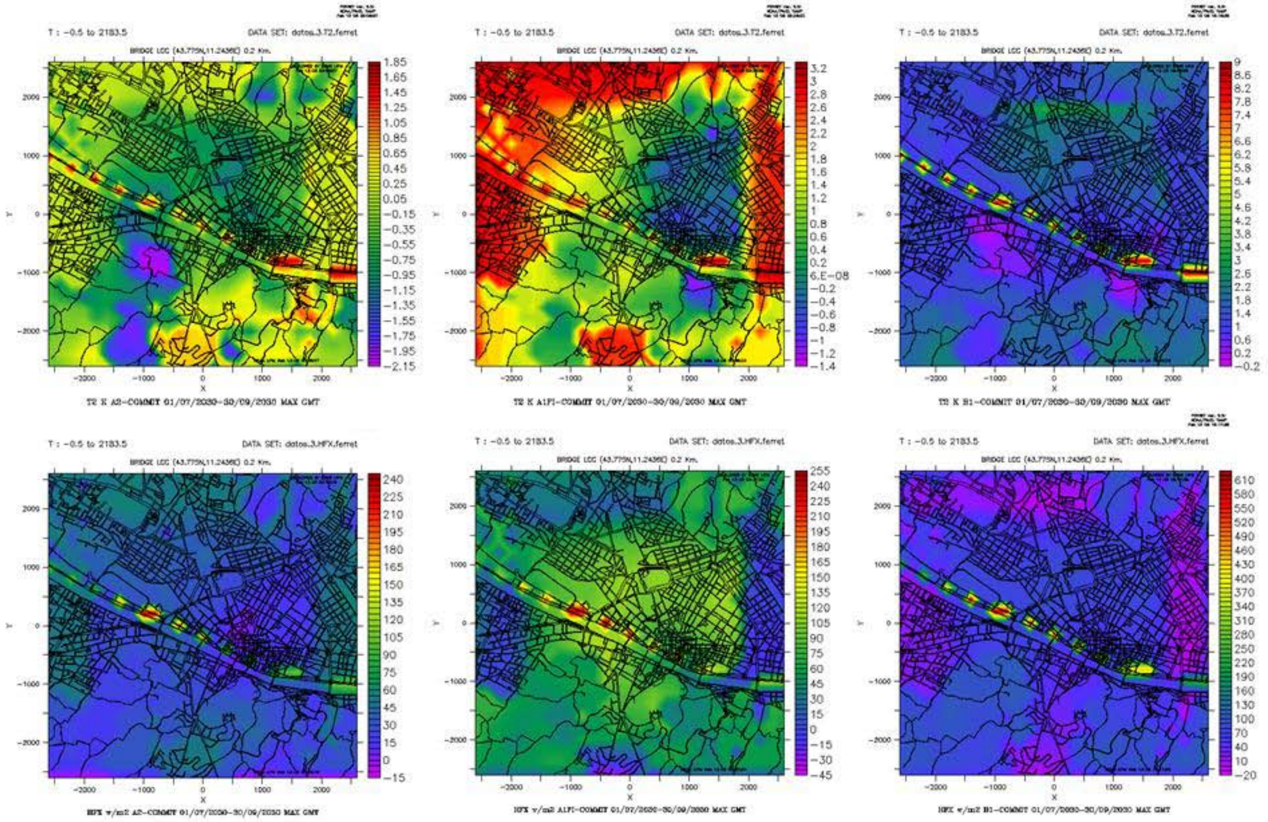

Figure 76: Differences between year 2030 and base run 2008, Scenario 1 (left), Scenario 2 (middle), Scenario 3 (right). Annual maximum of Sensible heat flux (bottom) and Air temperature (top), domain 0.2 km resolution over Firenze.

3 CAMx AND URBAIR. UAVR MODELS.

3.1 CAMx. UAVR OFF-LINE MESOSCALE MODEL.

The initial modelling approach by UAVR in BRIIDGE was to apply the MM5 meteorological model to drive the air quality simulations with model CAMx (please refer to Deliverable 4.1 – Model Selection Report). However, during the continuation of the project and resulting from discussion with project partners, for sake of consistency and to avoid the duplication of work, it was decided that CAMx air quality model would instead be driven by WRF outputs obtained by UPM partner.

CAMx air quality model will only be applied to the base situation of the case studies; the impacts of the different planning alternatives in terms of air quality will be analysed by UAVR team making use of URBAIR model (please refer to section 4 of this document).

3.1.1 Brief description.

The Comprehensive Air quality Model with extensions (CAMx) was developed by ENVIRON International Cooperation, from California, United States of America. CAMx [Morris et al., 2004] is an Eulerian photochemical dispersion model that allows the integrated “one-atmosphere” assessment of gaseous and particulate air pollution over many scales ranging from sub-urban to continental.

CAMx simulates the emission, dispersion, chemical reaction, and removal of pollutants in the troposphere by solving the pollutant continuity equation for each chemical species on a system of nested three-dimensional grids. The Eulerian continuity equation describes the time dependency of the average species concentration within each grid cell volume as a sum of all of the physical and chemical processes operating on that volume. The continuity equation is numerically marched forward in time over a series of time steps. At each step, the continuity equation is replaced by an operator-splitting approach that calculates the separate contribution of each major process (emission, advection, diffusion, chemistry, and removal) to concentration change within each grid cell [ENVIRON, 2010].

CAMx carries pollutant concentrations at the center of each grid cell volume, representing the average concentration over the entire cell. Meteorological fields are supplied to the model to quantify the state of the atmosphere in each grid cell for the purposes of calculating transport and chemistry. CAMx incorporates two-way grid nesting, which means that pollutant concentration information propagates into and out of all grid nests during model integration. Any number of grid nests can be specified in a single run, while grid spacing and vertical layer structures can vary from one grid nest to another. The nested grid capability of CAMx allows cost-effective application to large regions in which regional transport occurs, yet at the same time providing fine resolution to address small-scale impacts in selected areas [ENVIRON, 2010].

The CAMx gas-phase chemical mechanisms include the 2005 version of Carbon Bond [CB05; Yarwood et al., 2005b], SAPRC99 [Carter, 2000] and several versions of Carbon Bond IV [CB4; Gery et al., 1989]. The gas phase chemical mechanisms currently supported are listed in the next table.

Table 1 – Chemistry mechanisms currently implemented in CAMx [ENVIRON, 2010].

Mechanism ID	Description
6	CB05, the 2005 version of the Carbon Bond mechanism developed for use in EPA atmospheric modelling studies. This mechanism optionally includes the same aerosol and mercury chemistry as Mechanism 4. 156 reactions and up to 89 species (54 state gases, up to 22 state particulates, and 13 radicals).
5	The fixed parameter version of the SAPRC99 gas-phase mechanism. This mechanism optionally includes the same aerosol and mercury chemistry as Mechanism 4. 217 reactions and up to 114 species (76 state gases, up to 22 state particulates, and 16 radicals).
3	CB4 gas-phase chemistry with revised PAN chemistry, additional radical-radical termination reactions and updated isoprene chemistry. 96 reactions and 36 species (26 state gases and 10 radicals).
4	Mechanism 3 with additional inorganic gas-phase reactions important for regional modelling. This mechanism optionally includes aerosol and mercury chemistry. 113 reactions and up to 76 species (up to 44 state gases, up to 22 state particulates, and 10 radicals).
10	A user-defined simple chemistry mechanism can be developed for any gas and/or particulate species.

3.1.2 Architecture and domains

CAMx model was applied to 3 of the 5 BRIDGE study cases (see Figure 2), namely: Helsinki, Gliwice and London. The air quality simulations were performed for 2 domains for each city, corresponding to the WRF simulation domains presented in section 2.2 of this report. The first domain (with 5.4 km x 5.4 km resolution) was used to drive the second domain's simulations (0.2 km x 0.2 km resolution). Both domains were simulated with 17 vertical levels.

3.1.3 Computing platform

Due its complexity and computer resources needs, CAMx model will not integrate the BRIDGE DSS; the model was run separately and the output data are sent to DSS system database. The simulations were performed on a 25-node Beowulf Linux Cluster belonging to UAVR's research group.

3.1.4 Input data preprocessing.

CAMx requires input files that configure each simulation, define the chemical mechanism, and describe the photochemical conditions, surface characteristics, initial/boundary conditions, emission rates, and various meteorological fields over the entire modelling domain. Preparing this information requires several pre-processing steps to translate “raw” emissions, meteorological, air quality and other data into the final input files for CAMx. Some changes have been performed in order to implement WRF-CAMx system. The following figure presents the structure of the model, including the pre- and post-processors, and relations between them.

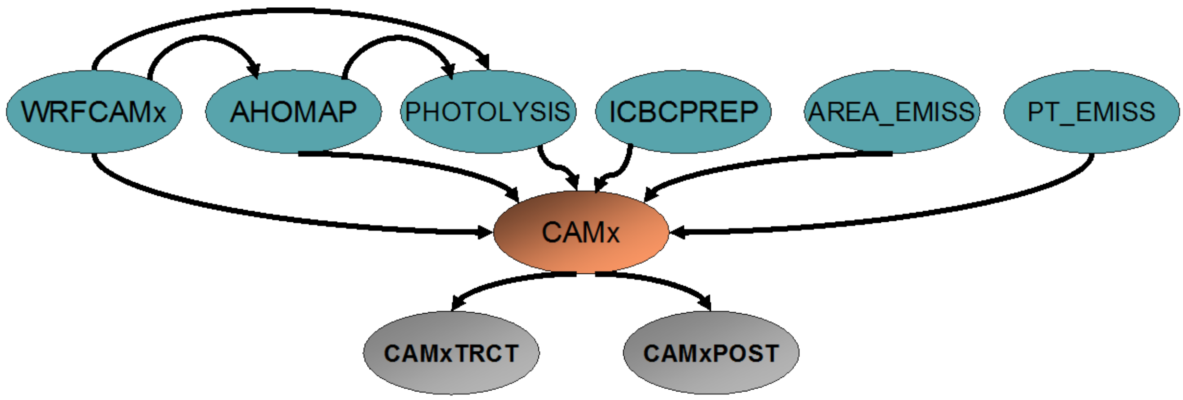

Figure 77: The CAMx modelling system

3.1.5 Meteorology, topography and land use

The WRFCAMx pre-processor generates CAMx meteorological input files from the WRF output files, including land use, altitude/pressure, wind, temperature, moisture, clouds/rain and vertical diffusivity. . The program offers four horizontal interpolation options, for BRIDGE simulations the CAMx grid was defined on the same projection and horizontal grid resolution as WRF. In this case WRFCAMx simply windows data from a portion of the WRF grid and outputs the subset to the CAMx files. The CAMx physical height layer structure (meters AGL) is defined from the geopotential heights at each of WRF's "eta" levels, and thus varies in space and time.

Land use information was also provided by the WRF model through the WRFCAMx pre-processor. However the program considered only the 24 USGS land use categories originally present in WRF model; AS these categories were changed (refer to section 2.4.3) WRFCAMx was altered in order to consider the additional land use classes: low density urban, high density urban and commercial/industrial and transportation.

3.1.6 Initial and boundary conditions

Initial concentrations and hourly boundary conditions were created from output concentration files from the LMDz-INCA chemistry-climate global circulation model [Hauglustaine et al., 2004] for gaseous species, and from the global model GOCART [Ginoux et al., 2001] for aerosols.

In order to use the output files from the global models, an ICBCPREP interface program, developed within collaboration between the University of Santiago de Compostela and the University of Aveiro, was used. The program allows the reading of the global model's output data and the writing of these data in a CAMx-compatible format. This program executes all the interpolation operations necessary to adapt the data given by the global models (with a grid resolution between 0.5 and 1 degree) to those needed for the air quality simulations (a few kilometres resolution). The application of the interface program results in the production of 12 IC and 12 BC files, containing different concentration values for each month of the year.

3.1.7 Emissions

3.1.7.1 TNO dataset

The emission dataset described in this section was used as input for the air quality simulations for Helsinki (both domains), Gliwice (both domains) and London's domain 1, with 5400 m x 5400 m resolution. For London's domain 2 the London Atmospheric Emission Inventory was used (see next section for more details).

CAMx air quality simulations were performed using the TNO European emission data set prepared for the EU FP project GEMS, for the year 2003, with 1/8 x 1/16 degree resolution [Visschedijk et al., 2007]. The inventory includes emissions for SO2, NOx, NH3, CO, NMVOC, CH4, PM10 and PM2.5, given at the SNAP 97 1st level that consists of 11 source categories, commonly adopted in air quality modelling (see Table). In addition, the inventory also includes emission data for international shipping.

Table 2 – Description of source categories [Visschedijk et al., 2007].

SNAP	Description
1	Public electricity and other energy transformation
2	Small combustion plants
3	Industrial combustion and processes with contact
4	Industrial process emission
5	Fossil fuel production
6	Solvent and product use
7	Road transport
8	Other (non-road) transport and mobile machinery
9	Waste disposal
10	Agriculture
11	Nature

An example of the gridded emission data for Europe is given in the next Figure for NOx emissions from all sectors.

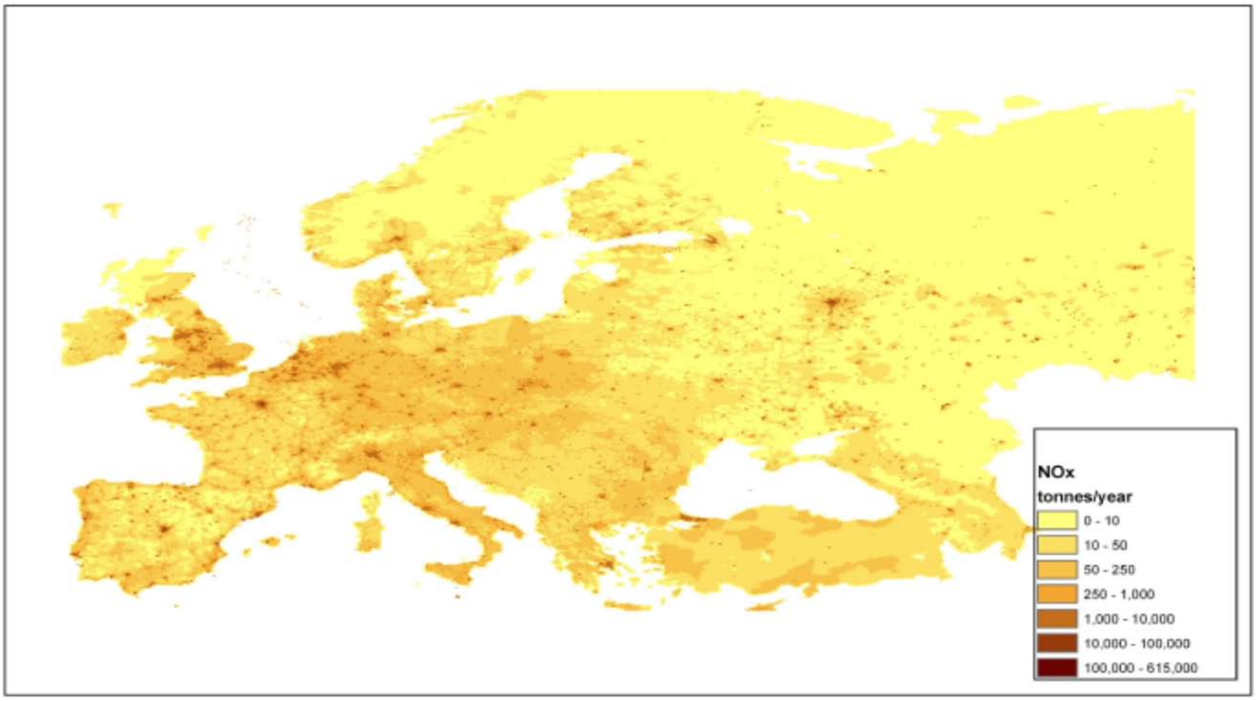

Figure 78: NOx emissions from all sectors in 2003 [Visschedijk et al., 2007]

However, for the high-resolution air quality simulations in BRIDGE, the above mentioned inventory had to be further spatially disaggregated. The spatial disaggregation of emissions was done according to Corine Land Cover 2006 data with 100m resolution [www.eea.europa.eu/data-and-maps/data/corine-land-cover-2006-clc2006-100-m-version-12-2009], following the methodology developed by Maes et al. [2009].

The next figure shows an example of the spatial distribution of emissions for NOx (all source categories except shipping) for Helsinki's 200m x 200m resolution.

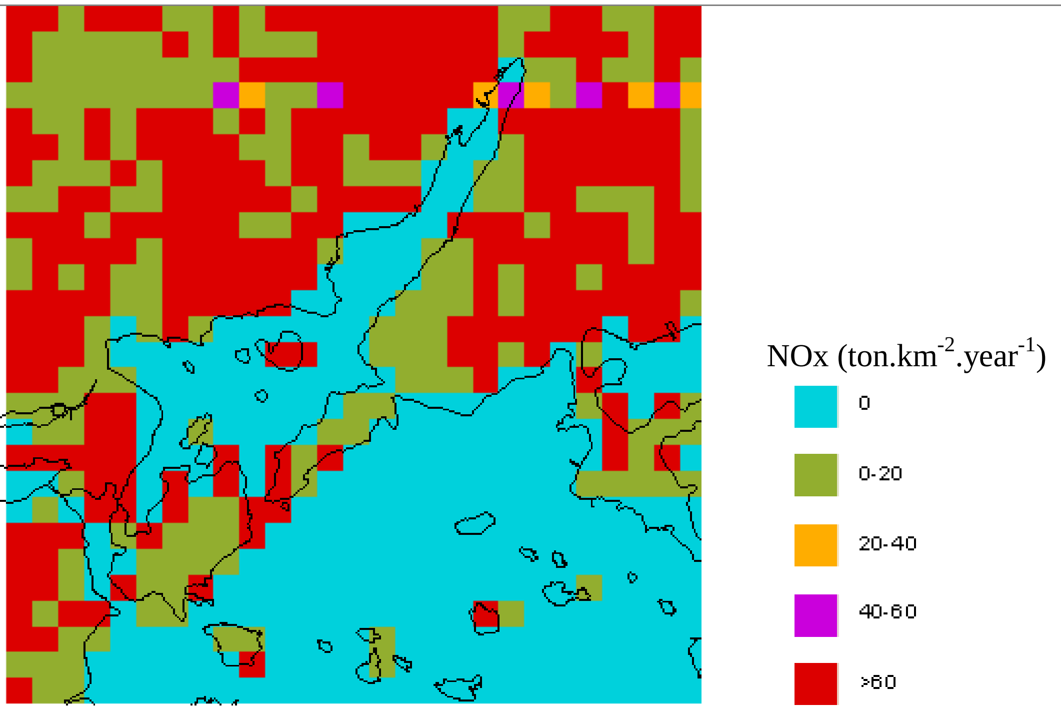

Figure 79: NOx emissions from all except shipping for Helsinki (domain 2).

3.1.7.2 London Atmospheric Emission Inventory (LAEI) dataset

The London Atmospheric Emissions Inventory (LAEI) was used for the air quality simulation of London's domain 2. Although it was not possible to use it for the larger domain, as the LAEI does not cover the entire domain, it was decided that it would be used for the smaller one due to its high spatial resolution.

The LAEI (http://static.london.gov.uk/mayor/environment/air_quality/research/emissions-inventory.jsp) is a database with information on emissions from all sources of air pollutants in the Greater London area The LAEI includes detailed emission information on several air pollutants including: NOx, SO2, CO, NMVOC, PM10 and PM2.5. Traffic emissions are provided on a road link basis for the major roads; other sources, including domestic and commercial emissions, minor roads, airport, rail and shipping, are given on a 1km x 1km grid square basis.

To furher spatially disaggregated the LAEI to the 200 m x 200 m resolution the above mentioned methodology (see 3.3.3.1) was once more applied.

3.1.8 Output data

CAMx post-processors allow the extraction of time series simulated concentrations for predefined locations, and bi-dimensional concentration fields for a given pollutant. The complete list of outputs was already described in D4.1 (Model selection Report).

UAVR's CAMx simulations supplied three datasets for the DSS database, one for each city, that are available for on-line models and that will also be used to calculate the indicators. The datasets include hourly gridded concentrations for O_3, NO_2, PM10 and PM2.5 for each city case's smallest domain with 200 m x 200 m spatial resolution, for the entire year of 2008, in a total of 79056 files (3 cities x 3 pollutants x 366 days x 24 hours), corresponding to around 12 Gigabytes.

3.1.9 Results

This section includes a brief analysis of the models results and the values obtained for the indicators established for BRIDGE project regarding air quality. A more detailed analysis with the assessment of the quality of the modeling process, including the air quality modeling with CAMx, is presented in D4.3 (Quality Assurance / Quality Control Report).

3.1.10 Gliwice

The next Figures present the annual average concentrations for NO_2, PM10 and PM2.5 for Gliwice's domain 2. Both pollutants present annual concentrations considerably below the legislated values (2008/50/EC): 40 $\mu g.m^{-3}$ for NO_2 and 48 $\mu g.m^{-3}$ (40 + 20% tolerance) for PM10.

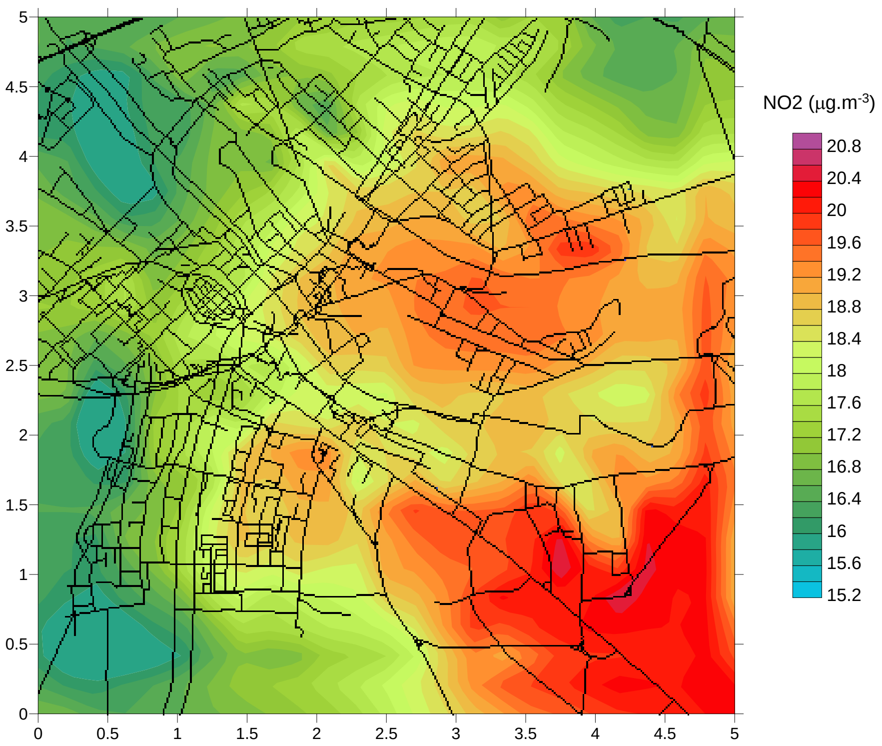

Figure 80: NO_2 annual average concentrations for Gliwice (domain 2).

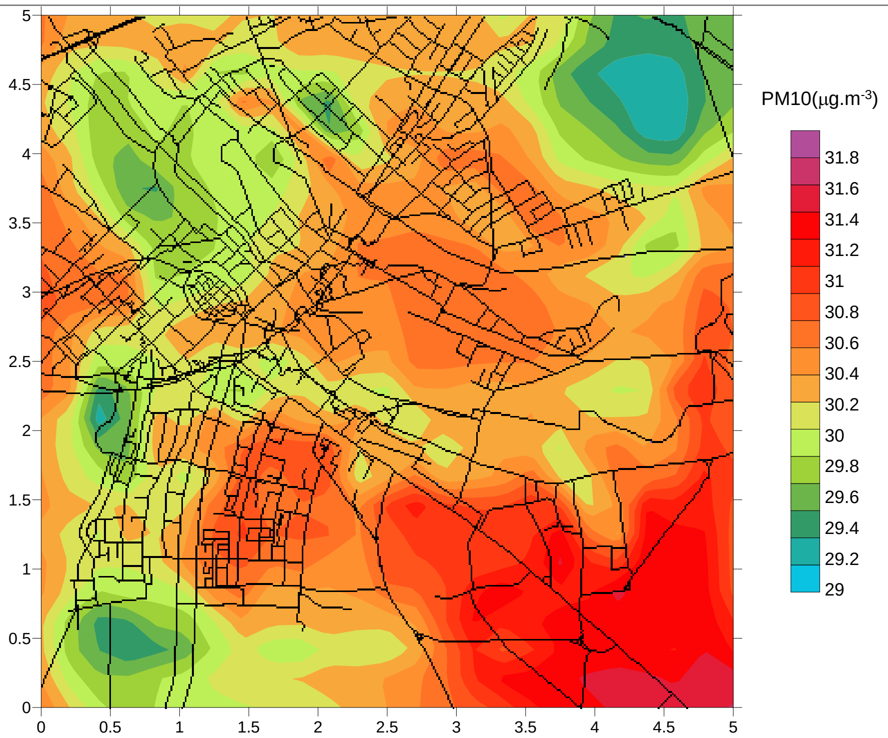

Figure 81: PM10 annual average concentrations for Gliwice (domain 2).

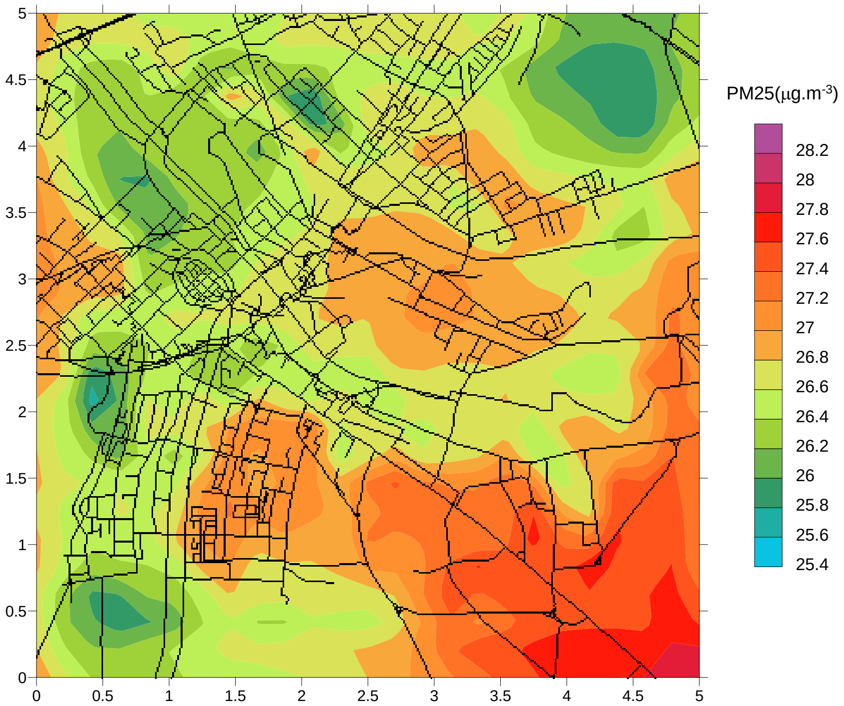

Figure 82: PM2.5 annual average concentrations for Gliwice (domain 2).

3.1.11 Helsinki

The next present the annual average concentrations for NO_2, PM10 and PM2.5 for Helsinki's domain 2. As for Gliwice, both pollutants present annual concentrations considerably below the legislated values.

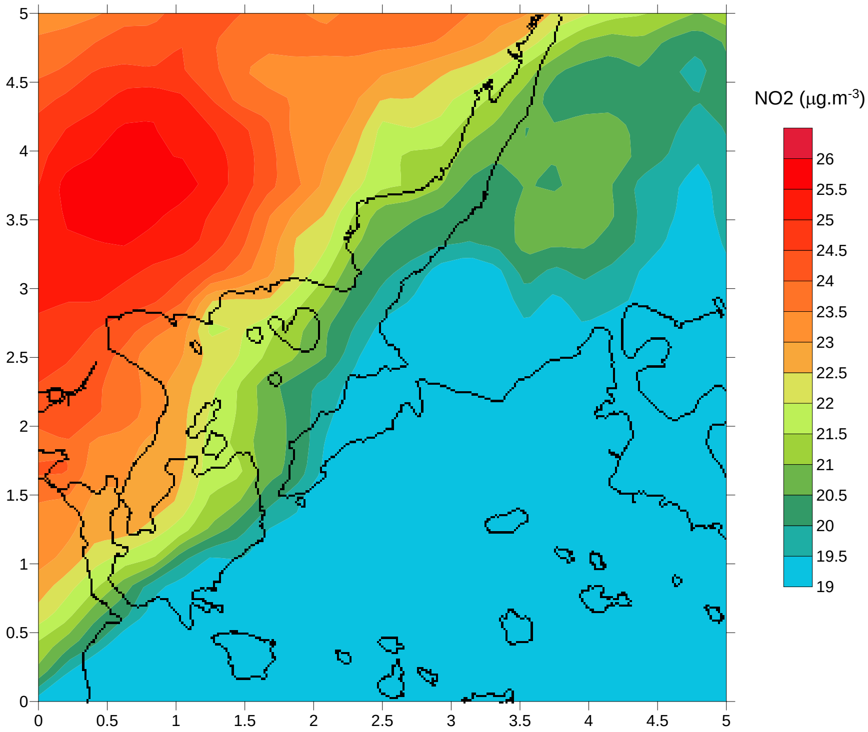

Figure 83: NO_2 annual average concentrations for Helsinki (domain 2).

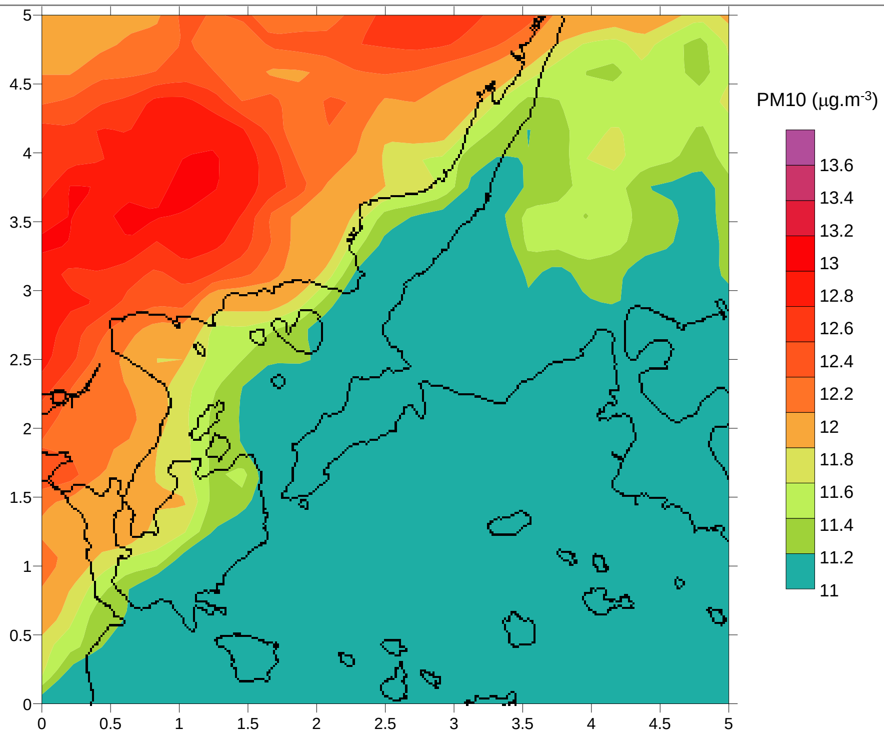

Figure 84: PM10 annual average concentrations for Helsinki (domain 2).

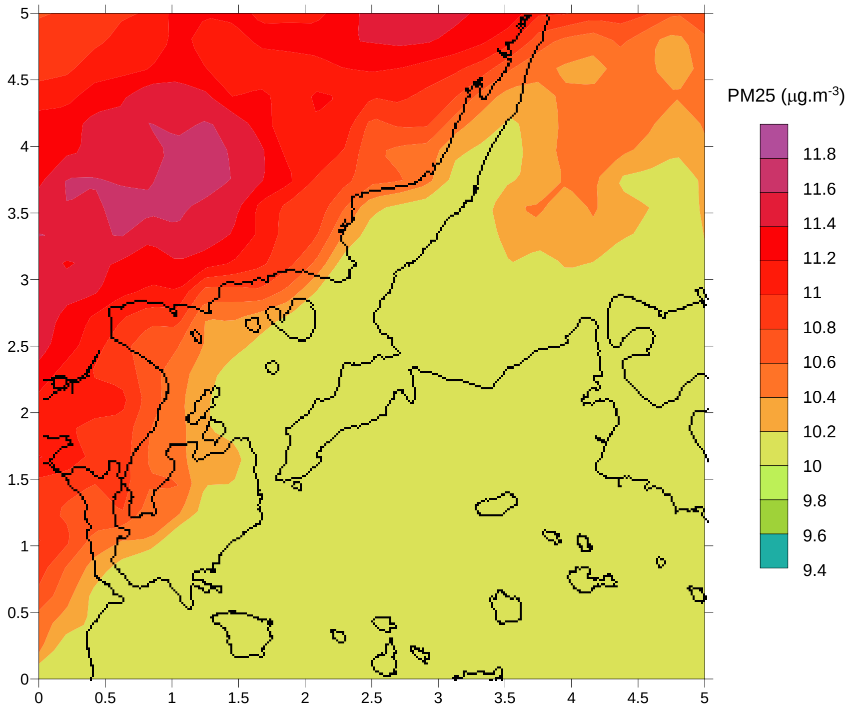

Figure 85: PM2.5 annual average concentrations for Helsinki (domain 2).

3.1.12 London

The next figures the annual average concentrations for PM10 and PM25, respectively, for London's domain 2.

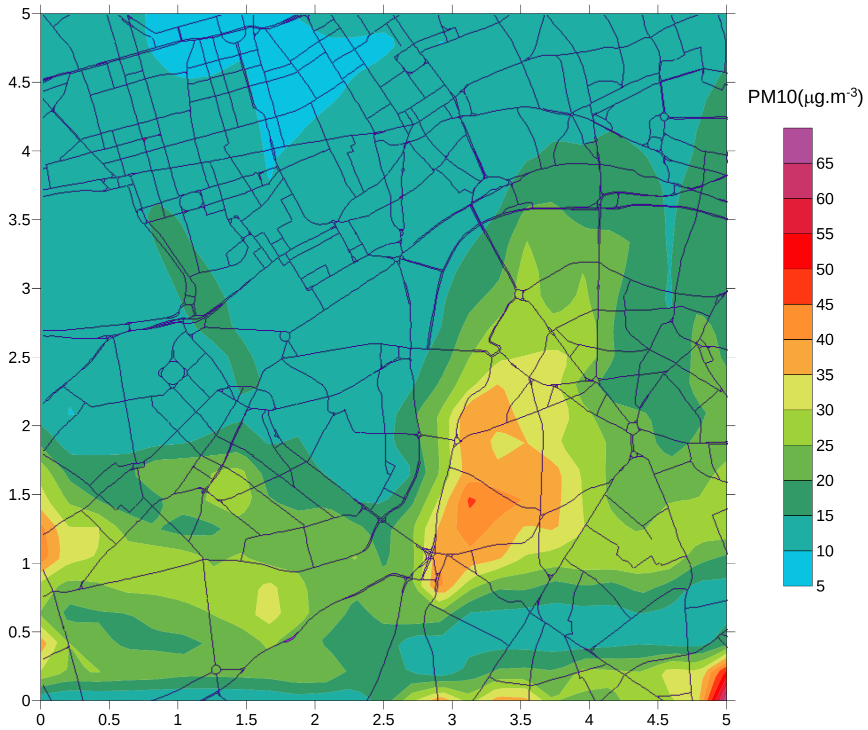

Figure 86: PM10 annual average concentrations for London (domain 2).

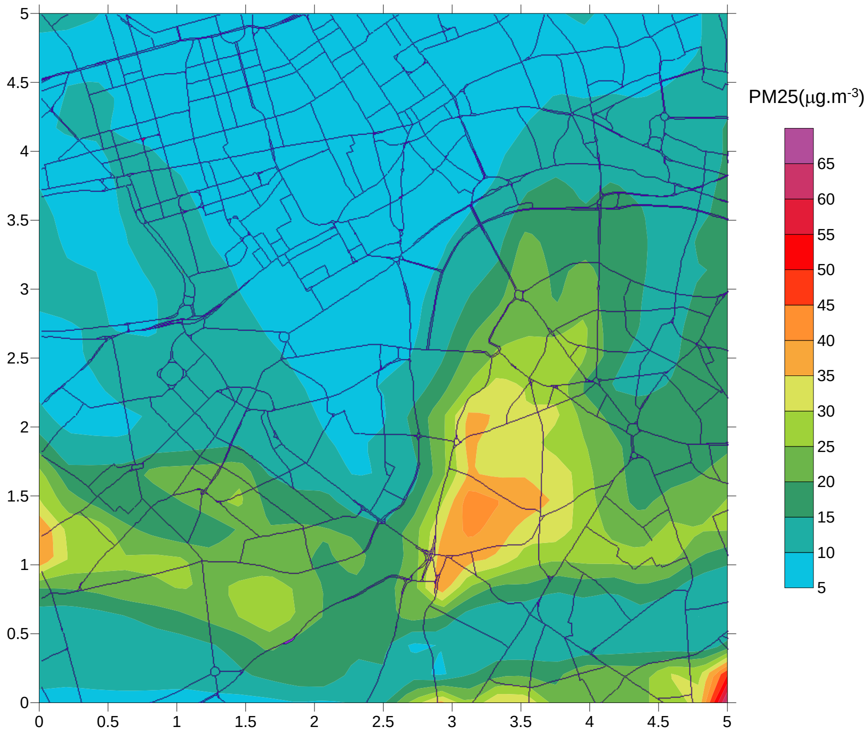

Figure 87: PM2.5 annual average concentrations for London (domain 2).

3.1.13 Indicators

Deliverable 5.3 (Indicators Definition Report) defined the set of indicators of environmental, socio-economic and sustainability impacts. The next table presents the air quality indicator values obtained with CAMx for its three study cases.

Table 3 – Air quality indicators produced by CAMx for Helsinki, Gliwice and London

Indicator Name	Indicator value			
	Helsinki	Gliwice	London	*Threshold*
annual [NO_2] ($\mu g.m^{-3}$)	25	20	-	*50 $\mu g.m^{-3}$*
annual [PM10] ($\mu g.m^{-3}$)	11	28	14	*48 $\mu g.m^{-3}$*
annual [PM2.5] ($mg.m^{-3}$)	10	24	9	*No limit defines*
maximum 8-hour [O_3] ($\mu g.m^{-3}$)	107	113	149	*120 $\mu g.m^{-3}$ for 8- hour averages*
No. of NO_2 exceedances	0	0	-	*200 $\mu g.m^{-3}$ not to be exceeded more than 18 times a year*
No. of PM10 exceedances	0	13	7	*50 $\mu g.m^{-3}$ not to be exceeded more than 35 times a year*
No. of O_3 exceedances	0	0	3	*120 $\mu g.m^{-3}$ for 8- hour averages no more than 25 times a year*

4

4.1 URBAIR . UAVR ON-LINE MODEL.

4.1.1 Brief description.

Within the scope of BRIDGE, and specifically with the purpose of developing a DSS for sustainable urban planning, it proved important to develop and implement an on-line air quality model capable of providing air pollutant levels at the urban scale, with higher spatial resolution than the one obtained with mesoscale models, but with much lower computational effort than the one resulting from the application of a CFD model.

The Urban Air Quality (URBAIR) model is an on-line second generation Gaussian model. It integrates a number of functionalities, namely the estimation of road traffic emissions, and the simulation of the resulting air quality patterns for a given spatial domain and time period (usually one year, in compliance with the Directive) for a number of air pollutants, namely: particulate matter with aerodynamic diameter smaller than 10 µm (PM10), nitrogen dioxide (NO_2), sulfur dioxide (SO_2) and carbon monoxide (CO).

Because of the capability to simulate the effect of buildings on air pollutants dispersion, URBAIR offers the possibility to assess the impact of urban planning strategies and traffic management scenarios on air quality.

4.2

4.2.1 Model structure.

URBAIR model integrates the pre-processing of urban morphology, meteorological information and air pollutants emission data in a single tool specifically developed to run online in a Decision Support System (DSS) build under a GIS platform. The URBAIR structure is organized into 4 modules as schematically shown in Figure 88. URBAIR includes also a series of other pre-processors that prepare the input data namely in terms of format to use by the model.

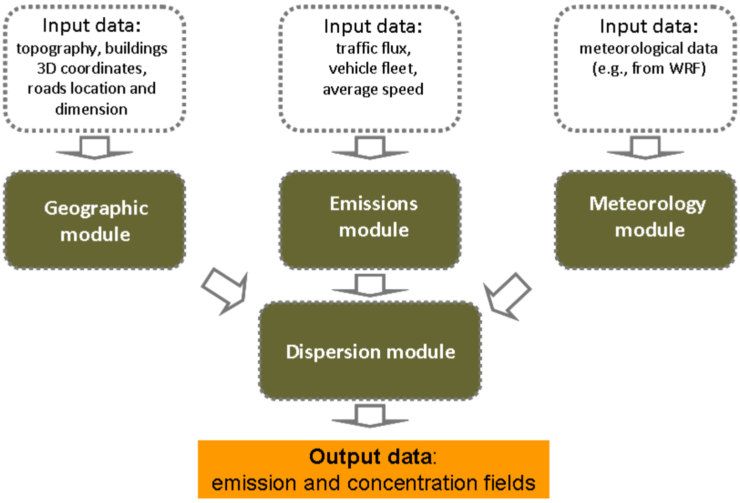

Figure 88 – URBAIR model structure.

The estimation of road traffic emissions is performed with the Transport Emission Model for Line Sources (TREM), a model that has been originally developed by the UAVR team (Borrego et al., 2003) and was coupled with URBAIR under the scope of BRIDGE.

Transport and dispersion of the emitted air pollutants (gaseous and particles) is modeled applying an improved version of the second generation Gaussian model POLARIS (Borrego et al., 1997), also developed in the University of Aveiro. This model is significantly different from traditional Gaussian dispersion models, because considers the presence of buildings during the dispersion simulation and its dispersion parameters have a continuous variation with the atmospheric stability. URBAIR is suitable to be used for distances up to about 10 km from the source, and is based in a steady state atmospheric dispersion model, based on boundary layer scaling parameters, such as the Monin-Obukhov Length instead of relying on Pasquill-Guifford stability classification. A pre-processor calculates the meteorological parameters needed by the dispersion model, namely the atmospheric turbulence characteristics, mixing heights, friction velocity, Monin-Obukov Length and surface heat flux. Furthermore, URBAIR requires meteorological information that is provided by the mesoscale meteorological model WRF. Alternatively, surface measurements and upper air soundings databases can also be used.

Topography and build-up structures characteristics have a significant influence on the dispersion of atmospheric pollutants, in particular in urban areas. In this sense, URBAIR requires also the characterization of the spatial variation of terrain surface elevation, buildings 3D coordinates and emission sources location and dimensions, which are usually provided by Geographical Information System (GIS) maps. The geographic module relies on a Cartesian coordinate system in which, regular and discrete gridded data can be used to characterize and spatially distribute terrain, receptors and sources. Representative terrain-influence heights and ‘projected’ building structures influence are determined following widely used modelling approaches. Topography is specified in the form of terrain heights at receptor locations. The influence of buildings on air pollutants dispersion depends on the orientation of the building with respect to the source,

the wind direction and the shape of the building. Direction-specific downwash parameters, in the form of projected building height and width dimensions, are estimated using the EPA's Building Profile Input Program PRIME (BPIP-PRIME) modelling approach.

4.2.2 Input data pre-processing.

As previously referred the major categories of input data need by the integrated air quality system URBAIR are the meteorological conditions, the geographic/geometric characteristics and road traffic fluxes. The procedures for defining these data are hereafter analysed.

The methodology adopted to preprocess the input data for URBAIR starts with the definition of the study area based on the information relating the proposed planning alternatives (PA) and using ArcGIS maps. Due to the high number of buildings within the study areas (which are in the order of some thousands) it was necessary to use a simplified approach. This was done by simply grouping building in blocks delimited by the adjacent roads, this way the computational time of URBAIR was greatly reduced. An example of the methodology adopted for the simplification of buildings is presented in Figure 89, which refers to the London study case.

Figure 89 – Methodology for building simplification in London study case.

Traffic is considered as the main pollutant source in the study areas. Emissions are calculated by the preprocessor TREM using traffic counts provided by each city and average speeds. In URBAIR roads are spatially discretized by defining an adequate number of point sources along each road. Previous sensibility analysis has demonstrated that a spacing of 10 to 15 meters between adjacent point sources guarantees the needed accuracy in the representation of the roads existing in the domain. Meteorological input data, including vertical profiles, were obtained from the WRF mesoscale model simulations over the different case studies domains. The meteorological data from WRF required to run URBAIR is divided in two categories: surface meteorological parameters and vertical profiles, the different parameters are presented in Table 4.

The meteorological output data from WRF was not in a format that URBAIR could use; a pre-processor was built to extract and prepare the input data for URBAIR.

Table 4 – Surface and Upper meteorological data.

Surface Meteorological data	Upper air meteorological data
Point location latitude.	Station location latitude.
Point location longitude.	Station location longitude.

Year	Year
Month	Month
Day	Day
Julian day	Julian day
Hour	Hour
Sensible heat flux	Height at which the temperature/pressure/wind speed is computed
Surface roughness length	Temperature
Albedo	Pressure
Wind speed	Wind speed
Wind direction	Wind direction
Height at which the wind is computed	
Temperature	
Height at which the temperature is computed	
Precipitation amount	
Relative humidity	
Air pressure	

Next section details how the different PAs were configured in URBAIR.

4.2.3 Implementation of planning alternatives in URBAIR

4.2.3.1 Athens

The intervention area is centered at the Brownfield industrial area. The computational domain for URBAIR has an area of approximately 4000×4000 m^2, with a spatial resolution of 100×100 m^2. The urban built-up area of the study domain was simplified by considering 151 rearranged building blocks with different configurations both in geometry and heights (baseline scenario). PA 2 considers more buildings and an increase in traffic flows being considered as the same as nearby roads in the Egaleo area. In PA 3 the intervention area is a green zone without buildings and with a reduction of 90% in traffic flows in the nearby roads to the green zone compared with the baseline scenario.
In Figure 90 a representation of the baseline, PA 2 and PA 3 is presented, with modifications on urban morphology and traffic flows.

Baseline

PA 2
Urban fabric

PA 3
Green area

Figure 90 – Baseline and PA 2 and PA 3.

4.2.3.2 Helsinki

Three preliminary alternatives have been proposed with varying combinations of housing density and office space, and differing relative footprints. All alternatives include the protection of the waterfront and geological heritage on site. These alternatives consider the configuration of three different building scenarios with different number or roads and consequently traffic fluxes.
The URBAIR computational domain, with approximately 4000×4000 m^2, with a resolution of 100 m, was defined at the center of the study area. The urban built-up area of the study domain was simplified by considering 234 rearranged building blocks with different configurations both in geometry and heights (baseline scenario). PA 1 considers 251 building blocks and an increase in the number of roads. In PA 2, 254 blocks were defined with a different configuration also with different roads configuration. In PA 3, 263 blocks were defined also with different road configuration.
Figure 91 presents the modifications on urban morphology and traffic flows for the different alternatives in comparison with the baseline.

Figure 91 – a) Baseline, b) PA1, c) PA 2 and d) PA 3, red triangle indicates the intervention area.

4.2.3.3 Gliwice

The URBAIR computational domain, with approximately 5400×5400 m^2 and a horizontal grid resolution of 100 m, was defined at the center of the study area. The urban built-up area of the study domain was simplified by considering 92 rearranged building blocks with different configurations both in geometry and heights (baseline scenario). PA 1 and PA 2 simply add 1 building to the baseline situation, while in PA 3 2 additional buildings are introduced. The most significant change is the increase of traffic flows due to the implementation of the sports hall and the center for new technologies.
Figure 92 presents the baseline and the modifications on urban morphology and traffic flows for the different planning alternatives.

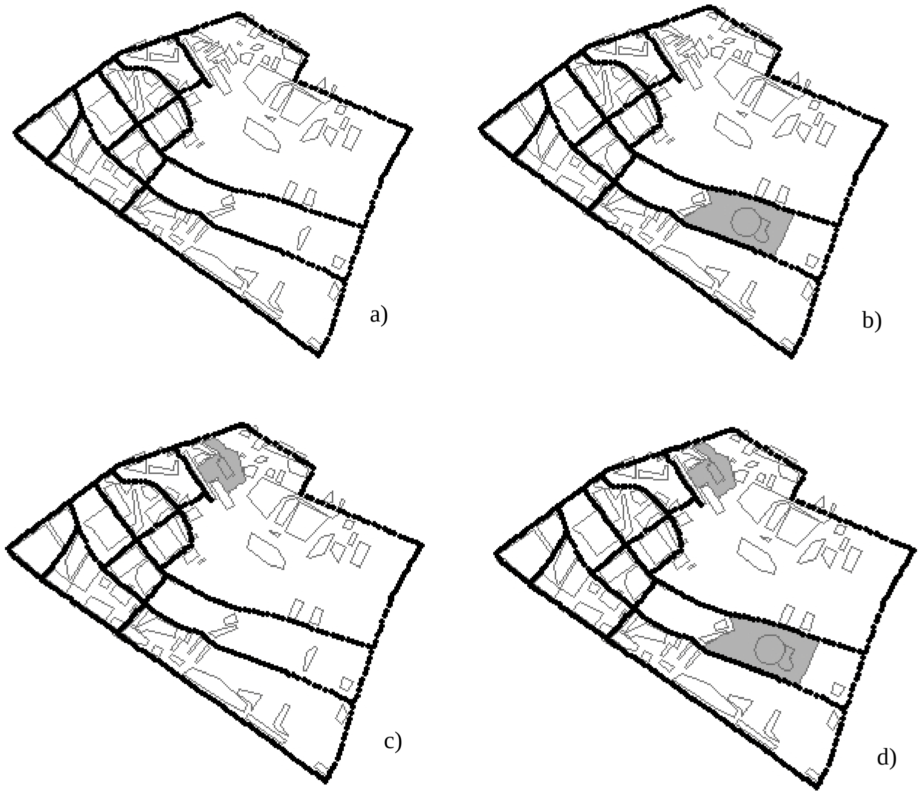

Figure 92 – a) Baseline, b) PA1, c) PA 2 and d) PA 3.

4.2.3.4 Firenze

Planning alternatives in Firenze are only related with meteorology changes and do not involve modifications in the urban structure. This implementation in URBAIR only requires the modification of the meteorological input files.

4.2.3.5 London

As in the case of Firenze, planning alternatives in London are only related with meteorology changes and do not involve modifications in the urban structure. This implementation in URBAIR only requires the modification of the meteorological input files.

4.2.4 Output data

The output data from URBAIR includes the meteorological parameters and pollutant concentration at user-specified receptor points or spatially distributed over a regular grid. Different mean averaged concentration values can be defined, depending on the purposes.

4.2.5 Air quality results for baseline and planning alternatives.

4.2.5.1 <u>Athens</u>

As an example for a specific summer day in the Athens study case, in Figure 93 the simulation results are presented for the pollutant PM10 in an intercomparison for the baseline with PA 1, PA2 and PA 3. PA1 is only related with modifications in meteorology.

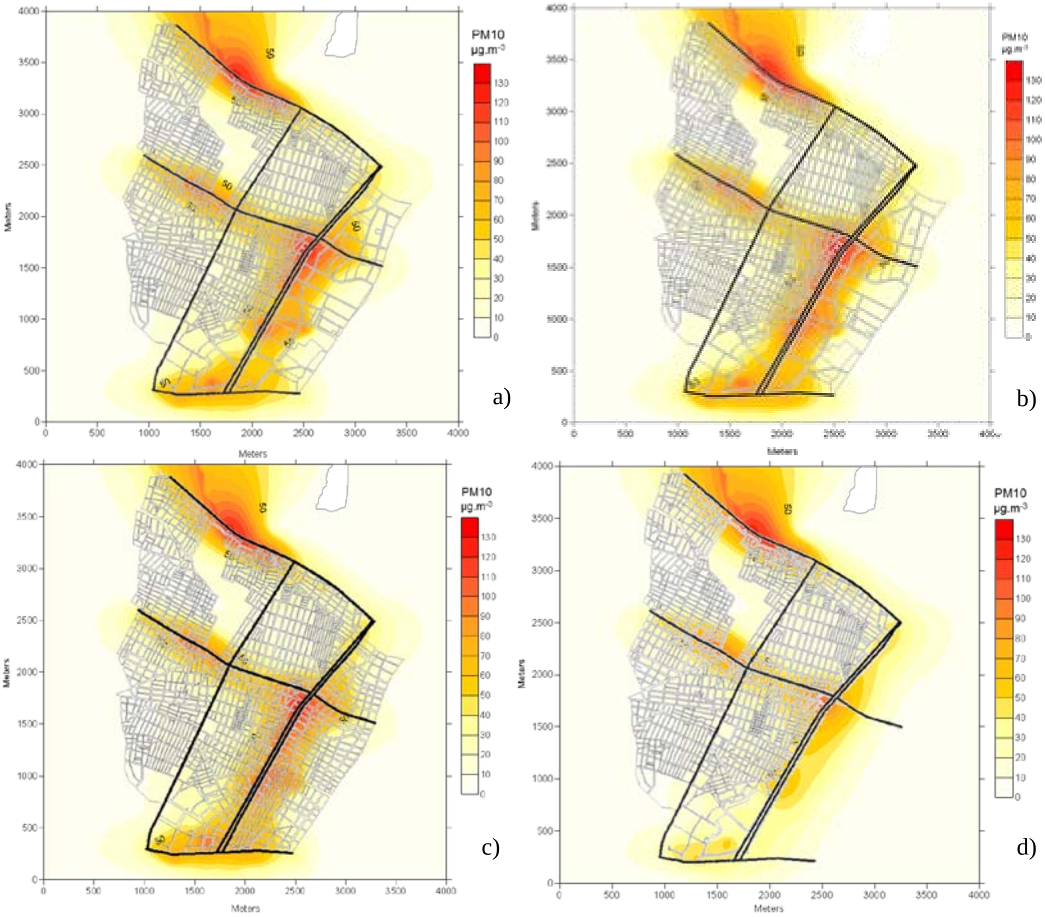

Figure 93 - Comparison of 1.5 m high horizontal 24 hour average PM10 concentration fields in 22 September 2008 for: a) baseline, b) PA 1, c) PA 2, d) PA 3.

Analysing the results presented in Figure 93, it is clear that PA 3 is the one that presents the most significant reduction on PM10 levels in the intervention area as a consequence of the decreased traffic flow induced by the implementation of the green area. According to the URBAIR simulations PA 1 and PA 2 have little impact over the dispersion pattern and magnitude of the concentrations attained when comparing with the baseline.

4.2.5.2 Helsinki

In Figure 94 the PM10 simulation results are presented for Helsinki study case during the 25 July 2008 for baseline situation and PA1, PA2 and PA3.

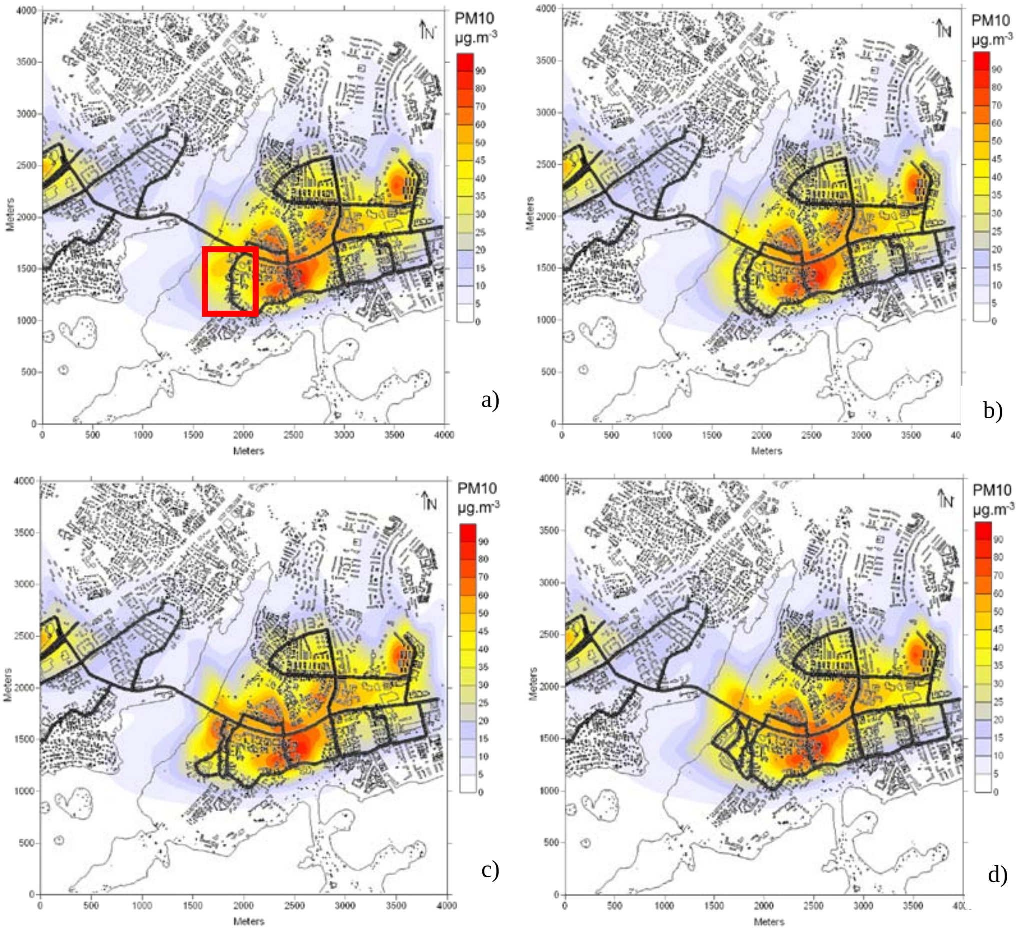

Figure 94 - Comparison of 1.5 m high horizontal 24 hour average PM10 concentration fields in 25 July 2008 for: a) baseline, b) PA 1, c) PA 2 and d) PA 3. Red rectangle indicates the intervention area.

Comparing the results observed in Figure 94 it is possible to conclude that despite the changes on the number of roads and respective traffic fluxes, and also on the number and location of buildings, the different alternatives do not induce significant modifications of the dispersion patterns for this particular summer day. However, and according to the simulations, PA 2 and PA 3 have a higher influence over the PM10 levels in the intervention area and, particularly in PA 3, in an area located to the north of the new buildings and roads.

In Figure 95 the hourly NO_2 concentrations for the entire year of 2008 are presented for a specific computational cell of the domain.

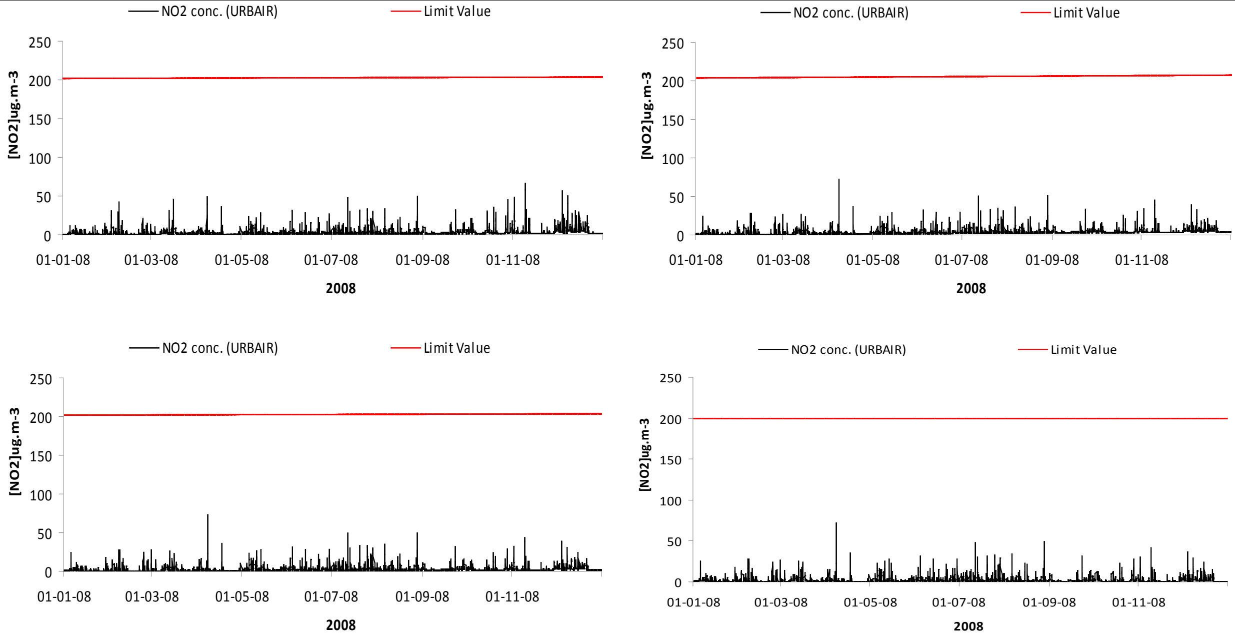

Figure 95 - Comparison of simulated NO_2 concentrations for baseline scenario, PA 1, PA 2 and PA 3 for a specific cell of the domain (X,Y=2000,2000) for the entire year of 2008.

Comparing the obtained results, there is an increase of the maximum NO_2 values for PA 1, PA 2 and PA 3 in relation to the baseline situation, although in all cases there are no exceedances to the limit value from the European legislation (2008/50/CE) for this particular cell of the domain. It should be mentioned, however, that no information on urban background was available.

4.2.5.3 Gliwice

In Figure 96 the PM10 simulation results for Gliwice study case are presented for the 2nd of January 2008 for baseline situation and PA1, PA2 and PA3.

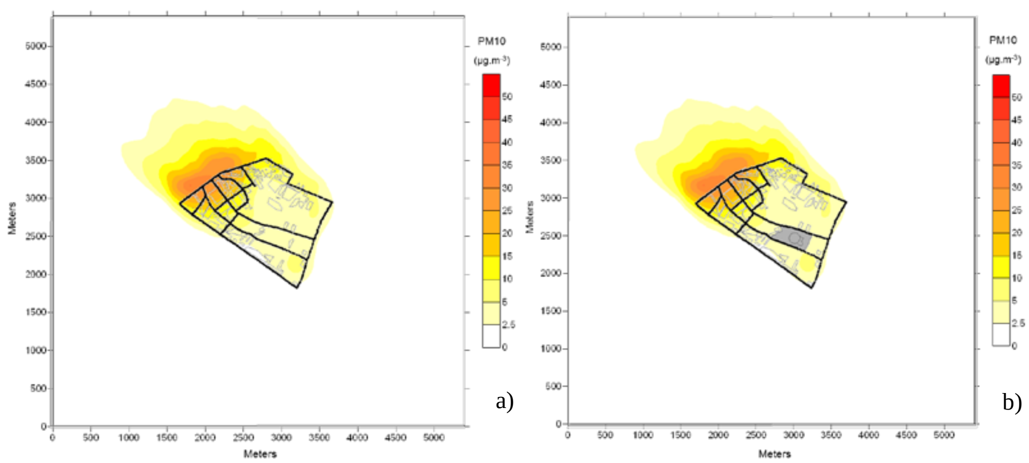

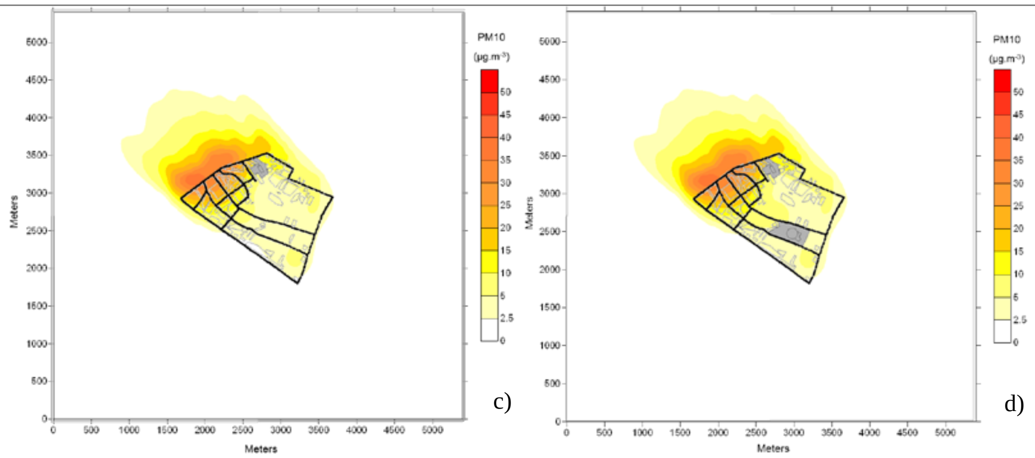

Figure 96 - Comparison of 1.5 m high horizontal 24 hour average PM10 concentration fields in 2 January 2008 for: a) baseline, b) PA 1, c) PA 2, d) PA 3.

Comparing the obtained results for the baseline, PA 1, PA 2 and PA 3, no major differences in PM10 concentrations are visible, since the implementation of the new buildings and the increase in traffic fluxes in the nearby roads do not induce a significant impact in PM10 concentrations.

4.2.5.4 Firenze

In Figure 97 the PM10 simulation results for Firenze study case during the 9 January 2008 are presented for baseline situation and PA1, PA2 and PA3.

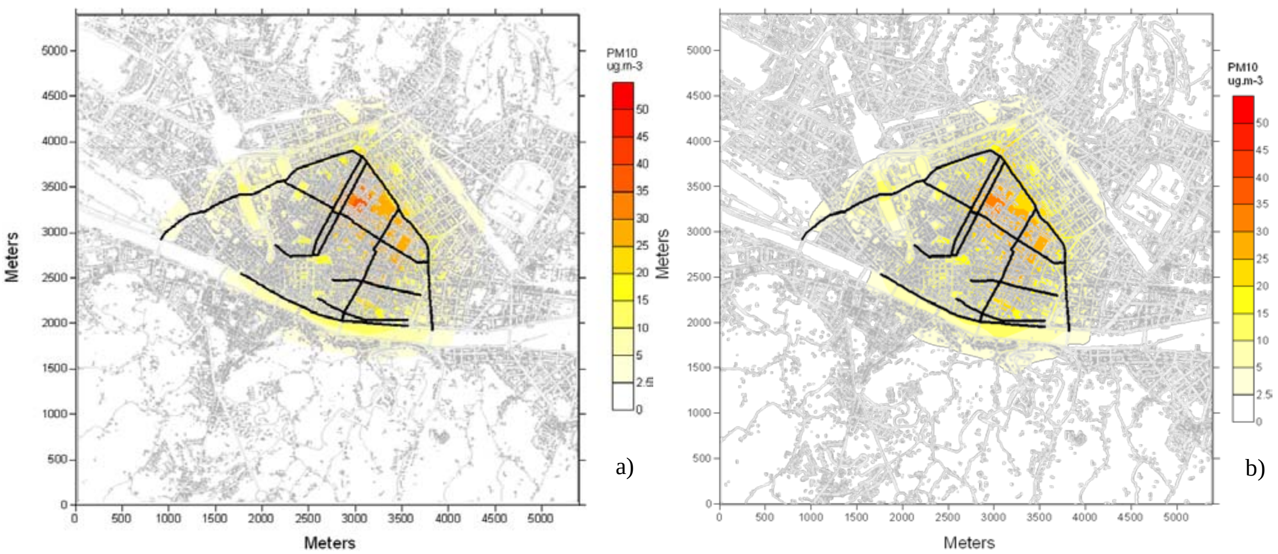

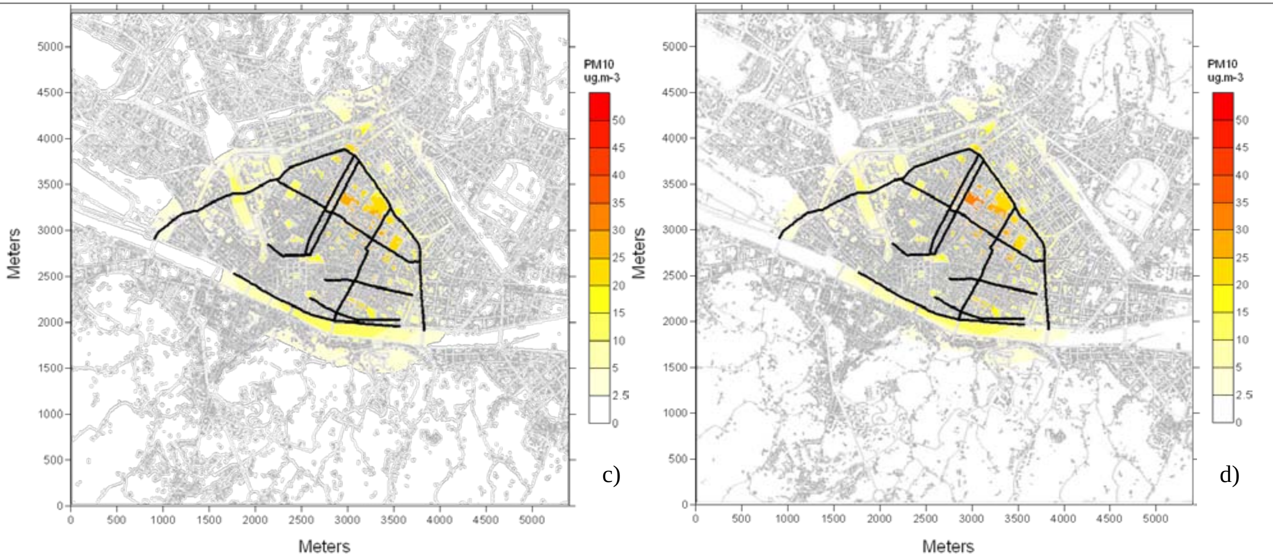

Figure 97 - Results of 1.5 m high horizontal 24 hour average PM10 concentration fields in 9 January 2008 for: a) baseline, b) PA 1, c) PA 2, d) PA 3.

Since the modifications on PA 1, PA 2 and PA 3 are only related with modifications in the meteorology, there aren't significant modifications in PA 1 and PA 3, and in PA 2 the PM10 concentration field has lower values when compared with the other cases for this particular day.

4.2.5.5 London

In Figure 98 the PM10 simulation results for London study case during the 7 November 2008 are presented for baseline situation and PA 1, PA 2 and PA 3.

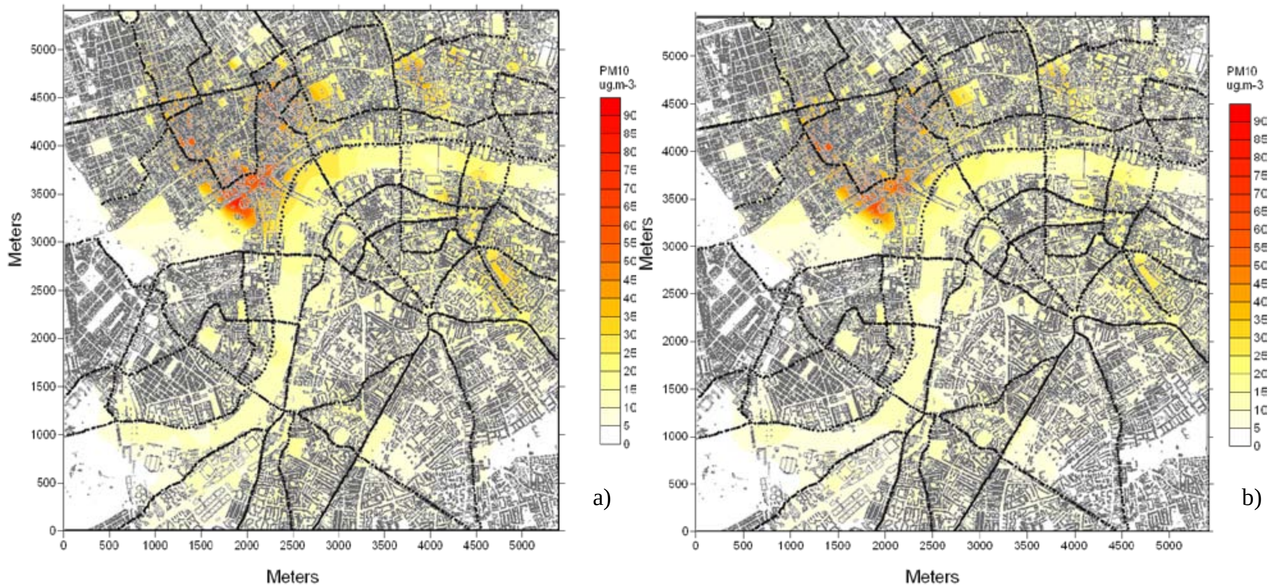

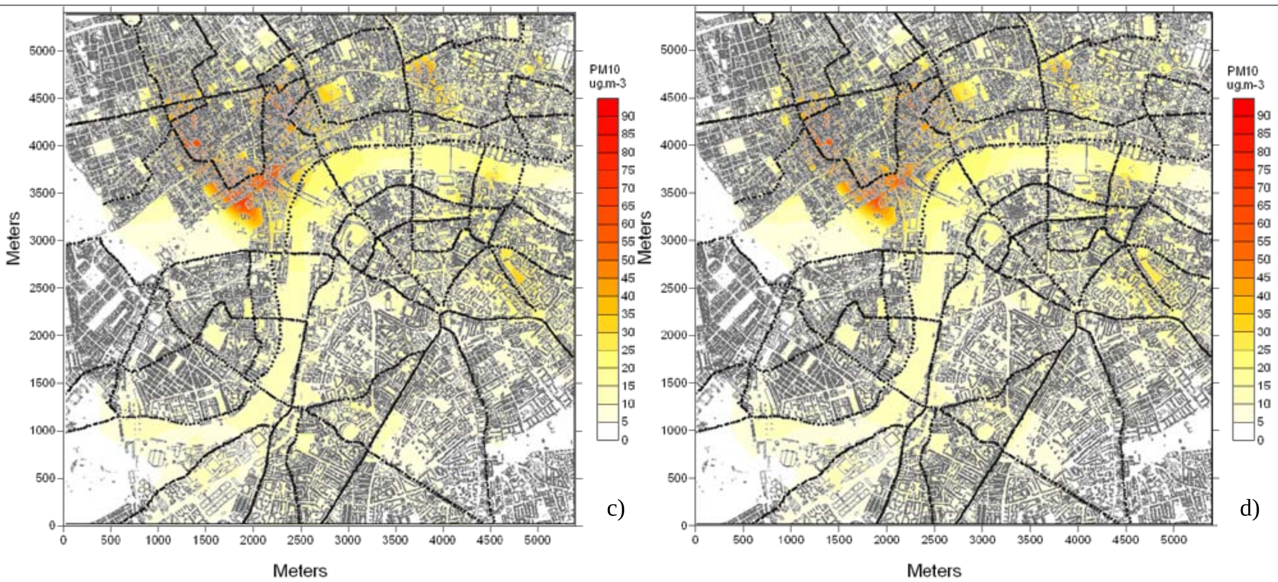

Figure 98 - Results of 1.5 m high horizontal 24 hour average PM10 concentration fields in 7 November 2008 for: a) baseline, b) PA 1, c) PA 2, d) PA 3.

Analysing Figure 98 it is clearly visible a PM10 concentration hotspot in all the situations. No major differences in the concentrations and dispersion patterns are observed with the different planning alternatives.

4.3 VADIS. UAVR OFF-LINE MICROSCALE MODEL.

The Computational Fluid Dynamics (CFD) model VADIS (Borrego et al., 2003), developed at the University of Aveiro, provides highly detailed 3D wind and concentration fields in built-up areas and enhanced capability to assess the impact of urban planning alternatives and traffic management scenarios on air quality and human comfort (for more details see deliverable 4.1). Under the scope of BRIDGE, this CFD code was improved with some new capabilities to fully address the requirements of the application to the different city-cases, namely in what relates to inflow boundary conditions, and vegetative canopy modelling.

The original objective was to apply VADIS to all the city-cases. However, due to the goals of BRIDGE, and specially the importance of having an on-line air quality model that could provide comparisons for different planning alternatives, UAVR team made a significant effort to develop, test and implement into the DSS the URBAIR model (described in the previous section). In this sense, the microscale VADIS model was applied only to then Helsinki city-case. Simulations were performed for a typical summer day of 2008 considering baseline situation and planning alternatives. Results were used to evaluate the simulations carried out with URBAIR and to understand the effect of buildings positioning/configuration and green spaces on wind flow conditions and carbon monoxide dispersion. The impact of each planning alternative on local air quality levels has been evaluated.

The defined computational domain has an area of 1500×2000 m^2, as can be seen in Figure 99 in comparison with URBAIR’s study area.

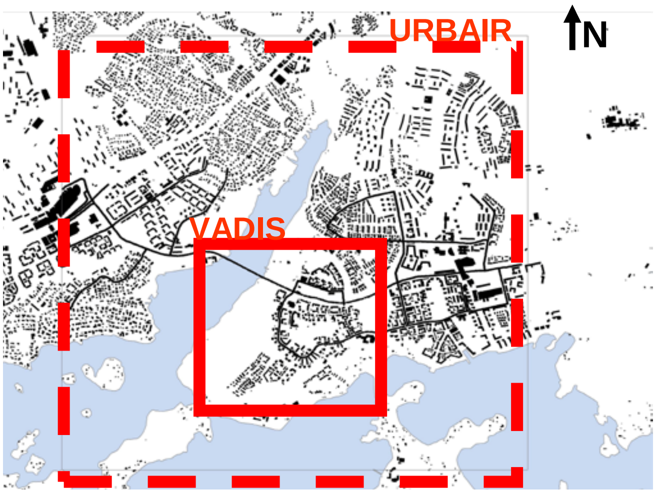

Figure 99 – Helsinki study domains for VADIS and URBAIR models.

Meteorological conditions for the simulation were defined based on climate data (see Figure 100). From this analysis it was concluded that the average wind speed in July is 3.74 m.s^{-1} and average wind direction is 225º.

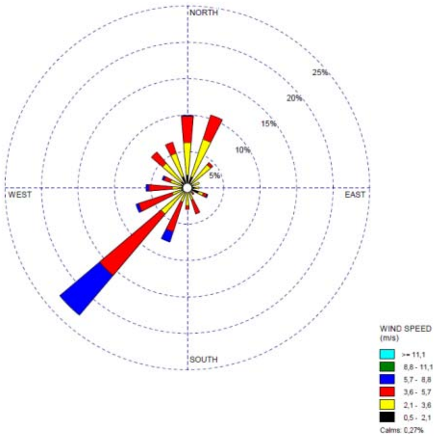

Figure 100 – Wind rose for Helsinki.

Road traffic emissions were estimated applying the traffic emission model TREM (Borrego et al., 2003). Because Helsinki traffic fluxes were provided as an average yearly value for each road, a typical hourly traffic distribution was applied. Traffic fluxes for the new roads in each planning alternative were estimated from the fluxes of nearby roads.

In what relates to urban morphology definition the 3D coordinates of buildings and roads were extracted from the GIS files shown in Figure 101.

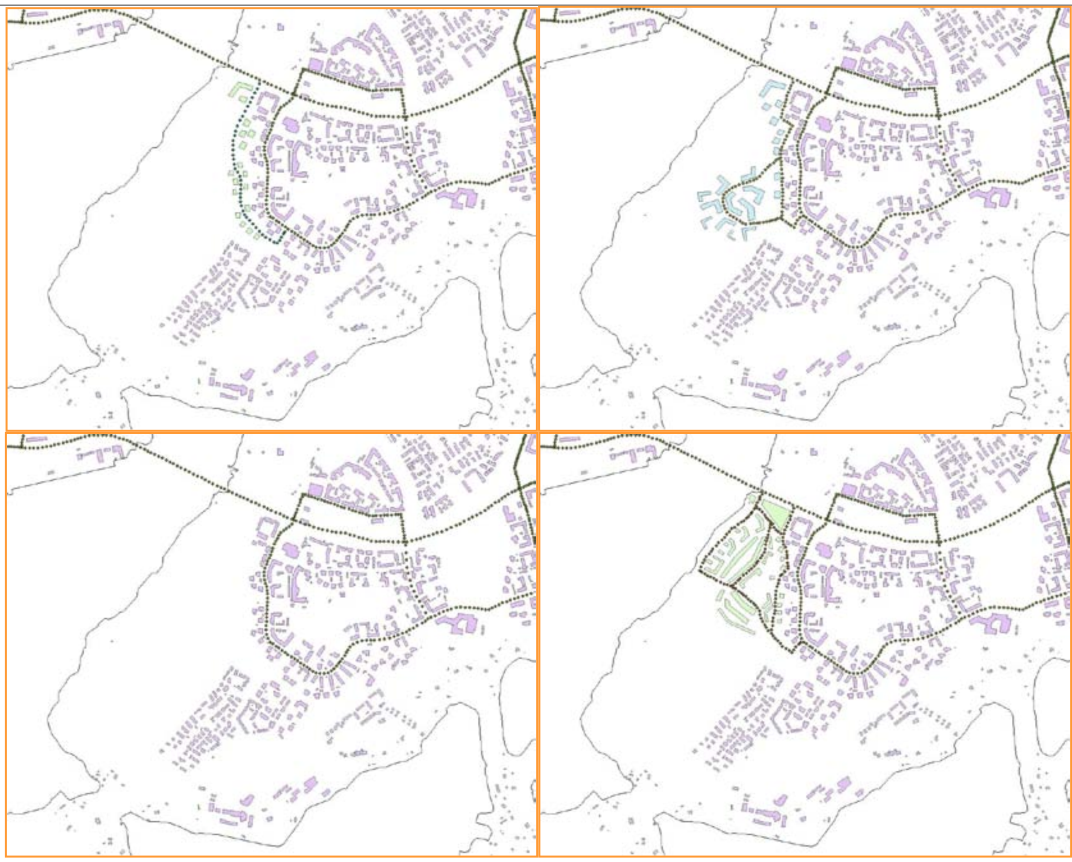

Figure 101 – Configuration of buildings and roads in Helsinki.

The definition of buildings involves the rearrangement of the existing structures based on their morphology. Table 5 shows the total number of “regrouped” buildings and “rearranged” roads.

Table 5 – Parameters for the definition of buildings and roads in VADIS.

	Baseline	PA1	PA2	PA3
Total number of “regrouped” buildings	331	349	353	375
Total number of “rearranged” roads	19	21	24	26

The 3D coordinates of trees for the baseline were extracted from satellite imagery (Google Earth – see Figure 109). For the planning alternatives green space was reduced correspondingly to the increase of the built-up area.

Figure 102 – Green area location in the study area of Helsinki.

CO concentration patterns are shown in Figure 103 for the baseline configuration, PA1 and PA3. Results are shown for the hourly period between 10 and 11 a.m. in July 2008 because it corresponds to a traffic peak in this area of Helsinki.

Baseline:

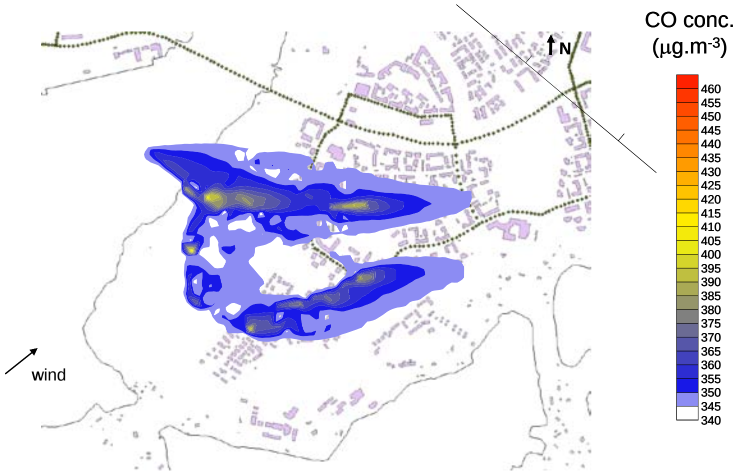

PA1:

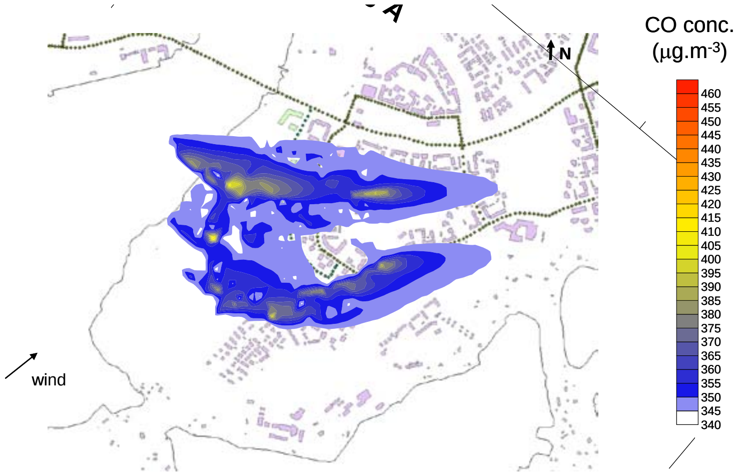

PA3:

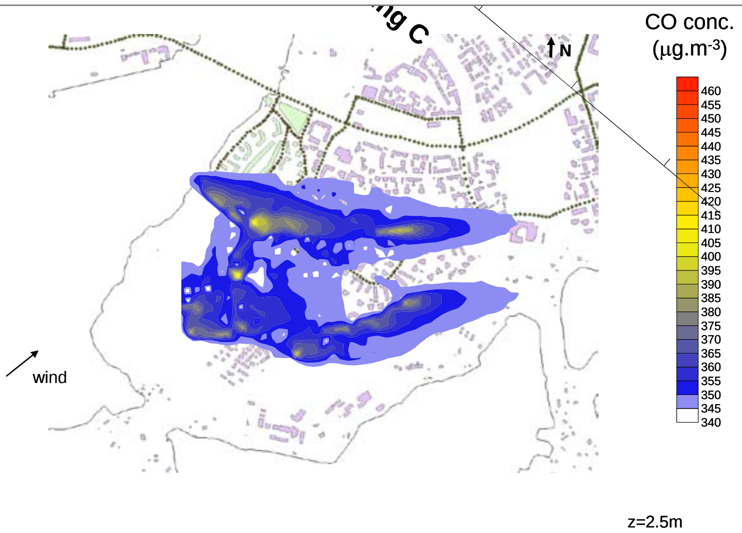

Figure 103 – CO concentration patterns at 2.5 m high obtained with VADIS for Helsinki and corresponding to the hourly period from 10 to 11 a.m. in July 2008. The results are shown for the baseline and planning alternatives PA1 and PA3.

From these results it was concluded that although a larger area is affected by CO dispersion in the alternatives (more evident in the case of PA3), no significant increase on CO hot-spots is attained.
In terms of micro-meteorological conditions, the construction of new buildings ant the modification of the green space has significant effects especially on wind speed, as can be inferred from Figure 104.

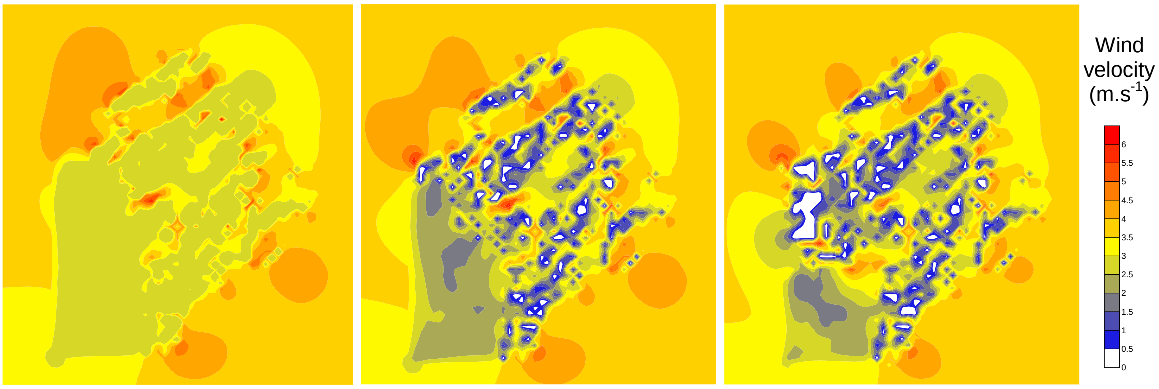

Figure 104 – Wind speed patterns at 2.5 m high obtained with VADIS for Helsinki and corresponding to the hourly period from 10 to 11 a.m. in July 2008. The results are shown for the baseline and planning alternatives PA1 and PA3.

5 LUMPS-LUCY. KCL MODELS

King's College London, in association with others, has developed a series of models (This consists of three sections which are the manuals for the software.

(1) LUCY
(2) GreaterQF
(3) SUEWS/LUMPS

Table 6 that are incorporated into the Decision Support System (DSS) or can be used to generate data for them. In this report we summarize how to use these models. This consists of three sections which are the manuals for the software.

(4) LUCY
(5) GreaterQF
(6) SUEWS/LUMPS

Table 6: Modelling sub-projects that King's College London (with others) have been associated with that relate to the BRIDGE project.

Model Name/Sub-Project	*Description*	*Publications*[1]
LUCY	Anthropogenic Heat flux for all cities globally	Allen et al. (2010)[2]
GreaterQF	Anthropogenic heat flux for London	Lamarino et al. (2011)[3]
LUMPS	Radiation and energy balance model	Loridan et al. (2011)[4]
SUEWS	Radiation, energy and water balance model	Jarvi et al. (2011)[5] in review

[1] For copies of papers please contact Prof Sue Grimmond (Sue.Grimmond@KCL.ac.UK)

[2] Allen L, F Lindberg, CSB Grimmond (2010)Global to city scale model for anthropogenic heat flux, International Journal of Climatology doi: 10.1002/joc.2210 http://onlinelibrary.wiley.com/doi/10.1002/joc.2210/pdf

[3] Iamarino M, Beevers S, CSB Grimmond (2011) High Resolution (Space, Time) Anthropogenic Heat Emissions: London 1970-2025 *International Journal of Climatology (in press)*

[4] Loridan T, CSB Grimmond, BD Offerle, DT Young, T Smith, L Jarvi, F Lindberg. Local-Scale Urban Meteorological Parameterization Scheme (LUMPS): longwave radiation parameterization & seasonality related developments Journal of Applied Meteorology&Climatology.**50**: 185-202doi: 10.1175/2010JAMC2474.1

[5] JärviL, CSB Grimmond, A ChristenThe**S**urface**U**rban **E**nergy and **W**ater Balance **S**cheme (SUEWS): Evaluation in Vancouver and Los Angeles. *Journal of Hydrology (in review)*

5.1 Global Model of Anthropogenic Heat Flux[6]: Manual V2.2 [A: Lindberg, Kotthaus, Grimmond]

5.1.1 Introduction: Manual and Changes from Previous Versions

This manual describes how to install and make use of the LUCY[**L**arge scale **U**rban **C**onsumption of energ**Y**]that is able to compute anthropogenic heat flux for a number of cities or regions around the world. A detailed description of the model can be found in Allen et al. (2010).

5.1.1.1 Version 2.2

Released: 18 January 2011

Changes from earlier versions: Possibility to run large model domains

5.1.1.2 Version 2.1

Changes from earlier versions: Possibility to change model inputs

5.1.1.3 Version 2.0

Changes from earlier versions:

a) Introduction of improved response to air temperature which extends latitudinal range (see Lindberg et al 2011 Manuscript in preparation – contact Sue Grimmond for a copy)
b) Graphical User Interface (GUI) introduced

5.1.1.4 Version 1.0

As published in Allen et al. (2010)

5.1.1.5 Version 0.0

As described in Allen (2009) Master's thesis

5.1.2 Installation

This model is written in MATLAB and is executed using the MATLAB Compiler Runtime (MCR), which can be distributed royalty free. Hence, the user can run the model without having a MATLAB license or any skills in MATLAB programming. The MCR runs on WINDOWS NT/2000/XP/Vista7 platforms.

To be able to run the model the MCR must be installed locally on the computer that will be used. The MCR can be downloaded from: **http://geography.kcl.ac.uk/micromet**

Files to download:

LUCY_GUI_v22.exe	-	Main model
AHF_model_ExportImport_MCR_v2.exe	-	Translation tool between Matlab binary format and ASCII raster
Lucy_v21_Data.zip	-	Model input datasets tounzip. IMPORTANT! Do not change the file and

[6] This section comes from the published paper by Allen et al. (2010 early view).

folder structure!

5.1.3 Running the model and changing the input data

To run the model the user simply needs to run the **LUCY_GUI_v22.exe**. The cities that are included in the current version are found in the section 5.1.8.

5.1.4 Running Guidance

Version 2.2 LUCY comes with a Graphical User Interface (GUI) which opens the following window when the program is executed:

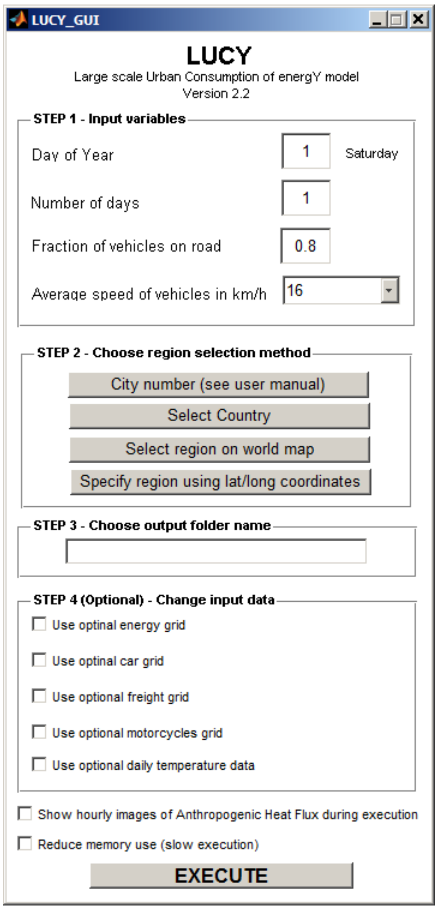

5.1.4.1 <u>Step 1 - Input variables</u>

1. ***Day of year:*** The date must be converted to the day of year (1-365) e.g. 1st January is day 1, 30th December is day 364. Current version of the model is designed to run for non-leap years only. The day of week of the specific day of year is shown left of the box. The current version uses 2005 data.
2. ***Number of days to run model:*** Note than increasing the number of days that the model is run for, the significantly increases the run time (approx 5 minutes per day run). The day of year plus number of days cannot exceed 365.
3. ***Factor (0-1) multiplying total vehicles to get number of vehicles on road:*** Traffic statistics are based on number on total number of vehicles. This factor allows for what fraction of the vehicles are

actually operational so a value of 0.8 assumes that the fleet of operational vehicles is 80% of the total number of vehicles.

4. ***Average speed of vehicle in km h^{-1}:*** This determines the amount of fuel and hence, the amount of heat exhausted by each vehicle in each grid cell based on Smith et al. (2009).

5.1.4.2 Step 2 - Choose region selection method

Due to the relatively high spatial resolution of the model the computational time for running the whole world is very high. Therefore, a number of options to select smaller model domains are available.

1. ***City number:*** Choose this first option if you want to model a city specified in section 5.1.8.

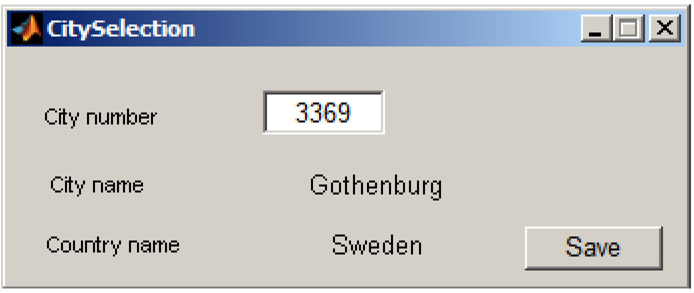

2. ***Select region from world map:*** This option makes is possible to define a larger region on a global map to be modelled. Remember, the larger region selected the longer the model run will take. Choosing too large a region may cause memory failure and the model will not run.

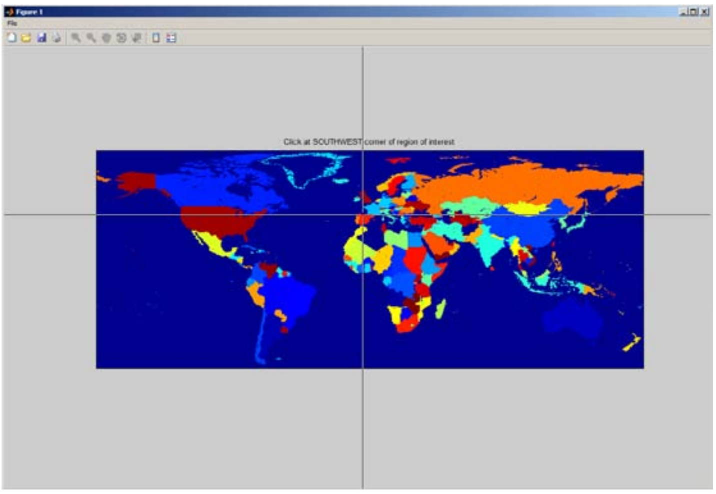

3. Specify region using lat/long coordinates: Latitude: positive are Northern Hemisphere, Longitude: positive are west). ***To run whole world:*** The easiest way to do this is to specify the following coordinates

Min latitude:-58	Min Longitude=-180
Max Latitude=85	Max Longitude=180

Note: this will be very slow if more than a day (e.g. 2h/day) and there may be memory issues depending on your computer.

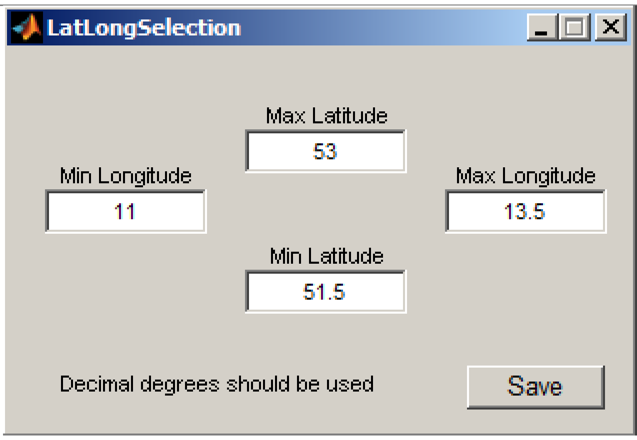

5.1.4.3 Step 3 - Choose output folder name

The specified name written in this box will create a subfolder under the location where the LUCY-model if located on your computer

5.1.4.4 Step 4 - (Optional) Change input data

This makes it possible to load grids stored as netCDF-files obtained from KUMA (**K**ing's College London **U**rban **M**icromet data **A**rchive).

5.1.4.5 Additional options

Show hourly map of Anthropogenic Heat Flux during execution: This will output a map of the hourly evolution of the AHF for the model domain. If this option is chosen the model will take longer to execute.

Reduce memory use (slow execution): This option should be used if the model is crashing due to memory issues using very large model domains (e.g. North America). The execution will slow down considerably.

5.1.5 Changing the Data in the Model

It is possible to change some of the input datasets used without using netCDF files and add a city which is not already included in Table A1. It is also possible to export the input data grids to explore it into another software system. To export and import new data, run: **AHF_model_ExportImport_MCR_v2.exe**. Any newly imported data should be in ASCII raster format and have the same spatial extent and resolution as all the other input datasets. The easiest way to obtain this information is to export the current datasets using: **AHF_model_ExportImport_MCR_v2.exe** .In the current version it is possible to change the temperature input data but it has to be done via KUMA (see Section 3.4).To model a city which is not included in the Appendix, the user can export the *CityID*-grid as an ASCII raster to obtain the CityID for a specific city of interest. When the city is identified, it should be added in the CityID.txt found in the Data folder.
The ASCII raster grids that can be retrieved in the current version (2.2) are:

1. Population density
2. Energy consumption

3. Number of cars per 1000 people
4. Number of freight vehicles per 1000 people
5. Number of motorcycles per 1000 people
6. CityID grid
7. CountryID grid
8. Default monthly temperature grids

If new data set is prepared we would appreciate receiving a copy to allow others to use it. Please create a readme file to indicate what has been updated.

1. Data set that has been updated (i.e. which of the above)
2. Time period data is valid for
3. Reference for source of data
4. Spatial area that has been updated (e.g. Germany)
5. Reference to cite/acknowledge you for this work

For multiple years please create a new data set for each year. Note the current year is 2005.

5.1.6 Output data

The output data files from the model will be created in the same file path as where the model is executed. Files that are created are:

1. A statistics file consisting of time series of anthropogenic heat flux
2. Hourly ASCII matrices (.txt) of AHF as well as an averaged matrix for the whole model period.
3. An ASCII raster headerwhich could be used for importing the results into GIS software systems as well as obtaining information about spatial resolution and location. The header includes the following information:

ncols	number of columns of the matrix
nrows	number of rows of the matrix
xllcorner	geographic “x” coordinate of the lower corner of the matrix
yllcorner	geographic “y” coordinate of the left side of the matrix
cellsize	in lat long
NODATA_value	-9999

To create an ASCII raster simply paste the header above any of the AHF matrices in a text editor.

5.1.7 References

Allen L, F Lindberg, CSB Grimmond (2010) Global to city scale model for anthropogenic heat flux, *International Journal of Climatology*,DOI: 10.1002/joc.2210.

Smith, C., Lindley, S. and Levermore, G. (2009) Estimating spatial and temporal patterns of urban anthropogenic heat fluxes for UK cities: the case of Manchester. *Theoretical Applied Climatology*, 98(1-2), 19-35.

5.1.8 Appendix 1: City Codes

Table A1: Current cities included in the model(Latitude: positive are Northern Hemisphere, Longitude: positive are west)

Note complete list given in full manual

CITY	COUNTRY	LAT (°)	LONG	CITYID
Athens	Greece	37.94	23.65	11919
Helsinki	Finland	60.19	24.97	2748
London	United Kingdom	51.48	-0.17	5012

5.1.9 Appendix 2: LUCY input submission

As part of KUMA (KCL Urban Micromet Archive) an open source database has been developed in order facilitate data exchange of input for the LUCY model. Everybody who is registered as a LUCY/KUMA user can contribute to the database in order to improve model performance which is highly dependent on the quality of information provided.From the website[7] an overview of currently available submitted datasets can be obtained.

In order to participate in the open source project, the user needs to

1. Provide appropriate meta information
2. Submit the data file

The following instructions provide details on how these steps are accomplished.

5.1.9.1 Submit meta information

To include new data into the KUMA metadataneeds to be provided. **Please complete the form at. (please email us for the location)**

It is assumed that categories: annual energy consumption, population density and vehicle numbers are constant through at year. Hence only the year needs to be specified in the form. In general a separate form for each submitted dataset needs to be completed.

However, if you submit new temperature information, please specify the covered time period. Except if several maps for daily temperature are provided, only one form is required.

Be aware that all data and metainformation you submit to the open source system might be accessible for other registered LUCY/KUMA users.

5.1.9.2 Data file

On completion of the form (above) you will be provided with the details to submit the data.

Currently the system uses the following four categories of data:

[7] http://geography.kcl.ac.uk/micromet/

- Annual energy consumption
- Population density
- Vehicle numbers, subdivided into
    - Cars
    - Motorbikes
    - Freight
- Daily mean air temperature

To use these data they need to be downloaded from KUMA. (Running LUCY requires datasets in all four categories).The user can load the dataset into MatLab using the **readGrid.m** code provided. All LUCY files consist of grid datasets with a resolution of 2.5 arc min and a latitudinal extent of 85°N-58°S.

We expect that most users havean interest in a specific region (e.g. a country or city) so havenew information that is more detailed (or is able to improve the existing dataset in terms of quality or temporal coverage). The new information needs to be at 2.5 arc min resolution. Once this is done, the base dataset can be saved as a .mat file (matlab binary format) or innetCDF. Please use the following filename convention in order to link your name, the data category and the represented time to the dataset:

YourLastName_DataCategory_YearMonthDay.mat

5.1.9.3 Use new input data

The KUMA system will perform some quality control on the new data and include it into the open source database. We will email you as soon as your new data are ready for download.

5.2 GreaterQF [Authors: Iamarino, Grimmond]

5.2.1 Overview

The model GreaterQF has been developed for computing of spatial and temporal profiles of the main components of the anthropogenic heat flux Q_F [W m^{-2}] within Greater London for the years 2005-2008. The heat sources considered are energy consumption in buildings, road traffic and human metabolism. Output data are characterized by high spatial (200 m x 200 m) and temporal (30 min) resolution and can be obtained for selected areas or for the whole of Greater London. Partition of Q_F into its main components (atmospheric sensible heat, latent heat and heat to wastewater) is also possible for every contribution or as total. Software is provided for easy computing and visualization of results.

Buildings appear to be the major source of anthropogenic heat emissions in Greater London and account for about 80% of the nearly 150 TWh of total waste energy annually emitted across the city. The method used to estimate the spatial variability of Q_F in buildings is a novel top-down approach based on high resolution resident and workplace population data and has been described in detail in Iamarino *et al*. (2011); further contributions to the methodology adopted here are derived from Hamilton *et al*. (2009) and from Sailor and Lu (2004).

5.2.2 Greater London geographical hierarchy

Greater London is the top-level administrative subdivision covering London, England, with a surface of 1596 km^2, a resident population of 7620000 (mid-2008 estimate) and an usual population of about 8200000 (2001 estimate). According to the Neighborhood Statistics (NeSS) geographical hierarchy adopted by the UK Office for National Statistics (ONS) to report area statistics from the 2001 UK national census, the territory of Greater London can be subdivided into Local Authorities (LA, corresponding to the 32 London boroughs plus the City of London), Middle Level Super Output Areas (MLSOA, minimum size of 5000 residents and 2000 households), Lower Level Super Output Areas (LLSOA, minimum size of 1000 residents and 400 households) and Output Areas (OA, with a minimum size of 100 residents and 40 households).

The NeSS units are characterized by comparable total population and produce, therefore, more detailed spatial description in dense populated areas while lacking accuracy in lower population density zones. For a more homogeneous representation, further spatial levels are added, given by a coarse grid (1730 1 km^2 square cells) and a finer grid (40632 square cells of 200×200 m$^{2)}$. The intersection of the NeSS areas with the square grids produces an additional operative level (termed here SubOA) from which all other spatial units introduced above can be generated. The SubOA level is made up of 147315 areas. All spatial units used in this work are summarized in Table 7, where the corresponding average surface and resident population are also given.

Table 7: Spatial units according to the NeSS hierarchy, square grids and their intersection (SubOA).

	N	Average area [km²]	Average residents
Greater London	1	1596	7172091
NeSS Hierarchy:			
LA	33	48.4	217336
MLSOA	983	1.62	7296
LLSOA	4765	0.33	1505
OA	24410	0.065	297
Square grids			
200×200 m	40632	0.04	177
1000×1000 m	1730	1	4146
SubOA	147315	0.011	

5.2.3 Data flow

Since external data on energy consumption in buildings, on fuel consumption for road traffic and on metabolic heat are available at different spatial levels, the information is disaggregated offline and allocated onto a new common spatial level (SubOA) from which data at all other spatial units can be generated (Figure 105).

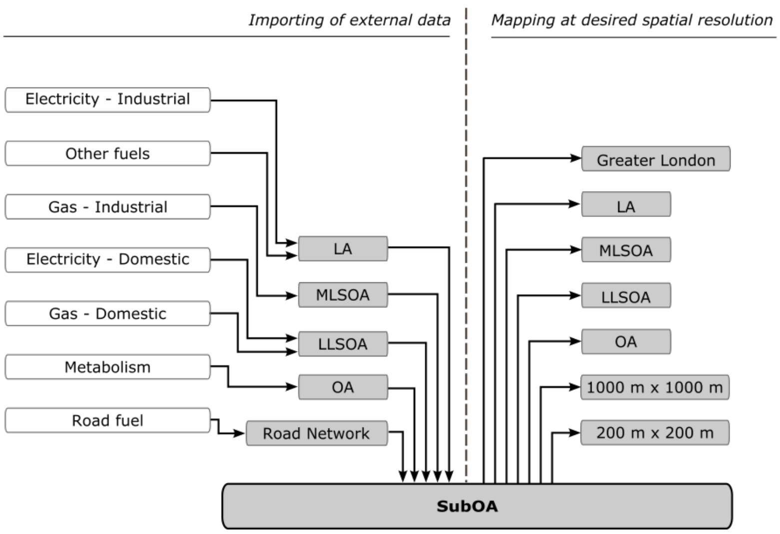

Figure 105: Data flow within the model GreaterQF.

Energy fluxes at the original spatial level are reallocated onto SubOA level based on relations with resident and workplace population and, for traffic, on the basis of the road length fraction in each SubOA area with respect to total road length in the parent square cell. Energy allocated at SubOA level can be then re-aggregated up to the desired macro-area j belonging to one of the NeSS levels or to the square grid according to the expression:

$$Q_{F,j} = \frac{\sum_{i=1}^{N} \left(A_i Q_{F,i} \right)}{\sum_{i=1}^{N} A_i} \quad (1)$$

where A_i is the surface of each area i out of the N SubOA areas belonging to macro-area j, and $Q_{F,i}$ and $Q_{F,j}$ are the anthropogenic heat fluxes in area i and j, respectively.

5.2.4 The software GreaterQF

The software GreaterQF (current version: 3.2) is an executable Microsoft Windows application built within the development environment Embarcadero Delphi® XE. It has been developed for an easier computation and visualization of results obtained by the model.

The software package, containing the executable file and a number of supplementary files, can be downloaded as compressed WinRAR archive from http://geography.kcl.ac.uk/micromet/. Installation is not necessary: decompressing the package in a given folder and starting the GreaterQFv32.exe file is enough to run the software (as long as all decompressed files are located in the same directory). Refer to *Readme.docx* for software instructions. The *csv* files use a semicolon to separate numerical values as this allows better compatibility with most GIS applications.

In detail, the following files are provided:

File name	Description
GreaterQFv32.exe	main program
Readme.docx	software user's guide
SubOA200Data.csv	stores information on heat emissions (by source and year) in W m^{-2} at the smallest spatial level (SubOA)
AreaList.csv	full list of area codes for each spatial level different than SubOA (see Table 7)
Index1_Transportation.csv	list of temporal indexes used to resolve annual Q_F values in the transportation sector
Index2_EnergyHourly.csv	list of temporal indexes used to build half-hourly Q_F profiles in the building sector starting from daily values
Index3_EnergyDaily.csv	list of temporal indexes used to build daily Q_F values in the building sector starting from annual values
Index4_Metabolism.csv	list of temporal indexes used to build temporal metabolic Q_F profiles
GORData.csv	stores information (by source and year) for the whole of Greater London
LAData.csv	stores information (by source and year) at LA level
MLSOAData.csv	stores information (by source and year) at MLSOA level
LLSOAData.csv	stores information (by source and year) at LLSOA level

OAData.csv	stores information (by source and year) at OA level
Gridkm2Data.csv	stores information (by source and year) according to a 1 km^2 square grid
Grid200Data.csv	stores information (by source and year) according to a 200 m x 200 m square grid
List.txt	example of area code list for computing multiple time profiles
Shapefile_Grid1000x1000	subdirectory with ArcGis shapefile of square grid 1000 m x 1000 m
Shapefile_Grid200x200	subdirectory with ArcGis shapefile of square grid 200 m x 200 m

The shapefiles for the NeSS spatial units (see Table 7) are not provided and can be requested directly from the UK Office for National Statistics.

5.2.5 Running the software

Different main panels can be accessed when starting the software:

- Time Profiles
- Spatial Profiles
- Preprocessing
- Exit

Time Profiles

This panel allows computation of Q_F customized time profiles. The following options are available:

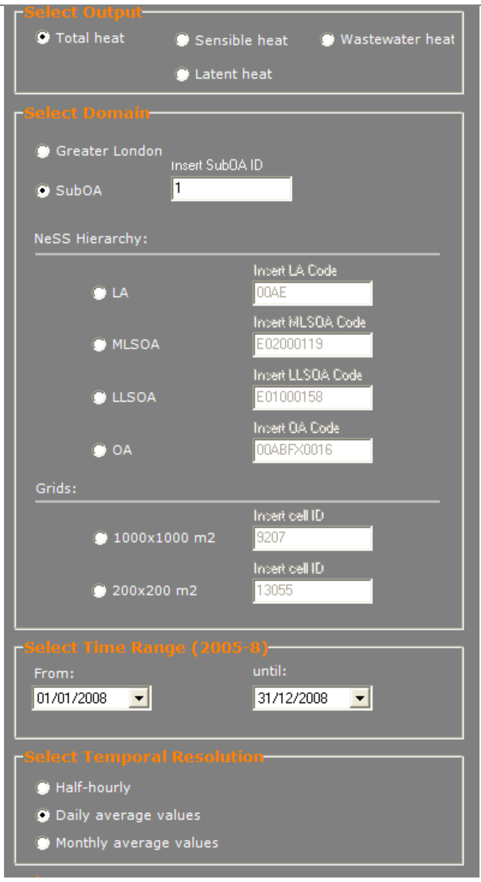

- *Select output:* results can visualized as sensible, latent or wastewater heat or as total (sum of previous terms).
- *Select domain*: to be chosen among the whole of Greater London, or the spatial units belonging to the NeSS hierarchy, or to one of the square grids (1000 x 1000 m^2 and 200 x 200 m^2) or to the common level SubOA. The selected unit is univocally individuated by its code; for NeSS units, this is given by the official NeSS code introduced by the Office for National Statistics; for grids and SubOA areas, the code has to be retrieved by the corresponding shapefiles provided with the software package.
- *Temporal range*: from one single day (to be selected between 01.01.2005 and 31.12.2008) up to 4 years.
- *Temporal resolution*: output can be provided with temporal resolution of 30 min, 1 day or 1 month.

Output is visualized graphically for each single heat emission source; these are grouped by sector (buildings, transportation, metabolism, total). For the sake of comparison, a second profile (obtained by changing any of the settings above) can be drawn on the same graphs (the new curves are characterized by dots). To visualize further profiles, old graphs have to be cleared first (*Clear Charts* command). An example of the graphs are shown in Figure 106.

By accessing the window under the *Save Current Profile* command, results can be saved as txt file. This function is not available when multiple or no profiles are displayed in the graphs.

Under the *Save Multiple Profiles* command, it is possible to start a routine that computes multiple Q_F profiles (according to the settings above) for a full list of areas. The desired area codes have to be provided as a textfile named List.txt, this file needs to be in the same directory of the main program. See an example of List.txt file in the software package. The area codes must belong to the same spatial level as selected in the *Spatial Domain* frame (see above).

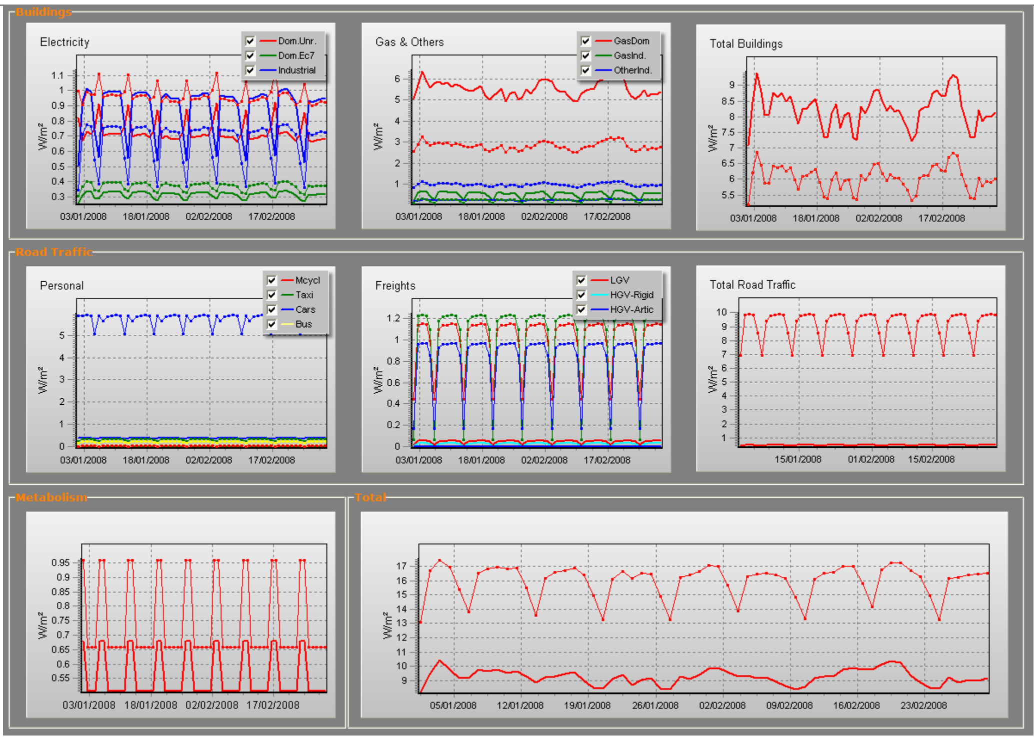

Figure 106: Example of graphs obtained with GreaterQF v.3.2

Spatial Profiles

This panel allows computation of Q_F customized spatial profiles and generates GIS-supported data characterized by different spatial resolution. The following options are available:

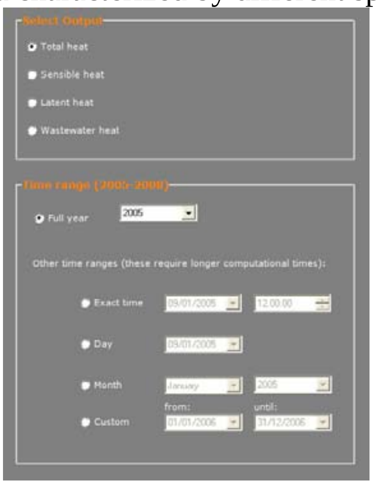

- *Select output:* results can visualized as sensible, latent or wastewater heat or as total (sum of previous terms).
- *Temporal range*: from one single day (to be selected between 01.01.2005 and 31.12.2008) up to 4 years.
- *Select Spatial Resolution*: from whole Greater London to the 200 x 200 m^2 square grid.

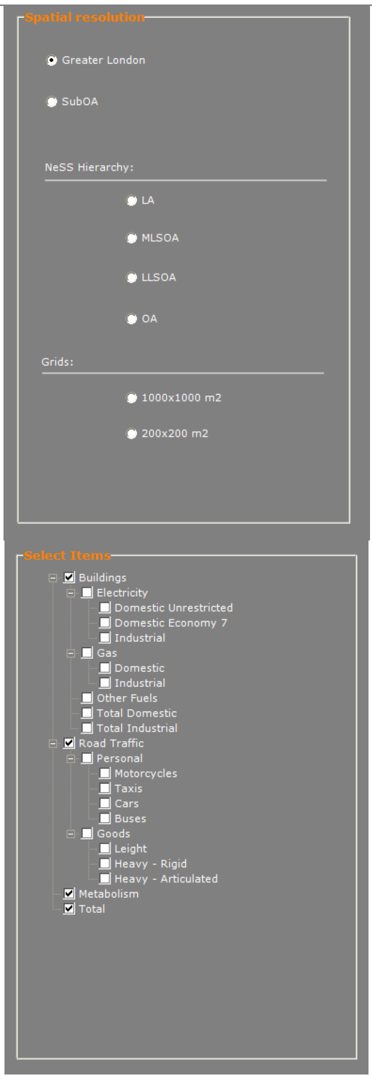

- *Select Source*: heat emissions sources can be selected one by one or by group. In detail, these components are: for the buildings sector domestic electricity unrestricted, domestic electricity Economy 7, industrial electricity, domestic gas, industrial gas and other fuels; for the transportation sector motorcycles, cars, buses, taxi, LGV, HGV-articulated, HGV-rigid; and finally the metabolic heat emission.

Output is saved as textfile with assigned name. The output files report single area codes and the corresponding heat fluxes [W m^{-2}] for each selected source in a format that is suitable for importation into GIS-representation environments (see Figure 107 for an example of GIS).

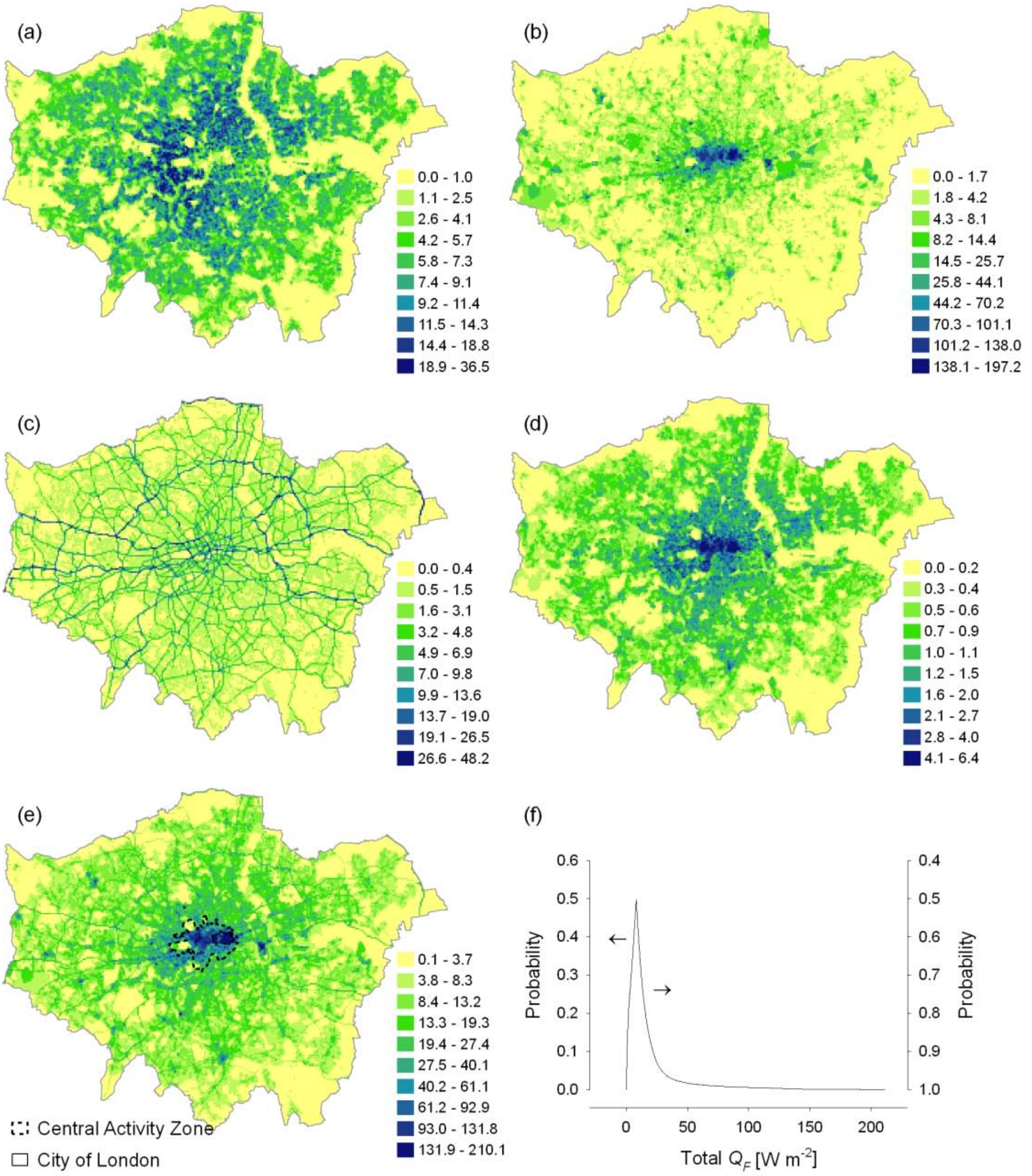

Figure 107: GIS representation of individual Q_F *[W m*$^{-2}$*] components (average for 2005–2008) at 200 m × 200 m resolution by sector: (a) domestic, (b) industrial, (c) road traffic, (d) metabolism and (e) total (classes by Jenks natural breaks); and (f) folded cumulative distribution function of total* Q_F *(f). From: Iamarino* et al. *(2011).*

Preprocessing

This is a password protected feature and is not available for external users. When unblocked, the program checks whether the data csv files need an update, *i.e.*, if a more recent version of the file *SubOA200.csv* is available. If needed, new data files can be created.

Exit

Closes the program.

5.3 LUMPS/SUEWS: Manual [Author: Järvi, Loridan & Grimmond]

5.3.1 Introduction

Surface **U**rban **E**nergy and **W**ater Balance **S**cheme (SUEWS)[8] is able to simulate the urban radiation, energy and water balances using only commonly measured meteorological variables and information about the surface cover. SUEWS utilizes an evaporation-interception approach[9] similar to that used in forests to model evaporation from urban surfaces.

In the model the urban surface is divided into seven types: paved, buildings, coniferous trees/shrubs, deciduous trees/shrubs, irrigated grass, non-irrigated grass and water. The surface state for each surface typeat each time step is calculated from the running water balance of the canopy where the evaporation is calculated from the Penman-Monteith equation. The soil moisture below each surface (excluding the water) is taken into account.

Horizontal movements above and below ground level are allowed. SUEWS runs with 60-min[10]time step and for water balance calculations it adopts a 5-min (300 s) time step. The model provides the radiation, energy balance components, surface and soil wetness and drainage of each surface, and surface and soil runoff.

The model contains several submodels:

1. NARP (*Net All-wave Radiation Parameterization*) radiation scheme[11,12] models net all wave radiation
2. Storage heat flux (ΔQ_S), calculated with OHM (the objective hysteresis model)[13,14,15], captures the magnitude and diurnal hysteresis[16]
3. LUMPS[7](*Local-scale Urban Meteorological Parameterization Scheme*) is used for the initial calculations of turbulent heat fluxes of sensible and latent heat and for stability calculations
4. a simple anthropogenic heat flux model
5. a simple urban water use model

---

[8]Järvi L.,Grimmond C.S.B. & Christen A. The **S**urface **U**rban **E**nergy and **W**ater Balance **S**cheme (SUEWS): Evaluation in Los Angeles and Vancouver *J. Hydrol. (submitted)*

[9]Grimmond C.S.B. & Oke T.R. (1991).An Evaporation-Interception Model for Urban Areas.*Water Resour. Res.* 27, 1739-1755.

[10] The model can be run at other time steps e.g. 30 minutes but needs to undergo further testing (v1.0)

[11]Offerle B., Grimmond C.S.B. & Oke T.R. (2003).Parameterization of Net All-Wave Radiation for Urban Areas.*J. Appl. Meteorol.* 42, 1157-1173.

[12] Loridan T.,Grimmond C.S.B, Offerle B.D., Young D.T., Smith T., Järvi L.&Lindberg F. (2010). Local-Scale Urban Meteorological Parameterization Scheme (LUMPS): longwave radiation parameterization & seasonality related developments*J. Appl. Meteorol. Clim.*doi: 10.1175/2010JAMC2474.1

[13]Grimmond C.S.B., Cleugh H.A. & Oke T.R. (1991).An objective urban heat storage model and its comparison with other schemes.*Atmos. Env.*25B, 311-174.

[14]Grimmond, C.S.B. & Oke, T.R. (1999) Heat storage in urban areas: Local-scale observations and evaluation of a simple model. *J. Appl. Meteorol.* 38, 922-940.

[15]Grimmond C.S.B. & Oke T.R. (2002). Turbulent Heat Fluxes in Urban Areas: Observations and a Local-Scale Urban Meteorological Parameterization Scheme (LUMPS). *J. Appl. Meteorol.* 41, 792-810.

[16]ΔQ_S is non-symmetric relative to solar noon

The formal reference for this model probably will be:
Järvi L., Grimmond C.S.B.& Christen A.The **S**urface**U**rban **E**nergy and **W**ater Balance **S**cheme (SUEWS): Evaluation in Los Angeles and Vancouver *J. Hydrol.* (*submitted*)
Please contact us if you would like to have a copy of the manuscript.

The model distributed with this manual can be run in two standard ways:

1) for an individual area
2) for multiple areas that are contiguous.

There is no requirement for the areas to be of any particular shape but here we refer to these as 'grids'.

5.3.2 Differences between SUEWS and LUMPS

The largest difference between LUMPS and SUEWS is that the latter simulates the urban water balance in detail while LUMPS takes a simpler approach for the sensible and latent heat fluxes and the water balance ("water bucket"). The calculation of evaporation/latent heat in SUEWS is more biophysically based.Due to its simplicity, LUMPS requires less parameters in order to run. Table 1.1 lists the differences between LUMPS and SUEWS. SUEWS gives turbulent heat fluxes calculated with both models as an output. The model can run LUMPS alone without running SUEWS (Table 4.1 – *SuewsStatus*).

Table 1.1: Similarities and differences between LUMPS and SUEWS.

	LUMPS	**SUEWS**
Net all-wave radiation (Q^*)	Input or NARP	Input or NARP
Storage heat flux (ΔQ_S)	Input or from OHM	Input or from OHM
Anthropogenic heat flux (Q_F)	Input or calculated	Input or calculated
Latent heat (Q_E)	DeBruin and Holtslag (1982)[17]	Penman-Monteith equation[2]
Sensible heat flux (Q_H)	DeBruin and Holtslag (1982)	Residual from available energy minus Q_E
Water balance	No water balance included	Running water balance of canopy and water balance of soil
Soil moisture	Not considered	Modelled
Surface wetness	Simple water bucket model	Running water balance
Irrigation	Only fraction of surface area that is irrigated	Input or calculated with a simple model
Surface cover	buildings, paved, vegetation	buildings, paved, coniferous and deciduous trees/shrubs, irrigated and unirrigated grass

[17] de Bruin H.A.R. & Holtslag A.A.M. (1982). A simple parameterization of surface fluxes of sensible and latent heat during daytime compared with the Penman–Monteith concept. *J. Appl. Meteor.*, 21, 1610–1621.

5.3.3 Notation (in alphabetical order)

λ_F	frontal area fraction
ΔQ_S	storage heat flux
b	coefficient in drainage equation
CT	coniferous trees and shrubs
D_0	coefficient in drainage equation
DT	deciduous trees and shrubs
GI	irrigated grass
GU	unirrigated grass
$L\downarrow$	incominglongwave radiation
LUMPS	Local scale Urban Meteorological Parameterization Scheme
NARP	Net All-wave Radiation Parameterization
NN	model area (Grid) identification code
OHM	Objective Hysteresis Model
Q^*	net all-wave radiation
Q_E	latent heat flux
Q_F	anthropogenic heat flux
Q_H	sensible heat flux
SS	two letter code for the measurement site
tt	time step of data
WB	water balance
YYYY	year
z_{0m}	roughness length for momentum

5.3.4 How to run SUEWS

The compiled version of the SUEWS version 1.0 (SUEWS_v1) is available for download from the KCL Urban Micromet Webpage[18]. The files contained within the zipped file (SUEWS_v1.zip) and the location they should be put are listed in Table 3.1.

[18] http://geography.kcl.ac.uk/micromet/

Table 3.1: Files included in the SUEWS_v1.zip (example Ln08 data)

Filename	Purpose	Place to put it
SUEWS_v1.exe	Actual program	Directory where you want to run programme
SUEWSv1_IO.pdf	User manual	
salflibc.dll	Dynamic link library required to run the executable.	Same directory as programme
ModelledYears.txt	Required input file listing modeled periods	Same directory as programme
GridConnections2008.txt	Required input file listing connections between spatial grids	Same directory as programme
HeaderInputLn3004_2008.nml	Required input file with parameters and model run options for LUMPS	Same directory as programme
SuewsInputLn3004_2008.nml	Required input file with parameters and model run options for SUEWS	Input directory
CanopyMoistureInputLn3004_2008.nml	Required input file with information for horizontal surface water flows	Input directory
WaterUseProfileLn3004_2008.txt	Required input file for water use model.	Input directory
Ln3004_2008_data.txt	Meteorological input file of the example dataset	Input directory
Ln3004_2008.ohm	OHM	Input directory
Ln3004_2008.gis	GIS file	Input directory
Ln3004_2008.sahp	File withinformation for $Q_F$calculation	Input directory
Ln3004_2008_60.txt	60-min output file	example run
Ln3004_2008_ErrorFile.txt	Output file including possible error messages	example run
Ln3004_2008_Filechoices	File including the run options of the example run	example run
Ln3004_2008_MonthlyFile.txt	Output file containing monthly, seasonal and yearly output data	example run
Ln3004_2008_DailyFile.txt	Output file containing daily output data	example run
Ln3004_2008 _NARPOut.txt	Optional output file containing radiation balance components for the different sub surfaces.	example run
Ln3004_2008_5min.txt	Optional output file containing model outputs with 5-minute resolution.	example run

After you have unzipped the SUEWS_v1 file you should save the executable file (**SUEWS_v1.exe**) in the directory where you want to run it. *ModelledYears.txt*, *GridConnectionsYYYY.txt* and *HeaderInputSSNN_YYYY.nml* should be saved in the same file path as the executable file. *SSNN*is the site identification code where e.g. *SS* is the site name and *NN* is the code for the model area. *YYYY* is the year of the measurement defined in *ModelledYears.txt*. The other required input files (Section 3.1) should be in the file path chosen in *HeaderInputSSNN_YYYY.nml*(Figure 3.1). This means before running the model you must open the *HeaderInputSSNN_YYYY.nml* file and edit input and output file paths and the site identification (with a text editor such as Notepad, Editpad, Textpad etc.) so that they are correct for your setup. From the given site identification the model identifies the input files and generates the output files (Table 3.2).

For example if you specify FileOutputPath = “C:\FolderName\SUEWSOutputs\” and use site identification code (e.g. Ln3004_2008) the model creates an output file (***Remember to add the last backslash***):

C:\FolderName\SUEWSOutput\Ln3004_2008_60.txt.

If the file paths are not correct the program will return an error (Run-time Error, File path not found, see Appendix C for error messages) when run.Note that while running multiple grids all HeaderInputSSYY.nml files should be in the same directory as the executable while the input and output file can have separate file paths as defined in eachHeaderInput*SSNN_YYYY.nml*.

To run the model you can use Command Prompt[19] or just double click the executable file.Please, see FAQ (Appendix D) if you have problems running the model.

The zip file (Table 3.1) includes the library salflibc.dll which needs to be saved on the computer in order to run the model, and an example dataset with the required input data files and example output files (section 5). The library needs to be in a path that can be found by the programme.

[19] From Start select run –type cmd – this will open a window. Change directory to the location of where you stored your files. The following website may be helpful if you do not know what a command prompt is. http://dosprompt.info/

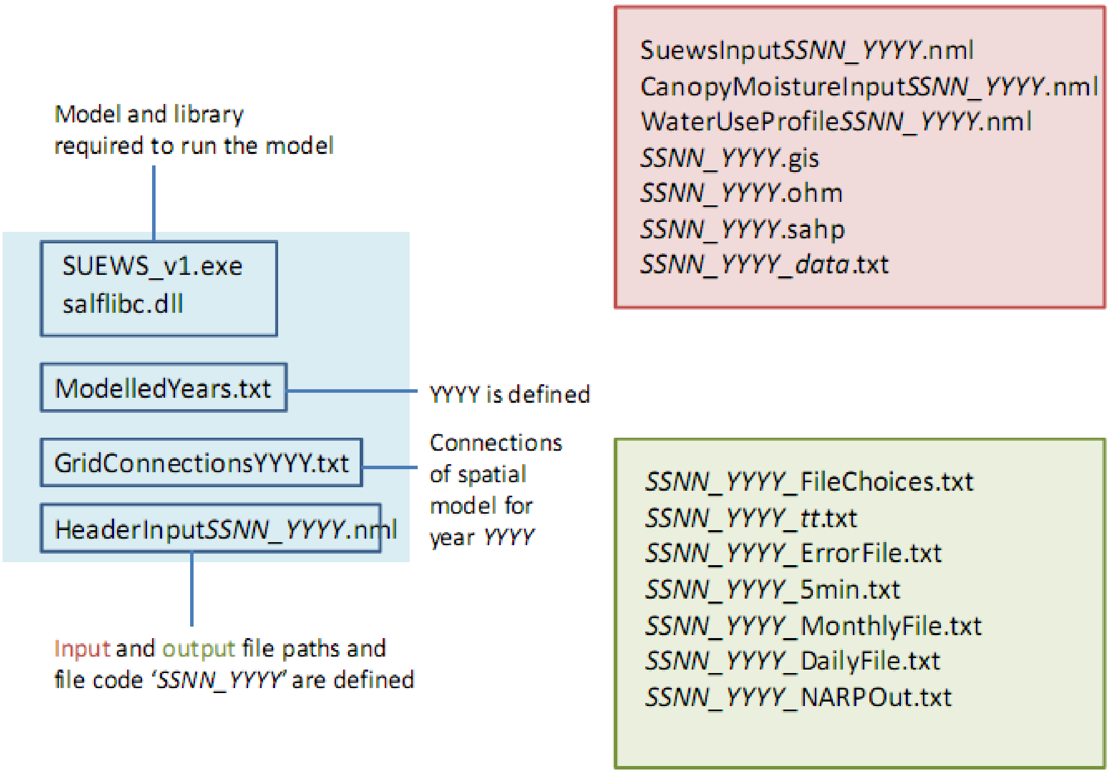

Figure 3.1. Input files needed and created output files of SUEWS version 1.0.

5.3.5 Input and output files

The input and output files required for SUEWS are listed in Table 3.2. For the user defined filenames (i.e. *SSYY*.ohm)*SS* represents a site name (usually a relevant two letter code is applied), and *YY* the year(typically a two digit year is used)or grid identification. Time step *tt* is set to 60-min with current version of the model.

Table 3.2:Input and Output files for SUEWS.

File Name	Description	Further Information
Input		
ModelledYears.txt	Listing of modelled years	Section 4.1
GridConnections***YYYY***.txt	Definition of modelled grids	Section 4.2
HeaderInput***SSNN_YYYY***.nml	Namelist: model parameters, file paths and run options.	List of variables – Table 4.1 Location: Same as the program code
SuewsInput***SSNN_YYYY***.nml	Namelist: model parameters and run options related to SUEWS	List of variables – Table 4.2 Location: Input file path
CanopyMoistureInput***SSNN_YYYY***.nml	File: water flows between surface stores	List of variables – Table 4.4 Location: Input file path
WaterUseProfile***SSNN_YYYY***.txt	File: parameters to calculate external water use	List of variables – Table 4.5 Location: Input file path
SSNN_YYYY.ohm	Parameter options for OHM.	List of variables – Table 4.7
SSNN_YYYY _data.txt	Meteorological forcing data	List of variables – Table 4.3
SSNN_YYYY.gis	GIS data	List of variables – Table 4.6
Output		
SSNN_YYYY _*tt*.txt	Model output with timestep*tt*	Output variables – Table 5.1
SSNN_YYYY _ErrorFile.txt	Model output with timestep*tt*	Output variables, including possible error messages – Table 5.1
SSNN_YYYY _NARPOut.txt	NARP file	List of variables - Table 5.4 Created if *NARPOutputChoice* = 1
SSNN_YYYY_MonthlyFile.txt	Monthly water balance	List of variables - Table

	(WB) file	5.2
SSNN_YYYY_DailyFile.txt	Daily WB file	List of variables - Table 5.2
SSNN_YYYY_5minFile	5-min WB file	List of variables - Table 5.3 Created if *write5min*=1

5.3.6 Input files

5.3.6.1 ModelledYears.txt

SUEWS can be used to model long time periods during what the forcing data, surface cover information and different input parameters may vary. The purpose of file **ModelledYears.txt** is to list the years which are modeled. In the example "!" indicates comments in the file. Comments are not read by the programme so they can be used by the user to provide notes for their interpretation of the contents.

Example of **ModelledYears.txt**

```
2     !Number of modelled years/time periods
  2008
  2009
```

This example would model two years: 2008 and 2009. This means that for both years all other input files with *YYYY*= 2008 and *YYYY*= 2009 are needed and output files created.

5.3.6.2 GridConnectionsYYYY.txt

SUEWS is a spatial model which can be run for several areas that are linked to each other as defined in **GridConnections*YYYY*.txt**. Connections concern water flows between the grids and the example describes a model run with two areas (in year 2008) Ln*3004_2008* and Ln*2926_2008* and 20% of water leaving grid Ln*3004_2008* as a runoff (either in pipes or above ground) will flow to grid Ln*2926_2008*. Similarly, as there are only two grids, the grid Ln*2926_2008* is not linked to any other grid.

Example of **GridConnections*YYYY*.txt**

```
2!Number of grid connections listed below
'Ln3004_2008'   0.2   'Ln2926_2008'
'Ln2926_2008'   0     'none'
!From  fraction   To
```

5.3.6.3 HeaderInputSSNN_YYYY.nml

The model run options and parameters are contained in **HeaderInput*SSNN_YYYY*.nml**. These are explained in Table 4.1

Table 4.1: Namelist and description of the parameters in **HeaderInput*SSNN_YYYY*.nml**. They can be in any order in the file (in total 84 parameters).
Req: R- parameters that are the most critical for the user to set for their model site.
VI: Variable that the parameter influences [F- anthropogenic heat flux, A – all fluxes, R radiation, S – Heat storage, W –multiple water balance fluxes, L- LUMPS, M – multiple heat fluxes].
CT = coniferous trees and shrubs, DT = deciduous trees and shrubs, GI = Irrigated grass, GU = unirrigated grass, W = water

Name	Req	VI	Units	Description
Model run options				
AnthropHeatChoice	R	F	-	Determines if Q_F is calculated [yes=3, no=0]
GISInputType	R	A	-	Declares GIS data file type (*see below*)
NARPOutput	R	R		Determines if NARP output file is printed [yes=1, no=0]
NetRadiationChoice	R	R	-	Determines net-radiation scheme (*see below*)
ldown_option	R	R	-	Determines which method is utilised for $L\downarrow$ (only relevant for *NetRadiationChoice*=2) (*see below*)
QSChoice	R	S	-	Identifies which ΔQ_S method is used – set to 1 to use OHM and - 2 to use measured
SuewsStatus	R	W	-	If SUEWS part is calculated [1] or only LUMPS [0]
Veg_type	R	W	-	Type of vegetation fraction used for LUMPS (*see below*)
z0_method	N	A	-	Defines method used to calculate roughness length (*see below*)
Parameters				
ALB(1)	N	R	-	Effective surface albedo for paved surfaces– sky view factor should be taken into account (see Appendix A)
ALB(2)	N	R	-	Same for roofs
ALB(3)	N	R	-	Same for CT
ALB(4)	N	R	-	Same for DT
ALB(5)	N	R	-	Same for GI
ALB(6)	N	R	-	Same for GU
ALB(7)	N	R	-	Same for water
ALB_SNOW	N	R	-	Effective surface albedo for snow (see Appendix A)
BaseT(1)	N	W	°C	Base temperature for leaf-on – CT (see Appendix A)
BaseT(2)	N	W	°C	Base temperature for leaf-on – DT (see Appendix

				A)
BaseT(3)	N	W	°C	Base temperature for leaf-on – GI (see Appendix A)
BaseT(4)	N	W	°C	Base temperature for leaf-on – GU (see Appendix A)
BaseTe(1)	N	W	°C	Base leaf-off (senescence) temperature – CT (see Appendix A)
BaseTe(2)	N	W	°C	Base leaf-off temperature – DT (see Appendix A)
BaseTe(3)	N	W	°C	Base leaf-off temperature – GI (see Appendix A)
BaseTe(4)	N	W	°C	Base leaf-off temperature – GU (see Appendix A)
BaseTHDD	N	W	°C	Base temperature for heating degree days (see Appendix A)
blgH	R	M	m	Mean building height
DayLightSavingDay(1)	R	M	d	Day of year (1-365/366) when the daylight saving time starts. Set to -999 if no daylight saving time occurs.
DayLightSavingDay(2)	R	M	d	Day of year (1-365/366) when the daylight saving time ends. Set to -999 if no daylight saving time occurs.
defaultFcld	N	R	-	Default cloud cover fraction (used if input data missing)
defaultPres	N	R	Pa	Default pressure (used if input data missing)
defaultRH	N	R	%	Default relative humidity (used if input data missing)
defaultT	N	R	°C	Default air temperature (used if input data missing)
defaulU	N	M	m s^{-1}	Default wind speed (used if input data missing)
DRAINRT	N	L	mm h^{-1}	Drainage rate of the “water bucket” (LUMPS; see Appendix A)
EMIS(1)	N	R	-	Effective bulk surface emissivity for paved surface– sky view factor should be taken into account (See Appendix A)
EMIS(2)	N	R	-	Same for roofs
EMIS(3)	N	R	-	Same for CT
EMIS(4)	N	R	-	Same for DT
EMIS(5)	N	R	-	Same for GI
EMIS(6)	N	R	-	Same for GU
EMIS(7)	N	R	-	Same for water
EMIS_SNOW	N	R	-	Effective surface emissivity for snow (See Appendix A)
FileInputPath	R	A	-	File path including the required input files.
FileOutputPath	R	A	-	File path where the output files are created.
FileCode	R	A	-	Total site identification code (e.g. SSNN_YYYY)
GDDFull(1)	N	W	°C	Growing degree days when leaf-on is over – CT (see Appendix A)
GDDFull(2)	N	W	°C	Growing degree days when leaf-on is over – DT (see Appendix A)
GDDFull(3)	N	W	°C	Growing degree days when leaf-on is over – GI

				(see Appendix A)
GDDFull(4)	N	W	°C	Growing degree days when leaf-on is over – GU (see Appendix A)
GrassFractionIrrigated	R	L	-	Fraction of irrigated grass used in LUMPS (0 to 1)
INTERVAL	R	A	min	Time interval of input data (Current version only 60 min)
LAIMax(1)	N	W	$m^2 m^{-2}$	Maximum LAI for CT (see Appendix A)
LAIMax(2)	N	W	$m^2 m^{-2}$	Maximum LAI for DT (see Appendix A)
LAIMax(3)	N	W	$m^2 m^{-2}$	Maximum LAI for GI (see Appendix A)
LAIMax(4)	N	W	$m^2 m^{-2}$	Maximum LAI for GU (see Appendix A)
LAIMin(1)	N	W	$m^2 m^{-2}$	Minimum LAI for CT (see Appendix A)
LAIMin(2)	N	W	$m^2 m^{-2}$	Minimum LAI for DT (see Appendix A)
LAIMin(3)	N	W	$m^2 m^{-2}$	Minimum LAI for GI (see Appendix A)
LAIMin(4)	N	W	$m^2 m^{-2}$	Minimum LAI for GU (see Appendix A)
lat	R	R	°	Latitude
lng	R	R	°	Longitude (NB. west of 0° should be set as POSITIVE)
numCapita	R	F	Capita ha^{-1}	Population density of the study area
PavedFractionIrrigated	R	L	-	Fraction of irrigated paved areas (0-1)
Qf_A(1)	R	F	$W m^{-2} (Capita\ ha^{-1})^{-1}$	Base value for Q_F on weekdays
Qf_A(2)	R	F	$W m^{-2} (Capita\ ha^{-1})^{-1}$	Base value for Q_F on weekends
Qf_B(1)	R	F	$W m^{-2} K^{-1} (Capita\ ha^{-1})^{-1}$	Parameter related to cooling degree days - weekdays
Qf_B(2)	R	F	$W m^{-2} K^{-1} (Capita\ ha^{-1})^{-1}$	Parameter related to cooling degree days - weekends
Qf_C(1)	R	F	$W m^{-2} (Capita\ ha^{-1})^{-1}$	Parameter related to heating degree days - weekdays
Qf_C(2)	R	F	$W m^{-2} (Capita\ ha^{-1})^{-1}$	Parameter related to heating degree days - weekends
RAINCOVER	N	L	mm	Limit when the surface is totally covered with water (LUMPS) (Appendix A)
RAINMAXRES	N	L	mm	Capacity of the surface to hold water (LUMPS) (Appendix A)
SDDFull(1)	N	W	°C	leaf-off ending degree day - CT
SDDFull(2)	N	W	°C	leaf-off ending degree day - DT
SDDFull(3)	N	W	°C	leaf-off ending degree day - GI
SDDFull(4)	N	W	°C	leaf-off ending degree day - GU

SkipHeaderGIS	R	A	-	Number of header lines to skip in GIS input file
SkipHeaderMet	R	A	-	Number of header lines to skip in meteorological input file
TIMEZONE	R	R	h	Time zone relative to UTC (OBS! east is positive)
TRANS_SITE	N	R	-	Atmospheric transmissivity (0-1) of the site (used in NARP)
TreeFractionIrrigated	R	L	-	Fraction of land in which trees are irrigated (LUMPS)
treeH	R	M	m	Mean height of trees
year	R	A	YYYY	Year of study (important to determine if a leap year)
z	R	M	m	Height of the meteorological measurements

GISInputType

For GIS data there are two possible temporal resolutions. The land cover data can
GISInputType = 3 stay constant with time
GISInputType = 4 vary with each timestep

NetRadiationChoice

NetRadiationChoice= 1 net all-wave radiation Q^* is observed
NetRadiationChoice= 2 modelled using the net all-wave parameterization (NARP)[3,4]

ldown_option[4]

There are three possible ways to take the downwellinglongwave radiation into account
ldown_option = 1 observations
ldown_option = 2 calculated from cloud cover fraction
ldown_option = 3 calculated from air temperature and relative humidity

QSChoice

QSChoice = 1 storage heat flux is modelled using the objective hysteresis model (OHM)[5,6,7]. The model is based on surface types

Veg_type

This determines how the vegetation fraction is used to model the turbulent heat fluxes in LUMPS
Veg_type= 1 total fraction of vegetation (sum of trees, grass, water) fractions from the total surface area
Veg_type= 2 fraction of vegetation that is irrigated (active evapotranspiring rather than dry vegetation)

z0_method

This determines how aerodynamic roughness length (z_{0m}) and zero displacement height are calculated
z0_method = 1 Values defined in GIS file are used
z0_method = 2 Calculated from mean building height with "Rule of Thumb"[20]
z0_method = 3 Calculated according to plan and frontal areal fractions[21]

[20] Grimmond C.S.B. & Oke T.R. (1999). Aerodynamic properties of urban areas derived from analysis of surface form. *J. Appl. Meteorol.* 38, 1262-1292.

5.3.6.4 SuewsInputSSNN_YYYY.nml

The parameters and model run options for SUEWS are specified in the file**SUEWSInputs*SSNN_YYYY*.nml**. These are explained in Table 4.2.

Table 4.2: Parameters used in SUEWS: SuewsInput*SSNN_YYYY*.nml. They can be in any order in the file (69parameters).
Req: R- parameters that are the most critical for the user to set for the site.
VI: Variable that the parameter influences [F- anthropogenic heat flux, A – all fluxes, R radiation, S – Heat storage, W –multiple water balance fluxes, L- LUMPS, M – multiple heat fluxes].
CT = coniferous trees and shrubs, DT = deciduous trees and shrubs, GI = Irrigated grass, GU = unirrigated grass, W =water

Name	Req	VI	Units	Description
Model run options				
RoughLen_heat	R	M	-	Method to calculate roughness length for heat (*See below*)
smd_choice	R	W	-	Soil moisture deficit is either modelled [0] or measured is used [1]
sm_input	N	W	-	Soil moisture deficit in the input file is either volumetric [1] or gravimetric [2] (set to -999 if modelled is used)
StabilityMethod	N	M	-	Atmospheric stability method used (*see below*)
write5min	R	W	-	Write 5-min output file [yes=1, no=0]
WU_choice	R	W	-	External Water use is either modelled [0] or the measured is used [1]
Parameters				
BldgStorCap	N	W	mm	Water storage capacity of buildings(see Appendix A)
BldgDrainCoef1	N	W	mm	Coefficient D_0 in drainage equation for buildings(see Appendix A)
BldgDrainCoef2	N	W	-	Coefficient *b* in drainage equation for buildings(see Appendix A)
BldgState	R	W	mm	Initial wetness state for buildings
ConifStorCap	N	W	mm	Water storage capacity of CT(see Appendix A)
ConifDrainCoef1	N	W	mm	Coefficient D_0 in drainage equation for CT(see Appendix A)
ConifDrainCoef2	N	W	-	Coefficient *b* in drainage equation for CT(see Appendix A)
ConifState	R	W	mm	Initial wetness state of CT
DecidStorCap	N	W	mm	Water storage capacity of DT(see Appendix A)
DecidDrainCoef1	N	W	mm	Coefficient D_0 in drainage equation for DT(see Appendix

[21] MacDonald R.W., Griffiths R.F.&Hall D.J. (1998). An improved method for estimation of surface roughness of obstacle arrays.*Atmos. Env.* 32, 1857-1864.

				A)
DecidDrainCoef2	N	W	-	Coefficient *b* in drainage equation for DT(see Appendix A)
DecidState	R	W	mm	Initial wetness state of DT
FlowChange	R	W	mm	Difference of input and output flows of the water surface type
G1	N	W	mm s^{-1}	surface conductance coefficient (see Appendix A)
G2	N	W	W m^{-2}	surface conductance coefficient (see Appendix A)
G3	N	W	kg g^{-1}	surface conductance coefficient (see Appendix A)
G4	N	W	g kg^{-1}	surface conductance coefficient (see Appendix A)
G5	N	W	°C	surface conductance coefficient (see Appendix A)
G6	N	W	mm^{-1}	surface conductance coefficient (see Appendix A)
GrassUStorCap	N	W	mm	Water Storage capacity of GU (see Appendix A)
GrassUDrainCoef1	N	W	mm	Coefficient D_0 in drainage equation for GU (see Appendix A)
GrassUDrainCoef2	N	W	-	Coefficient *b* in drainage equation for GU (see Appendix A)
GrassUState	R	W	mm	Initial wetness state of GU
GrassIStorCap	N	W	mm	Water Storage capacity of GI (see Appendix A)
GrassIDrainCoef1	N	W	mm	Coefficient D_0 in drainage equation for GI (see Appendix A)
GrassIDrainCoef2	N	W	-	Coefficient *b* in drainage equation for GI (see Appendix A)
GrassIState	R	W	mm	Initial wetness state of GI
HydraulicConduct	N	W	mm h^{-1}	Hydraulic conductivity of soil(see Appendix A)
InternalWaterUse	R	W	mm tt^{-1}	Internal water use on the study area (set to 0 if water use is modelled)
Kmax	N	W	W m^{-2}	Annual maximum hourly downward radiation. Change only if different surface conductance coefficients (G_1-G_6) are used. (see Appendix A)
PavStorCap	N	W	mm	Water storage capacity of paved areas(see Appendix A)
PavDrainCoef1	N	W	mm	Coefficient D_0in drainage equation for paved areas(see Appendix A)
PavDrainCoef2	N	W	-	Coefficient *b* in drainage equation for paved areas(see Appendix A)
PavState	R	W	mm	Initial wetness state of paved areas
PipeCapacity	R	W	mm	Storage capacity of the pipes
RunoffToWater	R	W	-	Fraction of water flowing to water surface type from above ground runoff
S1	N	W	mm	surface conductance coefficient (see Appendix A)
S2	N	W	mm	surface conductance coefficient (see Appendix A)

SDECStor	N	W	mm	Water Storage capacity of DT (leaf-on)(see Appendix A)
SmCap	N	W	kg m^{3} m^{-3} kg-^{1}/	Maximum water content in the soil (Needed if measured soil moisture is used)
SoilDensity	N	W	kg m^{-3}	Density of soil (Set to -999 if soil moisture is modelled)
SoilDepth	N	W	mm	Soil depth of the modelled soil moisture
SoilDepthMeas	N	W	mm	Soil depth of the measured soil moisture (Set to -999 if soil moisture is modelled)
SoilRocks	N	W	-	Fraction of soil without rocks (Set to -999 if soil moisture is modelled)
soilstorePav	N	W	mm	Maximum water soil storage of paved areas
soilstoreBldg	N	W	mm	Maximum water soil storage of buildings
soilstorePavstate	R	W	mm	Initial state of the soil water storage of paved areas
soilstoreBldgstate	R	W	mm	Initial state of the soil water storage of buildings
soilstoreConif	N	W	mm	Maximum water soil storage of CT
soilstoreDec	N	W	mm	Maximum water soil storage of DT
soilstoreGrass	N	W	mm	Maximum water soil storage of grass (same for irrigated and un-irrigated grass)
soilstoreConifstate	R	W	mm	Initial state of the water soil storage of CT
soilstoreDecstate	R	W	mm	Initial state of the water soil storage of DT
soilstoreGrassUnirstate	R	W	mm	Initial state of the water soil storage of GU
soilstoreGrassirrstate	R	W	mm	Initial state of the water soil storage of GI
SurfaceArea	R	W	ha	Area of the study site
TH	N	W	°C	Maximum temperature limit. Change only if different surface conductance coefficients (G_1-G_6) are used. (see Appendix A)
TL	N	W	°C	Minimum temperature limit for surface conductance. Change only if different surface conductance coefficients (G_1-G_6) are used. (see Appendix A)
Tstep	N	W	s	Timestep for the water balance calculations
WaterUseArea	N	W	ha	Area for water use (Set to -999 if soil moisture is modelled)
WaterState	R	W	mm	Initial state of the water storage in the water surface type
WaterStorCap	R	W	mm	Maximum water storage in the water surface type

RoughLen_heat

Roughness length for heat is calculated

RoughLen_heat= 1 as $0.1z_{0m}$

RoughLen_heat= 2 according to Kawai et al. (2009)[22]

RoughLen_heat= 3 according to Voogt and Grimmond (2000)[23]

[22] Kawai T., Ridwan M.K. & Kanda M. (2009). Evaluation of the simple urban energy balance model using selected data from 1-yr flux observations at two cities.*J. Appl. Meteorol. Clim.* 48, 693-715.

RoughLen_heat= 4 according to Kanda et al. (2007)[24]

StabilityMethod

Defines which stability function is used

StabilityMethod= 2 Momentum:
Unstable: Dyer (1974)[25], modified by Högstrom (1988)[26]
Stable: Van Ulden & Holtslag (1985)[27]
Heat:
Dyer (1974), modified by Högstrom (1988)

StabilityMethod= 3 Momentum:
Campbell & Norman[28]eqn 7.27 p 97
Heat:
Unstable: Campbell & Norman Stable:Dyer (1974) modifed by Högstrom (1988)

StabilityMethod= 4 Momentum and heat
Businger*et al.* (1971)[29]modifedby Högstrom (1988)

5.3.6.5 Meteorological input file (SSNN_YYYY_data.txt)

SUEWS is designed to run using commonly measured meteorological variables[1]. Table 4.3gives the required and optional additional input variables. Variables marked with # in the comment column are not compulsory and can be replaced with **-999.0** if the user's dataset does not include the variable. Columns 16 and 17 relate to the calculation of the downwellinglongwave radiation and in the current version there are three possibilities[3]:

1) Observed downward longwave radiation in column 16 (*ldown_option*= 1)
2) Downward longwave radiation is calculated from the cloud cover in column 17 (*ldown_option* = 2)
3) Downward longwave radiation is calculated from relative humidity and air temperature data (*ldown_option* = 3)

---

[23] VoogtJ.A&Grimmond C.S.B. (2000).Modeling surface sensible heat flux using surface radiative temperatures in a simple urban terrain.*J. Appl. Meteorol.* 39, 1679-1699

[24] Kanda, M., Kanega, M., Kawai, T., Moriwaki, R. & Sugawara, H., 2007. Roughness lengths for momentum and heat derived from outdoor urban scale models. *J. Appl. Meteorol. Clim.* 46, 1067-1079.

[25] Dyer A.J., (1974). A review of flux-profile relationships.*Boundary-Layer Meteorol*. 7, 363-372.

[26] Högström U. (1988).Non-dimensional wind and temperature profiles in the atmospheric surface layer: A re-evaluation.*Boundary-Layer Meteorol.*42, 55–78.

[27] van Ulden A.P. & Holtslag A.A.M. (1985). Estimation of atmospheric boundary layer parameters for boundary layer applications.*J. Clim. Appl. Meteorol.* 24, 1196-1207.

[28] Cambell G.S. & Norman J.M (1998).Introduction to Environmental Biophysics.Springer Science.

[29] Businger J.A., Wungaard J.C., Izumi Y. & Bradley E.F. (1971).Flux-Profile Relationships in the Atmospheric Surface Layer.*J. Atmos. Sci.*, **28**, 181–189.

Table 4.3: Meteorological input data to run SUEWS (*SSNN_YYYY*_data.txt)

Col	Variable	Model	Units	Comments
1	Day of year	id	-	
2	Time	it	-	
3	Decimal time	dectime	-	
4	Net all-wave radiation	qn1	W m^{-2}	#, With *NetRadiationChoice*=1
5	Observed sensible heat flux	qh	W m^{-2}	#
6	Observed latent heat flux	qe	W m^{-2}	#
7	Observed storage heat flux	qs	W m^{-2}	#
8	Anthropogenic heat flux	qf	W m^{-2}	#
9	Mean wind speed	avu1	m s^{-1}	
10	Mean relative humidity	avrh	%	
11	Mean air temperature	Temp_C	°C	
12	Station air pressure	Pres_kPa	kPa	
13	Rain	ph	mm t^{-1}	Reported for the time interval *t*
14	Mean incoming solar radiation	avkdn	W m^{-2}	#
15	Snow cover fraction	snow	-	#
16	Observed downward longwave radiation	ldown_obs	W m^{-2}	#
17	Observed cloud faction	fcld_obs	Tenths	#
18	External water use	wuh	m^3 t^{-1}	#
19	Soil moisture deficit	xsmd	m^3 m^{-3}/ kg kg^{-1}	#
20	Leaf Area Index	lai_hr	-	#

5.3.6.6 CanopyMoistureSSNN_YYYY.nml

CanopyMoisture*SSNN_YYYY*.nml file allows water to move between canopy storages within a grid/area. This way impervious connectivity can be taken into account. In this file the user sets the fraction of water flowing to runoff and to other surfaces from drainage(Table 4.4). E.g. if 0.05 of water from building flows to other surfaces:

BuildtoRunOff=0.95
BuildtoPaved=0.01
BuildtoConif=0.01
BuildtoDecid=0.01
BuildtoIrrGrass=0.01

BuildtoUnIrrGrass=0.01

Table 4.4: Variables in **CanopyMoisture*SSNN_YYYY*.nml** file.
CT = coniferous trees and shrubs, DT = deciduous trees and shrubs, GI = Irrigated grass, GU = unirrigated grass, W =water

Parameter name	**Description**	
PavedtoRunOff	Water from paved to runoff	Add up to one
PavedtoConif	Water from paved to CT	
PavedtoDecid	Water from paved to DT	
PavedtoIrrGrass	Water from paved to IG	
PavedtoUnirrGrass	Water from paved to UG	
PavedtoWater	Water from paved to water	
BuildtoRunOff	Water from roofs to runoff	Add up to one
BuildtoPaved	Water from roofs to paved surface	
BuildtoConif	Water from roofs to CT	
BuildtoDecid	Water from roofs to DT	
BuildtoIrrGrass	Water from roofs to IG	
BuildtoUnIrrGrass	Water from roofs to UG	
BuildtoWater	Water from roofs to water	
ConiftoSoil	Water from CT to soil	Add up to one
ConiftoPaved	Water from CT to paved surface	
ConiftoDecid	Water from CT to DT	
ConiftoIrrGrass	Water from CT to IG	
ConiftoUnirrGrass	Water from CT to UG	
ConiftoWater	Water from CT to water	
DecidtoSoil	Water from DT to soil	Add up to one
DecidtoPaved	Water from DT to paved surface	
DecidtoConif	Water from DT to CT	
DecidtoIrrGrass	Water from DT to IG	
DecidtoUnirrGrass	Water from DT to unirrigated grass	
DecidtoWater	Water from DT to water	
IrrGrasstoSoil	Water from IG to soil	Add up to one
IrrGrasstoPaved	Water from IG to paved surface	
IrrGrasstoConif	Water from IG to CT	
IrrGrasstoDecid	Water from IG to DT	
IrrGrasstoUnirrGrass	Water from IG to UG	
IrrGrasstoWater	Water from IG to water	
UnirrGrasstoSoil	Water from UG to soil	Add up to one
UnirrGrasstoPaved	Water from UG to paved surface	
UnirrGrasstoConif	Water from UG to CT	
UnirrGrasstoDecid	Water from UG to DT	
UnirrGrasstoIrrGrass	Water from UG to IG	
UnirrGrasstoWater	Water from UG to water	

5.3.6.7 File for water use model (WaterUseProfileSSNN_YYYY.txt)

SUEWS includes a simple model for external water use if it is not measured. The model calculates daily water use from the mean daily air temperature, days since rain and fraction of irrigated area using automatic/manual irrigation. Water use is divided into hours according to ready or user defined hourly profiles (Table 4.5).

Table 4.5: Input information for the external water use model.Doy- day of year

Name in Model	Units	Description
Ie_start	doy	Starting day of the irrigation period
Ie_end	doy	Ending day of the irrigation period
Faut	-	Fraction of irrigated area using automatic sprinklers
Ie_a(1)	mm	Coefficient for automatic irrigation model
Ie_a(2)	mm $°C^{-1}$	Coefficient for automatic irrigation
Ie_a(3)	mm d^{-1}	Coefficient for automatic irrigation
Ie_m(1)	mm	Coefficient for manual irrigation
Ie_m(2)	mm $°C^{-1}$	Coefficient for manual irrigation
Ie_m(3)	mm d^{-1}	Coefficient for manual irrigation
DayWat(1)		Irrigation allowed on Sundays [1], if not [0]
DayWat(2)		Irrigation allowed on Mondays [1], if not [0]
DayWat(3)		Irrigation allowed on Tuesdays [1], if not [0]
DayWat(4)		Irrigation allowed on Wednesdays [1], if not [0]
DayWat(5)		Irrigation allowed on Thursdays[1], if not [0]
DayWat(6)		Irrigation allowed on Fridays [1], if not [0]
DayWat(7)		Irrigation allowed on Saturdays [1], if not [0]
DayWatPer(1)		Fraction of houses following restrictions on Sundays [0-1]
DayWatPer(2)		Fraction of houses following restrictions on Mondays [0-1]
DayWatPer(3)		Fraction of houses following restrictions on Tuesdays[0-1]
DayWatPer(4)		Fraction of houses following restrictions on Wednesdays[0-1]
DayWatPer(5)		Fraction of houses following restrictions on Thursdays[0-1]
DayWatPer(6)		Fraction of houses following restrictions on Fridays[0-1]
DayWatPer(7)		Fraction of houses following restrictions on Saturdays[0-1]
HourResChoice		Hourly water use profile (*See below*)
HourWat		If *HourResChoice* = 0, set your own profile (*see below*).

HourResChoice

Defines what kind of hourly water use profile is used.

HourResChoice = 0 User defines own profile. Give the fractions of water used on each hour from the daily value. For example

HoutWat(5)=0.2
HourWat(6)=0.2
HoutWat(7)=0.2
HourWat(8)=0.2
HourWat(9)=0.2
allows irrigation to happen only between 4:00-8:00.

For ready options the fraction of daily water use occurring during fixed time period is given

HourResChoice= 1	7:00-16:00	0.35
	16:00-20:00	0.50
	20:00-23:00	0.15
HourResChoice= 2	7:00-16:00	0.40
	16:00-20:00	0.20
	20:00-23:00	0.40
HourResChoice= 3	7:00-16:00	0.19
	16:00-20:00	0.46
	20:00-23:00	0.35

5.3.6.8 GIS input file (SSNN_YYYY.gis)

This input file includes the plan area or 3-d (used in OHM) surface cover fractions for the different surface types, the roughness length for momentum and zero displacement height and frontal area fraction λ_F. Table 4.6 summarizes the GIS file format.

Table 4.6: *SSNN_YYYY*.gis**. That is is used when GISInputFormat = 3 or 4 (see Table 4.1). Note that the sum of columns from 4 to 11 has to equal 1. # indicates optional: Set to** -999 **if not used.** CT = coniferous trees and shrubs, DT = deciduous trees and shrubs, GI = Irrigated grass, GU = unirrigated grass, W =water

Col	Name in model	Description/Comment	
1	id	Day of year. Set to 3 if *GISInputFormat*=3	
2	it	Time in hours. Set to 3 if *GISInputFormat*=3	
3	iqual	Quality. Not used (set to 1)	
4	build	Areal cover fraction – buildings	
5	ximper	Areal cover fraction – paved	
6	unman	Areal cover fraction – unmanaged e.g. bare soil	
7	con_sh	Areal cover fraction – CT	
8	dec_sh	Areal cover fraction – DT	
9	Unirrgrass	Areal cover fraction – UG	
10	Irrgras	Areal cover fraction – IG	
11	watr	Areal cover fraction – water	
12	cany3D	Building fraction including walls	#
13	roof3D	Building fraction accounting slope of roofs	#
14	z0m	Roughness length for momentum	#
15	zdm	Zero displacement height	#
16	planFblg	Frontal area fraction for buildings	#
17	planFtr	Frontal area fraction for trees	#

5.3.6.9 OHM file (SSNN_YYYY.ohm)

The OHM file contains information on how the different surface types are taken into account in the calculation of net storage heat flux. That is what values should be used for the parameters in the OHM equation[5,6].The possible choices (Table 4.7) are followed by examples of OHM files.

Table 4.7: Description of choices in ***SSNN_YYYY*.ohm** file

Statement	Choice options	Comment
Are canyons included	[1] Yes [2] No	
Calculation of the coefficients for canyons	[2] Mean [3] Yoshida *et al.* (1990, 1991) – E-W canyon [4] Nunez (1974) – N-S canyon	Line added in the ohm-file only if **YES** was chosen on the previous line
Vegetation is calculated	[1] one [2] separated to grass/trees & shrubs/water	
Calculation of the coefficients for vegetation	[1] Mean [2] Mixed forest – McCaughey (1985) [3] Short grass -- Doll *et al.* (1985) [4] Bare soil -- Novak (1982) [5] Bare soil (wet) -- Fuchs & Hadas (1972) [6] Bare soil (dry) -- Fuchs & Hadas (1972) [7] Bare soil -- Asaeda & Ca (1993) [8] Water Shallow - Turbid -- Souch *et al.*(1998)	If option [1] is **NOT** used, put as many choices in the following rows as you want to take into account and add zero when finished
Calculation of the coefficients for roof	[1] Mean of all [2] Tar and gravel -- Yap (1973) [3] Taseler (1980) [4] Yoshida et al. (1990, 1991) [5] Average gravel/tar/conc. flat industrial -- Meyn (2000) [6] Dry -- gravel/tar/conc. flat industrial -- Meyn (2000) [7] Wet -- gravel/tar/conc. flat industrial -- Meyn (2000) [8] Bitumen spread over flat industrial membrane -- Meyn (2000) [9] Asphalt shingle on plywood residential roof – Meyn (2000) [10] Star - high albedo asphalt shingle residential roof -- Meyn (2000) [11] Star - Ceramic Tile -- Meyn (2000) [12] Star - Slate Tile -- Meyn (2000)	If option [1] is **NOT** used, put as many choices in the following rows as you want to take into account and add zero when finished
Impervious	[1] one	

areas are calculated as	[2] separated to concrete & asphalt	
Calculation of the coefficients for impervious areas	[1] Mean [2] Concrete – Doll *et al.*(1985) [3] Concrete -- Asaeda & Ca (1993) [4] Asphalt – Narita et al. (1984) [5] Asphalt -- Asaeda & Ca (1993) [6] Asphalt – Anandakumar (1999) [7] Asphalt (winter) – Anandakumar (1999) [8] Asphalt (summer) – Anandakumar (1999)	If option [1] is **NOT** used, put as many choices in the following rows as you want to take into account and add zero when finished

The **Ln*3004_2008*.ohm** file contained within the example dataset has the following structure.

```
%    # Ln08.ohm
%    2   Canyons included: [1] Y [2] N
%    2   Vegetation as one [1] Y [2] Separate grass/trees&shrubs/water
%    3   Vegetation: [3] Short grass -- Doll et al. (1985)
%    4               [4] Bare soil -- Novak (1982)
%    0
%    1   Roof: [1] Mean of all
%    2   Impervious as one [1] Y [2] Concrete & asphalt separate
%    2   Impervious surface: [2] Concrete – Doll et al. (1985)
%    4       [4] Asphalt – Narita et al. (1984)
%    0
```

In the model run, canyons are excluded, and vegetation is divided into trees/shrubs&shrubs/water, and paved surfaces into concrete and asphalt. For all surfaces the coefficients are calculated as the mean value of the assigned materials (Appendix B).

5.3.7 Output files

5.3.7.1 Model output files

SUEWS produces the main output file(***SSNN_YYYY_tt*.txt**)and an output file (***SSNN_YYYY*_ErrorFile.txt**) including possible error messages related to running the model (Appendix C). Both files have time resolution defined by *INTERVAL*. These contain a header with a selection of model run information. An example is presented below.

*Line 1*gives the model version and any additional modules that may have been run.
Line 2 indicates if multiple areas were used (always 1 in SUEWS_v1) and how the net radiation was calculated.
Line 3 indicates the method use to calculate the storage heat flux (OHM always used in SUEWSv1).
*Line 4*indicates*veg_type* usedin LUMPS and which *ldown_option* choice was used.

% Version= SUESWS_v1.0

% common[1]Common choices for all site Q*=[2]Modelled -NARP
% QS=[1]OHM [2] Dyer (1974) modified by Ho
% veg_type: 1 ldown_option: 1

The columns in the output file are explained in Table 5.1.

Table 5.1: SUEWS output file format: ***SSNN_YYYY _tt*.txt** where tt is set to 60 in the current version of the model

Col	Header	Name	Units
1	id	Day of Year	-
2	it	Time	-
3	dectime	Decimal Time	-
4	kdown	Incoming shortwave radiation	W m^{-2}
5	kup	Reflected shortwave radiation	W m^{-2}
6	ldown	Downwellinglongwave radiation	W m^{-2}
7	lup	Upwelling longwave radiation	W m^{-2}
8	Tsurf	Surface temperature	°C
9	qn	Net all-wave radiation	W m^{-2}
10	h_mod	Sensible heat flux-LUMPS	W m^{-2}
11	e_mod	Latent heat flux-LUMPS	W m^{-2}
12	qs	Storage heat flux	W m^{-2}
13	QF	Anthropogenic heat flux	W m^{-2}
14	QH	Sensible heat flux-SUEWS	W m^{-2}
15	QE	Latent heat flux-SUEWS	W m^{-2}
16	P/i	Rain per interval	mm
17	Ie/i	External water use on grass	mm
18	E/i	Evaporation per interval	mm
19	DR/i	Drainage per interval	mm
20	Ch/i	Change of surface and soil stores per interval	mm
21	ST/i	Land surface state per interval	mm
22	ROsoil/i	Soil runoff per interval	mm
23	RO/i	Runoff per interval	mm
24	ROpipe	Runoff in pipes per interval	mm
25	ROpav	Above ground runoff on paved surface per interval	mm
26	ROveg	Above ground runoff on vegetation surface per interval	mm
27	ROwater	Runoff occurring through water body per interval	mm
28	Ra	Aerodynamic resistance	s m^{-1}
29	Rs	Surface resistance	s m^{-1}
30	ustar	Friction velocity	m s^{-1}
31	L_mod	Modelled Obukhov length	m
32	SoilSt_pav	Soil moisture state of paved surface	mm
33	SoilSt _blg	Soil moisture state of building surface	mm

34	SoilSt _con	Soil moisture state of coniferous surface	mm
35	SoilSt _dec	Soil moisture state of deciduous surface	mm
36	SoilSt _Irrgr	Soil moisture state of irrigated grass	mm
37	SoilSt _Gr	Soil moisture state of unirrigated grass	mm
38	St_pav	State of paved surface	mm
39	St_blg	State of building surface	mm
40	St_con	State of coniferous surface	mm
41	St_dec	State of deciduous surface	mm
42	St_Irrgr	State of irrigated grass	mm
43	St_Gr	State of unirrigated grass	mm
44	St_water	State of the water body	mm
45	Fcld	Cloud cover fraction	-
46	SoilState	Soil moisture state	mm
47	smd	Soil moisture deficit	mm
48	LAI	Leaf area index	-
49	Fw	Additional water flow to the water body	mm
50	addWater	Water input from other grids	mm

5.3.7.2 Daily and monthly output files

In addition to the output files with time resolution defined by *INTERVAL* the model generates output files containing daily (***SSNN_YYYY_DailyFile.txt***) and monthly (***SSNN_YYYY_MonthlyFile.txt***) values. Table 5.2 give the content by column for both of these files.

Table 5.2: Output included in*SSYY*_DailyFile.txt and *SSYY*_MonthlyFile.txt files ordered by column (Col)

Col	Header	Name	Units
1	id	Day of Year	-
2	counter	Counter	-
3	qn	Net all-wave radiation	W m^{-2}
4	qs	Storage heat flux	W m^{-2}
5	qf	Anthropogenic heat flux	W m^{-2}
6	qe_S	Latent heat flux-SUEWS	W m^{-2}
7	pp	Precipitation	mm
8	ext_Ie	External water use on grass	mm
9	int_Ie	Internal water	mm
10	tot_Ie	Total (ext+int) water use	mm
11	E_S	Evaporation per day/month	mm
12	Change	Storage change	mm
13	R_Soil	Soil runoff	mm
14	R	Surface runoff	mm
15	Fw	Additional water flow to the water	mm

		body	
16	addWater	Water input from other grids	mm

5.3.7.3 5-min output file

If user chooses to have the 5 minute output which is specified by write5min=1 (in the file SuewsInput*SSYY*.nml), SUEWS will create an output file ***SSNN_YYYY*_5min.txt** including water balance results with 5-min resolution (Table 5.3). Note this will likely make the model runs much slower as there is going to be large amount of additional input.

Table 5.3: Structure of the 5 min ouput files:***SSNN_YYYY*_5min.txt**.

Col	Header	Name	Units
1	id	Day of Year	-
2	5min	Time	-
3	pp	Rain	mm
4	Ie	External water use	mm
5	E	Evaporation	mm
6	St_pav	State of paved surface	mm
7	St_blg	Moisture state of building surface	mm
8	St_con	Moisture state of coniferous surface	mm
9	St_dec	Moisture state of deciduous surface	mm
10	St_IrrGr	Moisture state of irrigated grass	mm
11	St_Gr	Moisture state of unirrigated grass	mm
12	St_water	State of the water surface type	mm
13	SoilSt_pav	Soil moisture state of paved surface	mm
14	SoilSt_blg	Soil moisture state of building surface	mm
15	SoilSt _con	Soil moisture state of coniferous surface	mm
16	SoilSt _dec	Soil moisture state of deciduous surface	mm
17	Sl_Irrgr	Soil moisture state of irrigated grass	mm
18	SoilSt_Gr	Soil moisture state of unirrigated grass	mm
19	D_pav	Drainage - paved surface	mm
20	D_blg	Drainage – buildings	mm
21	D_con	Drainage – coniferous trees	mm
22	D_dec	Drainage – deciduous trees	mm
23	D_Irrgr	Drainage – irrigated grass	mm
24	D_Gr	Drainage – unirrigated grass	mm
25	r_pav	Runoff - paved surface	mm
26	r_blg	Runoff - buildings	mm
27	r_con	Runoff - coniferous trees	mm
28	r_dec	Runoff - deciduous trees	mm
29	r_Irrgr	Runoff - irrigated grass	mm

30	r_ Gr	Runoff - unirrigated grass	mm
31	Soilr_pav	Soil runoff - paved surface	mm
32	Soilr_blg	Soil runoff - buildings	mm
33	Soilr_con	Soil runoff - coniferous trees	mm
34	Soilr_dec	Soil runoff - deciduous trees	mm
35	Soilr_Irrgr	Soil runoff - irrigated grass	mm
36	Soilr_ Gr	Soil runoff - unirrigated grass	mm

5.3.7.4 NARP output file

If *NARPOutput*= 1, SUEWS generates a NARP output file which includes radiation balance components and surface temperatures for each sub surface. Table 5.4 lists the variables included in this file.

*Table 5.4: NARP output file format:*SSNN_YYYY *_NARPOut.txt*

Col	Header	Name	Units
1	id	Day of Year	-
2	dectime	Decimal Time	-
3	kup_pav	Reflected shortwave radiation from paved areas	W m^{-2}
4	kup_blg	Reflected shortwave radiation from roofs	W m^{-2}
5	kup_con	Reflected shortwave radiation from coniferous area	W m^{-2}
6	kup_dec	Reflected shortwave radiation from deciduous area	W m^{-2}
7	kup_Irrgr	Reflected shortwave radiation from irrigated grass	W m^{-2}
8	kup_Gr	Reflected shortwave radiation from unirrigated grass	W m^{-2}
9	kup_wtr	Reflected shortwave radiation from water	W m^{-2}
10	lup_pav	Upwelling longwave radiation from paved areas	W m^{-2}
11	lup_blg	Upwelling longwave radiation from roofs	W m^{-2}
12	lup_con	Upwelling longwave radiation from coniferous area	W m^{-2}
13	lup_dec	Upwelling longwave radiation from deciduous area	W m^{-2}
14	lup_Irrgr	Upwelling longwave radiation from irrigated grass	W m^{-2}
15	lup_Gr	Upwelling longwave radiation from unirrigated grass	W m^{-2}
16	lup_wtr	Upwelling longwave radiation from water	W m^{-2}
17	Ts _pav	Surface temperature - paved areas	°C
18	Ts _blg	Surface temperature - roofs	°C
19	Ts _con	Surface temperature - coniferous trees	°C
20	Ts _dec	Surface temperature – deciduous trees	°C

21	Ts _Irrgr	Surface temperature - irrigated grass	°C
22	Ts _Gr	Surface temperature - unirrigated grass	°C
23	Ts_wtr	Surface temperature –water body	°C
24	qn _pav	Net all-wave radiation - paved areas	W m^{-2}
25	qn _blg	Net all-wave radiation - roofs	W m^{-2}
26	qn _con	Net all-wave radiation - coniferous trees	W m^{-2}
27	qn _dec	Net all-wave radiation – deciduous trees	W m^{-2}
28	qn _Irrgr	Net all-wave radiation - irrigated grass	W m^{-2}
29	qn _Gr	Net all-wave radiation - unirrigated grass	W m^{-2}
30	qn_wtr	Net all-wave radiation –water body	W m^{-2}

5.3.8 Appendix A. Suggested values for the parameters to run SUEWS.

Input	Value	Units	Source
ALB(1)	0.12	-	Oke (1987)
ALB(2)	0.15	-	Oke (1987)
ALB(3)	0.10	-	Oke (1987)
ALB(4)	0.18	-	Oke (1987)
ALB(5)	0.21	-	Oke (1987)
ALB(6)	0.21	-	Oke (1987)
ALB(7)	0.10	-	Oke (1987)
ALB_SNOW	0.50	-	Oke (1987)
BaseT	5	°C	Järvi *et al.* (2010)
BaseTe	11	°C	Järvi *et al.* (2010)
BaseTHDD	18.2	°C	Sailor and Vasireddy (2006)
DRAINRT	0.25	mm h^{-1}	Offerle (2002)
EMIS(1)	0.95	-	Oke (1987)
EMIS(2)	0.91	-	Oke (1987)
EMIS(3)	0.98	-	Oke (1987)
EMIS(4)	0.98	-	Oke (1987)
EMIS(5)	0.93	-	Oke (1987)
EMIS(6)	0.93	-	Oke (1987)
EMIS(7)	0.95	-	Oke (1987)
EMIS_SNOW	0.99	-	Oke (1987)
GDD(1-4)	300	°C	Järvi *et al.* (2010)
kmax	1200	W m^{-2}	Järvi *et al.* (2010)
LAIMax(1)	5.1	m^2 m^{-2}	Breuer *et al.* (2003)
LAIMax(2)	5.5	m^2 m^{-2}	Breuer *et al.* (2003)
LAIMax(3)	5.9	m^2 m^{-2}	Breuer *et al.* (2003)
LAIMax(4)	5.9	m^2 m^{-2}	Breuer *et al.* (2003)
LAIMin(1)	4	m^2 m^{-2}	Järvi *et al.* (2010)
LAIMin (2)	1	m^2 m^{-2}	Järvi *et al.* (2010)
LAIMin (3)	1.6	m^2 m^{-2}	Grimmond (1988)
LAIMin (4)	1.6	m^2 m^{-2}	Grimmond (1988)
RainCover	1.0	mm	Offerle (2002)

RainMaxRes	10.0	mm	Offerle (2002)
SDD(1-4)	-450	°C	Järvi *et al.* (2010)
Qf_A(1)	0.3081	W m^{-2} (capita ha^{-1})$^{-1}$	Järvi *et al.* (2010)
Qf_A(2)	0.3081	W m^{-2} (capita ha^{-1})$^{-1}$	Järvi *et al.* (2010)
Qf_B(1)	0.0099	W m^{-2} K^{-1} (capita ha^{-1})$^{-1}$	Järvi *et al.* (2010)
Qf_B(2)	0.0099	W m^{-2} K^{-1} (capita ha^{-1})$^{-1}$	Järvi *et al.* (2010)
Qf_C(1)	0.0102	W m^{-2} (capita ha^{-1})$^{-1}$	Järvi *et al.* (2010)
Qf_C(2	0.0102	W m^{-2} (capita ha^{-1})$^{-1}$	Järvi *et al.* (2010)
BldgStorCap	0.25	mm	Falk and Niemczynowicz (1978)
BldgDrainCoef1	10	-	Grimmond and Oke 1991
BldgDrainCoef2	3	-	Grimmond and Oke 1991
ConifStorCap	1.3	mm	Breuer et al. (2003)
ConifDrainCoef1	0.013	-	Grimmond and Oke 1991
ConifDrainCoef2	1.71	-	Grimmond and Oke 1991
DecidStorCap	0.3	mm	Breuer et al. (2003)
DecidDrainCoef1	0.013	-	Grimmond and Oke 1991
DecidDrainCoef2	1.71	-	Grimmond and Oke 1991
GrassUStorCap	1.9	mm	Breuer et al. (2003)
GrassUDrainCoef1	0.013	-	Grimmond and Oke 1991
GrassUDrainCoef2	1.71	-	Grimmond and Oke 1991
GrassIStorCap	1.9	mm	Breuer *et al.* (2003)
GrassIDrainCoef1	10	-	Grimmond and Oke 1991
GrassIDrainCoef2	3	-	Grimmond and Oke 1991
PavStorCap	0.48	mm	Davies and Hollis (1981)
PavDrainCoef1	10	-	Grimmond and Oke 1991
PavDrainCoef2	3	-	Grimmond and Oke 1991
SDECStor	0.80	mm	Grimmond and Oke 1991
G_1	16.48	mm s^{-1}	Järvi *et al.* (2010)
G_2	566.1	W m^{-2}	Järvi *et al.* (2010)
G_3	0.216	kg g^{-1}	Järvi *et al.* (2010)
G_4	3.36	g kg^{-1}	Järvi *et al.* (2010)
G_5	11.07	°C	Järvi *et al.* (2010)
G_6	0.018	mm	Järvi *et al.* (2010)
HydraulicConduct	0.000	mm s^{-1}	Belthier*et al.* (2006)

	5		
S_1	0.45	mm	Grimmond and Oke (1991)
S_2	15	mm	Grimmond and Oke (1991)
T_H	40	°C	Järvi *et al.* (2010)
T_L	0	°C	Järvi *et al.* (2010)
Tstep	300	s	Grimmond and Oke (1991)
Ie_a(1)	-84.54	mm	Järvi *et al.* (2010)
Ie_a(2)	9.96	mm °C^{-1}	Järvi *et al.* (2010)
Ie_a(3)	3.67	mm d-^{1}	Järvi *et al.* (2010)
Ie_a(1)	-25.36	mm	Järvi *et al.* (2010)
Ie_a(2)	3.00	mm °C^{-1}	Järvi *et al.* (2010)
Ie_a(3)	1.10	mm d-^{1}	Järvi *et al.* (2010)

5.3.9 Appendix B. Different coefficients for OHM file

Surface type		**Author**	**a_1**	**a_2**	**a_3**
Canyon	E-W canyon	Yoshida *et al.* (1990, 1991)	0.71	0.04	-39.7
	N-S canyon	Nunez (1974)	0.32	0.01	-27.7
Vegetation	Mixed forest	McCaughey (1985)	0.11	0.11	-12.3
	Short grass	Doll *et al.* (1985)	0.32	0.54	-27.4
	Bare soil	Novak (1982)	0.38	0.56	-27.3
	Bare soil (wet)	Fuchs & Hadas (1972)	0.33	0.07	-34.9
	Bare soil (dry)	Fuchs & Hadas (1972)	0.65	0.43	-36.5
	Bare soil	Asaeda & Ca (1993)	0.36	0.27	-42.4
	Water Shallow - Turbid	Souch *et al.* (1998)	0.50	0.21	-39.1
Roof	Tar and gravel, Vancouver	Yap (1973)	0.17	0.10	-17.0
	Uppsala	Taesler (1980)	0.44	0.57	-28.9
	Membrane and concrete, Kyoto	Yoshida et al. (1990,1991)	0.82	0.34	-55.7
	Average gravel/tar/conc. flat industrial, Vancouver	Meyn (2000)	0.25	0.92	-22.0
	Dry --gravel/tar/conc. flat industrial, Vancouver	Meyn (2000)	0.25	0.70	-22.0
	Wet -- gravel/tar/conc. flat industrial, Vancouver	Meyn (2000)	0.25	0.70	-22.0
	Bitumen spread over flat industrial membrane, Vancouver	Meyn (2000)	0.06	0.28	-3.0
	Asphalt shingle on plywood residential roof , Vancouver	Meyn (2000)	0.14	0.33	-6.0
	Star – high albedo asphalt	Meyn (2000)	0.09	0.18	-1.0

	shingle residential roof				
	Star - Ceramic Tile	Meyn (2000)	0.07	0.26	-6.0
	Star - Slate Tile	Meyn (2000)	0.08	0.32	0.0
Impervious	Concrete	Doll *et al.* (1985)	0.81	0.10	-79.9
	Concrete	Asaeda & Ca (1993)	0.85	0.32	-28.5
	Asphalt	Narita *et al.* (1984)	0.36	0.23	-19.3
	Asphalt	Asaeda & Ca (1993)	0.64	0.32	-43.6
	Asphalt	Anandakumar (1999)	0.82	0.68	-20.1
	Asphalt (winter)	Anandakumar (1999)	0.72	0.54	-40.2
	Asphalt (summer)	Anandakumar (1999)	0.83	-0.83	-24.6

5.3.10 Appendix C. Error messages.

"dectime 1000 avUU default data used=> 3"	**Your input wind speed data is unrealistic. Default data used. *Dectime* indicates the day and time in the day (as a decimal fraction) when the problem was seen and *avU* is the input wind speed value.**
"dectimexxxx dir30WD default data used=> 130"	Your input wind direction data is unrealistic. Default data used. *dir30* is the input wind direction value.
"dectimexxxxTem_CT default data used=> Default T "	Your input air temperature data is unrealistic. Default data used. *Temp_C* is the input meteorological value.
"dectimexxxxPres_kPaP default data used=> Default P"	Your input pressure data is unrealistic. Default data used.*Pres_kPa* is the input meteorological value.
"dectimexxxxavrhRH default data used=> Default RH"	Your input relative humidity data in unrealistic. Default data used.*avrh* is the input meteorological value.
If the error messages above arise from missing data (-999), you can consider filling the gaps in more sophisticated way before running the LUMPS.	
"%sat_vap_press.f temp=0.0000 pressure decime"	Temperature is zero and in calculation of water vapour pressure parameterization is used. You don't need to worry if the temperature should be 0°C. If it should not be 0°C this suggests that there is a problem with the data.
%T changed to fit limits [TL =0.1]/ [TL =39.9]	You may want to change the coefficients for surface resistance. If you have data from these temperatures, we would happily determine them.
"salflibc.dll is either not designed to run on Windows or it contains an error. Contact your system administrator or the software vendor	In this situation, your computer does not support the type of dll file and you are advised to download the Silverfrost compiler from the internet for free (http://www.silverfrost.com/32/ftn95/ftn95_personal

for support.”	_edition.aspx)
“Reference to undefined variable, array element or function result”	Parameter(s) missing from HeaderInput.nml, SuewsInput.nml, CanopyMoistureInput.nml or WaterUseProfile.txt

If the file paths are not correct the program will return an error when run (see How to run the model).

5.3.11 Appendix D: FAQ (Frequently Asked Questions)

1. **A pop-up saying “file path not found”**

This means the program cannot find the file paths defined in HeaderInputSSYY.nml file. Possible solutions:

- Check that you have created the folder that you have defined in HeaderInputSSYY.nml. Particularly the folder where the output files will be saved has to be existing
- Check that you have a single or double quote’s around the**FileInputPath**, **FileOutputPath**and **FileCode**

2. **How should I setup my filenames if I want to run only one time period for one area**

Example: If your forcing data are for 2005 and your site identification code is Ab01

ModelledYears.txt

```
1       !Number of modelled years/time periods
2005
```

GridConnections2005.txt

```
2!Number of grid connections listed below
'Ab01_2005'    0    'none'
!Fromfraction    To
```

The rest of the input files for this location should be

HeaderInputAb01_2005.nml
SUEWSInputAb01_2005.nml
CanopyMoistureInputAb01_2005.nml
WaterUseProfileAb01_2005.txt
Ab01_2005.gis
Ab01_2005.ohm
Ab01_2005.sahp
Ab01_2005_data.txt

6 SURFEX. CNRM MODELS.

6.1 Introduction

SURFEX is a numeric module that computes the energy and mass exchanges between the surface and the atmosphere (Figure 108). To be implemented, it needs atmospheric forcings (see the list of variables in Table 8) above the surface and a proper quantification of the parameters of the surface and among them, the descriptors of the urban area. Inside BRIDGE, the objective is to develop a DSS based on a GIS front end that will enable the user to modify the urban plan of the studied area. SURFEX will be integrated online inside this DSS, consequently in this document, we will present the method to calculate the parameters from the geographic information available from the case study for the base case. The implementation of the alternatives will be done online inside the DSS.

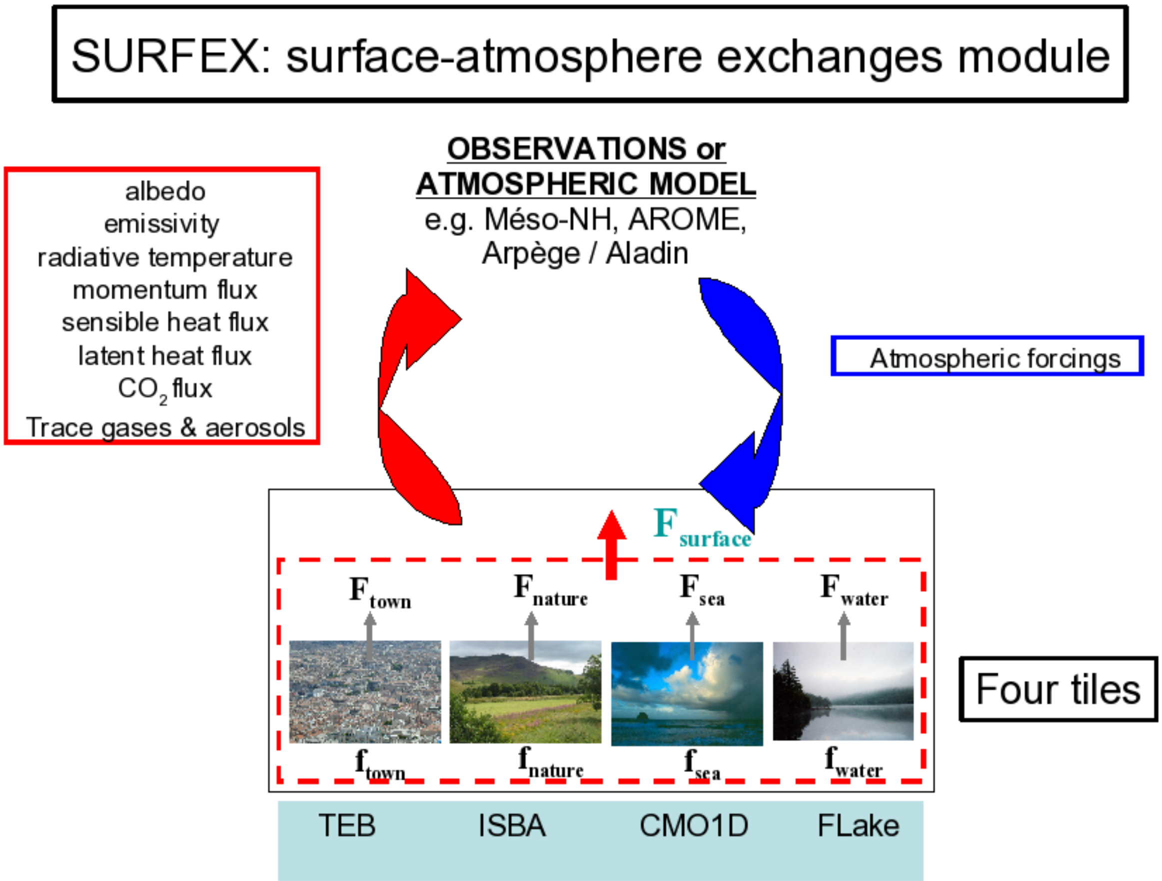

Figure 108: diagram of SURFEX structure.

Table 8: Atmospheric forcing for SURFEX

INPUTS	Units	Spatial resolution	Time resolution
Air temperature above canopy	K or °C	At each point of the grid	30 minutes to 3 hours
Specific humidity above canopy	kg/kg	At each point of the grid	30 minutes to 3 hours
Incoming solar radiation	$W\ m^{-2}$	At each point of the grid	30 minutes to 3 hours
Infrared solar radiation	$W\ m^{-2}$	At each point of the grid	30 minutes to 3 hours
Air pressure	Pa	At each point of the grid	30 minutes to 3 hours
Rain rate	$Kg\ m^{-2}\ s^{-1}$ (or mm/s)	At each point of the grid	30 minutes to 3 hours
Wind speed	$m\ s^{-1}$	At each point of the grid	30 minutes to 3 hours
Wind direction	°/N	At each point of the grid	30 minutes to 3 hours

6.2 Helsinki base case

This section aims at describing all the processes applied to the Helsinki GIS data to be incorporated into SURFEX simulations. The different steps to prepare a simulation with SURFEX are presented on the Figure 109. The work described here corresponds to the first step of *encoding or preprocessing* the GIS data to produce text files that can be read by SURFEX. The work has been done with Grass GIS (http://grass.osgeo.org/).

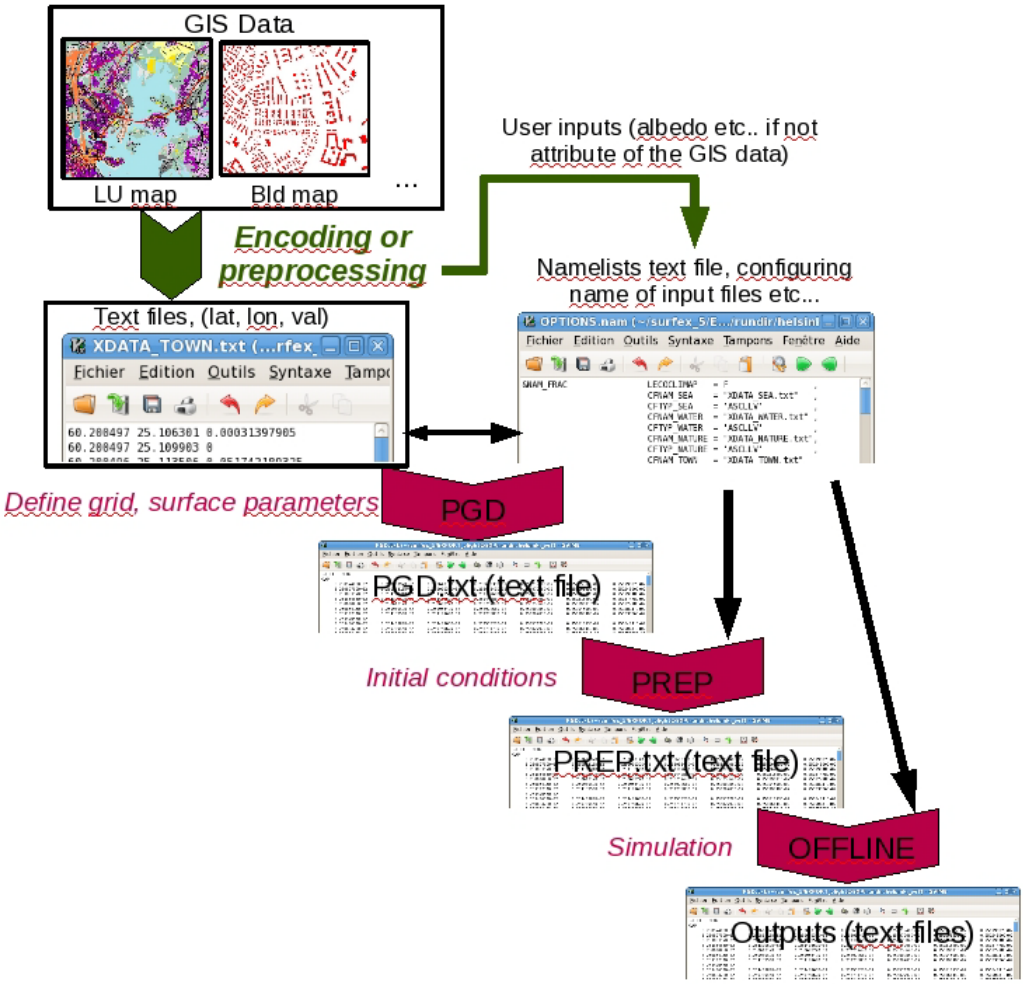

Figure 109: The different steps to prepare a SURFEX simulation from GIS data.

6.2.1 Definition of the projection, the domain and the grid

The projection, the domain and the grid are defined according to WRF-UPM simulations. The projection information are :

name	Lambert Conformal Conic
proj	Lcc
ellps	Sphere
Lat_1	30
Lat_2	60
Lat_0	60.1996
Lon_0	25.1045
X_0	0.00
Y_0	0.0

In this projection, the domain is –2700 to 2700 ; -2700 to 2700 respectively for south to north and west to east coordinates.

6.2.2 Reprojection of UHEL maps

Two maps provided by UHEL are used to compute the SURFEX parameters and are projected in this coordinate system. The maps are :

- uL4_10f raster layer (files uL4_10f.tif and uL4_10f.tfw)
- Buildings_as_regions_ETRSTM35_region vector layer (files Buildings_as_regions_ETRSTM35_region.*)

Only the region of these maps included in the domain of the simulation are extracted so a selection operation is performed over the Buildings_as_regions_ETRSTM35_region map. To have an idea of the resulting maps, Figure 110 represents the different layers land use map, building map and the simulation grid on the domain of interest.

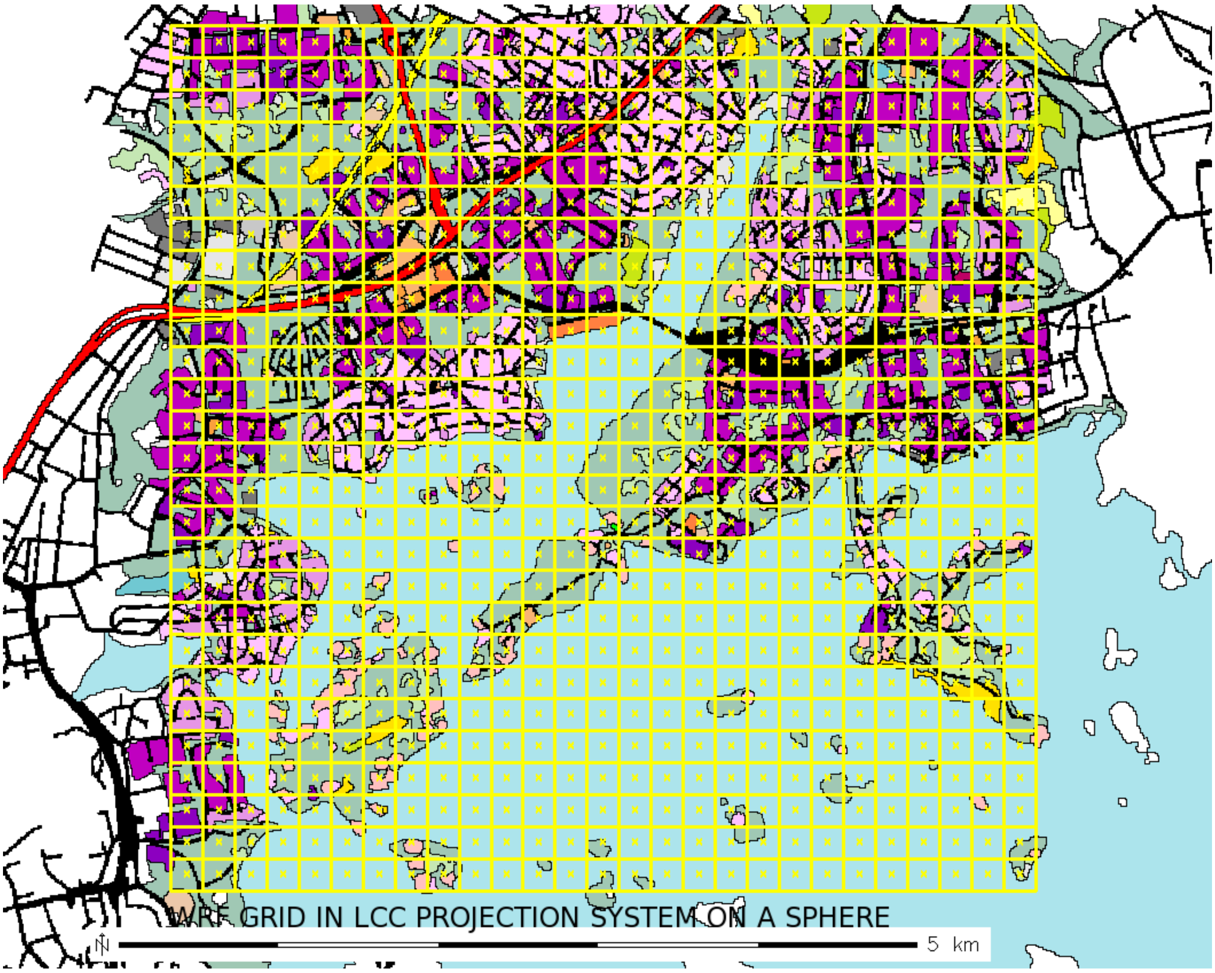

Figure 110: Overlay of the grid simulation, building and land use map.

6.2.3 Conversion of Land Use map from raster to vector

To compute area of each land use in the grid cells, the Land use map need to be converted from raster to vector format and the area of each land use polygon is added to the attribute table.

6.2.4 add information on the building map

New columns are added to the building map attribute table: area, perimeter, height, wall area. Area and perimeter are updated directly by the GIS functions. Height of the buildings are evaluated from the attribute CLASS according to Table 9. Wall area is computed as the product between building height and the building perimeter.

Table 9: Rules for the building height.

CLASS	TYPE OF BUILDING	NUMBER OF FLOORS	HEIGHT
42211	Residential building	1-2 storeys	6
42212	Residential building	3+ storeys	9
42221	Office or public building	1-2 storeys	6
42222	Office or public building	3+ storeys	9
42231	Vacation building	1-2 storeys	6
42241	Industrial building	1-2 storeys	6
42242	Industrial building	3+ storeys	9
42250	Ecclesiastical building	number of storeys unknown	9
42251	Ecclesiastical building	1-2 storeys	6
42252	Ecclesiastical building	3+ storeys	9
42260	Other building	number of storeys unknown	9
42261	Other type of building	1-2 storeys	6
42262	Other type of building	3+ storeys	9
42270	Church		15

6.2.5 overlay of maps and with the grid.

The land use map and the buildings map overlay because the land use map covers all The domain (Figure 4). To have no overlay between the land use and the building maps, an operation of subtraction is applied

Figure 111: Original land use map overlaid by building map. Land

Figure 112: Land use map after the subtraction operation. Building

use and building polygons intersect.	*polygons are removed from land use polygons.*

The next step is to make an intersection with the grid defined for the simulation so that we can aggregate the data according to the cell identifier working on the attribute table. Two new columns are added to the resulting map and computing from the topology of the map: the area of the polygons (buildings and land use) and the perimeter of building polygons only. Since, the overlay operation with the grid splits the buildings that are over 2 cells, an operation has to be applied to compute the length of the common boundaries between two polygons from the same buildings (Figure 113 and Figure 114).

Figure 113: a building is split between various polygons at each intersection with grid cells.

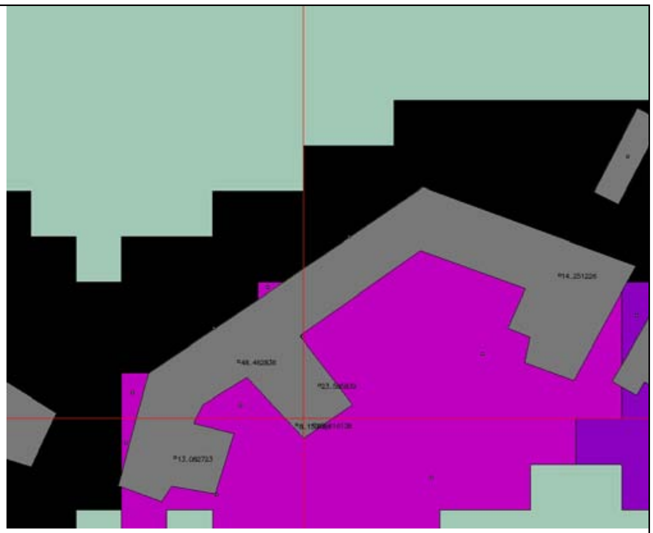

Figure 114: the length of the common boundary between two adjacent polygons of the same original building is uploaded to the attribute table.

This length is subtracted to the perimeter of the new building polygons to compute the wall surface in contact with the atmosphere.

6.2.6 Aggregation of results over the grid and calculation of SURFEX tiles fraction with rules

The following step of the processing consists to aggregate the results over the grid. The work has been done in *R* (http://www.r-project.org/) but it can be done in any other tools and specially in database manager systems. The principle is to compute in each grid cell, the sum of the surface of each class of Land use, of the buildings, of the surface of the walls.
Inside SURFEX the surface of each grid cell is classified between 4 tiles which are SEA, WATER (inland waters), NATURE and TOWN. For the different land use classes of the map, the rules presented in the table *tile_rules_surfex.xls* are applied (Table 10).

Table 10: Extract from the rules to be applied to the land use to compute the surface of SURFEX tiles.

Land use class	Pixel value	Step 1 : SURFEX TILE			
LU_CLASS	**LU_NUM**	SEA	WATER	NATURE	TOWN
A1. Housing areas	10	0	0	0	1
A11. Block house areas	11	0	0	0	1
A121. Row and attached small houses	13	0	0	0.5	0.5
A122. Detached housing areas	14	0	0	0.5	0.5
A21. Holiday resorts and cottage areas	21	0	0	0.5	0.5
A32. Areas of sport and recreational services	32	0	0	0.95	0.05

Consequently, for each grid cell, the fraction of each tile is computed as the sum of the surface of all the land uses multiplied by the corresponding fraction of the tile and then divided by the surface of the grid cell as in the following example for the NATURE tile:

$$F_{NATURE} = \frac{1}{S_{CELL}} \times \sum S_{LU} \times f_{NATURE,LU}$$

where LU are the different land use classes (Table 3, column LU_NUM), S is for the surface, F_{NATURE} is the NATURE fraction inside a grid cell and $f_{NATURE,LU}$ is the NATURE fraction in a specific Land use (Table 3, column NATURE).

For the TOWN tile, the buildings are added to the surface resulting from the land use rules and the calculation results in:

$$F_{TOWN} = \frac{1}{S_{CELL}} \times \left(\sum S_{LU} \times f_{TOWN,LU} + \sum S_{BLD}\right)$$

At the end of this operation, we create four text files containing as columns the latitude, the longitude and the fraction of the 4 tiles inside each grid cell (Figure 115). This is by this way that the quantitative information about the surface is integrated in SURFEX simulations.

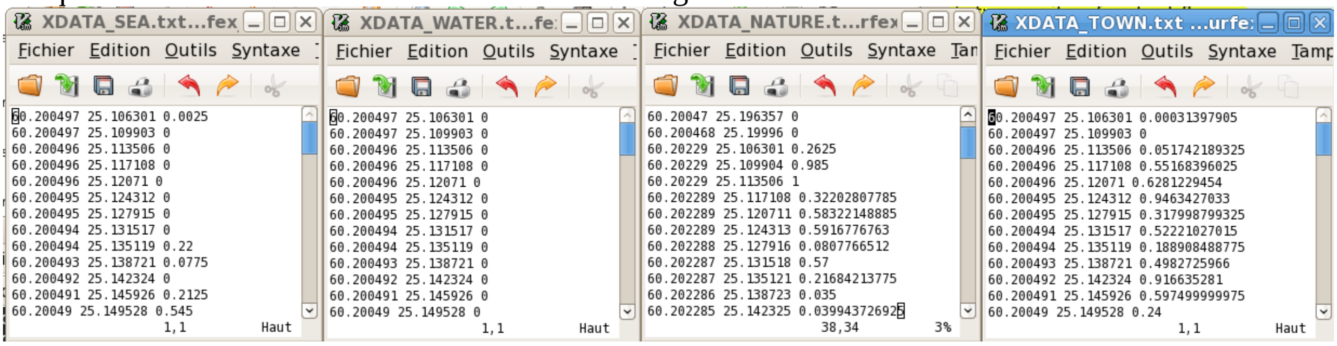

Figure 115 : Text files containing the tile fraction. The files should be included in the run directory of the simulation and their name in the OPTIONS.nam file.

6.2.7 Calculation and specification of TOWN tile parameters

The parameters for the TOWN tile are indicated in the *NAM_DATA_TEB* namelist in the *OPTIONS.nam* file (Figure 11). Considering the data provided from the Helsinki case study, three parameters of the TOWN tile vary for the different grid cells of the domain: the building fraction (parameter *BLD* and *XDATA_BLD.txt* file), the wall surface normalized by the town surface

(parameter *WALL_O_HOR* and the *XDATA_WALLOHOR.txt* file) and the building height (parameter *BLD_HEIGHT* and the *XDATA_HBLD.txt* file).

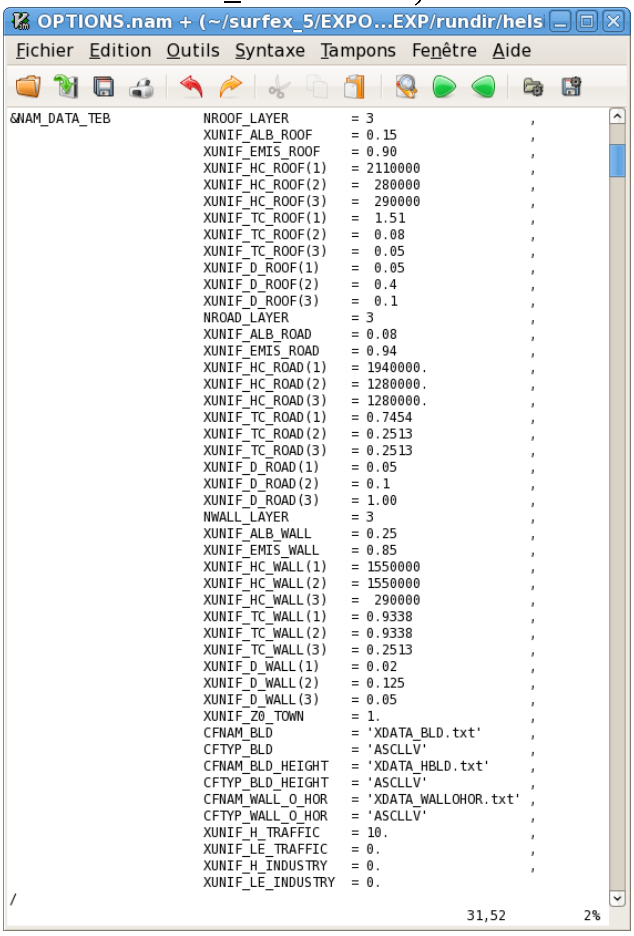

OPTIONS.nam + (~/surfex_5/EXPO...EXP/rundir/hels

Fichier Edition Outils Syntaxe Tampons Fenêtre Aide

```
&NAM_DATA_TEB        NROOF_LAYER        = 3                   ,
                     XUNIF_ALB_ROOF     = 0.15                ,
                     XUNIF_EMIS_ROOF    = 0.90                ,
                     XUNIF_HC_ROOF(1)   = 2110000             ,
                     XUNIF_HC_ROOF(2)   =  280000             ,
                     XUNIF_HC_ROOF(3)   =  290000             ,
                     XUNIF_TC_ROOF(1)   =  1.51               ,
                     XUNIF_TC_ROOF(2)   =  0.08               ,
                     XUNIF_TC_ROOF(3)   =  0.05               ,
                     XUNIF_D_ROOF(1)    =  0.05               ,
                     XUNIF_D_ROOF(2)    =  0.4                ,
                     XUNIF_D_ROOF(3)    =  0.1                ,
                     NROAD_LAYER        = 3                   ,
                     XUNIF_ALB_ROAD     = 0.08                ,
                     XUNIF_EMIS_ROAD    = 0.94                ,
                     XUNIF_HC_ROAD(1)   = 1940000.            ,
                     XUNIF_HC_ROAD(2)   = 1280000.            ,
                     XUNIF_HC_ROAD(3)   = 1280000.            ,
                     XUNIF_TC_ROAD(1)   = 0.7454              ,
                     XUNIF_TC_ROAD(2)   = 0.2513              ,
                     XUNIF_TC_ROAD(3)   = 0.2513              ,
                     XUNIF_D_ROAD(1)    = 0.05                ,
                     XUNIF_D_ROAD(2)    = 0.1                 ,
                     XUNIF_D_ROAD(3)    = 1.00                ,
                     NWALL_LAYER        = 3                   ,
                     XUNIF_ALB_WALL     = 0.25                ,
                     XUNIF_EMIS_WALL    = 0.85                ,
                     XUNIF_HC_WALL(1)   = 1550000             ,
                     XUNIF_HC_WALL(2)   = 1550000             ,
                     XUNIF_HC_WALL(3)   =  290000             ,
                     XUNIF_TC_WALL(1)   = 0.9338              ,
                     XUNIF_TC_WALL(2)   = 0.9338              ,
                     XUNIF_TC_WALL(3)   = 0.2513              ,
                     XUNIF_D_WALL(1)    = 0.02                ,
                     XUNIF_D_WALL(2)    = 0.125               ,
                     XUNIF_D_WALL(3)    = 0.05                ,
                     XUNIF_Z0_TOWN      = 1.                  ,
                     CFNAM_BLD          = 'XDATA_BLD.txt'     ,
                     CFTYP_BLD          = 'ASCLLV'            ,
                     CFNAM_BLD_HEIGHT   = 'XDATA_HBLD.txt'    ,
                     CFTYP_BLD_HEIGHT   = 'ASCLLV'            ,
                     CFNAM_WALL_O_HOR   = 'XDATA_WALLOHOR.txt' ,
                     CFTYP_WALL_O_HOR   = 'ASCLLV'            ,
                     XUNIF_H_TRAFFIC    = 10.                 ,
                     XUNIF_LE_TRAFFIC   = 0.                  ,
                     XUNIF_H_INDUSTRY   = 0.                  ,
                     XUNIF_LE_INDUSTRY  = 0.
/
                                                    31,52          2%
```

Figure 116: The NAM_DATA_TEB namelist where TOWN tile parameters are specificed in the OPTIONS.nam file.

In a grid cell, the building fraction (F_{BLD}) is computed as the surface of all the buildings from the GIS provided map divided by the TOWN surface. It means that the coefficient for the TOWN tile for the different land uses refer to the road. This value needs to strictly above 0 and below 1 and some points were not passing this condition (210 over the 729 of the grid). Consequently two more rules had been applied for these cases:

- when **F_{TOWN} > 0 and F_{BLD} = 0**. There were 201 grid points where there were a land use with a TOWN tile fraction but no buildings from the GIS map), F_{BLD} has been fixed to 0.05 as well *WALLOHOR* and the building height has been set to 3 m,
- when **F_{BLD} = 1**. There were 9 grid points where there were buildings but no land use with TOWN tile fraction. Those are probably isolated buildings. F_{BLD} has been reduced to 0.95 and *WALLOHOR* has been set to 0.1 to mimic isolated buildings.

Currently, the other parameters such as road, roof and wall radiative and thermal coefficient are considered uniform over the domain of simulation. If we plan to allow the end user of the DSS to change these parameters, a specific interface should be developed to change their value in the *OPTIONS.nam* file.

6.2.8 Calculation and specification of NATURE tile parameters

The parameters for the NATURE tile are specified in the *NAM_DATA_ISBA* namelist of the *OPTIONS.nam*. To describe, the NATURE tile, the land use classes have been classified according to the covers of the ECOCLIMAP database (Masson, 2003) present over Helsinki. The NATURE tile can be represented by a combination of 12 different vegetation types. Over Helsinki only 5 vegetation types were present: rocks, trees, coniferous, crops (C3 photosynthesis cycle) and grass. For each land use class of the GIS Helsinki dataset, the closest ECOCLIMAP cover has been selected to determine the the repartition between the different vegetation types (Figure 12), the leaf area index (LAI) and the height of trees. These rules are in the *nature_rules_surfex.xls* file.

LU_CLASS	LU_NUM	ROCKS (2)	TREE (4)	CONIF. (5)	C3 CROPS (7)	GRASS (10)	LAI1	LAI2	LAI3	LAI4	LAI5	LAI6	LAI7	LAI8	LAI9	LAI10	LAI11	LAI12	LA
A121. Row and attached small houses	13	0	0	0	0	1	1	1	1	1	1	1	1.1	1.1	1.2	1.3	1.4	1.5	
A122. Detached housing areas	14	0	0	0	0	1	1	1	1	1	1	1	1.1	1.1	1.2	1.3	1.4	1.5	
A21. Holiday resorts and cottage areas	21	0	0	0	0	1	1	1	1	1	1	1	1.1	1.1	1.2	1.3	1.4	1.5	
A32. Areas of sport and recreational services	32	0	0	0	0	1	1	1	1	1	1	1	1.1	1.1	1.2	1.3	1.4	1.5	
A33. Parks	33	0	0	0	0	1	1	1	1	1	1	1	1.1	1.1	1.2	1.3	1.4	1.5	
C13. Areas of air traffic and aviation	66	0	0	0	0	1	1	1	1	1	1	1	1.1	1.1	1.2	1.3	1.4	1.5	
D111. Mines	82	1	0	0	0	0	0	0	0	0	0	0	0	0	0	0	0	0	
D112. Quarries	83	1	0	0	0	0	0	0	0	0	0	0	0	0	0	0	0	0	
D121. Peat production sites	85	1	0	0	0	0	0	0	0	0	0	0	0	0	0	0	0	0	
D122. Gravel and sand extraction sites	86	1	0	0	0	0	0	0	0	0	0	0	0	0	0	0	0	0	
D123. Other soil extraction sites	87	1	0	0	0	0	0	0	0	0	0	0	0	0	0	0	0	0	
E11. Fields	91	0	0	0	1	0	0.2	0.3	0.4	0.4	0.5	0.7	0.8	1	1.2	1.3	1.5	2	
E12. Perennial meads and grasslands	92	0	0	0	0	1	1	1	1	1	1	1	1.1	1.1	1.2	1.3	1.4	1.5	
E131. Fruit and berry plantations	94	0	0.5	0.5	0	0	1	1	1.2	1.3	1.5	1.6	1.7	1.8	1.9	2	2.1	2.6	
E132. Nursery gardens and covered cultivations	95	0	0	0	0	1	1	1	1	1	1	1	1.1	1.1	1.2	1.3	1.4	1.5	
E211. Long-term fallows	102	0	0	0	0	1	1	1	1	1	1	1	1.1	1.1	1.2	1.3	1.4	1.5	
E212. Agricultural land permanently removed from productive use	103	0	0	0	0	1	1	1	1	1	1	1	1.1	1.1	1.2	1.3	1.4	1.5	
F11. Forests	121	0	0.5	0.5	0	0	1	1	1.1	1.3	1.4	1.4	1.5	1.5	1.6	1.7	1.8	2.4	
F12. Scrubland	122	0	0.5	0.5	0	0	1	1	1.1	1.3	1.4	1.4	1.5	1.5	1.6	1.7	1.8	2.4	
G1. Brownfields	130	1	0	0	0	0	0	0	0	0	0	0	0	0	0	0	0	0	

Figure 117: Vegetation types fraction rules for the different land use classes.

At the end of this step, 5 files (*XDATA_VEGTYP02.txt*, *XDATA_VEGTYP04.txt*, *XDATA_VEGTYP05.txt*, *XDATA_VEGTYP07.txt*, *XDATA_VEGTYP10*.txt) have been created to describe the repartition of the vegetation type over the domain of simulation (Figure 13).

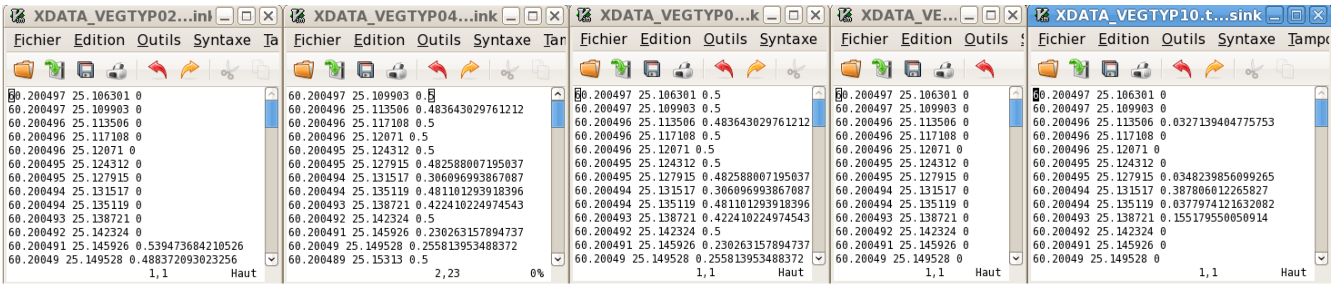

Figure 118: files describing the fraction of the vegetation types over the simulation domain.

Currently for each vegetation type, spatially uniform values have been taken to describe them such as: leaf area index (LAI), height of trees, roughness length (Z0), emissivity...

6.2.9 Maps of the surface parameters used in SURFEX.

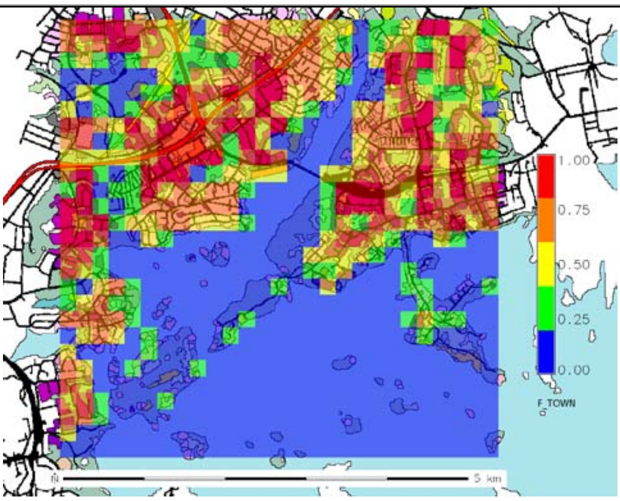

Figure 119: Town fraction

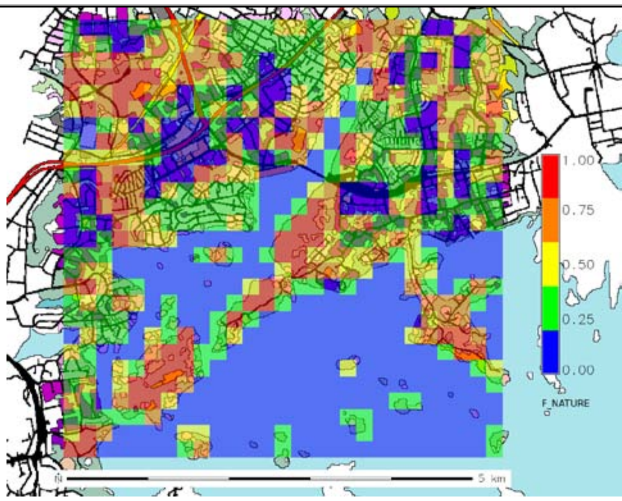

Figure 120: Nature fraction

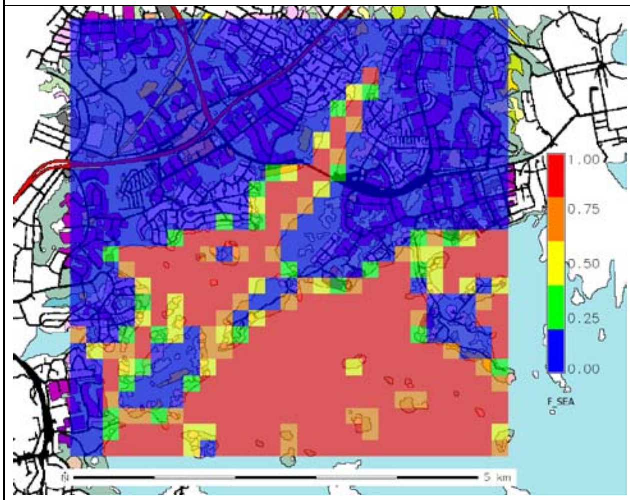

Figure 121: Sea fraction

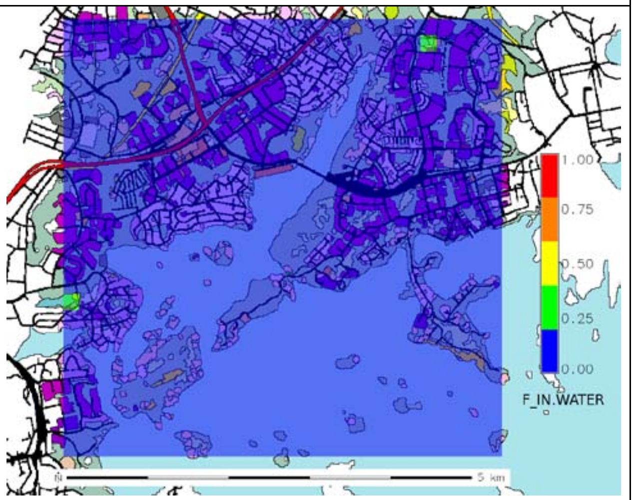

Figure 122: Inland waters fraction

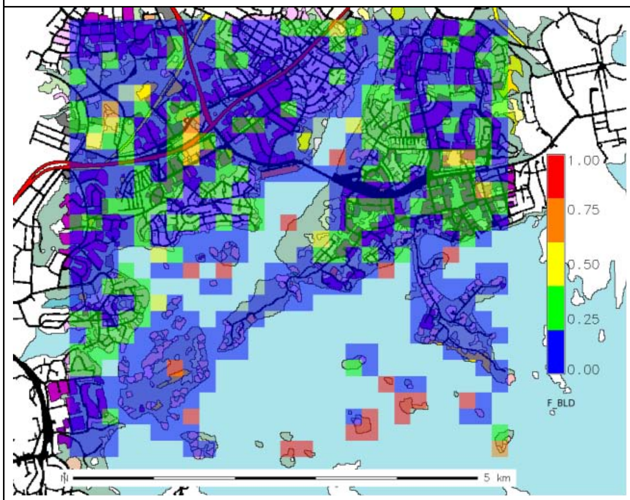

Figure 123: Building plan area density.

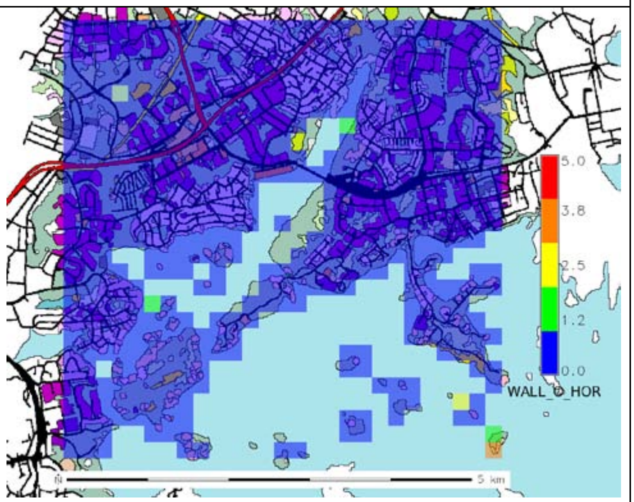

Figure 124: wall surface to urban horizontal surface ratio.

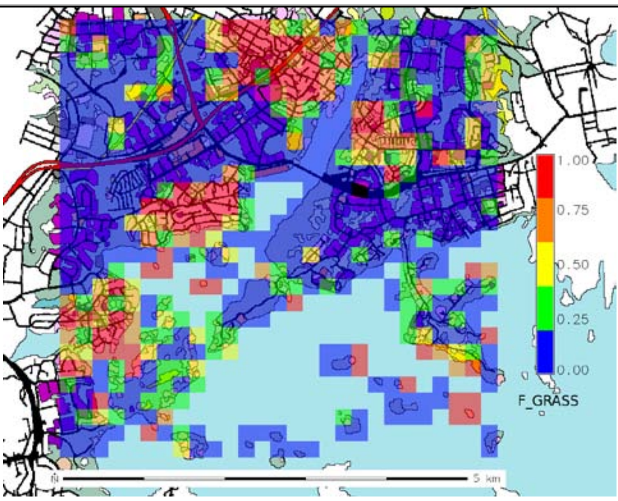

Figure 125: Grass surface fraction

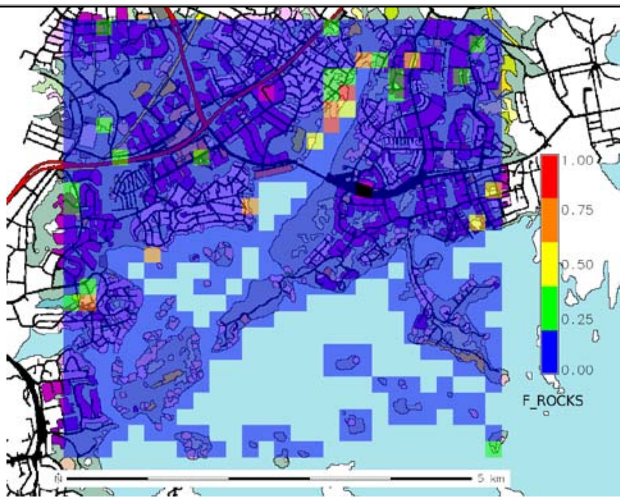

Figure 126: Rocks surface fraction

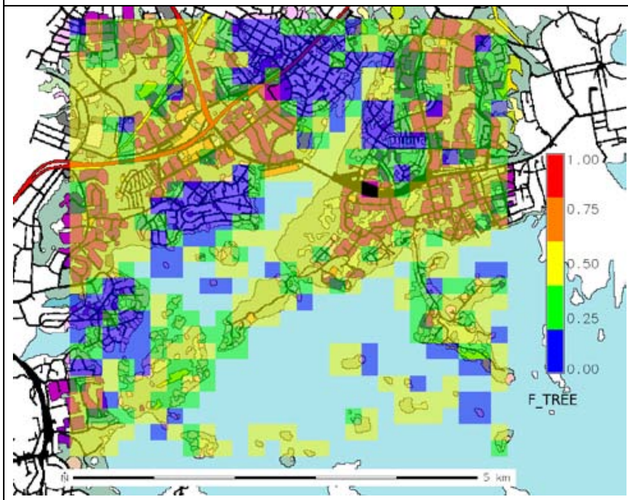

Figure 127: Broad leaf tree surface fraction

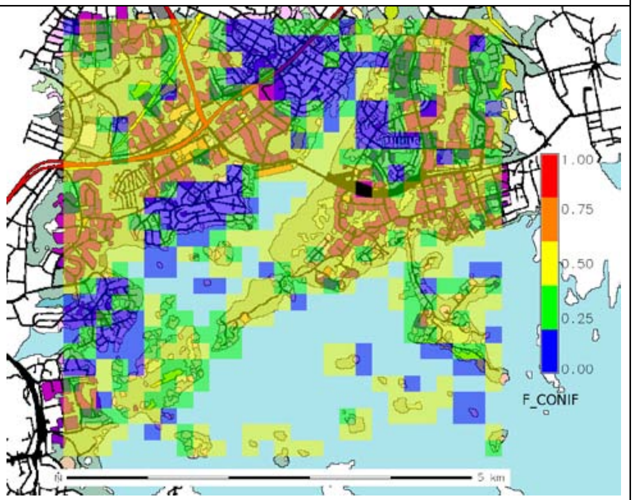

Figure 128: Coniferous surface fraction

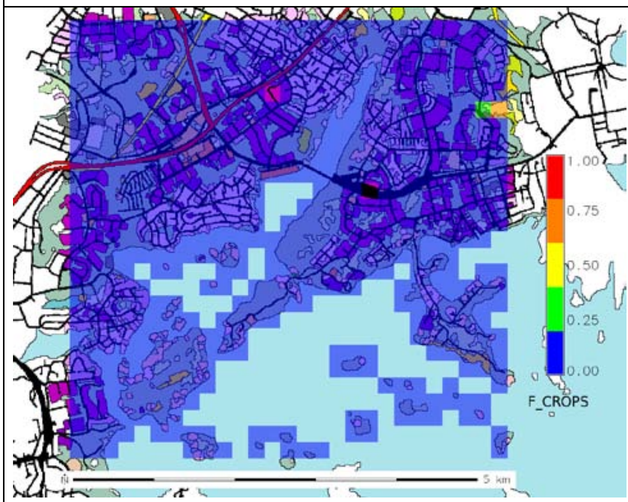

Figure 129: Crops surface fraction.

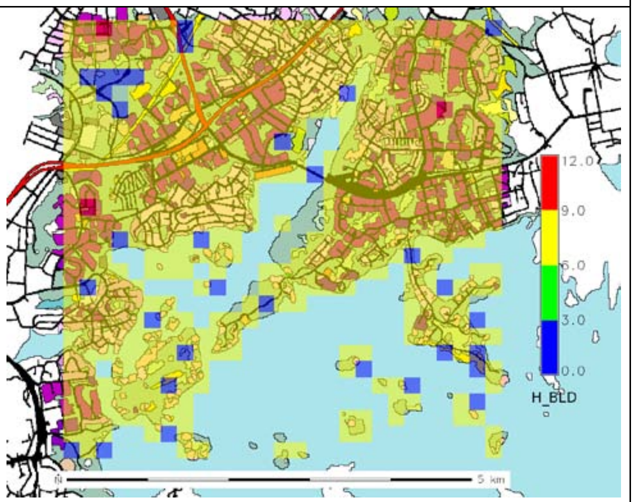

Figure 130: Building average height.

6.3 Egaleo, Athens base case

This section aims at describing all the processes applied to the Egaleo, Athens GIS data to be incorporated into SURFEX simulations.

6.3.1 Definition of the SURFEX domain

The domain for the SURFEX simulations was defined according to the extension of the available GIS data provided from the Egaleo case study. Consequently, this is not a square grid but an irregular grid of 200 x 200m cells (Figure 131).

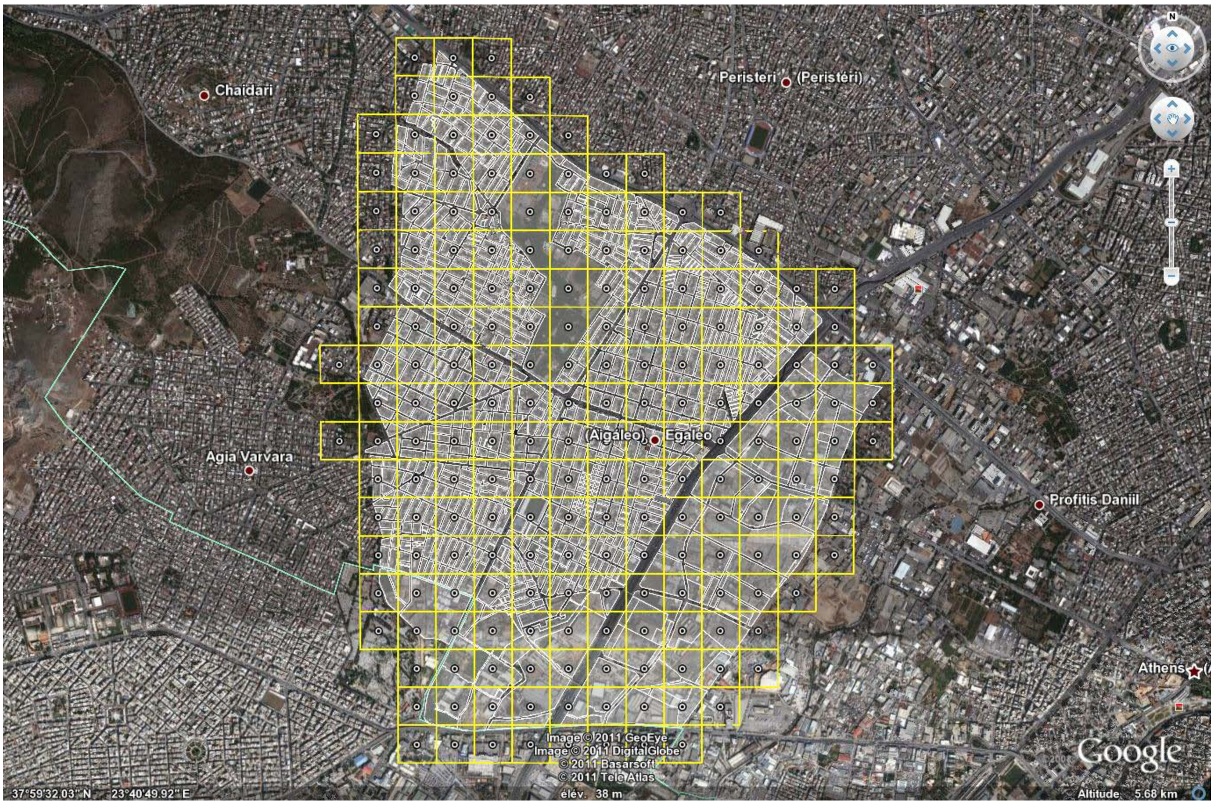

Figure 131: Surfex grid at 200m horizontal resolution overlapping the building block map inside Google Earth©.

6.3.2 Estimates of surface covered by vegetation

The surface covered by vegetation inside in grid cell of the SURFEX domain has been estimated using the Normalized Difference Vegetation Index (NDVI) image provided at 30m resolution. The method used to estimates the vegetation fraction from NDVI is a stretching of extreme values of NDVI measured on the domain:

- the lowest values are 0.15 and corresponds to the absence of vegetation (buildings, parking lot or bare ground),
- the highest values are 0.75 and corresponds to areas entirely covered by trees.

Those thresholds are in agreement with the literature in this field and the vegetation fraction VF is computed using the following equation:

$$VF = \left[\frac{NDVI - 0.15}{0.75 - 0.15}\right]^2$$

The estimates obtained from this calculation applied on the NDVI image are presented on Figure 132. From the comparison between the 2 graphics of this figure, it is possible to verify the ability of this method to represent the variability of the vegetation inside the domain of the study.

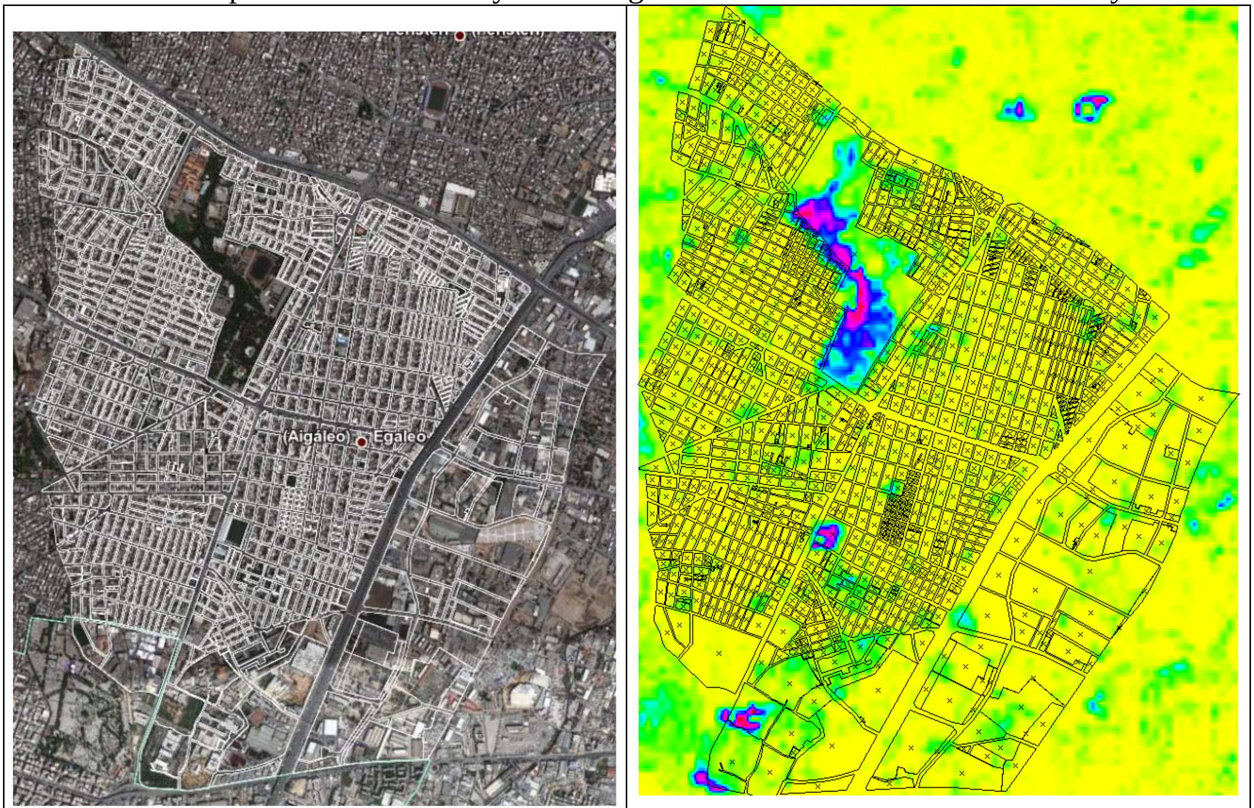

a. Building blocks map over Google Earth

b. Building blocks map over the vegetation fraction.

Figure 132: Estimates of the vegetation cover fraction over the Egaleo domain

6.3.3 Estimates of surface covered by buildings

The surface covered by the buildings has been calculated using this information of the vegetation cover fraction as well as the building blocks map. This last map was not describing individual buildings but blocks of buildings separated by roads. Consequently, inside each polygon of a block, some vegetation could be present as well as parking areas (Figure 133). The following steps have been applied to estimate the surface covered by the buildings:

- Step 1: the vegetation cover surface inside the blocks has been retrieved to the surface of the blocks,
- Step 2 : a ratio has been applied for the remaining surface to consider the possible presence of parking areas. The ratio is different for large blocks and for small blocks:
  - For blocks smaller than 9000m², it is considered that 90% maximum of the surface of the block can be occupied by the buildings,
  - For blocks larger than 9000m², this ratio is 50%.

a. details for large blocks	*b. details for small blocks*

Figure 133: Details of the surface covered by the blocks.

6.3.4 Calculation on the grid and maps of the surface parameters for SURFEX

Then given this information computed from the original maps provided from the Egaleo case study, the same kind of calculation as for Helsinki has been applied. It consists in intersecting the new maps with the grid defined for SURFEX. It results in the following maps of garden fraction (Figure 134), building fraction (Figure 135) and wall over horizontal area ratio (Figure 136). For this last parameters, an average building height of 15 m has been taken from the detailed description provided for 10 buildings for which the height was between 7.5 and 22.5m.

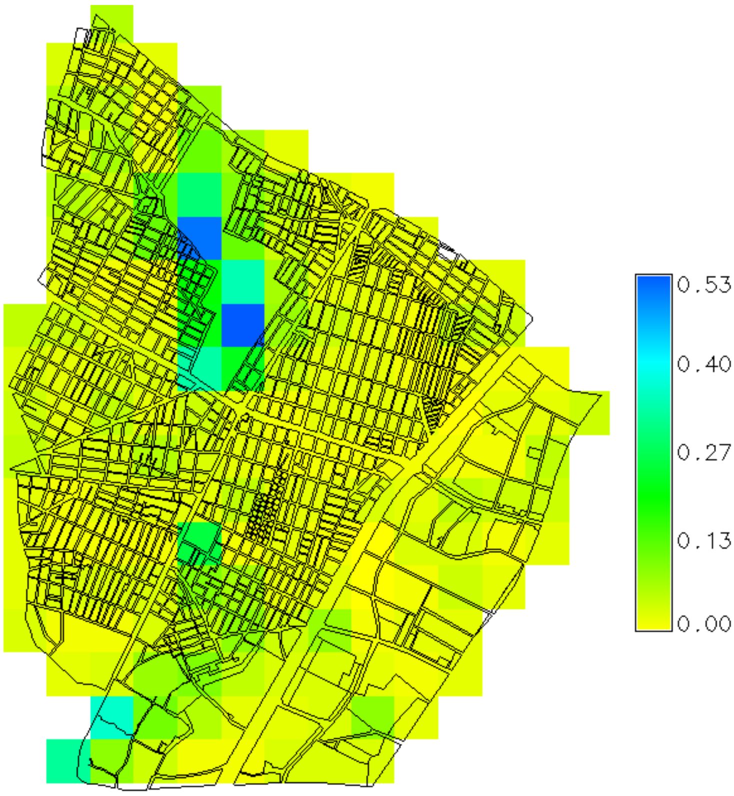

Figure 134: Fraction of vegetation inside the SURFEX grid celles.

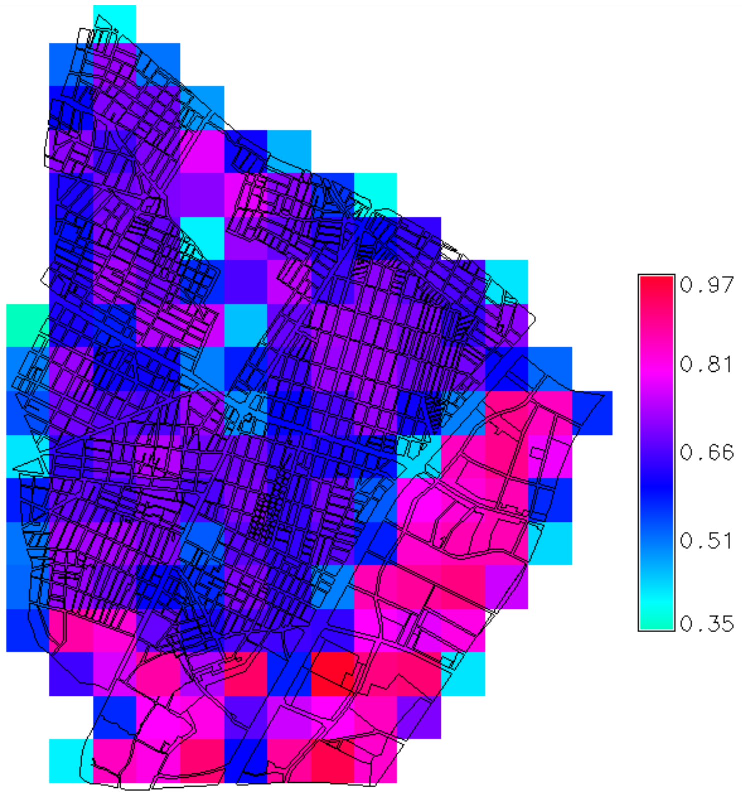

Figure 135: Building fraction inside the SURFEX grid cells

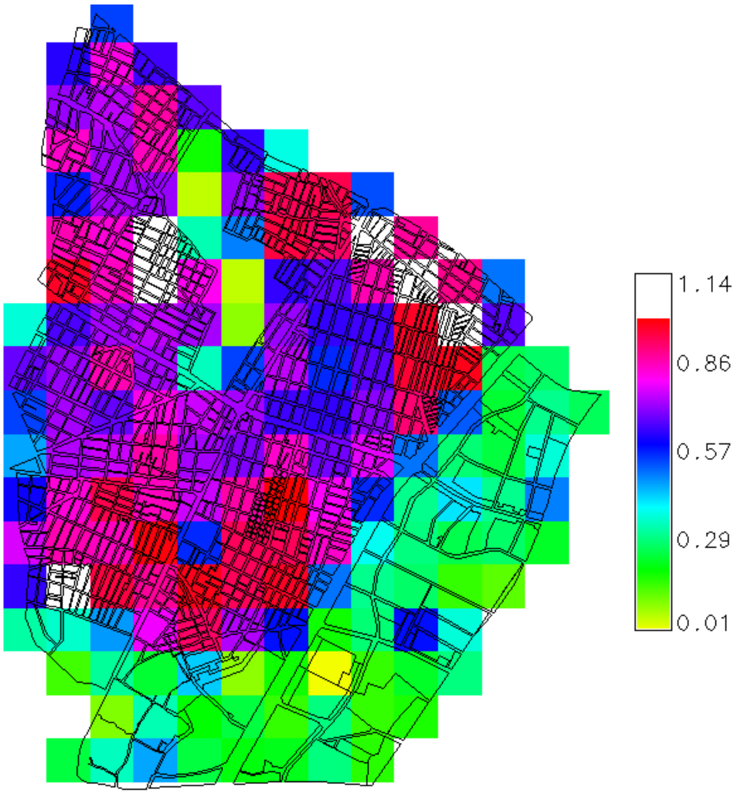

Figure 136: ratio between wall surface and horizontal surface inside the SURFEX grid cells.

7 SIMGRO. ALTERRA MODELS

7.1 Model description

SIMGRO is a physically based water balance model, and in this project used in the urban environment. The model is used for the analysis of effects land use changes have on the urban water balance. SIMGRO has been used as a decision support tool for water management issues before for the rural environment in the Netherlands (explained in SIMGRO manual 7.1.0 2010).

SIMGRO needs two types of data as input; 1) **time dependent data** and 2) **spatial data**. The BRIDGE project provides both types of data; time dependent climatological data and spatial variable land uses and elevation data. SIMGRO contains lookup tables that link land use types to pre-defined physical characteristics (see Table 11). The end user of the BRIDGE DSS can change land use types into other land use types presenting a scenario predefined in SIMGRO. After pre-processing the input data, SIMGRO-urban starts its calculations. In the end the calculated data is post-processed and the outputs are given as hourly ascii-grids, as prescribed by the BRIDGE programme. Figure 137 shows a schematisation of the processes around SIMGRO in the BRIDGE programme. The dashed line 'SIMGRO-urban' indicates which processes take place online by the model. The dashed line 'BRIDGE DSS' indicates the link to the BRIDGE DSS environment.

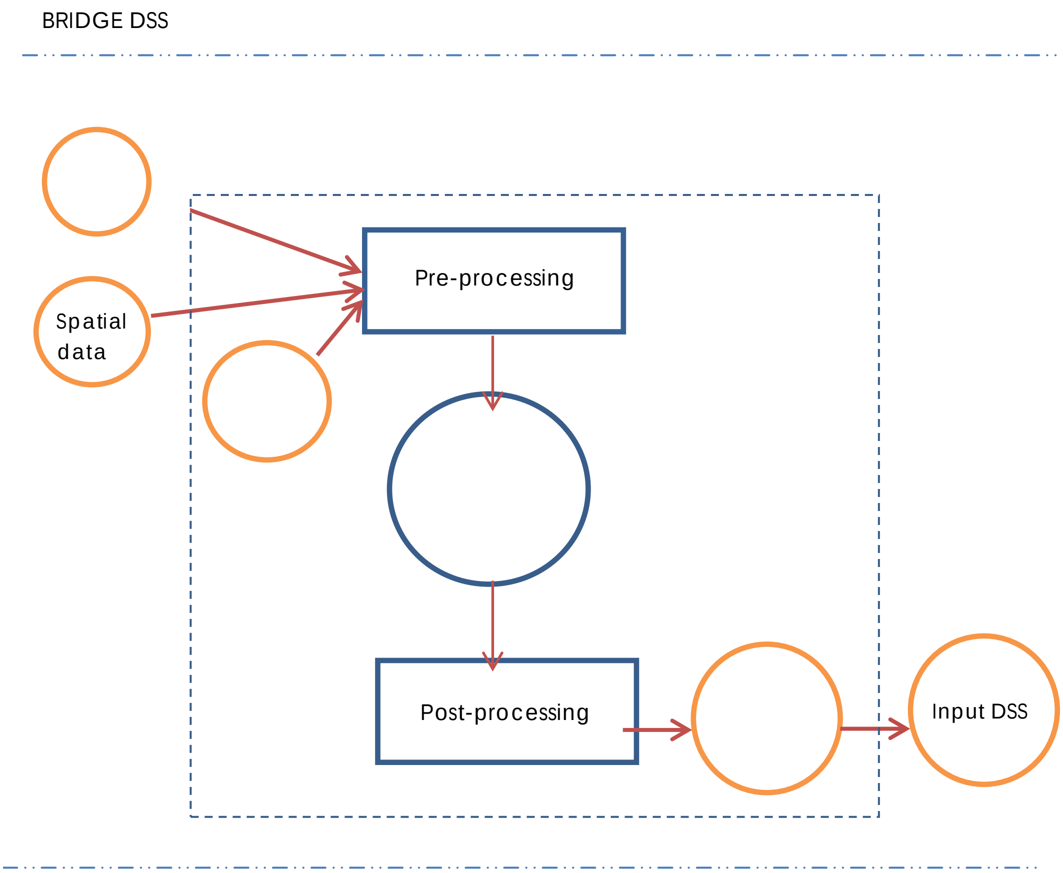

Figure 137: Schematization processes SIMGRO, within the BRIDGE DSS

SIMGRO is physically based and uses a reservoir approach to simulate the interaction between different components of the water balance. The order of the defined reservoirs is primarily vertical, representing the dominant water flow direction in the urban environment. The reservoirs can be categorized in for types based on their vertical order. The categories are;

1) **Interception reservoir**
2) **Surface reservoir**
3) **Soil reservoir**
4) **Groundwater reservoir**

Each reservoir can store water. SIMGRO used in the urban environment subdivides the surface into different urban land use types with specific reservoir characteristics. These units are called Urban Morphological Types (UMTs). Characteristics of the UMTs are pre-defined in tables (see Table 12). Figure 138 below gives an illustration of SIMGRO used in the urban environment (SIMGRO-urban).

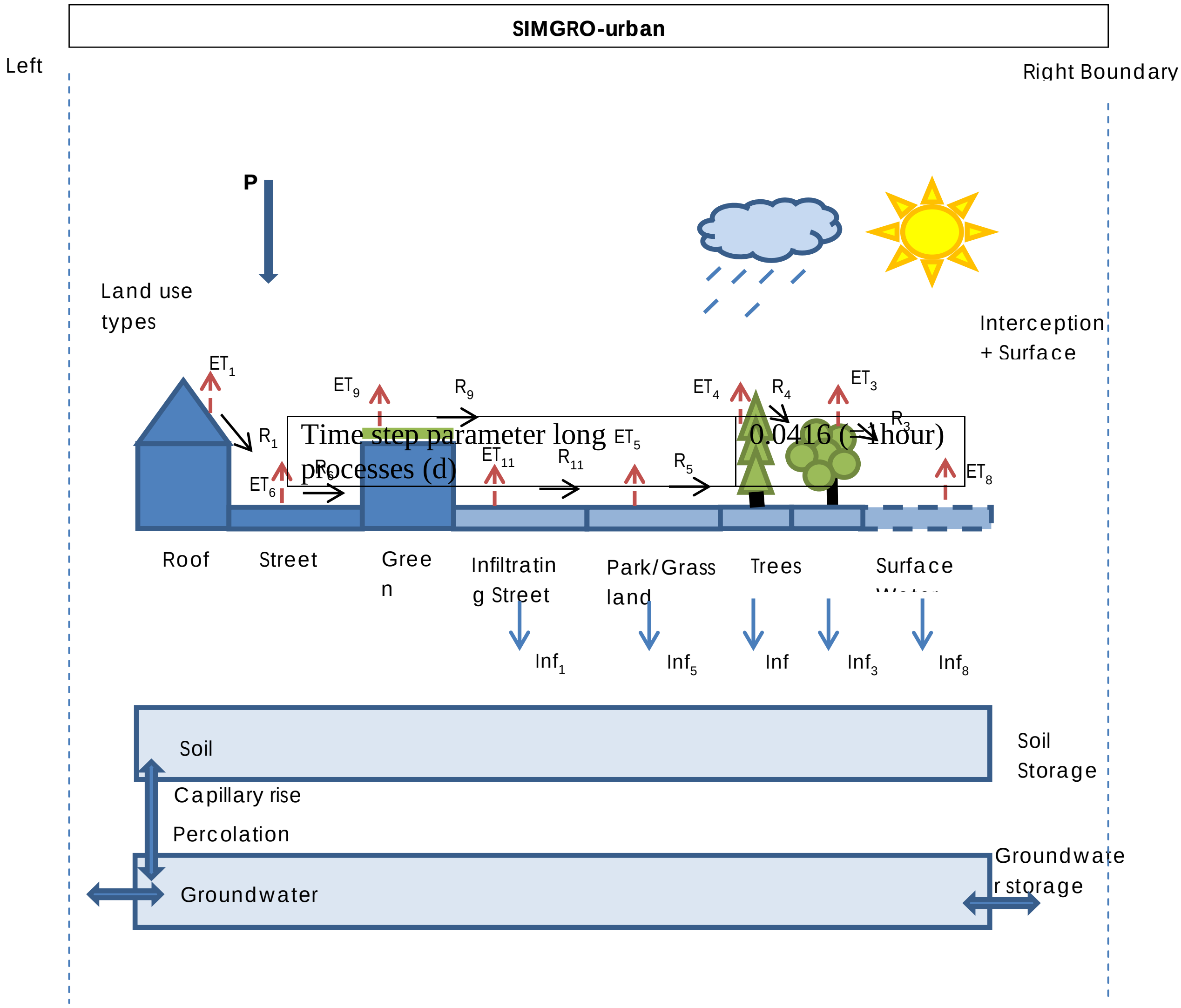

Figure 138: SIMGRO-urban reservoir presentation. Fluxes are indicated by arrows: P=precipitation, ET= evapotranspiration, R= runoff, Inf= infiltration. The number next to the arrow indicates to which UMT it is linked.

7.2 Scales

Time scales

SIMGRO is dynamic, and includes two different time scales. A long time scale for groundwater calculation and a short time scale for surface water calculations. The long time scale should be a multiple of the short time scale. The output is linked to the defined long time scales. The output time scale is prescribed by the BRIDGE project and set at 1 hour.

The length of calculation is 366 days (for 2008).

Time step parameter short processes (d)	0.0416 (=1hour)

Spatial scales

UMT index	Name of UMT	Infiltration capacity (m d^{-1})	Root zone (m)	Soil number	Coupling to SWNR unit	Micro-storage (m)	Coupling to Modflow

The total grid size for all case studies is 5.4 x 5.4 km. The land use maps given as inputs are pre-processes to ascii-grids with 4 m resolution. This results in a good presentation of all urban structures. These 4 m resolution grids are used to define UMTs to a 200 m resolution grid (prescribed by the BRIDGE programme).

7.3 Inputs

Time dependent inputs

SIMGRO needs time dependent meteorological inputs (the meteorological scenario chosen for the BRIDGE DSS). The meteorological data is provided by the WRF/UPM model. The model provides every case study with metrological data for the same grid size and resolution. The grid size is: 5.4x5.4 km; 27x27 cells, with a 200 resolution.

The WRF/UPM model provides hourly data for 366 days of the year 2008. The outputs used for SIMGRO-urban are: Rain (mm unit), Temperature (K at 2 meter height) and shortwave downward flux (W m^2). An average hourly value is calculated form the Rain data. Why this is done is described into detail in D 4.3 (QA/QC report).

Spatial inputs

The spatial inputs are needed to build the UMT grid for SIMGRO in which the different urban land use types are determined. SIMGRO needs a DEM, land use data, and groundwater level. These data are provided by the case studies of the BRIDGE project.

Table 11 gives the lookup table included in SIMGRO, that link the UMTs to their characteristics. The UMTs presented in this table include the land uses of the Helsinki and London case studies. The end-user can change land use types for each 4x4 grid cell into one of these types. Each land use type is coupled with reservoir characteristics, these characteristics cannot be changed. Even so, the end-user cannot define new land use types if no characteristics are available. Nevertheless, the end-user can determine land use types which can exist out of several UMT units in order to give a good representation of the land use type (see also section pre-processing).

		(m/d)	(m)			(m)	
1	Building	0	0.1	1	2	0.001	0
2	Undefined	0	0	0	0	0	0
3	Broad-leaved	0.1	0.4	16	1	0.004	1
4	Conifer	0.1	0.4	16	1	0.004	1
5	Grassland	0.1	0.4	16	1	0.004	1
6	Street	0.003	0.3	14	2	0.001	1
7	Street with vegetation	0.003	0.3	14	2	0.001	1
8	Surface water	0.1	0.3	16	3	0.1	1
9	Building green roof	0.07	0.2	14	2	0.03	-1
10	Building gravel roof	0	0.15	1	2	0.01	0
11	Street with infiltration	0.072	0.3	14	6	0.036	1

Table 11: Lookup table UMT-units and characteristics included in SIMGRO for BRIDGE

7.4 Pre- processing

Several pre-processing steps should be done before SIMGRO can be run. First the input data must be pre-processes to be incorporated with SIMGRO. This happens outside the 'SIMGRO box' (Figure 137). The second step includes the pre-processes to format UMT-grids.Before the pre-processing of the UMTs can be done the project, climate scenario, and land use alternative must be defined. The third step in the pre-processing is to define which water balance terms will be given as output (see section output).

Meteorological data

The meteorological data are provided in netCDF-formated tables. To be incorporated with SIMGRO these files are written into ascii-grids. Hourly ascii-grids were generated (27 rows, 27 columns, 200m resolution). The potential evapotranspiration (ETpot) was calculated with Makkink's formula. Both RAIN and ETpot are in mm h^{-1}, but SIMGRO needs these values in mm d^{-1}. This is included in the pre-processing. An average hourly value is calculated from the RAIN, this is used as input. All files used for the pre-processing are available in SIMGRO.

Spatial data

Spatial data (DEM, land use data) are needed to build the UMT grid for SIMGRO-urban in which the different land use types are determined. This data are provided by the BRIDGE project as .shp files and had to be transformed into ascii-grids in order to be incorporated with SIMGRO-urban. The resolution of these files is 4 x 4 m (1350 rows, 1350 columns), which results in a good representation of all urban structures.

UMTs

Land use maps are used in SIMGRO on a 4 m resolution, which is a good representation of urban structures. It was decided to calculate the fractions of land use per cell of 200 x 200 m, in order to guaranty a fast and stable calculation. This fractioning is illustrated in Figure 139. After this simplification of the land use the cells are treated as parallel stores. The end user can change land use types on the 4 m resolution, which leads to a new fracturing. With this pre-processer the UMT units are defined. Each calculation unit exist out of several UMT units.

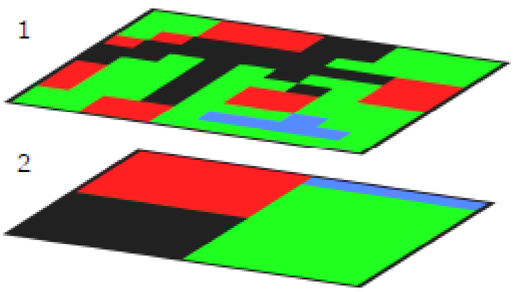

Figure 139: Calculation of fractions land use types, different colours represent different land use types. 1=ascii-grid, 2=UMT-units

The pre-processor is available in SIMGRO (pre_bridge.exe switched on by do_pre_bridge.bat). With this pre-processor the different input files needed to run SIMGRO are created. These files are available in SIMGRO in the folder 'imp'. The file fact_svat.inp (Table 12) gives an overview of the physical characteristics of the different urban land use types.

Table 12: Summary of Fact_svat.inp. Note that for some land use types interception capacity and vegetation fraction changes over season.

Land use	Description	Interception capacity (m)	Vegetation factor	Factor for interception evaporation	Factor for bare soil evaporation	Factor for ponding transpiration
1	building	0.00001	0.01	1.00	1.00	1.25
3	broadleaved	0.0035	0.85	2.20	1.00	1.00

4	conifer	0.0008	1.00	1.80	1.00	1.00
5	grassland	0.00011-0.00036	0.9-1	1.15	1.00	1.00
6	streets	0.00001	1.00	0.01	1.00	1.25
7	streets with vegetation	0.0025	1.00	0.01	1.00	1.25
8	fresh water	0.0000	1.25	0.00	1.00	1.25
9	building with green roof	0.0001	0.90	1.15	1.00	1.00
10	building with gravel roof	0.00001	1.25	0.00	1.00	1.50
11	street with infiltration	0.0001	1.00	1.00	1.25	1.50

7.5 Process

SIMGRO uses run_model.exe switched on by run_model.bat for its calculations. These files are available in SIMGRO. All files needed for the calculations are copied to the temporal folder (tmp). All calculation outcomes are stored in this folder as *.bda files. These files are used by in the post-processing for abstracting time series as ascii-grids (see section post-processing).

7.6 Post-processing

The water balance terms that should be given as outputs are defined in the pre-processing od the model. The output data generated by the post-processor are hourly ascii-grids for the year 2008, which means 8784 maps per parameter. These ascii-grids are input for the BRIDGE DSS (Figure 137). Table 13 gives the water balance parameters given as outputs in this study. How the data is presented in the end is based on statistical and spatial evaluation of the output data integrated in the BRIDGE DSS (e.g. annual sums, daily sums). Suggestions are provided in the section below.

Table 13: Output parameters SIMGRO for BRIDGE

Parameter	Abbreviation SIMGRO	Unit	Description
Precipitation	Pm	mm	Precipitation falling per UMT
Runoff	R	mm	Rainfall runoff per UMT
Actual	ETact	mm	Sum of Eic, Epd, Ebs, Tact per UMT

evapotranspiration			
Recharge	Qrech	mm	Recharge groundwater when negative, recharge soil reservoir when positive
Decrease soil moisture	dS	mm	Change in soil moisture storage, positive is decrease negative in increase soil moisture storgae

7.7 Outputs baseline scenario

This section gives examples of presenting outputs of SIMGRO after simulating the urban water balance. It should be noted that the model is not validated yet, mainly because of the lack of data. The results presented here are for the Helsinki case study. The baseline scenario is defined as the current situation. The alternatives 1, 2, and 3 are defined by the BRIDGE project, and will be discussed in the next section.

Figure 140 gives the land use map used for the simulation and the percentages of the different land use types. The graphs below give possible presentations of the model outcomes temporally and spatially.

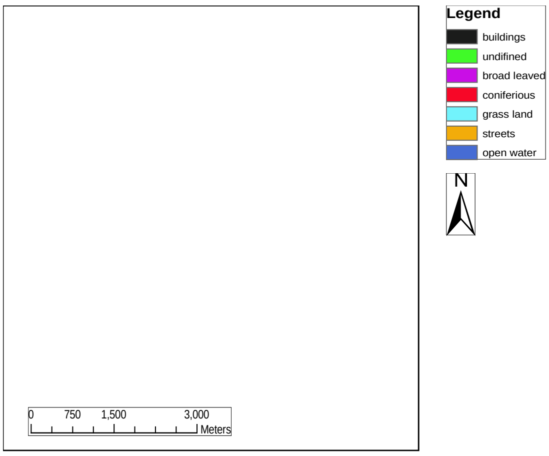

Land use type	%
Buildings	26
Undefined	1
Broad leaved trees	2
Coniferous trees	22
Grass land	2
Streets	10
Open water	36

Figure 140: Helsinki land use map baseline scenario

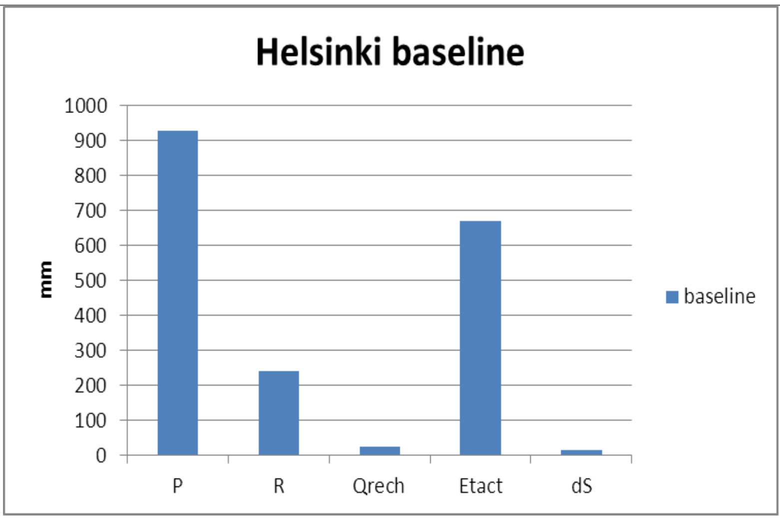

	P (mm)	R (mm)	Qrech (mm)	Etact (mm)	dS (mm)
baseline	927	241	24	670	17
% input	100	26	3	72	2

Figure 141: Yearly water balance baseline, and percentage of total input (P).

The Helsinki case study is not a general example of an urban area. The relative low amount of sealed surfaces leads to a low runoff sum. The relative high amount of urban green leads to a high actual evapotranspiration sum. In general it is expected that in the urban water balance runoff is the highest outflow. Less interaction takes place between the soil and groundwater reservoir (low Qrech and dS). This is typical for the urban environment with in general low groundwater levels.
Note that precipitation (P) is the only input term. All other terms are outputs and thus negative.

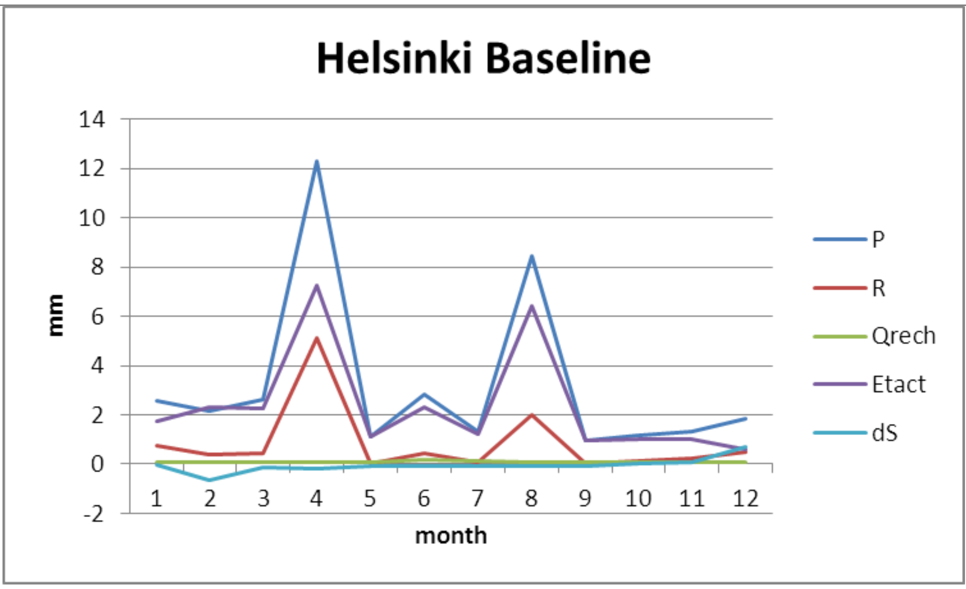

Figure 142: Monthly time step water balance Helsinki baseline

Precipitation (P) is the only input; runoff (R) is the only direct output, presented in this figure. Also actual evapotranspiration (ETact) follows the P input clearly. In this figure the influence of the input data (WRF meteorological forcing) on the model outcomes is indicated. This is further discussed in D 4.3. A monthly time step graph gives insides in the temporal changes of water balance terms and can indicate potential problems (e.g. for London, less soil water availability during summer which leads to low ETact values).

R ETact

Qrech dS

Low risk
Medium low risk
Medium risk
Medium high risk
High risk

Figure 143: Yearly spatial extend Helsinki baseline. Scaling indicates risk level.

The spatial pictures above show a clear relation with the urban land use types (Figure 140).A correlation between R and ETact is clearly visible. Areas with buildings and streets show high risk for runoff (red) as well as high risks for less ETact (red, explained as less ETact means to little water available for urban green). For the sealed areas also the Qrech and dS are small (red and orange). This risk mapping is a suggestion for the presentation of these outputs.

7.8 Outputs Alternatives

The table below gives the values of the water balance terms of the baseline scenario and the different alternatives defined for Helsinki.

Table 14: Outputs Alternatives Helsinki

	P	R	Qrech	Etact	dS
baseline	927	241	24	670	17
A1	927	241	27	679	20
A2	927	241	33	679	26
A3	927	241	31	679	24

It is concluded that the differences between the different scenarios and the baseline alternative are too small to be presented in the urban water balance outcomes. Therefore, the results are not further discussed here.

8 ANN. NKUA MODELS

Authors: D. Kolokotsa, K. Gobakis, A. Synnefa, M. Santamouris

8.1 Brief Model description

This model has been developed by the National Kapodestrian University of Athens for the estimation and prediction of the urban heat island intensity in various locations of a large urban area. The specific model is based on neural networks technology. Neural networks are a computational technique that simulates the operation of the human brain's neurons. To some extent, the NN approach is a non-algorithmic, black box strategy, which is trainable. The purpose is to train the neural black-box to learn the correct response or output (e.g. classification) for each of the training samples. This strategy is attractive to the system designer, since the required amount of a priori knowledge and detailed knowledge of the internal system operation is minimal. After training the internal (neural) structure of the artificial implementation the NN is self-organized to enable extrapolation when faced with new, yet similar, patterns, on the basis of experience with the training set.

Artificial neural networks (ANNs) have been used in a number of prediction studies that involve atmospheric time series data (Yi et al, 1996, Jiang et al, 2004, Maqsood et al, 2004, Ruano et al, 2006, Tasadduq et al, 2002). Additionally, a number of urban heat island prediction studies are based in the ANN technology (Santamouris et al, 1999, Mihalakakou et al, 2004, Kolokotroni et al, 2010). It should be underlined here that most urban heat island NN prediction studies require a large set of data to train the neural networks and predict the phenomenon in an accurate and acceptable manner. With this model an effort is made to predict the urban heat island intensity in Athens based on limited available data series using various neural networks architectures.

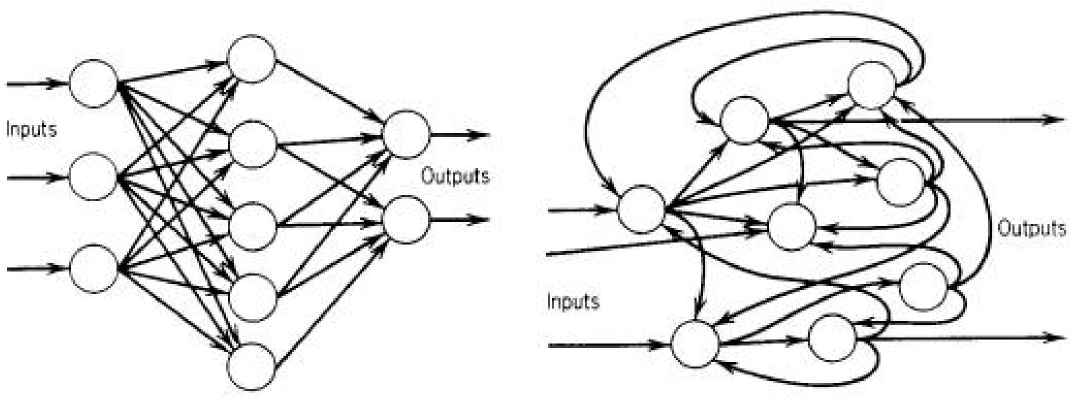

Figure 144 The neural network topology

8.1.1 Measurements

The application of NN model to the urban structure requires the following measurements for various urban positions:

- **Hourly ambient air temperature (°C)**
- **Global solar radiation (**MJ/m^2**)**

Moreover the NN model requires a series of urban stations and a reference station which is placed in a rural area.

8.1.2 List of input and output variables for NKUA NN model

8.1.2.1 Model the nighttime heat island intensity

The input parameters of the neural network model are the following:

Maximum daily values of the ambient air temperature (Tmax in °C), measured at each urban station: Maximum diurnal air temperature depends on various climatic factors such as the short-wave solar radiation, sunshine duration, vegetation and grounds' thermal properties, altitude and precipitation. Maximum daily air temperature is regarded as the representative urban parameter to the model, taking into account that it is the result of various major physical processes produced in the urban environment.

Nighttime values of the ambient air temperature (Tref in °C), measured at the reference station, at the time when ΔTmax,n is observed: Night time air temperature at the reference station is an important parameter contributing significantly to the heat island intensity estimation. The reference temperature is usually lower than the corresponding urban temperature, especially during calm and clear nights. This is mainly caused by the stronger rural cooling rates if compared with those of the urban environments.

$$\Delta T_{\max,n} = \left(T_{URBAN-}T_{REFERENCE}\right)_{\max,n}$$

The outputs of the neural network model are **the night time heat island intensity** values for each of the remaining twenty-two stations. Heat island intensity can be regarded as a measure of the numerous physical processes that produce the difference between rural and urban areas.

8.1.2.2 Model the daytime heat island intensity

The input parameters of the neural network model are the following:

Daytime values of the ambient air temperature (Tmax in °C) measured at each urban station at the time where $\Delta T_{\max,d} = \left(T_{URBAN-}T_{REFERENCE}\right)_{\max,d}$ is observed.

Maximum daily values of global solar radiation, (*Ig*, in MJ/m^2)

Daytime values of reference air temperature, (Tref, in _C), measured at the reference station at the time when the ΔTmax,d is observed.

The outputs of the neural network model are **the daytime time heat island intensity** values for each of the remaining twenty-two stations.

8.1.3 Implementation of the NKUA NN model in the DSS

The NKUA model can operate either on-line or off-line depending on the length of data provided. In case there are no data available or the monitoring period is short (less than 1 year) then the UHI intensity prediction should be based on historical data that should be continuously updated. In this case the model should be operated in on-line mode. If the monitoring period is long (higher than 3 years) then the prediction can be based in off line operation of the model.

8.1.3.1 Requirements for On- line System

Solution No.1

Each station

- Intel Pentium 4 and above RAM 512 MB (At least 1024 MB recommended)
- Windows XP or Vista 32bit (not Linux)
- Data Acquisition Card (see supported cards at http://www.mathworks.com/products/daq/supportedio.html)
- Internet connection (wired or wireless)

For this option a central computer is necessary to collect and analyze the data from all station. Using Matlab compiler we can transform our Matlab code into components witch can be used from Java, C# or .Net. Then a specially design program (in Java, C# or .Net with a Matlab module) must be written in order to acquire the measurement using the data acquisition card, prepare and transmit the data from each station to the central computer. The central computer must receive and verify the data from all station and store them. Then the data must be feed into The neural network , which will generate the desired output like a plot.

Solution No.2

Each station

- Data Acquisition Card with TCP/IP support (see supported cards at http://www.mathworks.com/products/daq/supportedio.html , like http://www.ueidaq.com/data-acquisition-chassis/ethernet-daq)
- Internet connection (wired or wireless)

For this option a central computer will communicate via TCP/IP with the data acquisition card's and collect the measurement. A program entire written in Matlab will make the necessary data manipulation and feed the data into neural network , which will generate the desired output like a plot.

In the course of the BRIDGE project it has been decided that the NKUA ANN model is going to be applied at the Athens case study area, considering the difficulties to apply the specific model to other cities. It is considered as a complementary model and will be implemented in the DSS as an on line model.

8.2 Urban heat island (UHI) intensity prediction in Athens through artificial neural networks (ANNs)

8.2.1 Experimental site description

The Greater Athens Area, (GAA), is situated on a small peninsula located on the southeastern edge of the Greek mainland (Figure 145). It is divided by high mountains in three main parts, which are connected by small openings. The central part is the Athens basin which covers an area of 450 km^2, with a population density of 8000 inhabitants per square kilometer, with the main axis orientated from SSW to NNE. Athens basin is surrounded by high mountains in the north (Parnitha, 1426 m), in the west (Egaleo, 458 m) and in the east (Hymettus, 1026 m and Penteli, 1107 m), while it is open to the sea from the south (Saronikos Gulf). The other parts of the Athens area are the Thriassion plain west of the Athens basin and the Mesogia plain in the east. There are only small openings through which the Athens basin communicates with these plains as well as the rest of Greek mainland. These openings play an important role in air mass exchange between the Athens basin and the Thriassion and Mesogia plains.

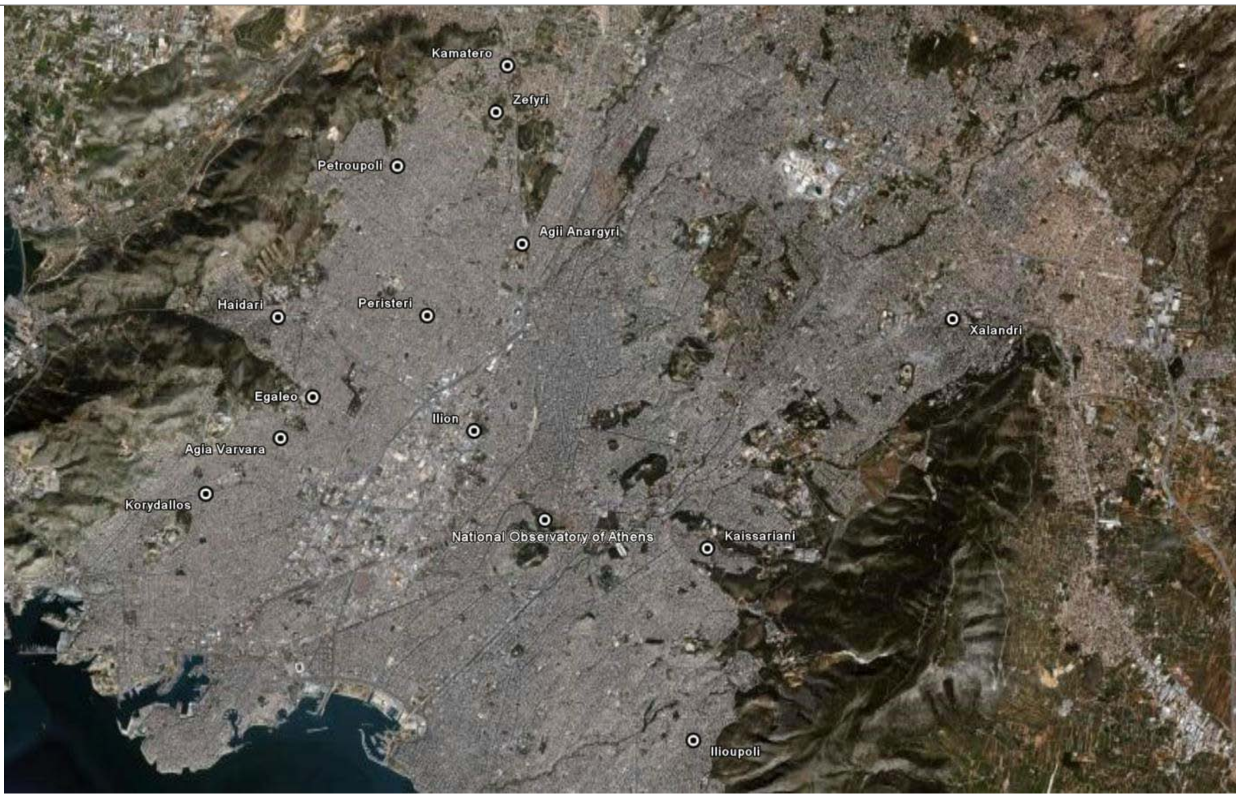

Figure 145 The location of 14 meteo stations in the GAA

The city of Athens is characterised by a strong heat island effect, mainly caused by the accelerated industrialisation and urbanisation during recent years.
In the present effort to predict the urban heat island effect in the area of Athens, a network of fourteen meteorological stations has been set up corresponding to the thirteen Athens municipalities plus the reference station (Table 15). The meteorological stations are placed on the administrative municipalities' buildings and are all 1.5 -2m above ground, north oriented, shaded and ventilated.

Table 15 The location of the experimental sites

i	**Municipality**	LATITUDE	LONGITUDE
1	Egaleo	**37°59'50"**	**23°40'5"**
2	Korydalos	**37°58'45"**	**23°38'33"**
3	Haidari	**38° 0'45"**	**23°39'35"**
4	Ag. Varbara	**37°59'22"**	**23°39'37"**
5	Peristeri	**38° 0'47"**	**23°41'43"**
6	Kamatero	**38° 3'35"**	**23°42'50"**
7	Zefyri	**38° 4'7"**	**23°43'4"**
8	Ilioupoli	**37°55'58"**	**23°45'29"**
9	Petroupoli	**38°2'26"**	**23°41'16"**
10	Agii Anargyri	**38°1'34"**	**23°43'3"**
11	Xalandri	**38°0'44"**	**23°39'34"**
12	Ilion	**38°1'54"**	**23°42'27"**
13	Kaissariani	**37°58'8"**	**23°45'41"**
14	National Observatory of Athens	**37°58'24"**	**23°43'5"**

Each meteorological station contains a fully calibrated high precision data logger (Tiny Tag data loggers) that measures air temperature every 15min.

The sensors' characteristics are:

- Reading Resolution 0.02°C or better
- Range -40°C to +125°C
- Temperature Stability ±0.01°C/°C change from 25°C

In addition, other meteorological data (solar radiation, wind velocity, etc) are collected from the National Observatory of Athens located at Thission, Athens (N′ 37° 58', E′ 23° 43'). The specific site is in a greenery area and is considered as the reference station of the overall analysis although it is positioned almost in the center of the peninsula. The experimental period started on April 2009. The present analysis uses data for one year period (from April 2009 until May 2010) targeting to minimise the need for long term historic data. Measurements were performed until November 2010. This last data set was used for additional validation of the model. This work is presented in the Deliverable 4.3.

8.2.2 Application of ANN for Urban heat island intensity prediction

8.2.2.1 Data sets

The measured and collected data are used as input in order to develop the ANN model and prediction procedure.

The input parameters for the neural network are as follows:

i) Date to represent the yearly climatic variations (the date is converted into the number of days starting from the 1st of January) and ranges within $[1,365]$

ii) Time, the time is converted into minutes of the day and ranges within $[0,1380]$.

iii) Ambient temperature (^oC) measured by the various experimental sites described in the previous section.

iv) Global solar radiation (W/m^2) measured by the National Observatory of Athens.

Neural networks generally provide improved performance when the data are normalised. The use of original data as input to the neural network may cause a convergence problem. All the temperature and global solar radiation data sets are, therefore, normalised in the range $[-1,1]$ by dividing the difference between the actual value x and minimum values by the difference between the maximum x_{max} and minimum values x_{min} i.e.

$$x_{nor} = \frac{x - x_{min}}{x_{max} - x_{min}}$$

The main goal of normalisation, in combination with the weight initialisation, is to allow the squashed activity function to work at least at the beginning of the learning phase. Thus, the gradient, which is a function of the derivative of the non-linearity, will always be different from zero. At the end of each algorithm, the outputs are transformed into its original data format.

8.2.3 The neural networks architecture

The prediction problem using neural network models can be separated into three steps or sub problems: designing the neural network architecture, conducting the learning or training process, and testing.

8.2.3.1 **The NN architecture design**

In the present study three different neural networks are chosen:

i) The Cascade NN (Figure 146) which consists of the input layer, the layer of output neurons, and one or more hidden layers. The first layer has weights coming from the inputs and each subsequent layer has weights coming from the input and all previous layers. All layers have biases. The last layer is the network output (Hedayat et al, 2009).
ii) The Elman NN (Figure 147) which can be viewed as a feedforward neural network with an additional set of inputs from the context layer (Song, 2010).
iii) The Feed-Forward NN has all of the data information flows in one direction. The neurons of one layer are connected with the neurons of the following layer and there is no feedback (Figure 148).

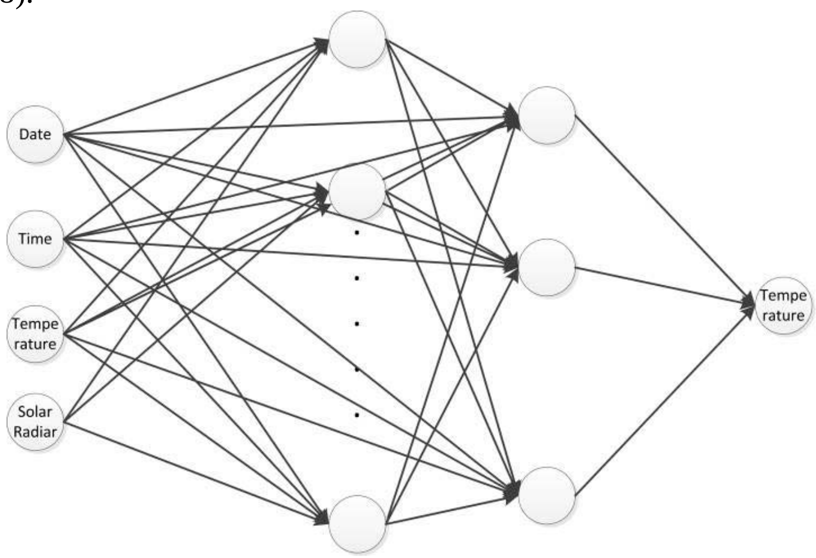

Figure 146 Schematics diagram for the Cascade neural network

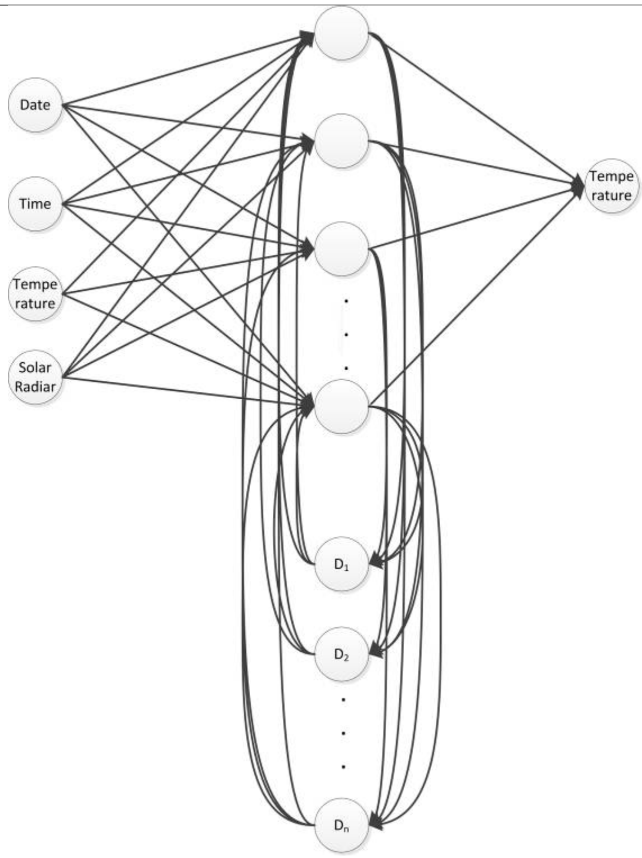

Figure 147 Schematics diagram for the Elman neural network

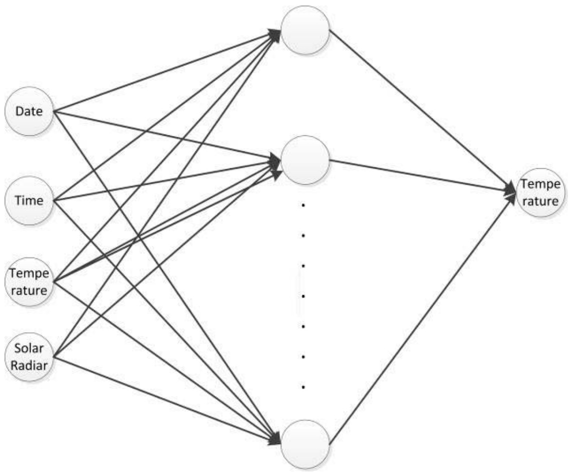

Figure 148 Schematics diagram for the Feed-Forward neural network

The selection of the networks' architecture is based on various results presented in the literature as well as in a preliminary trial and error procedure for various neural networks' types. Apart from the three above mentioned types, the NARX, Hopfield and Learning Vector Quantization (LVQ) neural networks are also tested without providing any encouraging results for the specific problem.

8.2.3.2 The learning and training process

For each different neural network architecture the optimal training function, transfer or activation function, hidden layers and number of neurons are investigated. Each neural network consists of one to three hidden layers with 20 to 40 neurons each, followed by an output layer of one neuron. For all three neural networks (Cascade, Elman and Feed Forward) the following training functions are considered:

- Levenberg-Marquardt (trainlm).
- Scaled conjugate gradient (trainscg).
- BFGS quasi-Newton (Trainbfg).
- Gradient descent (traingd).
- Gradient descent with momentum and adaptive learning rate (traingdm).
- Resilient back propagation training function (traingnrp).

The tangent sigmoid function is used as transfer function (Figure 149) for all the NN.

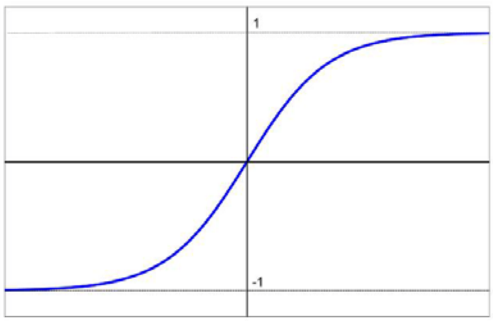

Figure 149 Tangent sigmoid function

Each neural network is trained using all the above training functions for the datasets from the Koridalos station for 1 hour and 24 hours prediction horizon respectively. The Koridalos site is randomly selected and the results are validated by the implementation of the same procedure in the Peristeri experimental site (see Table 16 and Table 17).
The best prediction performance is achieved by (see Table 16 and Table 17):

- The Cascade neural network using the BFGS quasi-Newton as training function.
- The Elman neural network with the Levenberg-Marquardt as training function.
- Feed-Forward neural network with scaled conjugate gradient as training function.

Table 16 Performance comparison of difference training functions for Koridalos site

		1 hour			24 hours		
	Training Function	Mean Value	Standard Deviation	MSE	Mean Value	Standard Deviation	MSE
Feed Forward	trainlm	2.220	1.601	0.621	2.513	2.274	0.955
	trainscg	**2.041**	**1.385**	**0.484**	**2.291**	**1.970**	**0.820**
	trainbfg	22.355	12.376	38.023	30.355	17.376	45.023
	traingd	7.471	7.215	6.859	8.873	6.997	8.285
	traingdm	15.643	10.772	20.319	18.323	12.033	26.518

	traingnrp	10.660	7.677	11.252	7.533	6.074	6.409
Cascade	trainlm	1.965	1.483	0.423	2.153	2.681	1.070
	trainscg	1.954	1.342	0.393	2.163	1.978	0.773
	trainbfg	**1.666**	**1.084**	**0.593**	**0.942**	**0.845**	**0.131**
	traingd	3.606	3.259	1.812	3.476	3.140	1.668
	traingdm	3.042	3.032	1.230	3.593	3.799	2.303
	traingnrp	2.088	1.547	0.535	2.325	2.487	1.052
Elamn	**trainlm**	**1.137**	**1.192**	**0.342**	**2.530**	**2.357**	**1.026**
	trainscg	1.897	1.295	0.367	1.517	1.085	0.303
	trainbfg	1.975	1.321	0.614	1.254	0.967	0.652
	traingd	2.560	1.723	0.780	1.556	1.294	0.314
	traingdm	2.443	1.445	0.574	1.383	1.068	0.235
	traingnrp	3.215	1.687	0.691	1.469	1.325	0.325

Table 17 Performance comparison of difference training function for Peristeri site

		1 hour			24 hours		
	Training Function	Mean Value	Standard Deviation	MSE	Mean Value	Standard Deviation	MSE
Feed Forward	trainlm	3.606	3.259	1.812	4.128	5.655	4.348
	trainscg	**3.174**	**2.457**	**1.407**	**3.087**	**3.087**	**2.253**
	trainbfg	7.707	5.638	9.454	14.607	10.348	23.870
	traingd	9.201	7.230	12.596	7.677	5.402	6.144
	traingdm	6.980	6.779	8.493	10.595	8.019	13.464
	traingnrp	6.890	6.391	7.157	11.877	10.265	14.669
Cascade	trainlm	2.930	2.269	1.166	3.691	3.908	2.745
	trainscg	2.805	2.155	1.043	2.764	2.682	1.454
	trainbfg	**2.890**	**2.281**	**1.157**	**2.912**	**2.636**	**1.411**
	traingd	6.317	7.253	6.964	5.172	5.109	3.599
	traingdm	6.831	5.684	5.880	4.689	4.776	3.540
	traingnrp	2.994	2.282	1.233	3.381	4.217	2.475
Elamn	**trainlm**	**2.234**	**1.351**	**0.911**	**1.142**	**0.736**	**0.151**
	trainscg	3.299	2.041	1.160	1.268	0.923	0.173
	trainbfg	3.754	2.545	2.840	3.412	1.785	0.985
	traingd	2.886	1.920	0.520	1.835	1.575	0.571
	traingdm	3.315	5.818	3.122	3.202	7.685	3.652
	traingnrp	3.125	2.958	2.958	3.587	2.218	2.504

8.2.3.3 The testing process

In this step the results from the three neural networks, for the various data sets are compared in order to examine the prediction accuracy. We choose the optimum results for each neural network.

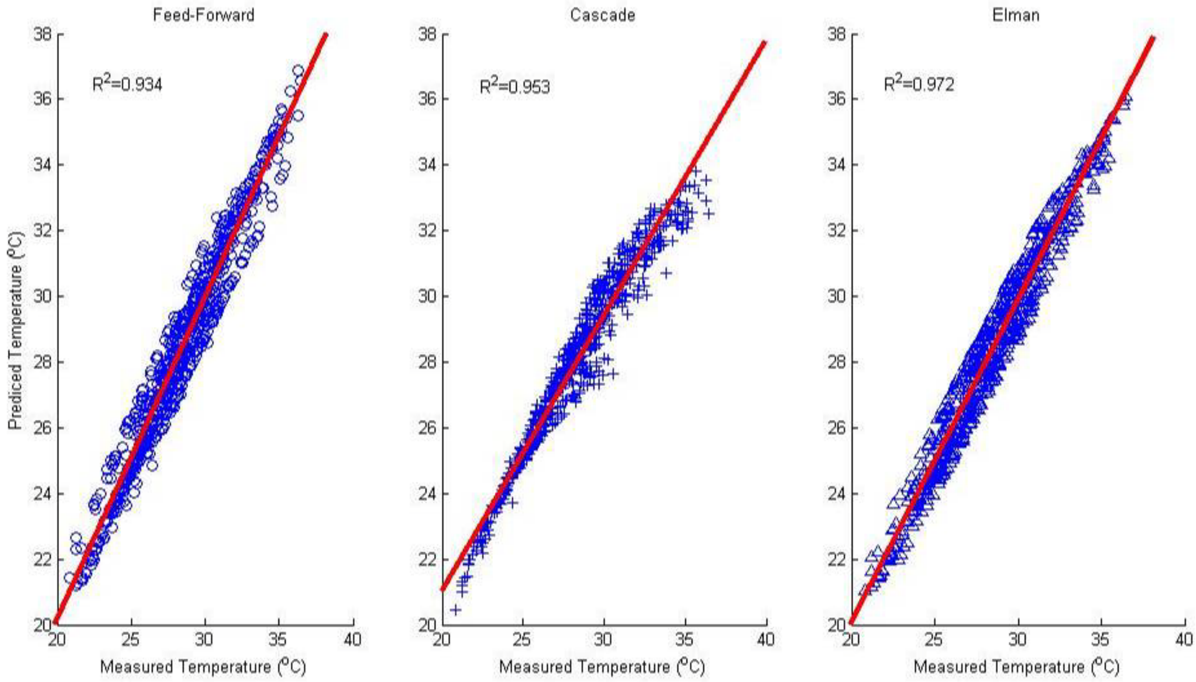

Figure 150 Comparison between the three different ANN for one-hour prediction horizon

Figure 150and Figure 151 present the measured versus the predicted values for Koridalos site for 1hour and 24 hours prediction horizon respectively. The best fit of the measured to the observed data is achieved by the Elman followed by the Cascade and the Feed-Forward architecture.
The percentage error and the mean square error are utilised to calculate the difference between the measured and the predicted temperature values.

$$PercentError = \frac{Experiment - Theoretical\ value}{Theoretical\ value} * 100\%$$

The mean value (MV) and the standard deviation (SD) of the percentage error for each neural network architecture and for 1 hour prediction horizon are 1.8±1.0 % for Elman, 2.8±2.2 % for Feed Forward and 2.4±1.5 % for Cascade. The same results apply for the 24 hours prediction horizon as tabulated in Table 16. The mean squared error (MSE) of the three neural networks and for Koridalos site is for Feed-Forward 1.12, for Cascade 0.65 and for Elman 0.35.
The above results show that the most suitable NN architecture for the urban heat island intensity prediction is the Elman type using Levenberg-Marquardt as transfer function. The above results are verified by following the same procedure for another site, placed in a quite different location, i.e. the Peristeri site. The results of the analysis performed in Peristeri site are tabulated in Table 17 and verify that the optimum neural network is the Elman. The specific network architecture is then used for predicting the urban heat island intensity in all sites.

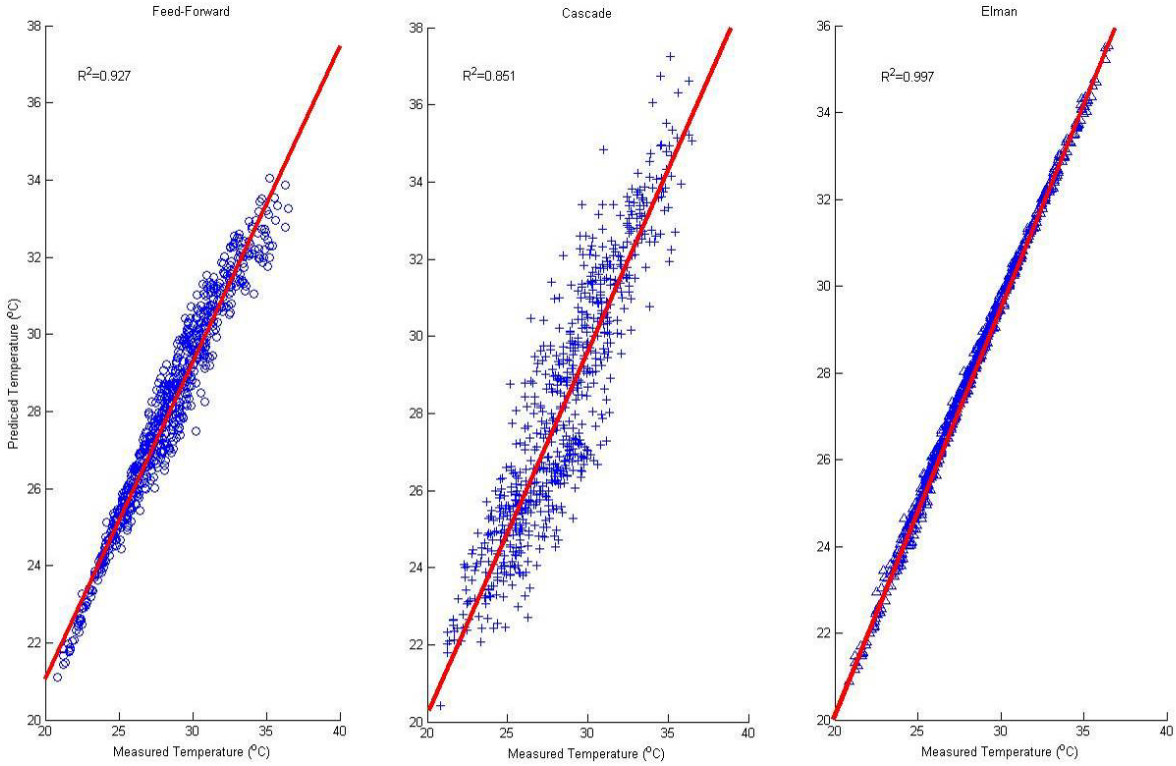

Figure 151 Comparison between different ANN for 24-hour prediction horizon

8.3 Results and discussion

Training and verification of the ANN is performed using the data collected during the period from 06/04/2009 to 07/09/2009 for each experimental site. Therefore the training and verification period is shortened to five months.

The data are fed into the ANN as blocks of 24 values corresponding to each hour of the day. The neural network has a training period of 40-60 days. The remaining data are used to verify the quality of network and adaptation of the neural network to the new data.

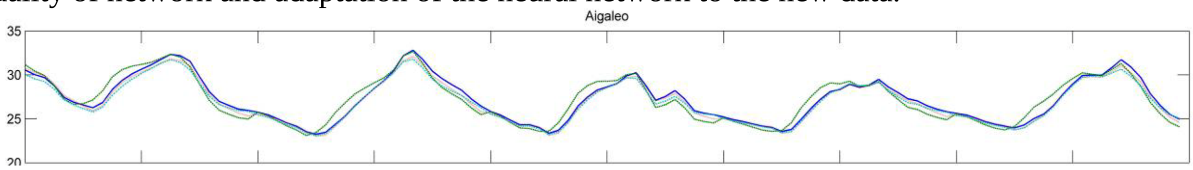

shows the measured and predicted temperatures the Bridge case study area (Aegaleo) for two different dates 19-20/06/2009 and 05-06/07/2009 respectively.

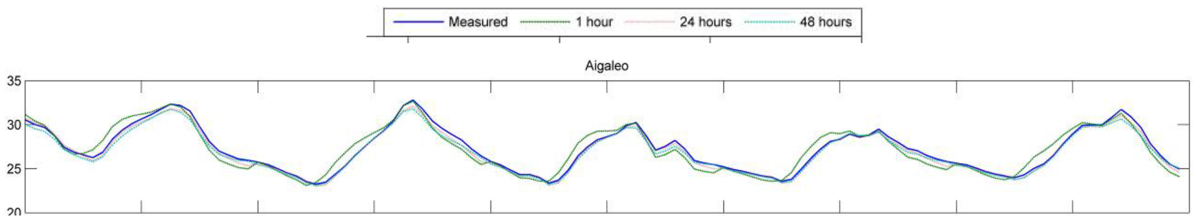

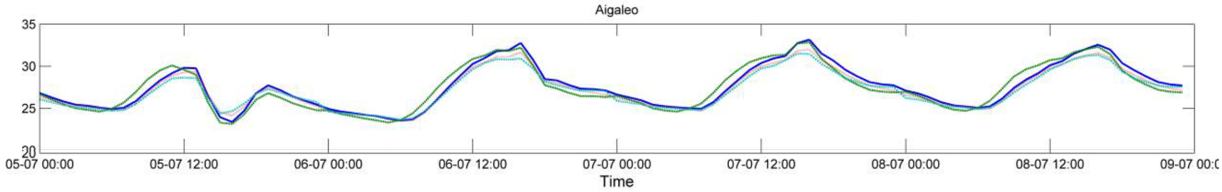

Figure 152 Measured – predicted temperatures for 19-20/06/2009and 05-06/07/2009

The diurnal fluctuation of temperatures is quite smooth and is followed by the 1 hour and 24 hours Elman prediction algorithms quite accurately.

Isothermal images have been developed to imprint the UHI intensity over Athens. The mapping of the region is performed is using Google Earth while the isothermal lines are added by Surfer 8 software. For each day that the UHI over Athens is analyzed, a set of four images is constructed to visualize the ANN prediction:

- The first image maps the isotherms over Athens using the measured data of the specific day and time.
- The second image represents the isotherms of Athens urban heat island based on the 1 hour prediction results for the specific day and time.
- The third image maps the isotherms of Athens urban heat island based on the 24 hour prediction results for the specific day and time.
- The fourth image plots the isotherms of Athens urban heat island based on the 48 hour prediction results for the specific day and time.

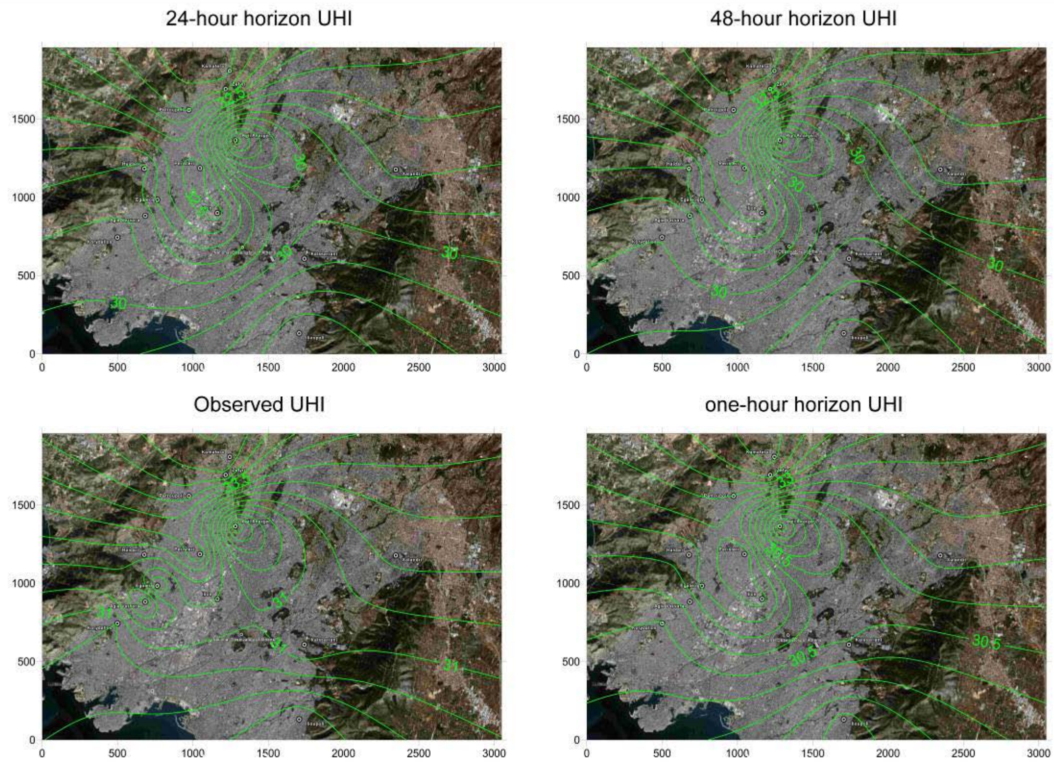

Figure 153The UHI in Athens during 01/07/2009

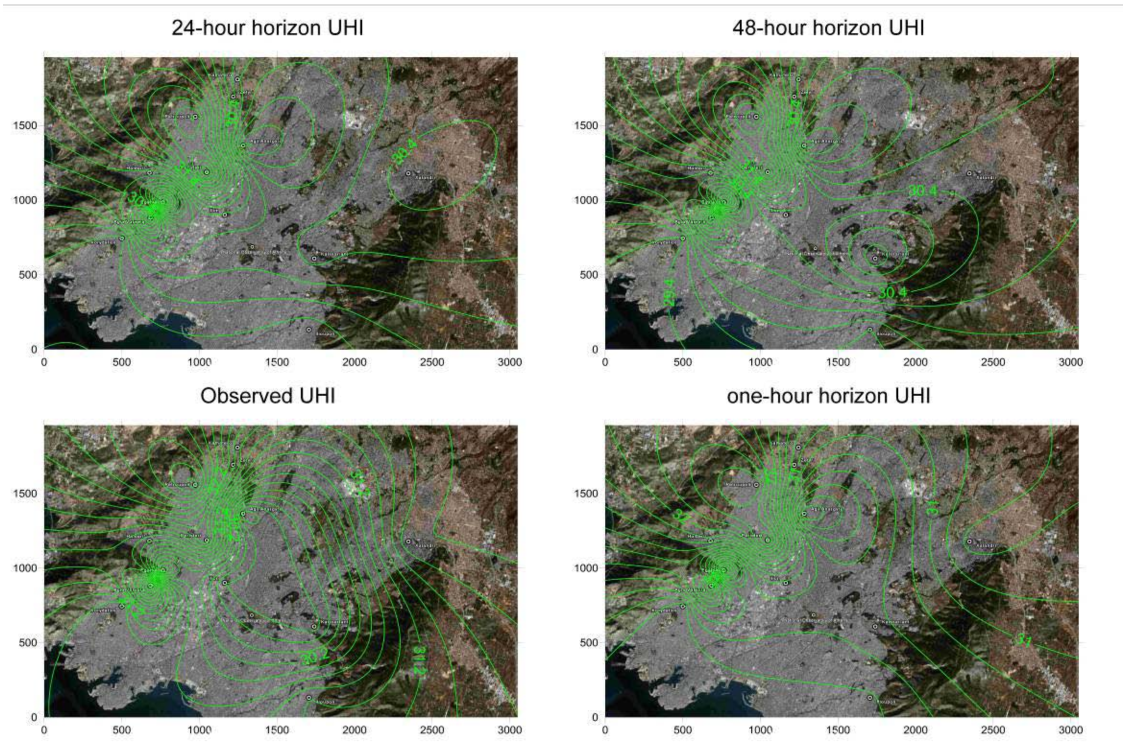

Figure 154 The UHI in Athens during 18/06/2009

Indicatively the isothermal maps of the UHI intensity over Athens for two days (i.e. 1/7/2009 and 18/6/2009) are illustrated in Figure 153 and in Figure 154. The prediction of the maximum temperatures for the 1/7/2009 has a maximum error of 1.6 ^{0}C and 1.9 ^{0}C for the 24 hour and 48-hour prediction horizon respectively. Moreover the visualization of UHI intensity prediction shows that the isotherms of the 24 hours prediction are very close to the actual measured ones while the 48 hours prediction has a slightly different picture. Therefore the specific NN architecture and methodology followed is quite accurate for the 24 hours prediction horizon.
The urban heat island intensity is then calculated versus the reference station, i.e. National Observatory of Athens.

8.4 Conclusions

Important heat island studies have been performed in Europe during the last decades showing that the deep understanding of the phenomenon plays an important role in fighting its consequences to the climate change. Advanced artificial intelligence techniques such as neural networks offer on the other hand a valuable tool to be used for the prediction of the specific phenomenon. The neural networks prediction accuracy is mainly based on the quality and quantity of the available data.
The aim of the present work was to investigate the feasibility of predicting the urban heat island phenomenon using a limited data series. The Athens case study was used to demonstrate the feasibility and accuracy of the overall approach.
The methodology presented here showed that the urban heat island intensity can be predicted quite accurately for at least a 24 hours prediction horizon using a limited set of data.

Therefore the NN prediction methodology can be an important tool for peak energy load predictions during heat waves and hot summer days contributing to the demand and supply energy management.

9 WRF-ACASA. CMCC MODEL

9.1 Brief description.

The **Advanced Canopy-Atmosphere-Soil Algorithm** (**ACASA**) model (Pyles et al., 2000; 2003), first developed by University of California, Davis (UCD), is a SVAT (Soil-Vegetation-Atmosphere-Transport) model, used to simulate the exchanges of heat, water vapour and CO_2 within and above a canopy. It treats the surface and associated fluxes as an interconnected system, and the atmosphere, the urban surface, and the soil are represented as a multilayer system. In ACASA, the canopy is represented as a horizontally homogeneous medium with all leaves and branches arranged with spherical symmetry. The surface-layer domain simulated by ACASA represents average conditions and fluxes for a 30-minute time intervals at each spatial point in WRF. Twenty equally spaced atmospheric layers represented by a steady-state 3rd order turbulence extend to twice the canopy height (Meyers and Paw U 1986; 1987) with the canopy occupying the lowermost 10 layers (Figure 155). All sources of heat and mass fluxes occur within the canopy and at the soil- (or snowpack)-atmosphere interface only, while constant-flux assumptions prevail in the 10 layers above the canopy. Within the soil horizon, the model includes thermal and hydrologic diffusion among an adjustable number and depth of soil layers; varying by soil type. Short-wave (solar) radiative transfer within the canopy initially occurs among 100 layers to suit the numerical needs of the radiative transfer equations, which are solved for both beam and diffuse PAR (0.36-0.72 µm) and NIR (0.7 – 2.0 µm) wavelength bands. The short-wave radiation flux streams needed by the rest of the model are then interpolated to 10 layers. The latter are used to help drive the calculations of surface temperatures, terrestrial-infrared radiative transfer, physiological conditions, and associated fluxes needed for the turbulence calculations; all of which come into iterative numerical convergence. To properly work in urban environment, the model has been modified to account for the anthropogenic contribution to heat exchange and carbon production (Marras et al., 2010).

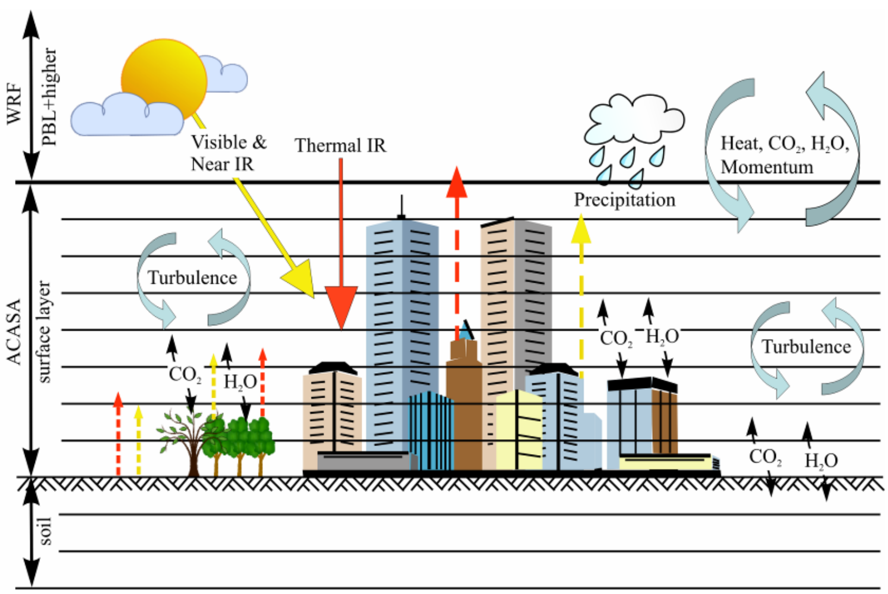

Figure 155: Scheme of the processes modelled by the coupled model WRF-ACASA.

ACASA has been recently coupled with the well known Weather Research and Forecasting model (WRF) (Skamarock et al., 2008). WRF is a mesoscale numerical weather prediction system which, thanks to its flexibility and computational efficiency, is largely used for both operational forecasting and atmospheric research. In particular, the ACASA model was adopted as an alternative to the existing suite of surface-layer schemes available in WRF due to the need to establish more flexible and realistic representations of surface-layer physics and physiology (Falk et al., 2010). The WRF model, in our case driven by North American Regional Reanalysis data (NCAR-NCEP), is run down to its planetary boundary layer, where ACASA is called (Figure 155).

The WRF-ACASA coupling is able to identify how multiple environmental factors, in particularly climate variability, population density, and species distribution, impact future carbon cycle prediction across a wide geographical range. A scheme representing the WRF-ACASA coupling is reported in Figure 156

Specifically, all urban fluxes in ACASA are parameterized in a manner where the urban canopy density and associated anthropogenic flux components are proportional to population density: the more people there are in an area, it is assumed, the more building surfaces there are that can be flux sources and sinks. Total roof area index, *RAI*, is linearly proportional to population density (*PD*, people m^{-2}) as $RAI=1000*PD$, with a maximum value of 50% of the horizontal surface-area at population densities greater than or equal to 5000 people km^{-2}. Only roof surfaces can maintain standing water or ice, and they do so in the same way that is modelled for plant canopy elements. Wall area (WAI) makes up the majority of the urban canopy for cities of sufficient population density. In ACASA, this assumption is kept by making total wall area index (WAI) vary in a manner proportional to the cube of the population density. The vertical distribution of roof and wall area is unimodal and is the same for all urban land points: only the magnitudes vary with measured or specified values population density and maximum canopy height. For coupled simulations, WRF-ACASA population density values are keyed in by WRF-specific urban land use representations for the baseline and alternative scenarios, in order of urban land use intensity, as containing 1000, 1500, and 2000 people per square kilometre, respectively. Soil surface types representing surface drainage capacity range from sand-loam to sand to bedrock for WRF urban-classes 1, 2 and 3, respectively, in order of increasing urban land use intensity.

All nonpoint sources of carbon dioxide (autos, furnaces, etc.) are represented as proportional to population density times the input vehicle flux density, whenever available, preferably as a 30-minute “forcing” time series. As long as internal combustion dominates the transportation web of most population centers, it is advisable that the assumption that vehicles are mostly responsible for the nonpoint anthropogenic CO_2 fluxes be kept. Whenever diurnal time series of vehicle flux density data are not available, anthropogenic carbon dioxide flux sourcing is proportional to population density-normalized Lorentz-fit to measured averages of the composite-diurnal carbon monoxide exposure (Marco et al., 2005), which varies throughout the diurnal cycle as a proxy for vehicle flux density. Vegetation contributions are nontrivial whenever total LAI is specified as nonzero. Vegetation density decreases linearly with population density above 1000 people km^2, with 0 values for population densities exceeding than 10,000 people km^2. For all simulations, the mean leaf area index was set to 0.5 for cities of moderate to high urban development. Wall conduction fluxes that affect surface energy exchanges are handled using the same conduction scheme as for soil, but for a fixed (dry) moisture specification and thermal conduction parameters

set for concrete. Total anthropogenic surface sensible heat fluxes are weighted by total building surface area, which is proportional to total population density.

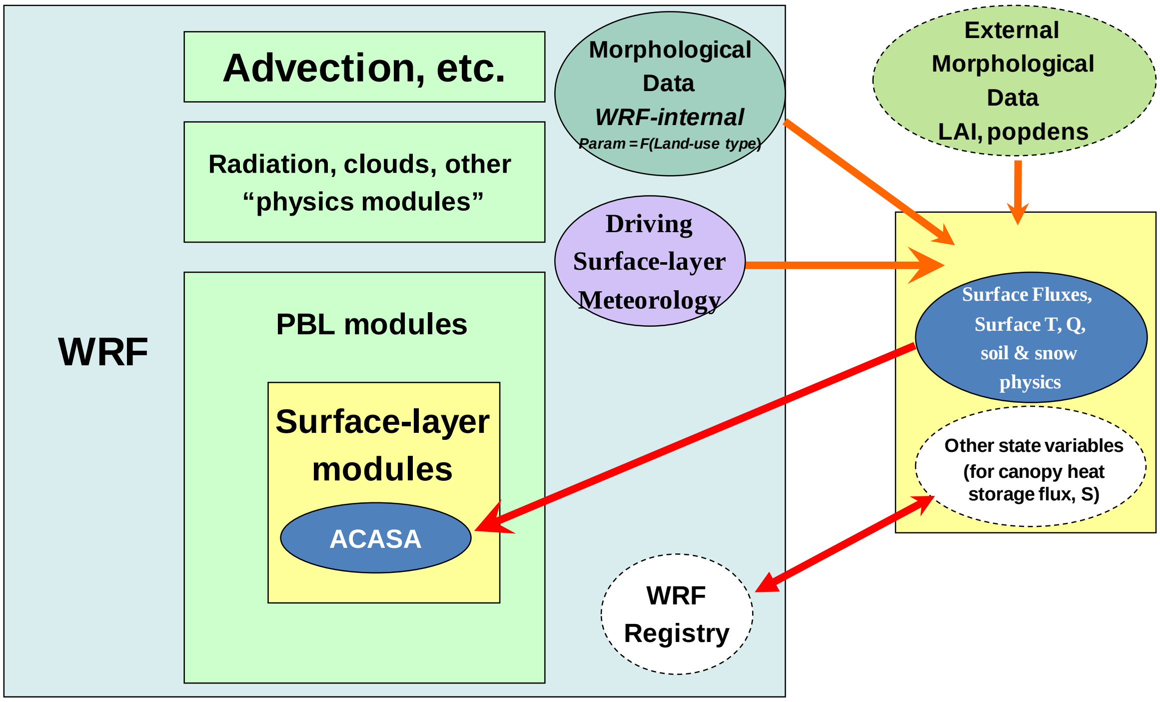

Figure 156Visual schematic of WRF-ACASA coupling.

9.2 Architecture and domains.

The implemented WRF-ACASA model has been run over two European cities completely different from each other for topographical and environmental characteristics: Helsinki and Firenze.

We have run the WRF-ACASA model using the initial and boundary conditions received from the UPM partner. The coupled WRF-ACASA model is designed to be WRF-compatible, meaning that WRF-ACASA compiles and runs in a manner using exactly the same procedure as WRF-original, with no additional pre-processing. Results from 8 sets of runs (Firenze Scenarios Baseline, Alt1, Alt2, Alt3, and Helsinki Scenarios Baseline, Alt1, Alt2, Alt3) on a 200-meter horizontal grid are provided for both 5km by 5km domain locations.

A second set of runs uses WRF-ACASA for all of Europe, with concentric nesting down to a 7km by 7km area at 200m horizontal grid spacing for each city. The domain configuration and input data feeds are logistically set, and the Baseline and the Alternatives 1-3 scenario simulations are ready to proceed as soon as computational resources become available. The vertical resolution will be significantly increased, to 30 or more layers in the PBL regime, to allow for more complete representations of the surface-layer physics.

9.3 Set up and configuration.

We have implemented the following configuration in WRF:

-Cumulus parameterization: Option 1 (Kain-Fritsch scheme)

-PBL scheme and diffusion: Option 2 (Mellor-Yamada-Janjic scheme)

-Explicit moisture scheme: Option 3 (Hong-Dudhia-Chen scheme)

-Radiation schemes: option 1 (Dudhia scheme from MM5)

All model configuration flags were kept as given to us by Land surface model: the existing model NOAHLSM scheme in WRF has been replaced by the ACASA multilayer model. We aliased ACASA as "surface-layer physics, option 2" (NOAHLSM), but kept all else the same, in the configuration files provided to us by UPM. Due to ACASA features described above, a more flexible and realistic representation of surface-layer physics and physiology was achieved.

The ACASA coupling to WRF proceeds in a subroutine structural manner that parallels NOAHLSM, with a similar front-end for each. This allows parallelization using multiple processors. ACASA provides a suite of surface and surface-layer quantities that help to drive WRF, the most important (WRF-sensitive) being sensible heat and moisture flux density, surface "skin" temperature and humidity. Included also are updates to snowpack and/or soil thermal and hydrological states, each of which affect the surface forcing. Carbon dioxide flux density and other diagnostic variables, also provided as outputs, do not 'force' WRF directly.

9.4 Input data preprocessing.

The required set of driving meteorological data from the lowest WRF atmospheric layer, applied to ACASA on a half-hourly basis, are: precipitation rate and form (kg m^{-2} $timestep^{-1}$), specific humidity (kg kg^{-1}), wind speed (m s^{-1}), downwelling short-wave radiation (W m^{-2}), downwelling long-wave radiation (W m^{-2}), air temperature (K), air pressure (hPa), and carbon dioxide concentration (ppm). Furthermore, initial soil temperature (K) and moisture (volumetric) profiles for the first model timestep are provided by the WRF initialization routines. Surface morphological parameters that drive the physiological responses also have to be specified, which vary by WRF land use type. The set of key morphological parameters includes: total (green) leaf area index (m^2 m^{-2}), maximum canopy height (m), leaf-scale ideal photosynthetic potential (μmol m^{-2} s^{-1}), human population density (# people/ km^{-2}), and eventually vehicle flux density (# vehicles/ m^2). Morphological parameters not represented in the WRF land-use parameter suite, quantities such as mean leaf diameter and basal respiration rates for plant tissues, are specified with constant near-cardinal values for all land points. Marras et al. (2011) and Staudt et al. (2010) provide additional background information on morphological parameters and model sensitivities to each.

9.4.1 Emissivity:

WRF values used as constants for input, values for canopy-elements in ACASA scaled 1:1 with WRF values.

9.4.2 Albedo:

WRF values used as input-constants, translated to leaf-scale visible and near-IR values, with soil surface values changing with moisture content.

9.4.3 Topography:

land slope affects radiation calculations in the same manner as WRF-original

9.4.4 Land uses:

land use type provided by WRF; with related parameters keyed in with the same procedure as WRF-original.

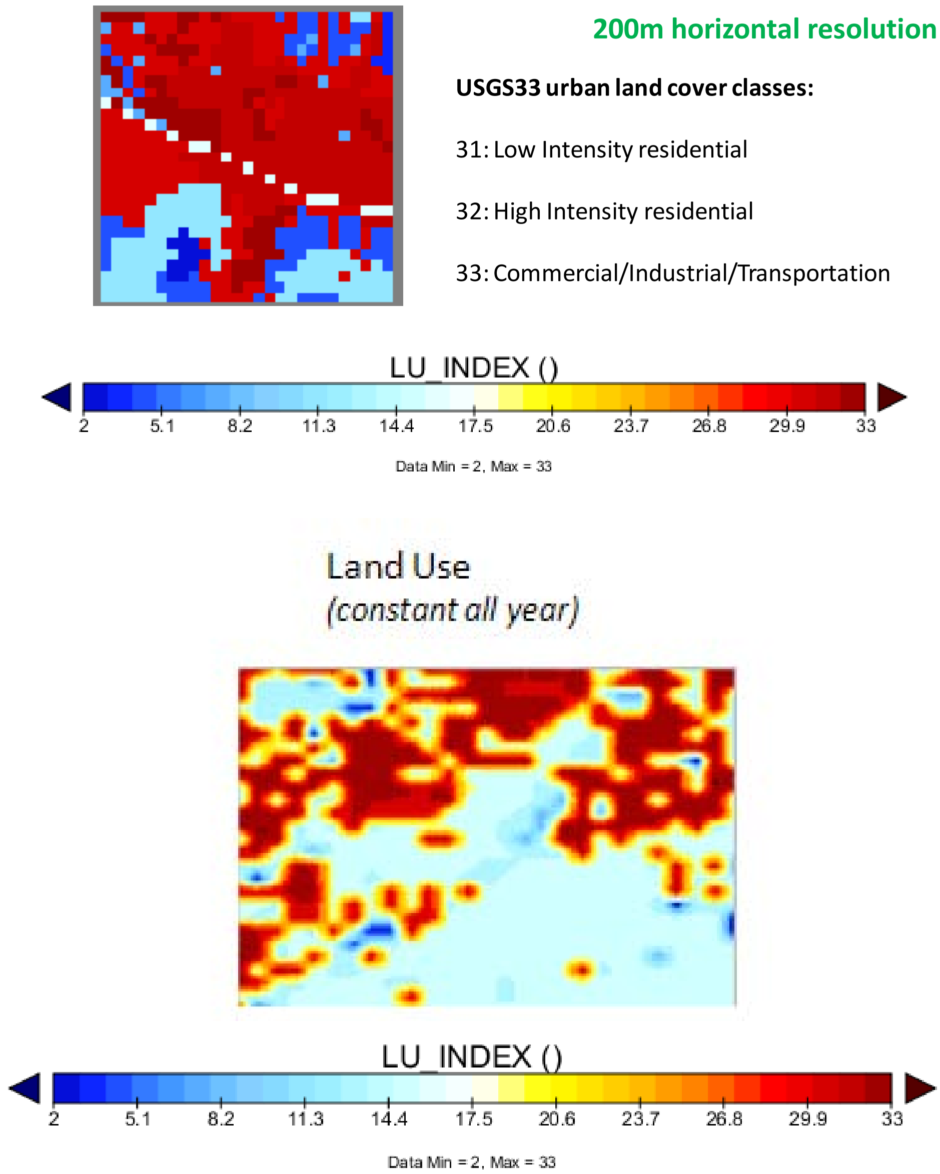

Figure 157Land use maps for Baseline scenarios, Firenze (top) and Helsinki (bottom).

The most crucial ACASA model output that drives the WRF-simulations from below include half-hourly vertical fluxes of heat (Wm^{-2}), water vapour ($kg\ m^{-2}\ s^{-1}$), momentum flux density (as friction

velocity, m s^{-1}), turbulence kinetic energy (m^2 s^{-2}), and surface (bulk skin) temperature (K). In addition, snowpack and/or soil and canopy thermal and hydrological states, needed for adequate simulation of the surface-layer, are updated at all land points and are stored between time steps. Land use changes in the Alternative Scenarios: The WRF-ACASA Alternatives simulations were driven with the forcing meteorology as given by UPM partners. Each Alternative simulation, however, involved a slightly different land use map (Figure 158 ,Figure 159).

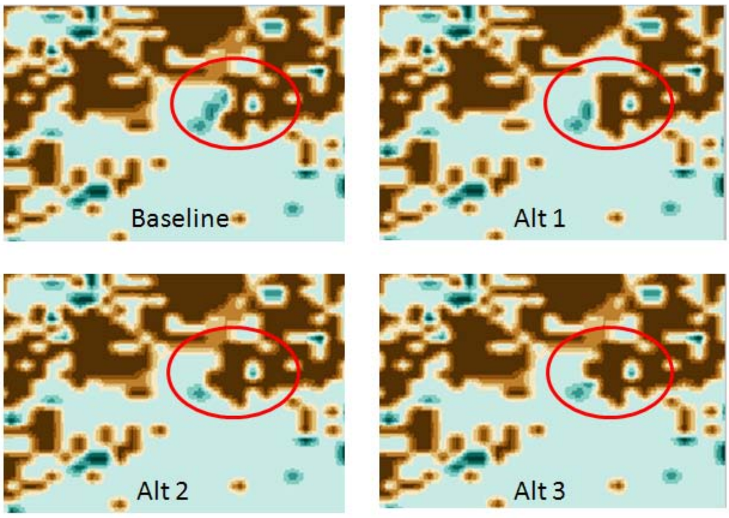

Figure 158a. Areas of Helsinki Alternative Scenario land use changes are circled in red. Brown areas are urban zones; vegetation in green.

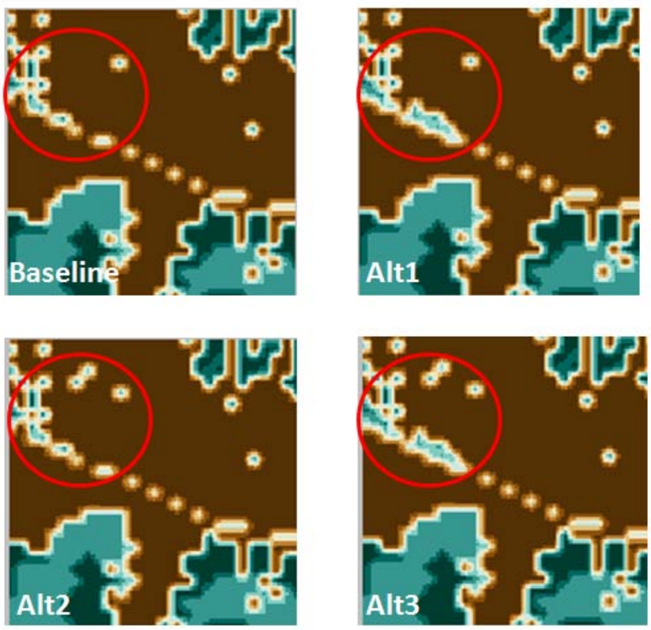

Figure 159b. Areas of Firenze Alternative Scenario land use changes are circled in red. Brown areas are urban zones; vegetation in green.

9.5 Output data.

CMCC model has been run in off-line mode. The output produced by WRF-ACASA model have been uploaded in an internal ftp website and are actually available to be downloaded into the DSS: daily files containing hourly time series; and files containing composite “days” averaged at monthly, seasonal, and annual timescales. All output files are in NetCDF format, and contain the following:

Hourly data appear in 365 daily files for each city and case. The data were post-processed from raw WRF-ACASA output files using no filtering; only the requested data arrays with simple unit transformations were performed. Composite-diurnal cycles (also hourly) for monthly, seasonal, and annual averages are single files with 24 “composite-hours” each, and are in the same format. The files contain 25 time points, hours 1-24 in each file correspond with the file’s temporal array values 2-25. The temporal array value “1” in each file is either blank or irrelevant.

All output files contain hourly (daily files), or hourly-composite values (for monthly-, seasonal-, and annually-averaged files), of the following quantities:

1) BowenRatio(Time, south_north, west_east) ;
   BowenRatio:description = "UPWARD HEAT FLUX AT THE SURFACE" ;
   BowenRatio:units = "--" ;
2) QFX(Time, south_north, west_east) ;
   QFX:description = "UPWARD MOISTURE FLUX AT THE SURFACE" ;
   QFX:units = "mm3_h2o m-2 s-1" ;
3) FCO2(Time, south_north, west_east) ;
   FCO2:description = "CO2 FLUX" ;
   FCO2:units = "microg m-2 s-1" ;
4) UDROFF(Time, south_north, west_east) ;
   UDROFF:description = "UNDERGROUND RUNOFF" ;
   UDROFF:units = "mm3_h2o m-2 s-1" ;
5) SFROFF(Time, south_north, west_east) ;
   SFROFF:description = "SURFACE RUNOFF" ;
   SFROFF:units = "mm3 m-2 s-1" ;
6) Infiltration(Time, south_north, west_east) ;
   Infiltration:description = "H2O infiltration rate" ;
   Infiltration:units = "mm3 m-2 s-1" ;
7) Temperature_2m(Time, south_north, west_east) ;
   Temperature_2m:description = "TEMP at 2 M" ;
   Temperature_2m:units = "degrees Celsius" ;
8) EMISS(Time, south_north, west_east) ;
   EMISS:description = "SURFACE EMISSIVITY" ;
   EMISS:units = "" ;
9) HFX(Time, south_north, west_east) ;
   HFX:description = "UPWARD HEAT FLUX AT THE SURFACE" ;
   HFX:units = "W m-2" ;
10) LH(Time, south_north, west_east) ;
   LH:description = "LATENT HEAT FLUX AT THE SURFACE" ;
   LH:units = "W m-2" ;
11) SMOIS(Time, soil_layers_stag, south_north, west_east) ;

SMOIS:description = "SOIL MOISTURE" ;
SMOIS:units = "m3 m-3" ;

12) S_anthro(Time, south_north, west_east) ;
S_anthro:description = "Anthropogenic thermal storage flux dens." ;
S_anthro:units = "Wm-2" ;

13) S_bio(Time, south_north, west_east) ;
S_bio:description = "Biogenic thermal storage flux dens." ;
S_bio:units = "Wm-2" ;

File names

The filename nomenclature is designed to be self-explanatory. The NetCDF format contains descriptor metadata as well. WRF-ACASA output fields (to appear in the DSS) come in several forms:

1. Daily files containing hourly reports (non-averaged) for the above set of variables for all days in 2008, for Firenze and Helsinki; each for Baseline and Alternative Scenarios 1-3 (2928 total).

   Example filename for December 23, 2008, Baseline (Alternative Scenario 0), Firenze:
   WRFACASA_Firenze_Scenario0_Endotherm_2008-12-23.nc
   Example filename for December 23, 2008, Alternative Scenario 1, Firenze:
   WRFACASA_Firenze_Scenario1_Endotherm_2008-12-23.nc

2. Monthly-averaged composite set, each file containing 24 “composite hourly” reports of all variables (96 total).
   Example filename for monthly composite-averaged hourly values (24 total), December 2008, Firenze:

   WRFACASA_Firenze_Scenario0_Endotherm_2008-12.nc

3. Annual-averaged composite set, each file containing 24 “composite hourly” reports of all variables (8 total).
   Example filename for annual composite-averaged hourly values, 2008, Firenze:

   WRFACASA_Firenze_Scenario0_Endotherm_2008.nc

4. Seasonal composite-difference files*:* Each file contains (Scenario – Alternative) differences for seasonally-averaged (3-month) values. Each file contains 24 “composite hourly” reports of differences for each variable (24 total).
   Example filename for differences (Alternative Scenario 1 minus Baseline, or “1m0”) for summer 2008, Firenze:

   WRFACASA_Firenze_Endotherm_2008-Summer_1m0.nc

9.6 Base run results.

The base runs for both Firenze and Helsinki for all of 2008 have been completed. In the deliverable 3.4, a number of these were shown on a monthly basis. Here, for the sake of brevity, annual results are presented.

9.6.1 Helsinki

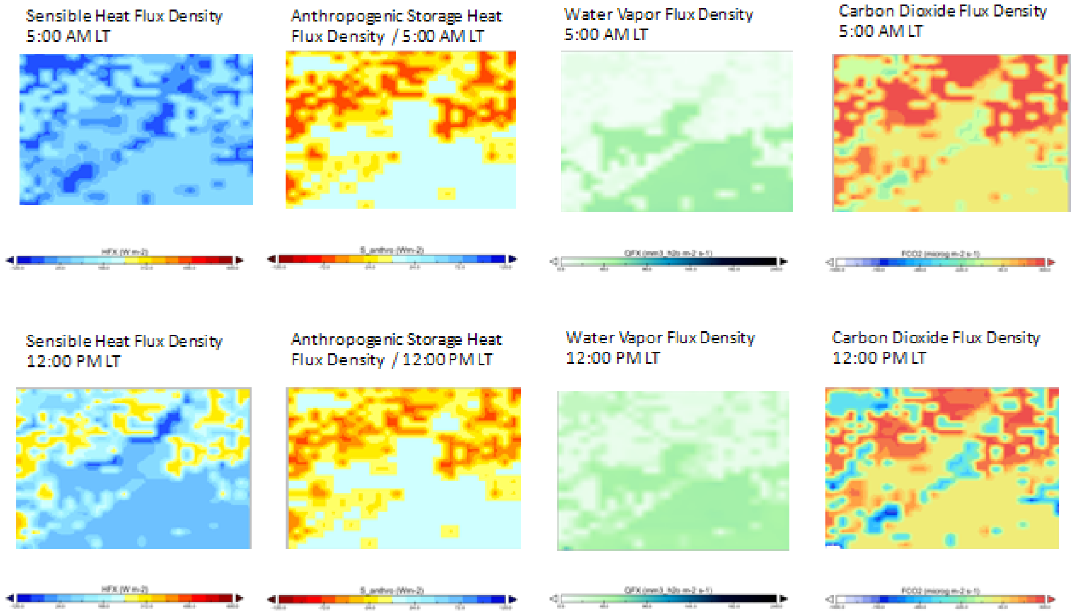

Figure 160. Helsinki, Baseline case: anually-averaged composite-hourly nighttime and daytime surface flux values.

9.6.2 Firenze

1 - Annual Composite-Averages (24 hours total; 2 are presented here)

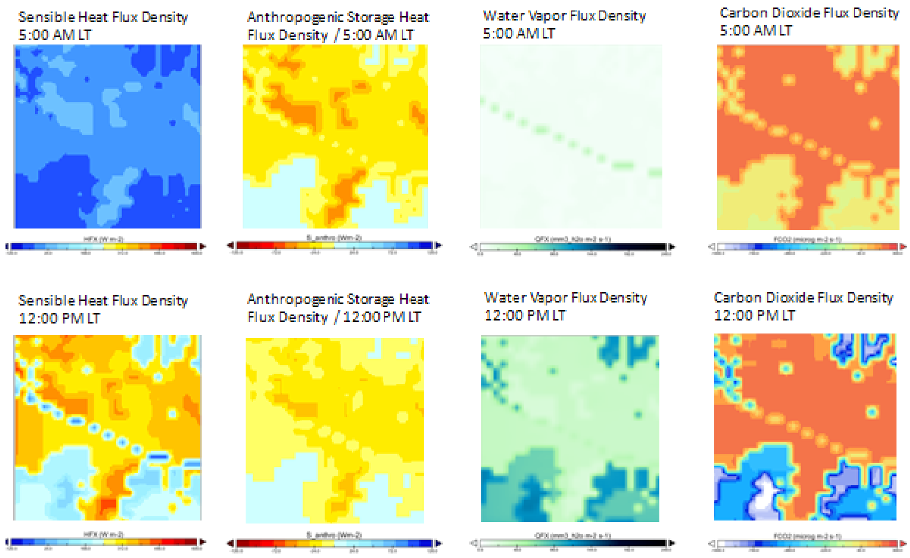

Figure 161 Firenze, Baseline case: anually-averaged composite-hourly nighttime and daytime surface flux values.

9.7 Alternatives implementation.

9.7.1 Helsinki

Implementation of the variations corresponding to development scenarios 1, 2, and 3 was the same as it was for the baseline case: we used all WRF-input and land use data provided as-is by UPM partner for each scenario.

9.7.2 Firenze

Implementation of the variations corresponding to development scenarios 1, 2, and 3 procceded as they did for Helsinki, but using Firenze data provided by UPM partner.

9.8 Alternatives results.

Differences in 2m air temperatures, heat, moisture, and carbon dioxide fluxes between each of the Alternative Scenarios and the Baseline simulation were nontrivial in the regions of land use change for both Helsinki and Firenze. A very brief summary of each is presented here.

The largest differences tend to occur during the summer months during daytime hours, but differences exist over all hours for all times of the year. Alternative minus Baseline differences are generally most prevalent on cloud-free days when photosynthesis is most active, but some significant differences occur at night during the cold months. Most difference fields generally show that Alternatives 1, 2 and 3 all provide a cooler, more evaporative, carbon-sinking regime in varying proportions, relative to Baseline. The urban heat island effect in the alternative scenarios appears somewhat mitigated during all hours and seasons as compared with Baseline.

Although these differences are nontrivial, the largest changes in fluxes and microenvironment tended to be confined to the points representing the land-use changes in each Alternative Scenario.
Visualizing finer details in these composite averages in order to see any downstream effects requires a careful calibration among scales that are close to the range of observational uncertainty. Such features would also tend to get lost in whole-domain averages. However subtle, the importance of downstream effects of any type of land use change scenario warrants further attention. An example of ‘downstream’ effects in the WRF-ACASA simulations described here is presented below for Helsinki. Note positive and negative differences to the south of the land use change zone, which is actually over open water, but these changes are small and most likely fall within measurement and statistical uncertainty bounds.

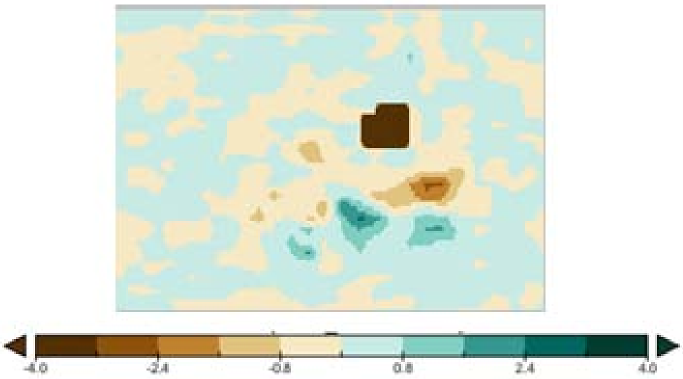

Figure 162 Baseline minus Alternative 3 Scenario, 12;00 PM LT summer composite, Helsinki.

Although the above tendency might in general be true at small scales for all quantities of concern, the vertical resolution (28 layers to 10,000m) in the current experimental design may be insufficient to allow advective features in the surface-layer and PBL to distribute these effects horizontally. By allowing sufficient vertical resolution throughout the planetary boundary layer, scaling arguments suggest that we might see additional statistically-significant changes further afield in the domain under the alternative development scenarios. Further simulations are planned that account for this.

9.8.1 Helsinki

The composite-averaged differences in 2-meter air temperature (Figure 163) show similar patterns for each set of land use changes during the extremes of winter and summer, with mostly warmer (near 1 degree Centigrade) temperatures prevailing in and near the changed grids during all times. At night during the winter, however, there appears to be a slight decrease in temperature adjacent to the land use change, Scenario 1 (Figure 163, far left).

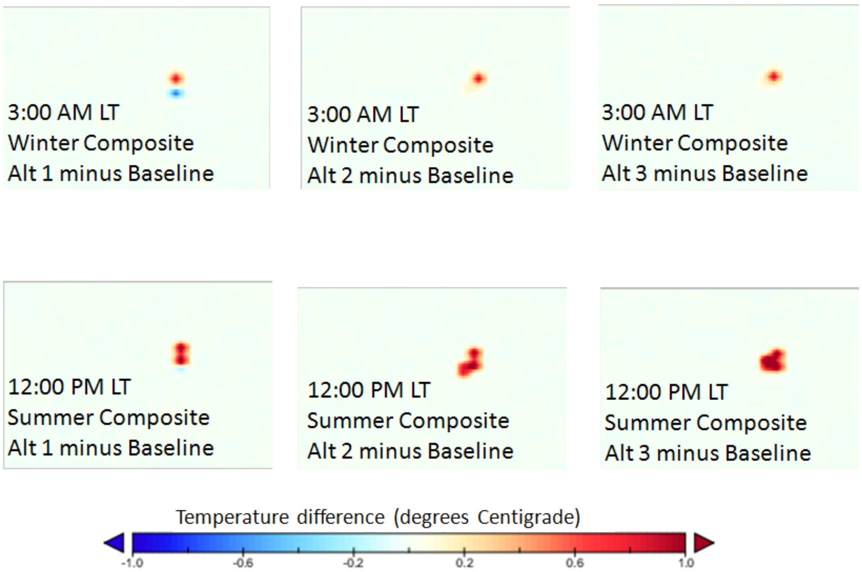

Figure 163 Helsinki composite 2-meter air temperature: Baseline minus Alternatives (difference) maps for winter-nighttime and summer-daytime conditions for Alternative Senarios 1, 2, and 3.

These changes are mainly due to changes from increased building zones that alter the partitioning of available energy into sensible and latent heat flux components, as shown below.

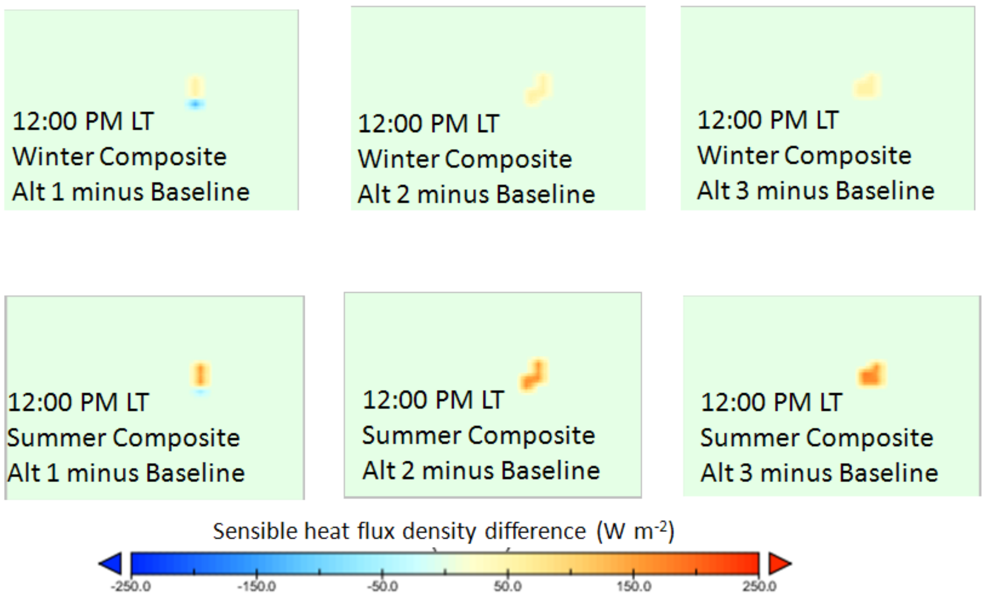

Figure 164 Helsinki composite difference maps for sensible heat flux density.

Changes to both sensible heat and moisture flux densities are relatively uniform in sign throughout most composite-hours, with the magnitudes of the differences increasing with increasing solar

radiation. Generally, there is more sensible heat flux in each of the alternative scenarios over areas local to the land use changes in each. Differences are most extreme during the summer daytime hours, when sensible heat flux difference values are between 100 and 200 Wm^{-2}. Differences showing less warming (more cooling) for the area immediately south of the land use change for Scenario 1 is on the order of -20 to -80 Wm^{-2} on average, matching thermal differences seen in Figure 163

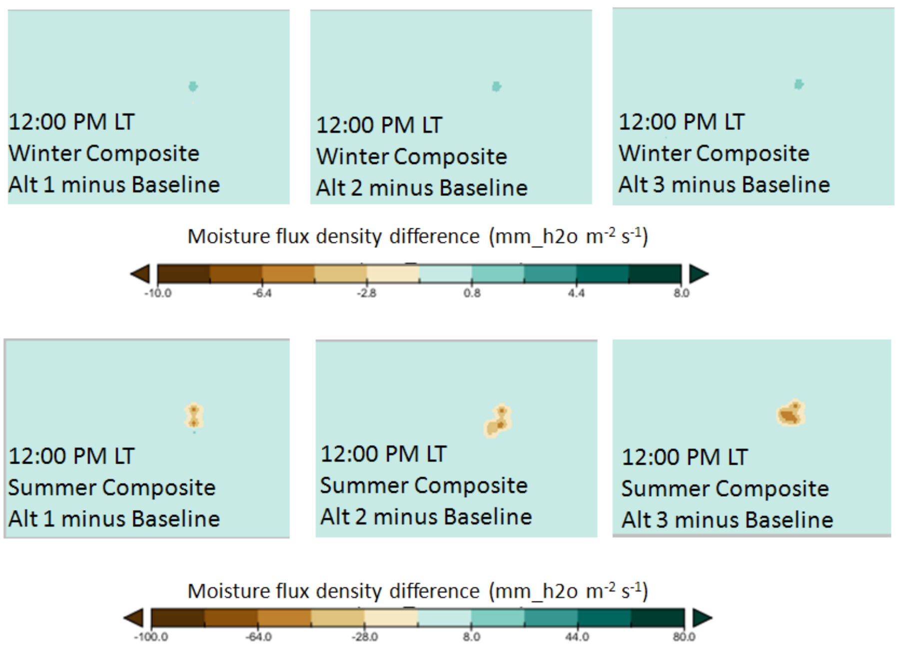

Figure 165 Helsinki composite difference maps for moisture flux density.

Seasonal difference plots for moisture flux show less evapotranspiration during the summer for all three Alternative scenarios, mostly due to the proposed building plans for each which would lessen the amount of vegetation while increasing building area. Differences are of much less magnitude during winter, but are of reversed sign. Note the finer calibration used for the winter plots (top 3 panels, Figure 165).

Seasonal composite difference fields for carbon dioxide flux densities show positive values for most hours and throughout most of the year, consistent with an increase in building intensity. During the daytime hours and particularly in the spring and summer, differences between baseline and the Alternatives are much larger in magnitude, a result of enhanced differences in carbon uptake between Baseline vegetation and each of the Alternative land use scenarios.

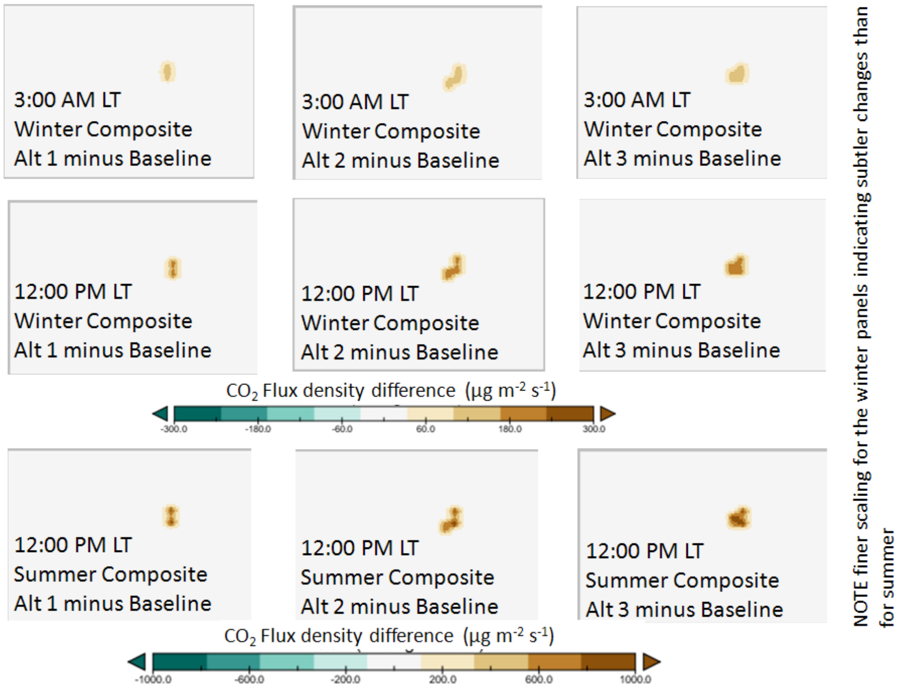

Figure 166 Helsinki composite difference maps for carbon dioxide flux density.

9.8.2 Firenze

The composite-averaged differences in 2-meter air temperature (Figure 167) show similar patterns for each set of land use changes during the extremes of winter and summer, with mostly cooler temperatures prevailing in and near the changed grids during all times. At night during the winter, however, there appears to be a slight enhancement in 2-meter air temperatures over several of the interior-changed grids in Scenarios 1 & 3. This positive feature diminishes during nighttime hours when it is warmer; and is most intense during the coldest nights of the winter. Scenario 2 results generally show the least amount of changes out of the three Scenarios, with Scenario 3 output changes appearing like a ‘sum’ of Scenarios 1 & 2.

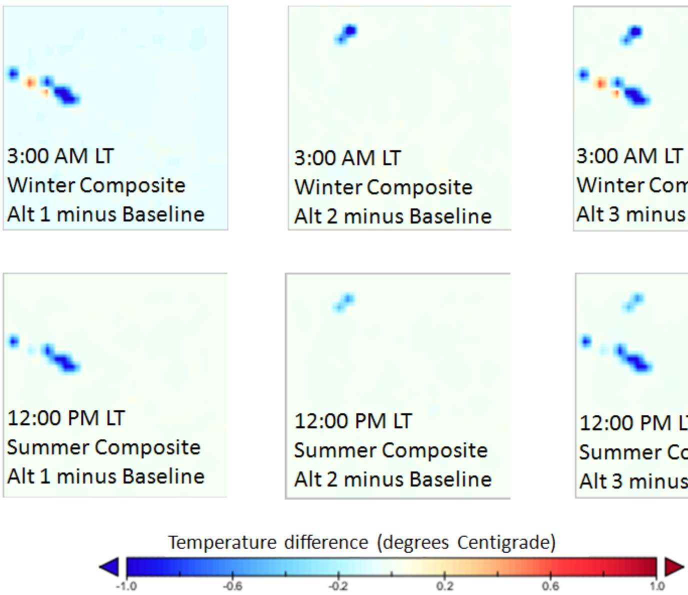

Figure 167. Firenze composite 2-meter air temperature difference maps for winter-nighttime and summer-daytime conditions.

These changes are mainly due to vegetation-related changes in the partitioning of available energy into sensible and latent heat flux components, as shown below.

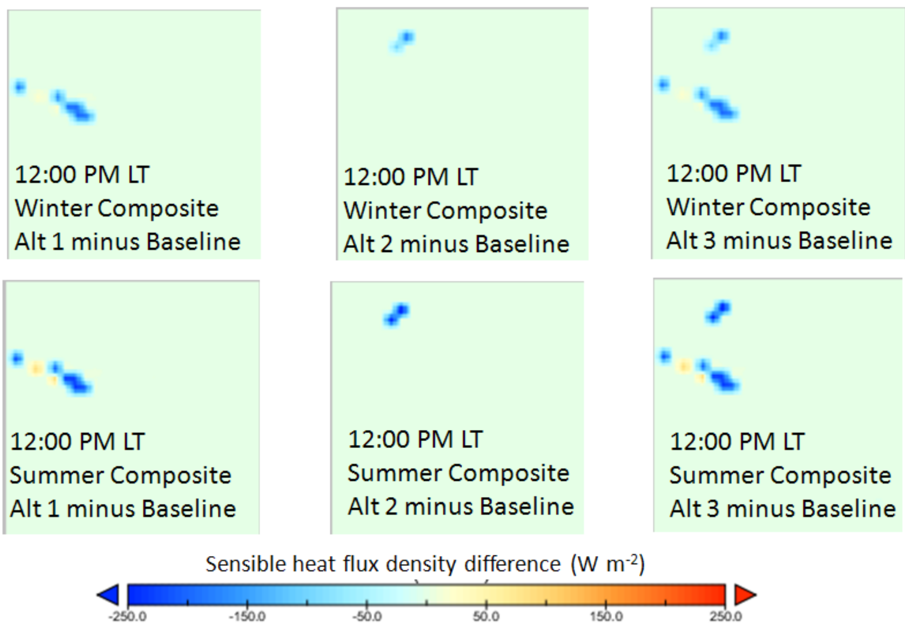

Figure 168Firenze composite difference maps for sensible heat flux density.

Changes to both sensible heat (Figure 168) and moisture flux (Figure 169) densities are relatively uniform in sign throughout most composite-hours, with the magnitudes of the differences increasing with increasing solar radiation. Generally, there is less sensible heat flux (more evapotranspiration) in each of the alternative scenarios over areas local to the land use changes in each. Differences are

most extreme during the summer daytime hours, when sensible (latent) heat flux values are between 100 and 200+ Wm^{-2} less (more) than for the baseline case.

A preliminary examination of composite nighttime values (not shown) reveals that sensible heating is lessened in the Alternative scenarios (on the order of 100 Wm^{-2}) during the coldest periods, lessening to near-negligible values in the summer. This latter pattern in the simulated results is most likely due to the ectothermic effects of vegetation replacing dry endothermic buildings over most points in the alternative land use Scenarios. Flux values appear nearly unchanged over the unaffected areas in the domain in all cases.

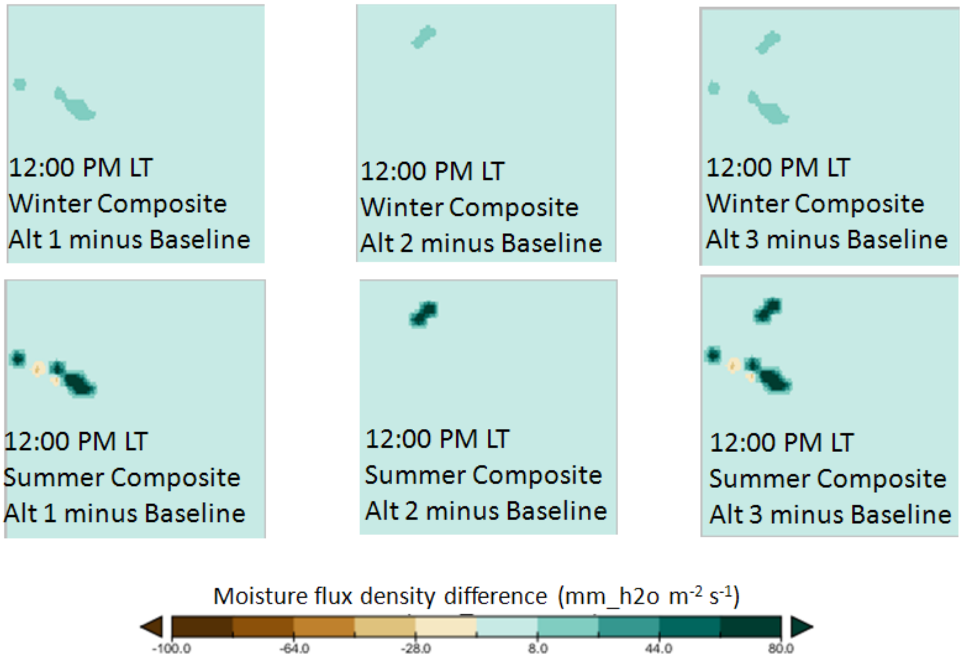

Figure 169 Firenze composite difference maps for moisture flux density.

Seasonal composite difference fields for carbon dioxide flux densities show negative values for most hours and throughout most of the year. Nighttime respiration (CO^2 emissions) of the enhanced vegetation areas in the Alternative Scenarios is of a lesser magnitude than that of existing (Baseline) land use patterns. During the daytime hours and particularly in the spring and summer, differences between baseline and the Alternatives are much larger in magnitude, a result of enhanced photosynthetic uptake.

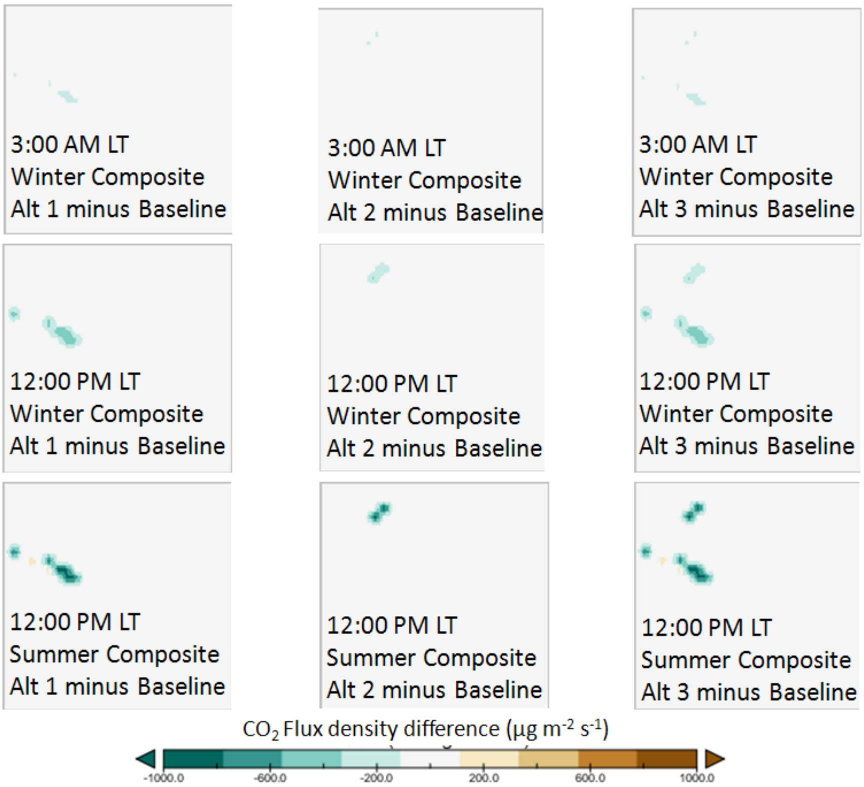

Figure 170. Firenze composite difference maps for carbon dioxide flux density.